

Methods to prepare amorphous material for rapid dissolution solid dosage forms

Runglawan Viboonkiat

*A thesis submitted to the University of London as a partial requirement
for the degree of Doctor of Philosophy*

Department of Pharmaceutics
The School of Pharmacy
University of London

March 2003

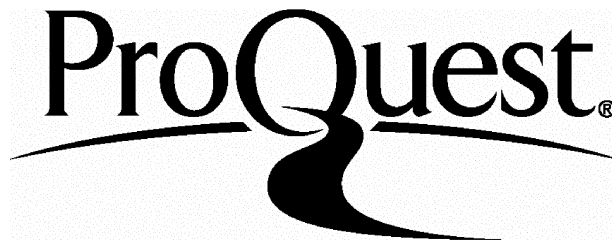
ProQuest Number: 10104822

All rights reserved

INFORMATION TO ALL USERS

The quality of this reproduction is dependent upon the quality of the copy submitted.

In the unlikely event that the author did not send a complete manuscript and there are missing pages, these will be noted. Also, if material had to be removed, a note will indicate the deletion.



ProQuest 10104822

Published by ProQuest LLC(2016). Copyright of the Dissertation is held by the Author.

All rights reserved.

This work is protected against unauthorized copying under Title 17, United States Code.
Microform Edition © ProQuest LLC.

ProQuest LLC
789 East Eisenhower Parkway
P.O. Box 1346
Ann Arbor, MI 48106-1346

Abstract

Poorly water-soluble drugs with dissolution as the rate-limiting step in gastrointestinal absorption commonly show increased bioavailability when dissolution is improved by conversion to the amorphous form. In this study, different techniques were employed to convert a model drug, indomethacin, into the amorphous state. The techniques involved the use of spray-drying and supercritical carbon dioxide (sc-CO₂) as an antisolvent and as a solvent. The products were characterised using differential scanning calorimetry (DSC) and Powder X-ray diffraction (PXRD).

In the spray drying method, indomethacin was co-spray dried with microcrystalline cellulose (MCC) and polyvinylpyrrolidone (PVP) at various proportions. At 20% PVP and above, amorphous indomethacin could be produced but MCC had no effect on crystallinity. When sc-CO₂ was used as an antisolvent, it was not possible to form amorphous indomethacin or coprecipitates of indomethacin-PVP. After modification of the rig, sc-CO₂ was employed as a solvent. Coprecipitated indomethacin at various PVP weight fractions were successfully prepared, and amorphous products were obtained at PVP weight fraction of 0.80 and above. The dissolution rates of indomethacin-PVP mixtures prepared using sc-CO₂, physical mixing and solvent evaporation methods were compared. PVP enhanced the dissolution of indomethacin at low concentration but increase in PVP content above 30% retarded the dissolution rate. The dissolution was dependent on the PVP content and the preparation method. The stability of indomethacin-PVP mixtures at different temperatures and relative humidities was monitored over a 3-month period. Coprecipitation of indomethacin-PVP retarded the crystallization process. The coprecipitates where indomethacin existed in completely amorphous form did not crystallize after storage at 30, 50 and 70°C for 3 months. Similarly, coprecipitation of indomethacin with PVP also retarded the crystallization process at 35% RH for 3 months. At 76% and 98% RH, products absorbed large quantities of water but did not crystallize.

In summary, a solvent free, porous and rapid dissolution amorphous indomethacin can be prepared by sc-CO₂ based process. This method could provide a viable and practical alternative to spray drying for the production of amorphous material.

Acknowledgements

The completion of this work would not have been possible without the valuable supervision of Professor Graham Buckton for which I am most grateful. I have also appreciated his guidance, encouragement and optimism throughout the period of this work.

I am also particularly indebted to Dr. Jawwad A Darr for his practical advice, countless discussions and encouragement throughout this work. My gratitude is also extended to Dr. Ihtesham Ur Rehman for his kindness, support and valuable advice. I am especially grateful to James Stewart and Dr Peh Kok Khiang who took their time to listen to my frustration and helped me through the hard times while I was writing this thesis. Their assistance in reviewing this manuscript is also greatly appreciated. I am grateful to Keith Barns and Dave Porter for all their assistance. Special thanks are due to all the staff involved at the School of Pharmacy and Queen Mary University of London, particularly Dave McCarthy for his help with the Scanning Electron Microscopy.

I also would like to thank all my friends at Maria Assumpta Student Residence for understanding and companionship during the time I have been away from home.

As with any undertaking of this nature, I wish to thank my family for their constant love and encouragement over the years. Finally and most importantly, I would like to thank my fiancé, Uthen whose love, understanding and endless inspiration has aided me in the completion of this thesis.

To my parents.

With love and grateful thanks.

Table of contents

Abstract	2
Acknowledgements	3
Dedication	4
Table of contents	5
List of tables	10
List of figures	14
Chapter 1. Introduction	20
1.1 Crystalline materials	21
1.1.1 Crystallization	22
1.1.2 Polymorphism	24
1.1.3 Solvates and hydrates	26
1.2 Amorphous materials	27
1.2.1 Glass transition temperature (T_g)	27
1.2.2 Physico-chemical properties	28
1.3 Techniques for preparing amorphous solid materials	28
1.3.1 Spray drying	29
1.3.1.1 Spray drying process	30
Atomisation	30
Spray-gas contact	31
Drying of the sprayed droplets	32
Separation of dried sample from air	34
1.3.1.2 Effect of spray drying experimental parameters on the product	34
Inlet temperature	34
Outlet temperature	34
Aspirator speed	35
Spray flow rate	35
Feed rate	35
Feed concentration	35
1.3.2 Supercritical fluid technology	36
1.3.2.1 Supercritical fluids	36

1.3.2.2 Precipitation using a supercritical carbon dioxide	38
Rapid Expansion of Supercritical Solution	39
Precipitation from Gas Saturated Solutions/Suspensions	45
Precipitation using sc-CO ₂ as an Antisolvent	48
Batch operation techniques	49
Semicontinuous operation techniques	51
1.4 Techniques for characterizing amorphous solids	60
1.5 Dissolution studies	60
1.5.1 Factors affecting the dissolution rate of drugs	60
1.5.1.1 Solid phase characteristics	60
1.5.1.2 Polymorphism	61
1.5.1.3 Particle size and surface area	61
1.6 Thesis aims	62
Chapter 2. Materials and Methods	63
2.1 Materials	64
2.1.1 Drug	64
2.1.2 Polymers	66
2.1.3 Organic solvents	70
2.1.4 Excipients	71
2.1.5 Distilled water	72
2.1.6 Dissolution medium	72
2.2 Methods	73
2.2.1 Scanning electron microscopy	73
2.2.2 Differential scanning calorimetry	73
2.2.3 Powder X-ray Diffraction Analysis	75
Chapter 3. Spray Drying	79
3.1 Introduction	80
3.2 Materials and Methods	80
3.2.1 Materials	80
3.2.2 Preparation of spray dried indomethacin	80
3.2.3 Preparation of indomethacin and microcrystalline cellulose mixture	82

3.2.4 Preparation of indomethacin and polyvinylpyrrolidone mixture	82
3.2.5 Preparation of indomethacin and PVP mixtures with inclusion of MCC or silicified microcrystalline cellulose	82
3.2.6 Thermal analysis	83
3.2.7 X-Ray diffraction analysis	83
3.2.8 Preparation of tablets	83
3.2.9 Dissolution study	84
3.3 Results and Discussion	84
3.4 Conclusions	97
Chapter 4. Precipitation using supercritical CO₂ as an antisolvent	98
4.1 Introduction	99
4.2 Materials and Methods	99
4.2.1 Materials	99
4.2.2 Precipitation of indomethacin using water as an antisolvent	99
4.2.3 Construction and design of PCA apparatus	100
4.2.4 Procedure	105
4.2.5 Precipitation of indomethacin from dichloromethane	105
4.2.6 Precipitation of indomethacin from various organic solvents	106
4.2.7 Precipitation of indomethacin and PVP	106
4.2.8 Scanning electron microscopy	106
4.2.9 Thermal analysis	106
4.2.10 X-ray diffraction analysis	106
4.3 Results and Discussion	107
4.4 Conclusions	122
Chapter 5. Precipitation using supercritical CO₂ as solvent	123
5.1 Introduction	124
5.2 Materials and Methods	125
5.2.1 Materials	125
5.2.2 Design and construction of apparatus	125
5.2.3 Procedure	129

5.2.4 Investigation of the effect of sc-CO ₂ on the characteristics of indomethacin	130
5.2.5 Precipitation of indomethacin and PEG	130
5.2.6 Precipitation of indomethacin and PVP	130
5.2.7 Scanning electron microscopy	131
5.2.8 Particle size analysis	131
5.2.9 Thermal analysis	131
5.2.10 X-ray diffraction analysis	132
5.2.11 Statistical analysis	132
5.2.12 Determination of the crystallinity of indomethacin	132
5.3 Results and Discussion	134
5.4 Conclusions	146
Chapter 6. Dissolution and stability studies	147
6.1 Introduction	148
6.2 Materials and Methods	149
6.2.1 Materials	149
6.2.2 Preparation of indomethacin and PVP physical mixtures	149
6.2.3 Preparation of indomethacin and PVP solid dispersions	149
6.2.4 Preparation of indomethacin and PVP mixture using supercritical CO ₂	149
6.2.5 Preparation of amorphous indomethacin	150
6.2.6 Preparation of α-metastable indomethacin	150
6.2.7 Drug content determination	150
6.2.8 Solubility determination	151
6.2.9 Dissolution study	151
6.2.10 Statistical analysis	152
6.2.11 Stability study	152
6.3. Results and Discussion	153
6.4 Conclusions	183
Chapter 7. Conclusions and Recommendations	184
7.1 Introduction	185

7.2 General conclusions	185
7.3 Recommendations for future work	187
References	189
Appendix	207

List of Tables

Table	Description	Page
1.1	Physical properties of gases, supercritical fluids and liquids	37
1.2	Critical data for some supercritical solvents	38
1.3	Solubility of Pharmaceutical compounds in Supercritical carbondioxide	44
1.4	Experimental results on the supercritical antisolvent precipitation of compounds	58-59
2.1	Indomethacin solubility in different solvents at 25 °C	65
2.2	The functions and their corresponding concentrations of MCC	68
3.1	Spray drying parameters investigated for indomethacin	81
3.2	The composition of indomethacin and different polymer for spray dried solutions	83
3.3	Results of % yield for indomethacin spray dried under different conditions	85
3.4	The powder X-ray diffraction results of indomethacin and PVP mixture at various compositions	94
3.5	The powder X-ray diffraction results of indomethacin with various amount of PVP and MCC or SMCC	95
3.6	The powder X-ray diffraction results of indomethacin and PVP with various percentages of MCC or SMCC	96
4.1	The physical appearance, SEM, DSC and PXRD results of indomethacin prepared at different concentrations precipitated using water as anti-solvent	109
4.2	The physical appearance, SEM, DSC and PXRD results of indomethacin precipitated from different concentrations and flow rates of drug solution	114
4.3	The maximum concentration, physical appearance, SEM, DSC and PXRD results indomethacin precipitated from various organic solvents using sc-CO ₂ as antisolvent	116

Table	Description	Page
5.1	Results of the particle size analysis for indomethacin precipitated under different conditions	134
5.2	Glass transition temperature and degree of crystallinity for indomethacin coprecipitates with PVP obtained by Differential Scanning Calorimetry and PXRD, respectively	143
5.3	One-way analysis of variance (ANOVA) results of T_g	144
5.4	Tukey HSD test results of T_g	145
6.1(a)	ANOVA table of $T_{50\%}$ values of amorphous, α and γ forms of indomethacin	156
6.1(b)	Tukey HSD test results of $T_{50\%}$ values of amorphous, α and γ form indomethacin	157
6.2	The indomethacin content in various mixtures of indomethacin and PVP	158
6.3(a)	ANOVA table of $T_{50\%}$ values of physical mixture of indomethacin with 20-83% of PVP	159
6.3(b)	Tukey HSD test results of $T_{50\%}$ values of physical mixture of indomethacin with 20-83% of PVP	160
6.4	Glass transition temperature and degree of crystallinity for solid dispersions of indomethacin and PVP obtained by Differential Scanning Calorimetry and PXRD, respectively	160
6.5(a)	ANOVA table of $T_{50\%}$ values of solid dispersion indomethacin with 20-83% of PVP prepared using solvent evaporation method	163
6.5(b)	Tukey-HSD test results of $T_{50\%}$ values of solid dispersion indomethacin with 20-83% of PVP prepared using solvent evaporation method	164
6.6(a)	ANOVA table of $T_{50\%}$ values of coprecipitates indomethacin with 20-83% of PVP prepared using supercritical CO_2 based technique	165

Table	Description	Page
6.6(b)	Tukey HSD test results of $T_{50\%}$ values of coprecipitates indomethacin with 20-83% of PVP prepared using supercritical CO_2 based technique	166
6.7	$T_{50\%}$ of mixtures of indomethacin and various proportion of PVP prepared using physical mixing, solid dispersion and supercritical fluids based technique	167
6.8(a)	ANOVA table of $T_{50\%}$ values of indomethacin from indomethacin and 20% PVP prepared by three different methods	167
6.8(b)	Tukey HSD test results of $T_{50\%}$ values of indomethacin from indomethacin and 20% PVP prepared by three different methods	167
6.9(a)	ANOVA table of $T_{50\%}$ values of indomethacin from indomethacin and 30% PVP prepared by three different methods	168
6.9(b)	Tukey HSD test results of $T_{50\%}$ values of indomethacin from indomethacin and 30% PVP prepared by three different methods	168
6.10(a)	ANOVA table of $T_{50\%}$ values of indomethacin from indomethacin and 50% PVP prepared by three different methods	168
6.10(b)	Tukey HSD test results of $T_{50\%}$ values of indomethacin from indomethacin and 50% PVP prepared by three different methods	169
6.11(a)	ANOVA table of $T_{50\%}$ values of indomethacin from indomethacin and 60% PVP prepared by three different methods	169
6.11(b)	Tukey HSD test results of $T_{50\%}$ values of indomethacin from indomethacin and 60% PVP prepared by three different methods	169

Table	Description	Page
6.12(a)	ANOVA table of $T_{50\%}$ values of indomethacin from indomethacin and 83 % PVP prepared by three different methods	170
6.12(b)	Tukey HSD test results of $T_{50\%}$ values of indomethacin from indomethacin and 83% PVP prepared by three different methods	170
6.13	Degree of crystallinity of indomethacin and PVP coprecipitated using solid dispersion and supercritical fluid technique	175
6.14	The time measured for the changing of appearance from powder to sticky mass of indomethacin–PVP coprecipitates at various RH at 25 °C	182

List of Figures

Figure	Description	Page
1.1	Plot of heat <i>versus</i> temperature for crystalline material	22
1.2	The seven possible primitive unit cells in crystals	26
1.3	Diagram of the Buchi 190 Mini spray dryer	31
1.4	A drying graph depicting the relationships between drying rate and moisture content	33
1.5	Diagram of the particle features along the drying step of spray Drying	33
1.6	Pressure-Temperature diagram for a pure substance	37
1.7	Requirements of an ideal particle formation process for pharmaceutical products	39
1.8	RESS equipment	40
1.9	Particle from Gas Saturated Solutions (PGSS) equipment	46
1.10	Gas antisolvent (GAS) or supercritical antisolvent (SAS) recrystallization equipment	49
1.11	Factors influencing particle properties when prepared by the gas antisolvent or supercritical antisolvent recrystallization	50
1.12	PCA/ASES equipment	52
1.13	SEDS equipment concept along with a cross section of the two and three coaxial-passages nozzle	54
2.1	Structural formula of Indomethacin	64
2.2	Structural formula of Polyvinylpyrrolidone	66
2.3	Structural formula of microcrystalline cellulose	68
2.4	A typical thermogram generated from power compensation DSC	75
2.5	Geometrical relationships among X-ray beam wavelength, diffraction angle and the distance of lattice space	76
2.6(a)	Typical spectra of crystalline material	77
2.6(b)	Typical spectra of partially amorphous	78

Figure	Description	Page
3.1	DSC scan of spray-dried Indomethacin in Ethanol/water	86
3.2	DSC scan of spray-dried dispersion of MCC in solution of Indomethacin in Ethanol/water	87
3.3	DSC scan of spray-dried ground mixtures of Indomethacin and MCC in Ethanol/water	87
3.4	X-ray diffraction pattern of spray-dried Indomethacin in Ethanol/water	88
3.5	X-ray diffraction pattern of spray-dried dispersion on MCC in solution of Indomethacin in Ethanol/water	89
3.6	X-ray diffraction pattern of spray-dried ground mixtures of Indomethacin and MCC in Ethanol/water	89
3.7	DSC scan of spray-dried Indomethacin with PVP 5%	90
3.8	DSC scan of spray-dried Indomethacin with PVP 10%	91
3.9	DSC scan of spray-dried Indomethacin with PVP 20%	91
3.10	DSC scan of spray-dried Indomethacin with PVP 60%	92
3.11	X-ray diffraction pattern of spray-dried Indomethacin with 5% PVP	92
3.12	X-ray diffraction pattern of spray-dried Indomethacin with 10% PVP	93
3.13	X-ray diffraction pattern of spray-dried Indomethacin with 20% PVP	93
3.14	X-ray diffraction pattern of spray-dried Indomethacin with 60% PVP	94
3.15	Dissolution profiles of spray-dried Indomethacin with polymer	97
4.1	PCA apparatus schematic diagram	101
4.2	The PCA reaction vessel	102
4.3	PCA apparatus	103
4.4	The CO ₂ pump for PCA apparatus	104
4.5(a)	SEM photograph of unprocessed indomethacin particles	108

Figure	Description	Page
4.5(b)	SEM photograph of indomethacin particles precipitated from 33.3% w/v ethanolic solution using water as an antisolvent	108
4.6	DSC scan of indomethacin recrystallized from 12.5% w/v of ethanolic solution using water as an antisolvent	109
4.7	DSC scan of indomethacin recrystallized from 20 % w/v of ethanolic solution using water as an antisolvent	110
4.8	DSC scan of indomethacin recrystallized from 33.33 % w/v of ethanolic solution using water as an antisolvent	110
4.9	PXRD scan of indomethacin recrystallized from 20% w/v of ethanolic solution using water as an antisolvent	111
4.10	PXRD scan of indomethacin recrystallized from 33.33% w/v of ethanolic solution using water as an antisolvent	111
4.11	Typical SEM photograph of indomethacin particles prepared using dichloromethane as solvent and sc-CO ₂ as antisolvent	113
4.12	Typical DSC scan of indomethacin particles prepared using dichloromethane as solvent and sc-CO ₂ as antisolvent	113
4.13	Typical PXRD profile of indomethacin particles prepared using dichloromethane as solvent and sc-CO ₂ as antisolvent	114
4.14(a)	SEM of indomethacin particles prepared using Acetone as solvent and sc-CO ₂ as antisolvent	117
4.14(b)	SEM of indomethacin particles prepared using chloroform as solvent and sc-CO ₂ as antisolvent	117
4.15	DSC of indomethacin particle prepared using ethanol as solvent and sc-CO ₂ as antisolvent	118
4.16	DSC of indomethacin particle prepared using dichloromethane:ethanol (1:1) as solvent and sc-CO ₂ as antisolvent	118

Figure	Description	Page
4.17	DSC of indomethacin particle prepared using acetone as solvent and sc-CO ₂ as antisolvent	119
4.18	DSC of indomethacin particle prepared using chloroform as solvent and sc-CO ₂ as antisolvent	119
4.19	PXRD of indomethacin particle prepared using dichloromethane: ethanol (1:1) as solvent and sc-CO ₂ as antisolvent	120
4.20	PXRD of indomethacin particle prepared using acetone as solvent and sc-CO ₂ as antisolvent	120
4.21	PXRD of indomethacin particle prepared using chloroform as solvent and sc-CO ₂ as antisolvent	121
5.1	CO ₂ pump with a built-in chiller	126
5.2	The stirred batch reaction vessel	127
5.3	Schematic diagram of an apparatus using CO ₂ as solvent	128
5.4	Peak intensity ratio versus degree of crystallinity (a) physical mixture of α form and noncrystalline solid, (b) physical mixture of γ form and noncrystalline solid	133
5.5	SEM images of indomethacin (a) original material and the precipitates obtained by SCF method at 20 °C (b) P=200 bar; (c) P=100 bar	135
5.6	SEM images of indomethacin and PVP mixture at ratio 1.7:8.3 prepared using sc-CO ₂ as solvent (T=40 °C and P=150 bar)	137
5.7	(a) and (b) SEM images of indomethacin and PVP coprecipitate at ratio 1.7:8.3 before grinding	138
5.8	Typical trace obtained from differential scanning calorimetry of indomethacin-PVP coprecipitates using sc-CO ₂ as solvent	139
5.9	XRD pattern of the coprecipitation of indomethacin and 0.2 PVP weight fraction prepared using sc-CO ₂ as solvent	140

Figure	Description	Page
5.10	XRD pattern of the coprecipitation of indomethacin and 0.3 PVP weight fraction prepared using sc-CO ₂ as a solvent	140
5.11	XRD pattern of the coprecipitation of indomethacin and 0.5 PVP weight fraction prepared using sc-CO ₂ as a solvent	141
5.12	XRD pattern of the coprecipitation of indomethacin and 0.6 PVP weight fraction prepared using sc-CO ₂ as a solvent	141
5.13	XRD pattern of the coprecipitation of indomethacin and 0.8 PVP weight fraction prepared using sc-CO ₂ as a solvent	142
5.14	XRD pattern of the coprecipitation of indomethacin and 0.83 PVP weight fraction prepared using sc-CO ₂ as a solvent	142
5.15	Plot of glass transition temperature <i>versus</i> weight percent of PVP for indomethacin-PVP coprecipitates using SCF based technique	144
6.1.	Paddle apparatus for dissolution testing	152
6.2	Solubility study of amorphous, α and γ form of indomethacin	155
6.3	The dissolution profiles of amorphous, α and γ indomethacin	156
6.4	Dissolution profiles of pure indomethacin and physical mixture of indomethacin with 20-83% of PVP	159
6.5	PXRD pattern of the solid dispersion of indomethacin and 0.2 PVP weight fraction prepared using solvent evaporation	161
6.6	PXRD pattern of the solid dispersion of indomethacin and 0.3 PVP weight fraction prepared using solvent evaporation	161
6.7	PXRD pattern of the solid dispersion of indomethacin and 0.5 PVP weight fraction prepared using solvent evaporation	162
6.8	Dissolution profiles of pure indomethacin and solid dispersion (SD) of indomethacin with 20-83% of PVP prepared using solvent evaporation method	163
6.9	Dissolution profiles of pure indomethacin and coprecipitates of indomethacin with 20-83% of PVP prepared using supercritical CO ₂ based technique	165

Figure	Description	Page
6.10(a)	percent crystalline phase vs time at 30 °C for the amorphous indomethacin	172
6.10(b)	plot of percent amorphous indomethacin remaining after storage at 30 °C for various time periods (t) after an induction time (t _i) for the amorphous indomethacin	173
6.11	Percent crystalline phase vs time at 50 °C for the amorphous indomethacin	173
6.12	Percent crystalline phase vs time at 70 °C for the amorphous indomethacin	174
6.13	Percent crystalline phase vs time at 30, 50 and 70 °C for the solid dispersion of indomethacin and 20% PVP	176
6.14	Percent crystalline phase vs time at 30, 50 and 70 °C for the coprecipitated indomethacin and 20% PVP prepared using the SCF based technique	177
6.15	Percent crystalline phase vs time at 30, 50 and 70 °C for the coprecipitated indomethacin and 50% PVP prepared using the SCF based technique	177
6.16	Plot of degree of crystallinity vs time of amorphous indomethacin stored at 35% and 76% RH and 25°C	179
6.17	Plot of degree of crystallinity vs time of amorphous indomethacin stored at 98% RH and 25°C	179
6.18	Percent crystallinity vs time at 35%, 76% and 98% RH for the solid dispersion of indomethacin and 20%PVP	181
6.19	Percent crystallinity vs time at 35%, 76% and 98% RH for the coprecipitated indomethacin and 20% PVP prepared using SCF based technique	181
6.20	Percent crystallinity vs time at 35%, 76% and 98% RH for the coprecipitated indomethacin and 50% PVP prepared using SCF based technique	182

Chapter 1
Introduction

Solids can either be crystalline or amorphous in their structures. In the case of polymers, it is even more common to find a combination of both crystalline and amorphous regions within the same polymer structure with one of them available in a higher concentration than the other. If this solid is heated, the crystalline part undergoes melting whereas the amorphous part undergoes glass transition.

1.1 Crystalline materials

A solid crystal is a mass of ions, atoms or molecules, which are packed in a neat, fixed, rigid and orderly fashion; having both short and long range, order. This high degree of order results in the development of definite external crystal faces resulting in a certain external shape called the crystal habit. The crystals may vary in the development of the various faces and size, but the angle between any two adjacent faces is a constant value, described by the law of constant interfacial angles, which was proposed in 1784 by Hauy (Mullin, 1997).

The basic unit in a crystal is called a unit cell and repetition of this unit cell in three dimensions gives the crystal. Depending on the structure of the molecule itself and many other factors such as crystallization conditions, different crystal habits can be obtained, such as needle, tabular, lamellar, and columnar (Florence and Attwood, 1998). If a crystalline solid is heated, it undergoes melting at a certain specific temperature which is characteristic to the material being heated.

Melting is a first order phase transition which entails a well-known process. Specifically, that upon heating a crystalline solid its temperature will start rising up to the melting point. Due to latent heat, the temperature will stop rising until all the solid mass melts. Once all have melted, the temperature resumes its rise while heating continues (Figure 1.1). Hence a first order transition involves both a latent heat and a change in the heat capacity.

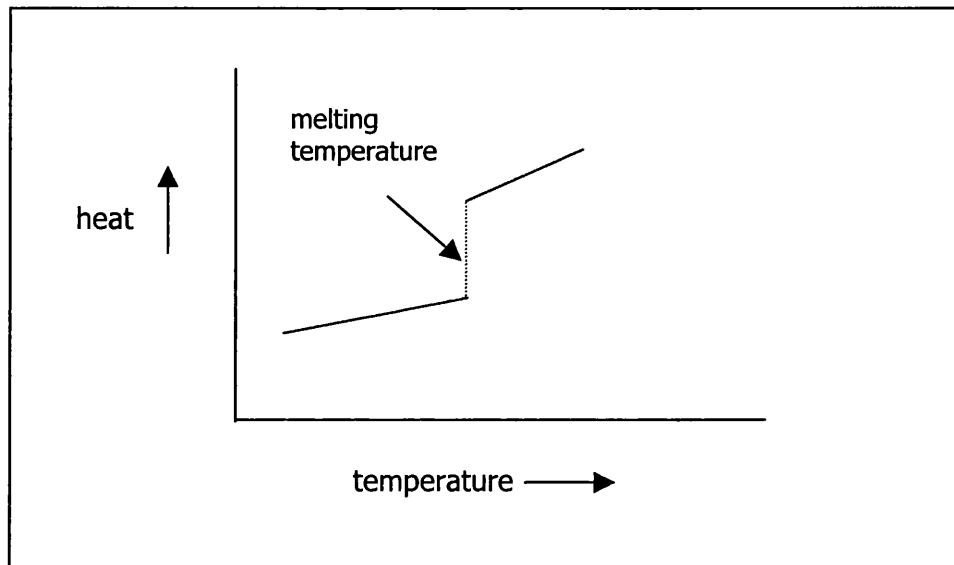


Figure 1.1 Plot of heat *versus* temperature for crystalline material.

1.1.1 Crystallization

Crystallization can be considered to pass through three successive phases.

- a. **Supersaturation of the solution:** can be achieved in different ways such as solvent evaporation; cooling; a chemical reaction which changes the properties of the solute, or by the addition of a precipitant.
- b. **Formation of crystal nuclei (nucleation):** It is not sufficient to have a supersaturated system for crystallization to take place. The presence of seeds or nuclei, on the surface of which the material can be deposited and crystallized, is essential. These nuclei can be obtained through artificially seeding of the supersaturated solution with particles of the same compound to enhance deposition and precipitation from solution on the surface of these seeds. Dust particles, impurities or even container particles can act as seeds that enhance deposition of crystals from solution on their surfaces. Nucleation can be triggered in different ways such as mechanical shock, application of high pressure or friction within the solution and agitation (Mullin, 1997). Spontaneous nucleation can sometimes be achieved without the need for

seeding; in this case collision between molecules of the solute in solution takes place and leads to nuclei formation. Primary nucleation is a term given to the type of nucleation which is either spontaneously triggered or where seeds are already present and not added deliberately such as dust particles. On the other hand, secondary nucleation is the type of nucleation which is artificially induced by deliberately adding seeds of a crystalline material to enhance crystallization.

- c. **Crystal growth:** There are many theories which are proposed in order to explain crystal growth. These are as follows:

1. Diffusion theories:

Can be looked upon as the reverse process of dissolution. According to Noyes-Whitney(1897) and Nernst(1904), matter is continuously deposited on the surface of a crystal at a rate that is proportional to the concentration gradient between the surface of the crystal and bulk of solution.

$$dm/dt = A k_m (C_{ss}-C_s)$$

Where m: mass of solid deposited on the surface of crystal at time t

A: surface area of the crystal

C_{ss} : concentration at supersaturation.

C_s : solute concentration at saturation.

$$k_m = D/\delta$$

Where D: diffusion coefficient of solute.

δ : Thickness of diffusion layer.

It should be noted that rapid cooling results in smaller crystals whereas a slow cooling rate gives more chance for crystal growth and therefore larger crystals are obtained.

2. Surface energy theory

In this case, a growing crystal is compared to an isolated liquid droplet in which case the droplet would assume the minimum surface area resulting in minimum surface free energy, which is favoured thermodynamically.

This would mean that the final shape a crystal ends up having depends on the surface areas and hence surface free energies of individual faces. This theory means that during crystal growth the face with larger surface area would grow at faster rate than other faces having smaller surface areas and hence smaller surface free energies. Eventually the smaller, faster-growing faces will be eliminated.

The handicap of such theories is that they fail to relate solution movement and supersaturation to the rate of crystal growth.

3. Adsorption-layer theory

This theory was first suggested by Volmer in 1939 (Mullin, 1997). The theory explains crystal growth as a discontinuous process in which adsorption on the surface of the crystal takes place layer by layer.

In this case, ions, atoms or molecules of the crystallizing substance in solution migrate to the surface of an existing crystal and diffuse on the surface. Later, they connect to the surface of the crystal at a position where attractive forces are the highest. This type of growth will continue step by step until the whole face of the crystal is completed. Once one layer is completed, another layer will be formed in the same manner. A centre for crystallization or a so-called active site must be formed on the face of the crystal for this layer-by-layer deposition to continue.

1.1.2 Polymorphism

The presence of the same chemical entity in different crystal habits or crystalline forms is termed as polymorphism. One of the polymorphs will be the most stable one, this usually has a higher melting point and a lower solubility that may in turn lead to lower bioavailability. These properties are due to higher structural density caused by a closer and more stable packing of ions, atoms or molecules in the most stable polymorph. Eventually and given a sufficient period of time, the other less stable polymorphs (metastable polymorphs) will convert to the most stable form at different rates depending on free energy difference between the metastable and the

stable forms. It is well known that the most stable form is the one with the lowest free energy and the lowest entropy levels. It has to be mentioned that the formation of a certain form is favoured if it has higher entropy and lower free energy levels (Florence and Attwood, 1998).

Presence of different polymorphs can be triggered by one of the following:

1. Change in the crystallization conditions such as:

- a. Type of solvent used for crystallization purposes: A certain solvent may favour the formation of a certain polymorph over the other. This depends on types of interactions between solute and solvent.
- b. Change in temperature at which crystallization is performed.
- c. Change in cooling rate.

2. Milling

3. Granulation

4. Drying

Polymorphism is a phenomenon demonstrated by compounds that are able to crystallize in more than one crystal structure. Due to the different crystal packing arrangements, polymorphs display different chemical and physical properties such as melting point, solubility, enthalpy of fusion, density, X-ray diffraction patterns and refractive index (Rustichelli et al, 2000). Some of these differences can be quite serious. If for example the polymorph suffers from low solubility or stability, this can have serious biopharmaceutical implications affecting bioavailability or activity.

In three-dimensional crystalline structure, there are seven possible crystal systems resulting in seven independent different unit cell shapes (Florence and Attwood, 1998; West, 1997). These are: cubic, tetragonal, orthorhombic, hexagonal, trigonal, monoclinic, and triclinic (Figure 1.2). A cubic unit cell exhibits the ultimate and maximum symmetry (Florence and Attwood, 1998).

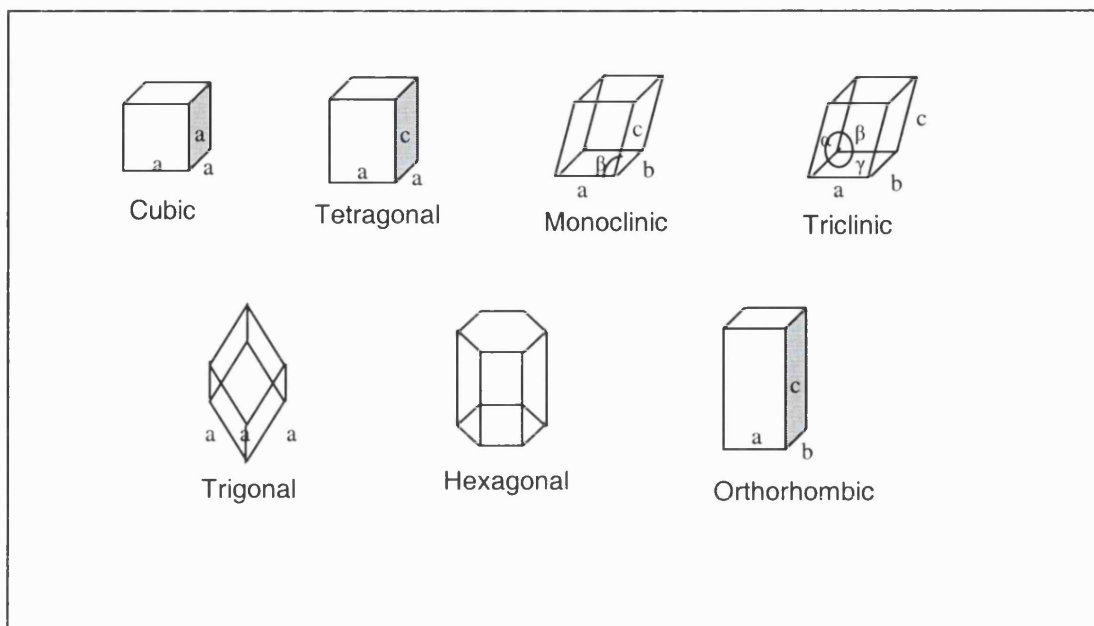


Figure 1.2 The seven possible primitive unit cells in crystals (Florence and Attwood, 1998).

1.1.3 Solvates and hydrates

Sometimes referred to as pseudopolymorphism, a solvate is formed when the solvent of crystallization gets trapped in the crystalline lattice. When the solvent is water it is called a hydrate. Anhydrous forms on the other hand reflect the absence of such water trapped in the crystalline structure. The investigation of the presence of solvates or hydrates is not by any means less important than investigating the presence of different polymorphic forms.

It has been noted that solvates exhibit different solubilities and melting points when compared with the non-solvated compound in which case solvates tend to be more soluble in water than the non-solvates.

On the other hand, hydrates tend to have lower water solubilities than the anhydrous forms. This can be attributed to the fact that when a hydrate was formed interaction with water took place during crystallization releasing some energy. Consequently less energy was left to enhance the interaction with water later on in order to solubilize the

drug and as a result the anhydrous form exhibited higher water solubility than the hydrated form (Florence and Attwood, 1998).

1.2 Amorphous materials

Amorphous solid, as the name suggests (a=without, morphe=shape), is a solid material which is randomly arranged, and lacks the presence of long range three dimensional molecular order, although it may have short range molecular order. Amorphous solids exist in many industrially important products, such as polymers and pharmaceuticals. Currently, interest in this area has been augmented by two developments: an increasing attention in the study of pharmaceutical solids especially polymorphs and solvates (Trelfall, 1995; Yu et al., 1998) and a revived interest in the glasses and in the phenomenon of glass transition (Angell, 1995; Ediger et al., 1996).

1.2.1 Glass transition temperature (T_g)

Glass transition temperature, T_g, is a point at which an amorphous substance changes from the glassy state to the rubbery state or vice versa. When an amorphous solid is cooled below its glass transition temperature (T_g), it will be in its glassy state. At this state, the molecules are held in an unstable kinetically frozen state, i.e. rigidly and randomly fixed in place with short-range molecular motion. Amorphous materials in this state are high viscosity undercooled liquids ($\eta > 10^{12}$ Pa s). Glassy materials are vitreous, hard, brittle and transparent. If an amorphous solid is heated above T_g, the material converts from the glassy state to the rubbery state. The molecules gain energy and therefore the molecular motion is increased. At this stage, the material has enough energy to revert to the crystalline form.

Many amorphous materials have a glass transition temperature above room temperature. For example, indomethacin, with an onset T_g of 40 °C (Matsumoto and Zografi, 1999). As the temperature increases above T_g, the molecular mobility increases with a decrease in viscosity. It is known that water can cause a lowering of the T_g of materials. Apart from water, there are many other compounds, which act as plasticizers, for example, glycerol and liquid paraffin (Andronis and Zografi, 1998).

1.2.2 Physico-chemical properties

Amorphous solids have higher molecular mobility and energy than the crystal form. These properties render the amorphous systems with higher apparent solubility and dissolution rate, hence possibly an enhanced bioavailability compared to the crystalline form. Usually, drugs, in solid dosage forms, are used in their crystalline state. As the amorphous state can improve drug dissolution behaviour (Gil et al, 1994), its use has attracted interest in the preparation of solid dosage forms (Yonemochi et al, 1997). However, this is very difficult to achieve and maintain the stability of the amorphous state because this system is thermodynamically unstable. It has the tendency to undergo solid-state transformation to lower energy, and more stable, crystalline form upon storage. For this reason, the amorphous state of the drugs needs to be maintained throughout their shelf-life. It is therefore important to study how to form and stabilise the amorphous state and the way that this preparation can affect drug dissolution.

1.3 Techniques for preparing amorphous solid materials

Different pharmaceutical processing techniques can lead to an induction of an amorphous moiety in a crystalline solid materials. These processes include super cooling of a melt (such as quench cooling), grinding, solid dispersion (melting or solvent method), rapid precipitation by antisolvent addition, freeze-drying and spray-drying.

Egawa et al (1992) reported that amorphous cefalexin could be prepared by lyophilization. Grinding could decrease % crystallinity. The longer the grinding time, the lower the % crystallinity. However, grinding could not produce a totally amorphous cefalexin. According to Yonemochi et al (1997), amorphous ursodeoxy cholic acid obtained by grinding and quenching methods, had a more rapid dissolution rate than that of the crystalline form.

Another way of turning crystalline materials into the amorphous state is by co-grinding them with microcrystalline cellulose (Nakai et al, 1978a; 1978b). It has been shown that the resulting ground mixtures have various properties, such as rapid dissolution and disappearance of melting endotherms on the thermograms (Nakai et

al, 1978b). These results were explained by the concept that the ground mixture was an “entropy frozen solution”, i.e. dissolving in cellulose without limited molecular mobility, thus limiting crystallisation.

The physicochemical properties of drugs can be modified by co-precipitation with hydrophilic polymers. Co-precipitation, or solid dispersion, is widely employed for enhancing the dissolution rate of poorly water-soluble drugs. Polyvinylpyrrolidone (PVP) and polyethylene glycol (PEG) are commonly used hydrophilic polymers. The enhanced dissolution rate of the drug-polymer complex is due to the formation of thermodynamically unstable amorphous drug phase and/or the molecular dispersion of the drug (Banakar, 1992).

Doherty and York (1987) prepared frusemide-PVP solid dispersions. The amount of PVP used in the preparation of solid dispersions played an important role in controlling the degree of crystallinity of the products. At PVP concentrations above 60%w/w, the product was in the amorphous form, whereas at concentrations below 10%, the product was in the crystalline form. It was found that solid dispersions had higher dissolution rates than the corresponding physical mixtures and unprocessed frusemide. The improved dissolution rate of solid dispersions could be attributed to the solubilizing effect of PVP and the amorphous drug phase.

Ochoa Machiste et al. (1995) improved the dissolution rate of poorly water-soluble carbamazepine using cross-linked polyvinylpyrrolidone (Polyplasdone XL-10). The drug-polymer mixtures were prepared by mixing, milling and solvent evaporation techniques. It was found that the dissolution rates of carbamazepine were significantly enhanced compared to that of the pure drug. The mixing and milling techniques were noted to be more effective in enhancing the dissolution rate than the solvent evaporation method.

1.3.1 Spray drying

To change the physical state of poorly water soluble drugs and thus to enhance their dissolution and potentially improve their bioavailability, the material can be co-spray dried with polymers and other glass forming solids (Corrigan et al, 1985; Bootsma et

al, 1989; Giunchedi and Conte, 1995). Yamaguchi et al. (1992) documented that the amorphous 16-membered macrolide compound, prepared by different conditions of spray drying, exhibited different dissolution rates. In addition, it was shown that the greatest physicochemical stability was achieved when the amorphous powders were prepared at temperatures between the recrystallization temperature (T_c) and the glass transition temperature (T_g). Corrigan and Timoney (1975) investigated the dissolution rates of hydroflumethiazide-PVP co-precipitates and the crystalline drug. Co-precipitates containing more than 40% PVP were found to be amorphous. The apparent solubility of the co-precipitates was found to be four times higher than that of the crystalline drug. Corrigan and Holohan (1984) produced amorphous hydroflumethiazide-PVP using a spray-drying technique. The apparent solubility of the complex increased as the PVP content increased. The complex also exhibited higher dissolution rates than those of the physical mixtures.

1.3.1.1 Spray-drying process

Spray drying is a process by which solution, suspension, emulsion, dispersion, slurry or paste is converted into a dry particulate system. It is not only a drying process but also has a dramatic effect on the product. Particularly in the pharmaceutical industry, it has been employed successfully to alter physicochemical properties to improve formulation, in as much as to transform crystalline material to an amorphous state, and to improve the compressibility of a powder for tableting. There are four sequential steps: atomisation, spray-gas contact, drying of the sprayed droplets and separation of dried sample from air. These steps are commented on as follows:-

Atomisation

Atomisation occurs in the atomiser in order to produce fine droplets of equal size. The fine droplets are immediately in contact with the gas from outside of the atomiser. Subsequently, this dried product is separated from the air stream in a cyclone and finally collected from the collecting vessel. Atomisation provides a feed which has a high surface area to mass ratio, creating the ideal evaporating conditions. As a result, a product with certain characteristics such as density, shape and particle size distribution could be obtained. There are many variables to be optimised during the process prior to producing the desired product.

There are three different atomization systems, which are classified by the nozzle design-rotary atomization, pressure atomization and pneumatic (two-fluid) atomization. A Buchi190 mini spray dryer (Buchi Laboratories-Technik AG, Flawil, Switzerland) composed of pneumatic atomisation was shown in Figure 1.3.

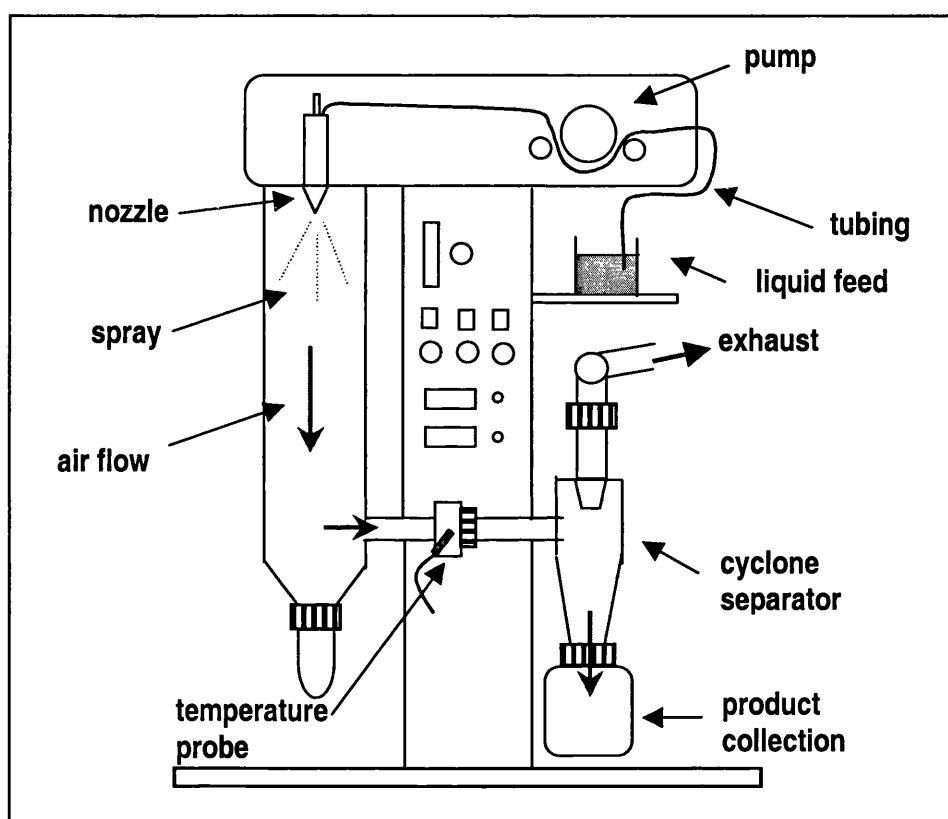


Figure1.3 Diagram of the Buchi 190 Mini spray dryer (adapted from Hill, 1999).

Spray-gas contact

Spray dryers are designed to perform in one of three manners in the spray-gas contact stage. Firstly, a co-current manner; the spray and the hot drying air enter the drying chamber in the same direction. Secondly, a counter-current manner; the spray and drying air pass through the chamber at opposite ends. Thirdly, a combined co-/counter-current manner; the product is sprayed upwards and remains in the hot zone

then it immediately drops down into the cool zone by gravitational force. The Buchi mini spray dryer used throughout the research operates in a co-current manner.

Drying of the sprayed droplets

The removal of solvents from the spray occurs at the drying stage. Heat and mass transfer between atomised droplets and drying air are simultaneous. In general, the evaporation process during spray drying can be divided into four stages (Figure 1.4). The first stage (a) occurs when the droplet immediately comes into contact with air evaporation of the solvent. The temperature of the droplet surface increases until equilibrium occurs between the droplet surface and the air. The second stage (b) is the stage of constant evaporation. The moisture of the droplet migrates from inside to outside prior to maintaining saturation at the surface and until a critical point is reached. This critical point indicates that the moisture within the droplet can no longer maintain surface saturation. The drying rate then dramatically falls at the third stage (c), accompanied by a droplet temperature increase. This stage depends on the air temperature and the liquid inside the droplet. If the boiling point of liquid inside the droplet is lower than the air temperature, the liquid vaporises. The pressure within the droplet increases, when the solid phase forms a crust around the surface. If the crust is porous, then the vapour will escape, otherwise the powder will break. The shape of the final products is determined by the type of crust formed. Figure 1.5 shows the types of product that occur during spray drying. In the last stage (d), when the droplet becomes absolutely dry, the evaporation rate continues to slowly decrease since the droplet surface provides resistance to drying. Eventually, there is an equilibrium of moisture content between the droplet and the surrounding air. However, the product is usually collected before equilibrium.

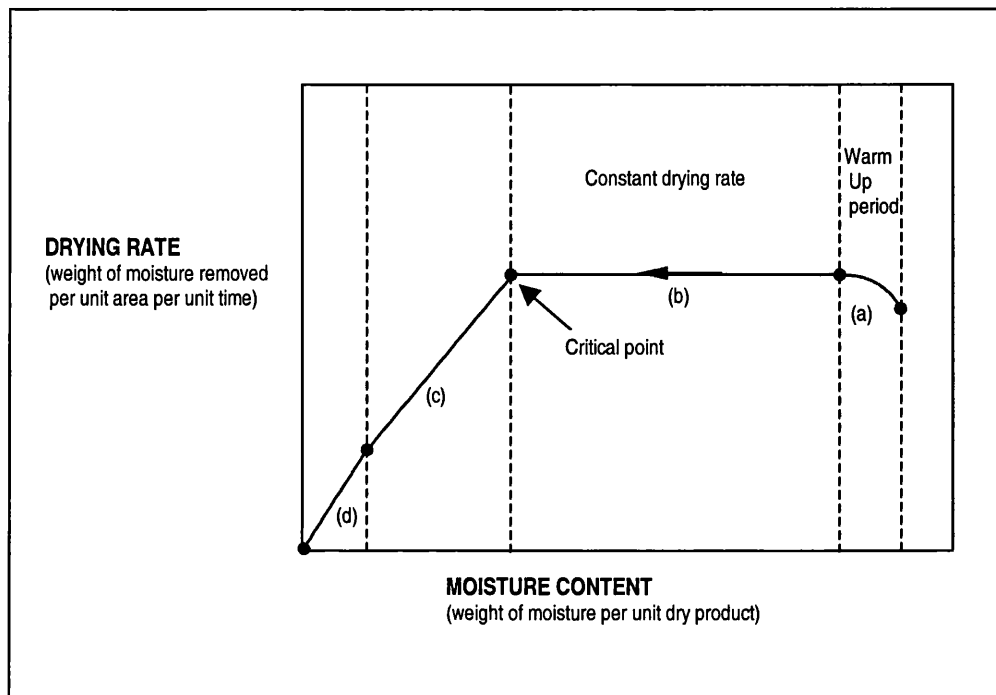


Figure1.4 A drying graph depicting the relationships between drying rate and moisture content. Data adapted from Masters (1990).

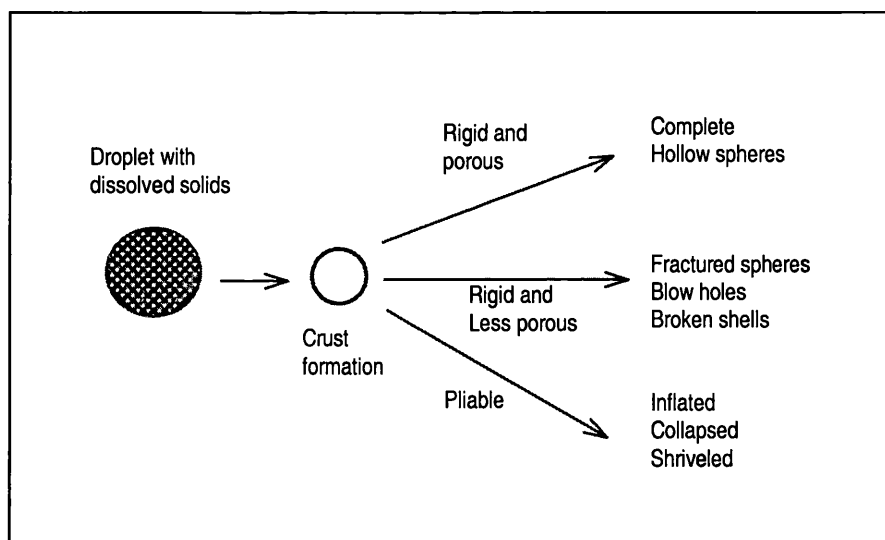


Figure1.5. Diagram of the particle features along the drying stage of spray drying (taken from Oakley ,1997).

Separation of dried sample from air

The last stage of the spray-drying process is product recovery, namely, the separation of the product from the air stream. The product can be separated from the air by cyclonic air flow which occurs in the cyclone separator. Many dryers also allow for product collection at the base of the drying chamber. In the Buchi mini spray dryer, the product can be collected from a collecting vessel only.

1.3.1.2 Effect of spray-drying experimental parameters on the product

The various settings on the spray-drying device are important in identifying the powder properties. There are many variables to be controlled throughout the process. These variables are the inlet and outlet temperatures, the aspirator speed, the spray flow rate, the feed rate and feed concentration. However, all the parameters are interdependent as adjusting one parameter can affect other parameters.

Inlet temperature

The inlet temperature is the temperature of the heated drying air, which is drawn in over a heater by an aspirator motor. The impact of inlet temperature on particle size depends on the materials being dried (Crosby and Marshall, 1958). It was noted that the temperature had little effect on mean particle size of crystalline sodium sulfate, whereas the mean particle size of coffee extract was significantly decreased as the inlet temperature increased. Conversely, the particle size of certain substances was shown to increase by increasing the inlet air temperature (Newton 1966, through Broadhead et al, 1992).

Outlet temperature

The outlet temperature is the temperature of the air of the particulate products before entering the cyclone. This temperature is not necessarily the product temperature because the vaporization of the water removes heat from the product. However, if this temperature is too high, the heat sensitive substances can be degraded. Increasing outlet temperature causes lower final moisture content. Hence, the bulk density also decreases.

Aspirator speed

The aspirator speed setting has influence on the drying performance of the instrument. High aspirator speed results in a higher degree of separation in the cyclone. However, if the particle size of products is too small, particles may be lost in the air stream exhaust.

Spray flow rate

The spray flow rate is different from the aspirator speed. The spray flow rate is the amount of compressed air from the main spray dryer, which is required to convert the liquid into fine droplets. The higher the spray flow rate, the smaller the particle size of the final product.

Feed rate

An increase in feed rate while holding the inlet temperature and aspirator flow rate at constant, results in an increase in the final moisture content of the spray-dried products. For this reason, the bulk density also increases (Masters, 1990).

Feed concentration

Spray drying of high concentration preparations of hydrophilic substances usually results in powder with a low bulk density. On the other hand, spray drying of high concentration of non-hydrophilic materials leads to an increase in bulk density. In addition, the feed concentration influences the particle size. The more concentrated feed mixtures usually produce larger and more porous particles. It is important to understand how all the variables interact, and to know how to modify and optimize both process and formulation variables in order to manufacture products with the most suitable characteristics.

1.3.2. Supercritical fluid technology

In the pharmaceutical industry, conventional processing of drugs involves extensive use of organic solvents as either reaction media in synthesis of drugs, or as so-called “antisolvents” for recrystallising drugs. During the last decade, replacement of traditional organic solvents with “environmentally benign” solvents, known as supercritical fluids (SCFs), in pharmaceutical processing is receiving increased attention. More recently, this technology has been commercialised. One such company using this technology is Bradford Particle Design (BPD), which was established in 1994 by University of Bradford, UK.

1.3.2.1 Supercritical fluids

A substance is termed supercritical when its pressure and temperature is greater than its critical pressure (P_c) and critical temperature (T_c), respectively. Near the critical point ($1-1.2T_c$), the density, transport properties (such as viscosity and diffusivity), and other physical properties (such as solvent strength and dielectric constant) can be varied from gas-like to liquid-like with relatively small changes around the critical pressure ($0.2-0.9 P_c$) (Subramaniam et al, 1997a). Thus, it is possible to realize unique fluid properties to suit various processing needs. In other words, small changes in the temperature or pressure near the critical point result in large changes in the fluid's density and, hence, its solubilizing power. The supercritical state of a material is shown in the pressure-temperature (P-T) diagram in Figure 1.6, and exists above a certain pressure and temperature for any substance.

A comparison of the physical properties of supercritical fluid (SCF) with those of liquid and gas is shown in Table 1.1. Supercritical carbon dioxide (sc- CO_2) has been found to have particular use as an environmentally acceptable ‘solvent’ alternative compared to some conventional hydrocarbon solvents. For this reason, the area of supercritical fluids is also better known as “Clean Technology”.

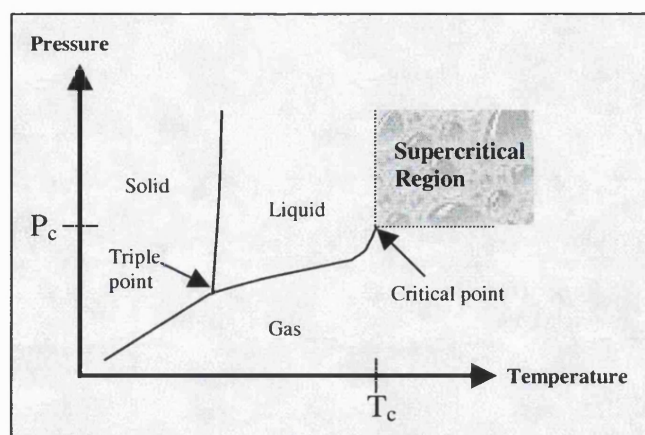


Figure 1.6 Pressure-Temperature diagram for a pure substance (McCabe et al, 1993).

Table 1.1 Physical properties of gases, supercritical fluids and liquids (Raynie, 1997).

	Density (g/cm ³)	Diffusivity (cm ² /s)	Viscosity (cp)	Surface Tension (mN m ⁻¹)
Gas	$(0.6-2) \times 10^{-3}$	0.1-0.4	0.01-0.03	0
SCF	0.2-1.0	$(2-7) \times 10^{-4}$	0.01-0.09	0
Liquid	0.6-1.6	$(0.2-2) \times 10^{-5}$	0.2-3.0	30-60

Table 1.2 lists some common supercritical fluids and their critical temperatures and pressures (Mchugh and Krukoni, 1986). For pharmaceutical applications, carbon dioxide is an ideal processing medium. The critical parameters of carbon dioxide (critical pressure $P_c = 73.8$ bar, critical temperature $T_c = 31.1$ °C) are both relatively low values for T and P compared to many other potentially useful supercritical fluids. Carbon dioxide is also non-toxic, relatively inert, non-flammable and recyclable.

Supercritical carbon dioxide is a relatively nonpolar solvent. A common rule of thumb is that if a substance dissolves in n-hexane, then that substance may also dissolve in supercritical carbon dioxide. While this rule is valid for many low molecular mass substances that have appreciable vapour pressures, it fails in the case of many polymers, which have negligible vapour pressures. sc-CO₂ has been employed both as a solvent and as an antisolvent in pharmaceutical applications (Subramaniam et al,

1997a). The ability to precisely and rapidly vary the solvent strength and thereby the rate of supersaturation and nucleation of dissolved compounds, is a unique aspect of supercritical fluids for particle formation.

Table 1.2 Critical data for some supercritical solvents

Solvents	Critical temperature	Critical pressure
	T _c (°C)	P _c (atm)
Ethylene	9.3	730.0
Carbon dioxide	31.1	72.8
Ethane	32.3	709.0
Nitrous oxide	36.5	1050.0
Propylene	91.9	45.6
Propane	96.7	41.9
Trichlorofluoromethane	198.1	43.5
Ammonia	132.5	111.3
Cyclohexane	280.3	40.2
Isopropanol	235.2	47.0
Benzene	289.0	48.3
Toluene	318.6	40.6
Water	374.2	217.6

1.3.2.2 Precipitation using supercritical carbon dioxide

Conventional processes for producing small drug particles include ball milling, recrystallization of drug particles from solution using organic antisolvents, freeze-drying and spray-drying from organic solvents and aqueous solutions. These methods can require excessive solvent use and a need for solvent disposal. Also thermal and chemical degradation of products can occur or sometimes solvent residues will remain in the drugs. Particle size control is also sometimes inconsistent. For this reason, the production of contaminant-free microparticles with controlled particle size is a major challenge. Any desirable method should provide those features identified for an ideal particle formation process (Figure 1.7) (York, 1999). Various particle-formation techniques have been developed that can take advantages of the properties of supercritical fluids. These techniques can be divided into three main topics: (i)

precipitation using sc-CO₂ as a solvent; (ii) precipitation from gas saturated solutions; and (iii) precipitation from saturated solutions using sc-CO₂ as a non-solvent or antisolvent. The subject of particle design using supercritical fluids has been reviewed previously (Subramaniam et al, 1997a; York, 1999; Reverchon and Perrut, 2000; Jung and Perrut, 2001), thus a short summary is given here.

Figure 1. 7 Requirements of an ideal particle formation process for pharmaceutical products (taken from York, 1999).

- Operates with relatively small quantities of organic solvent(s)
- Molecular control of process
- Single step, scalable process for solvent-free final product
- Ability to control desired particle properties
- Suitable for wide range of chemical types of therapeutic agents and formulation excipients
- Capability for preparing multi-component systems
- GMP compliant process

Rapid Expansion of Supercritical Solution

This process of particle formation has been called Rapid Expansion of Supercritical Solution (RESS) (Matson et al, 1987), consisting of dissolving a solute in a supercritical fluid, then depressurising this solution through a heated nozzle or capillary into a low pressure precipitator in order to cause a rapid nucleation of the substrate in the form of contaminant-free microparticles or fibers or films that are collected from gaseous stream. A process schematic of RESS is depicted in Figure 1.8.

Liquid carbon dioxide from a cylinder is pumped to the desired pressure and preheated to the extraction temperature through a heat exchanger. The supercritical fluid is then percolated through the extractor filled with one or more substrates. The supercritical solution is expanded in the precipitator, through a preheated nozzle to avoid blocking by substrate precipitation. The morphology of the resulting product depends on several factors such as the material structure (crystalline or amorphous,

composite or pure) on the RESS parameters (temperature/pressure) in the precipitator, distance of impact of the jet against the surface, dimensions of the expansion device, nozzle geometry and the RESS time scale (dictated by the expansion trajectory from the preheater and the expansion device) (York, 1999; Phillips and Stella, 1993; Reverchon et al, 1993).

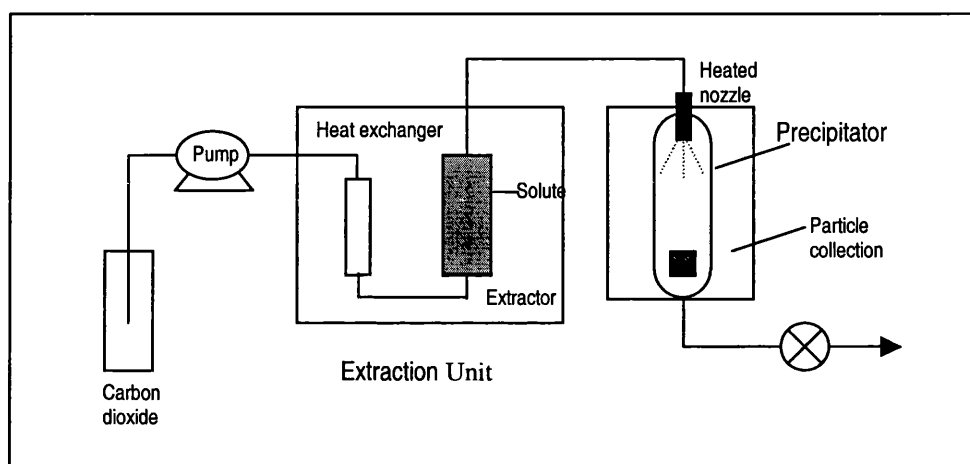


Figure 1.8 RESS equipment

The relationship between process parameters and the resulting particle size has been reported previously (Shaube et al, 1995; Reverchon and Pallado, 1996; Reverchon, 1999; Tom and Debenedetti, 1991; Lele and Shine 1994). Various types of materials have been processed by the RESS method, including organics, inorganics, ceramics and polymers, and also coprecipitation of polymer/drug systems. The particle dimensions obtained using RESS generally range from 0.5 to a few hundred microns (Reverchon, 1999; Reverchon and Perrut, 2000). Although in a few cases, particles smaller than 0.1 micron have been produced by this single-step process (Matson et al, 1987).

As sc-CO₂ is nonpolar, those solutes that are also non-polar can be expected to dissolve in sc-CO₂ and thus are suitable candidates for RESS method. Examples of pharmaceutical drug compounds soluble in scCO₂ include lovastatin (Larson and King, 1986), stigmasterol (Ohgaki et al, 1990), salicylic acid and theophylline (Subra

and Debenedetti, 1996). Expansion of such solutions to pressure conditions above ambient temperature, and thereby at lower levels of supersaturation, can result in agglomeration of particles. Whereas, increased supersaturation during expansion leads to rapid nucleation rates and micron- and submicron-sized particles.

The RESS process is a suitable technique for size reduction. Due to the high degree of supersaturation and rapid expansion characteristics of the RESS process, small particles with a uniform distribution can be obtained. Various pharmaceutical compounds such as ibuprofen (Charoenchaitrakool et al, 2000), griseofulvin (Martin et al, 2000; Reverchon, 1995), progesterone (Alessi et al, 1996) have been successfully micronised with the RESS technique. Using ibuprofen as an example, Charoenchaitrakool et al (2000) showed that the median particle size of the product was less than 2.5 μm , compared to the original material, which has highly non-uniform particle size distribution, with a median particle size of 42 μm . It was reported that the enthalpy of fusion obtained from DSC analysis and the intensity of the XRD peaks of the processed ibuprofen were slightly lower compared with the original material. These results indicated a reduction in the degree of crystallinity of ibuprofen after processing with RESS. Additionally, it was also demonstrated that ibuprofen after RESS processing has a powder dissolution rate of five times greater than that of the original material. The enhanced dissolution rate of ibuprofen was due to the reduction in both the particle size and the degree of crystallinity.

Martin et al (2000) studied the RESS processing of poorly soluble griseofulvin. Using trifluoromethane as a cosolvent, nano size griseofulvin particles were produced. However, the processed-griseofulvin was agglomerated, forming a spongy-like structure. The genuine particle size was approximately 200 nm. From DSC data, it was reported that the melting point of the RESS produced griseofulvin was lower than that of the crystalline product, which meant a reduction of crystallinity. The dissolution rate of the RESS-produced griseofulvin increased 1.6 times compared to the original sample. The increase in dissolution rate of griseofulvin was hence due to both the reduction in particle size and the degree of crystallinity.

Several polymers of pharmaceutical interest have been processed by RESS technique, including biodegradable polymers based on lactic acid (Tom and Debenedetti, 1991;

Debenedetti, 1994) and polyethylene glycol (Weidner et al, 1996). Likewise, particle shape and morphology have been affected for polymer-supercritical fluids systems, depending upon the point of saturation in the processing route. Phase separation at the pre-entry to the orifice and within the orifice results in formation of polymer fibres or elongated particles, respectively.

Tom and Debenedetti (1991) reported that the RESS process is feasible for the production of microspheres and microparticles of biodegradable polymers such as poly (hydroxy acid) polymers. Microparticles and microspheres of poly (L-lactic acid) (L-PLA) (MW 5,500) in the range of 4 to 25 μm were precipitated from CO_2 and CO_2 -acetone mixtures. Irregular-sized particles of poly(D,L-lactic acid) (DL-PLA) (MW 5,300) ranging from 10 to 20 μm were produced. The precipitation of poly(glycolic acid) (PGA) (MW 6,000) from CO_2 produced needle particles of 10-40 μm length and regular shape. The molecular weight of the precipitated polymers was found to be lower than that of the commercial polymers, indicated that RESS is limited to low molecular weight polymers.

Polymers are polydisperse to some degree and their solubility in supercritical fluids is a function of molecular weight, hence the precipitation of polymers by RESS differs from that of single molecular weight compounds. As the extraction begins, the molecular weight distribution of the polymer changes. Low molecular weight polymers with a low glass transition temperature, appeared to be extracted first and precipitated as a liquid or waxy paste (McHugh and Krukons, 1986). Due to the polydispersity of polymers, the ability to maintain consistency and reproducibility of the product characteristics still remains as a challenge in polymer processing by RESS. However, the successful production of polymer microspheres and microparticles is a promising step in developing the RESS process as a novel technique for polymer processing.

The application of RESS can be extended to microencapsulation. This can be simply accomplished by combining the extracted drug and polymer into one stream prior to expansion. The intimate drug/polymer mixture can then be precipitated in one processing step.

The formation of microparticles consisting of lovastatin crystals coated with DL-PLA polymer can be obtained via the RESS process (Tom and Debenedetti, 1992; Tom et al, 1993). A lovastatin concentration > 30% precipitated as a network structure while a low concentration precipitated as microparticles and microspheres. In the first case the network consisted of intertwining polymer fibres with the drug incorporated in the strands. In the latter case the particles consisted of drug needles coated with polymer. The production of polymer coated lovastatin needles suggested that lovastatin precipitated and grew first, and then acted as nucleating sites for the polymer.

Tom et al (1994) also investigated the coprecipitation of L-PLA (MW 10,000) and pyrene by RESS using sc-CO₂-CHClF₂ solutions. Pyrene, a fluorescent compound, was selected as a model solute. The uniformity of pyrene distribution in the polymer matrix was then assessed via fluorescence microscopy. Results from confocal fluorescence microscopy showed a uniform distribution of pyrene microparticles within polymer microspheres, which indicated efficient mixing of the solute and carrier in the RESS process.

Kim and co-workers (1996) also employed the RESS method in preparing coprecipitated naproxen and L-PLA using CO₂. The drug and polymer were premixed and loaded in the same extraction vessel. Mixtures of naproxen and L-PLA were coprecipitated using a 50 µm diameter capillary over a range of extraction pressures from 170 to 200 bar, pre-expansion temperatures of 90-115 C, and extraction temperature of 60 C. The distribution of the fluorescent naproxen within the precipitates was analysed using confocal laser scanning microscopy with fluorescence wand reflected light detection. Composite particles containing microcrystalline naproxen particles at the core, with coated polymer on the surface were observed. However, the drug loading in the composite precipitates was not reported.

As demonstrated in the above studies, microencapsulation by RESS is achievable. However, due to the low solubility of high molecular weight polymers in supercritical fluids, low production rates of microencapsulated products are obtained. Different modified supercritical fluids are required to obtain the enhanced solubility of high molecular weight polymers in supercritical solutions. Preconditioned or synthesized

polymer, which possesses low polydispersity and molecular weight, would be an ideal solute for RESS encapsulation. Microencapsulation by RESS processing also requires further refinement in order to produce a high yield of desirable polymer-drug particles with uniform drug distributions.

Table1.3. Solubility of Pharmaceutical compounds in Supercritical Carbondioxide (adapted from Subramaniam et al, 1997).

Solute	Cosolvent	Solubility*	Temp(°C)	P(bar)
Lovastatin	-	4a	40	345
	5%Methanol	10-45a	40	103-379
Efrotomycin	-	3a	40	345
Imipenem	-	0a	40	345
Lovastatin	-	0.09-3.4a	55	125-409
	-	0.1-6a	75	134-409
Digoxin	-	0.18b	50	241
	7.2 mol%Methanol	0.17b	50	241
Griseofulvin	-	1.5b	50	241
	3.5 mol%CH ₂ Cl ₂	1.4b	50	241
	3.4 mol%Butyl acetate	6.4b	50	241
Aspirin	-	0.12-26b	45	60-228
Salicylic acid	-	14b	45	138-241
Testosterone	-	0.23-5.0b	35	88-242
	-	0.04-7.0b	55	87-242
Progesterone	-	0.99-5.9b	35	105-244
	-	0.11-7.4b	55	109-243
Cholesterol	-	0.61-28b	55	102-276
Salicylic acid	-	10-53b	40	100-350
	-	8.3-67b	60	115-325
Ketoprofen	-	1.3-8.0b	39.4	100-220
	-	0.78-15b	58.4	116-220
Piroxicam	-	0.45-4.3b	39.4	100-220
	-	0.37-3.9b	58.4	130-220
Nimesulide	-	1.9-7.4b	39.4	130-220
	-	0.85-9.8b	58.4	130-220

* a , mass fraction (10⁴); b, mole fraction (10⁵)

Particle formation by the RESS technique offers several elements of the “ideal particle formation technique” (Figure 1.7). This process is attractive because it includes a single-step process with reduced organic solvent requirement and

capability of producing microparticles. Moreover, the gas generated after expansion can be recovered and recycled. Unfortunately, at moderate temperatures and pressures (<60 °C and 300 bar) many pharmaceutical substrates are not soluble enough into the supercritical fluid to lead to a profitable process. As shown in Table 1.3, the solubility of drugs is on the order of 0.01 wt % or less (Subramaniam et al, 1997). Hence, relatively large amounts of carbon dioxide are required for increased product throughput. To solve this problem, co-solvents, such as methanol, may be used to enhance this solubility. However, the solvent elimination step from the resulting powders is neither simple nor cheap. Other challenges with this method are the operational and scale-up issues associated with nozzle design in order to avoid particle agglomeration and freezing caused by the rapid expansion.

Precipitation from Gas Saturated Solutions/Suspensions

A more recent application of supercritical fluids to particle formation is the precipitation from gas saturated solutions/suspension (PGSS), which was developed in 1994 by Weidner et al.

Since the solubility of compressed gases in liquids and some polymers is normally high and larger than the solubility of such liquids and solids in the compressed gas phase, the process consists of the solubilisation of sc-CO₂ in melted or liquid suspended substances, leading to a so-called gas-saturated solution/suspension that is then rapidly expanded in an expansion unit. The gas evaporates and the solution is cooled down below the solidification temperature of the solute and solid particles are formed. The basic scheme of experimental equipment is shown on Figure 1.9.

This process can produce small particles from a variety of substances (inorganic powders, polymers, waxes, fat derivatives, natural products and pharmaceutical compounds) that need not be soluble in sc-CO₂, especially with polymers that absorb a high concentration (10-40 wt%) of CO₂ that either swells the polymer or melts it at a temperature much below its glass transition temperature (Jung and Perrut, 2001).

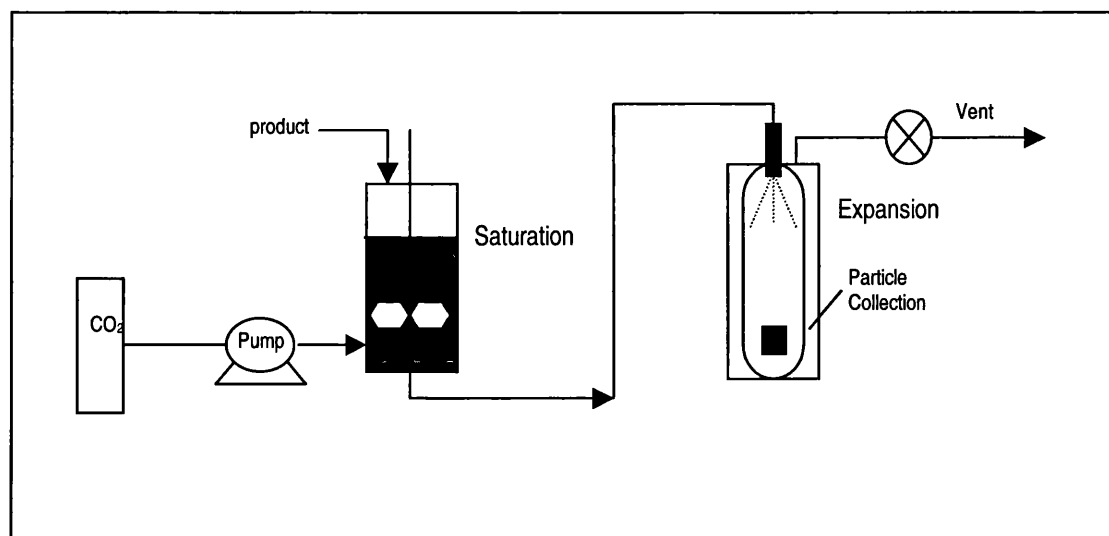


Figure 1.9 Particle from Gas Saturated Solutions (PGSS) equipment

With this method, even though the polymer is insoluble, sc-CO₂ causes it to swell. The higher the pressure, the greater the swelling. In this case the T_g of the polymer is decreased in the presence of CO₂, which makes it possible to incorporate the softened polymer with the insoluble additives added to the vessel. The polymer forms what is, in effect, “supercritical foam” with the insoluble additives within the polymer phase rather than the sc-CO₂ phase. Finally, the mixture is expanded through the nozzle and the foam breaks up into a fine powder. This process can also be used with suspensions of active substance(s) in polymers or other carrier substances leading to production of composite microspheres. The particle size and size distribution of product can be tailored to specific requirements by adjusting process parameters such as temperature, nozzle size and shape, and the amount of dense gas dissolved.

Moreover, it is possible to form microparticles when a suspension of active drug is mixed in a substrate into a carrier that is swollen with sc-CO₂ and then atomised. Shine and Gelb (1997) patented a process called “Polymer Liquifaction using Supercritical Solvation” (PLUSS). The advantage of this method is that the carrier (for instance, polymer) and the active substrate (drug), which are both insoluble in the supercritical fluid, can be employed. The mixture of the substrate and the polymer is mixed with a supercritical fluid capable of swelling the polymer. The pressure is then

rapidly released, resulting in the solidification of the polymer around the core material to form microcapsules.

Sencar-Bozic et al. (1997) prepared solid dispersions of the poorly water soluble calcium antagonist nifedipine and polyethylene glycol (PEG) 4000 using Particles from Gas Saturated Solution Process (PGSS). In the PGSS process, a sc-CO₂ is dissolved under pressure in a mixture of nifedipine and PEG to be micronized. Upon expansion of the gas saturated solution, nifedipine and PEG 4000 were coprecipitated as microparticles. The DSC profiles of nifedipine/PEG 4000 mixtures showed only a melting peak of PEG 4000. It implied that nifedipine dissolved in the PEG 4000 melt. The dissolution rate of nifedipine was enhanced significantly compared to that of the physical mixtures and unprocessed nifedipine. The enhanced dissolution rate of solid dispersions could be due to particle size reduction, interactions between the drug and PEG 4000 and the solubilization effect of the hydrophilic polymer.

Kerc et al (1999) also investigated the micronisation of nifedipine, felodipine and fenofibrate by PGSS process using sc-CO₂. It was shown that the mean particle size of micronized nifedipine and that of felodipine depended on the pre-expansion conditions. On the other hand, the particle size of processed fenofibrate increased due to agglomeration. In the DSC profiles of felodipine/ PEG 4000 mixtures, only a melting peak of PEG 4000 existed. Coprecipitated nifedipine/PEG 4000 and felodipine/PEG 4000 had enhanced dissolution rates. While, the dissolution profile of coprecipitated fenofibrate/PEG 4000 did not differ significantly from the dissolution profile of fenofibrate, its physical mixture. The mechanism of the rapid dissolution rate of felodipine/PEG 4000 coprecipitate via PGSS could be explained by a combination of three factors including particle size reduction, interactions between the drug and PEG 4000 and the solubilization effect of the hydrophilic carrier. In addition, decrease in % crystallinity or presence of amorphous mixture could have also contributed to the enhanced dissolution rate.

With the PGSS process, micronized drug or micronized drug/carrier can be obtained in one step without organic solvent. However, the development of the PGSS process is hindered because of the lack of data for phase behaviour of solute-dense gas

systems. In addition, there are two major limitations for this process, the problem of nozzle clogging and the relatively high operating temperatures involved. As a result, the stability issues of solute in molten form prohibit the use of this method for thermally labile pharmaceuticals and biological substrates.

Precipitation Using sc-CO₂ as an Antisolvent

Organic liquid antisolvent processes are extensively used in the pharmaceutical industry for drug precipitation. The basic concept is the use of two liquid solvents that are completely miscible. However, the drug is soluble in the first solvent, but it is insoluble in the second solvent. As a result, the addition of the antisolvent to a solution induces supersaturation and precipitation of the solute.

Supercritical fluid antisolvent processes have been recently proposed as alternatives to liquid antisolvent processes. When sc-CO₂ is used as an antisolvent, the solute of interest (usually a drug, polymer or both) is dissolved in a conventional solvent to form a solution. The preferred ternary phase behaviour is such that the solute is insoluble (or weakly soluble) in compressed carbon dioxide whereas the solvent is miscible with compressed carbon dioxide at the recrystallisation temperature and pressure.

There are some advantages. It is possible to completely remove the antisolvent by a pressure reduction to the gas phase. Nevertheless, this step is problematic for liquid antisolvents that require post-processing treatments for the complete elimination of liquid residues. Moreover, the supercritical fluid antisolvent can diffuse very fast into the liquid solvent. Therefore, It can produce the supersaturation of the solute and immediately precipitates the micronised particles in an effective fast single step. The narrow particle size distributions are also possible with these technologies.

Supercritical antisolvent micronisation has been performed using different process arrangements. To indicate the micronization process, different acronyms were also employed by the various authors. The process has been referred to as PCA (Precipitation by Compressed Antisolvent) (Dixon et al, 1993; Bodmeier et al, 1995), GAS (Gas Antisolvent) (Gallagher-Wetmore et al, 1994; Yeo et al, 1993; Randolph et

al, 1993), ASES (Aerosol Solvent Extraction System) (Bleich et al, 1993), SEDS (Solution Enhanced Dispersion by Supercritical Fluids) (Hanna and York, 1994; Palakodaty et al, 1998) and SAS (Supercritical Antisolvent) processes (Reverchon et al, 1993; Winters et al, 1996). A short description of the various techniques is presented as follows.

Batch operation techniques

Batch techniques are essentially 'one pot' methods that usually involve injection of an antisolvent into a reactor to bring about precipitation. This process has been called gas antisolvent (GAS) or supercritical anti-solvent (SAS) recrystallization. A batch of solution is expanded several folds by mixing with a dense gas in a vessel. Due to the dissolution of the solvent and compressed gas, and low solubility of solute in the compressed gas, the mixture becomes supersaturated and the solute precipitates as microparticles. The rate of supercritical antisolvent addition can be an important parameter in controlling the morphology and the size of the precipitated particles.

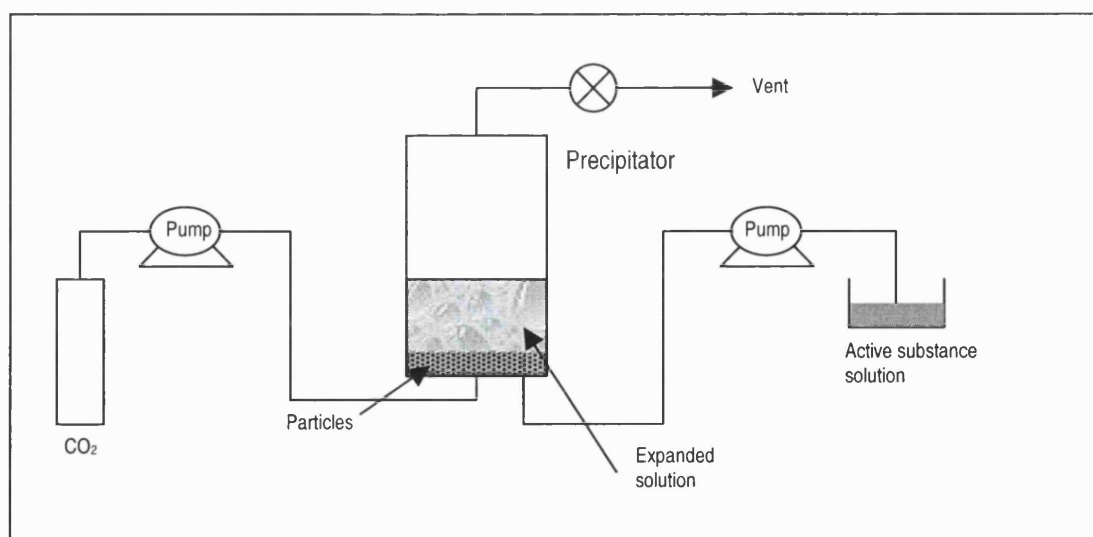


Figure 1.10. Gas antisolvent (GAS) or supercritical antisolvent (SAS) recrystallization equipment.

As depicted on Figure 1.10, the precipitator is partially filled with the solution of active compounds. Carbon dioxide is then pumped up to the desired pressure and introduced into the precipitation vessel. It can be added from the bottom or from the top of the vessel. To achieve a better mixing of the solvent and anti-solvent, Carbon dioxide should be introduced from the bottom of the vessel. After a holding time, the expanded solution is drained under isobaric conditions to wash and clean the precipitated particles. This mode of operation can be termed liquid batch operation.

In an alternative arrangement the precipitation vessel contains the antisolvent and the solution is then injected into it. This mode of operation can be referred to as gas batch operation. The difference between these two operational modes is that in the former case the precipitation occurs in a *liquid rich phase*, in contrast, in the latter case it occurs in a *supercritical fluid rich phase*. Therefore, the result can be very different for the two modes of operation.

It is difficult to analyse the effect of the process parameters on the final characteristics of the products because in both cases the operation performed is not at steady state. Hence, batch operation is not always suitable for industrial production. Factors influencing particle properties when prepared by GAS or SAS process are listed in Figure 1.11.

Figure 1.11. Factors influencing particle properties when prepared by the gas antisolvent or supercritical antisolvent recrystallization. (adapted from York, 1999)

- Solute solubility in organic solvent
- Solute insolubility in supercritical fluid antisolvent
- Degree of expansion of organic solvent in supercritical fluid (liquid batch operation)
- Organic solvent/supercritical antisolvent ratio
- Flow rate of supercritical antisolvent
- Critical parameters (pressure and temperature condition) in reaction vessel
- Phase process path followed during particle nucleation

At the last step of batch precipitation processes, the vessel is usually washed with the antisolvent to remove any residual organic solvent. This step is important for 'clean' production of particles. Indeed, if washing is not performed afterwards, the residue of liquid solvent is released from the supercritical solution mixture during the depressurisation of the apparatus and this may resolubilise some of the solutes.

Semicontinuous operation techniques

Semicontinuous techniques differ from batch techniques in that particles are produced under approximately steady-state conditions into a precipitation vessel. The liquid solution and the supercritical antisolvent are both delivered into the precipitator in co-current or counter-current fashion. The dissolution of the supercritical fluid into the liquid droplets is accompanied by a large volume expansion. As a result, a reduction in the liquid solvent power causes a sharp rise in the supersaturation within the liquid mixture and the consequent formation of small and uniform particles. In this method, the flow rates and the ratio between the solution and the supercritical antisolvent can all be controlled independently and are important for controlling the precipitation process. Pressure and temperature are also relevant process parameters. This process has been termed as Precipitation with Compressed Antisolvents (PCA) (Dixon et al, 1993) and employs either liquid or supercritical carbon dioxide as antisolvent. When using a supercritical antisolvent, the spray process has also been termed Aerosol Solvent Extraction System (ASES). A process schematic is shown in Figure 1.12.

The supercritical fluid is pumped to the top of the reaction vessel by a high pressure pump. Once the system reaches steady state (desired pressure and temperature), the solution of active substance is introduced into the vessel through a nozzle. The liquid solution is pumped at a pressure higher (approximately 20 bar) than the vessel operating pressure prior to producing small liquid droplets (Jung and Perrut, 2001). Precipitation happens when the non-aqueous drug solution mixes with sc-CO₂. The organic solvent can then be removed by the sc-CO₂ from the vessel. Particles are collected on a filter at the bottom of the vessel. After formation of sufficient quantity of particles, liquid solution pumping is stopped and pure supercritical fluid continues to flow through the vessel to eliminate the residual solvent from the particles. At the end of the precipitation process, the washing step with supercritical antisolvent is

required to clean the precipitated particles and avoid the condensation of liquid phase otherwise the characteristics of the powder will be changed.

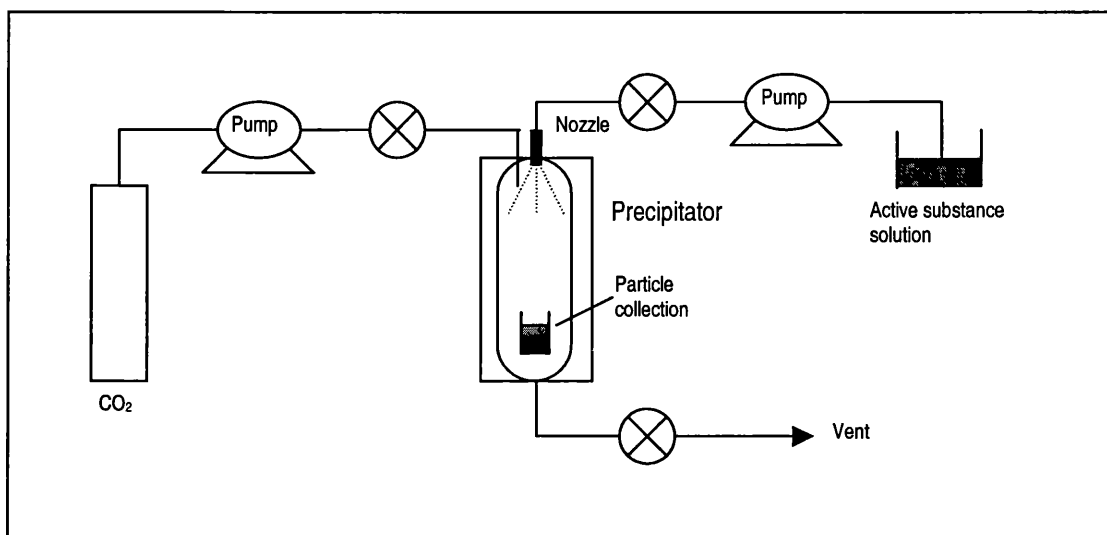


Figure1.12 PCA/ASES equipment.

An important factor in the semi-continuous process is the liquid solution injection device. The injector is designed to produce liquid jet break-up and the formation of small droplets which expand in the vessel. The solute is released from solution when its local concentration exceeds the saturation limit. Different kinds of injectors such as standard capillary nozzles, ultrasonic atomizers, and coaxial nozzles have been employed to spray the active substance solution. Reverchon et al (1998) employed an atomisation method, which involves spraying the solution through a 22 μm diameter stainless steel nozzle in the form of fine droplets into compressed carbon dioxide. Metal-organic nanoparticles reduced to about 100 nm were successfully obtained at very large expansion after subsequent heat treatment of the liquid solution. This process was used to prepare semiconductor particles. Debenedetti et al (1992) and Yeo et al (1993) proposed the adoption of an atomisation nozzle and tested a variety of nozzle diameters ranging from 5 to 50 μm . Other authors employed an atomisation nozzle (Saim et al, 1996; Bleich et al, 1993). Randolph et al (1993) used small internal diameter capillary (75 μm i.d.), or vibrating orifice nozzle (ultrasonic type). This

vibrating apparatus produces a spray by superimposing a high frequency vibration on the liquid jet that exits from an orifice. Submicron size L-PLA microspheres with a narrow size distribution were produced when 0.6 wt% PLA/methylene chloride solution was sprayed into supercritical carbon dioxide *via* both capillary and vibrating nozzles. This led researchers to speculate that interphase mass transfer rates, rather than initial droplet size, control final particle size. Using 100 μm capillary orifices, Bodmeier et al (1995) reported that at higher L-PLA concentrations ($> 4 \text{ wt } \%$) with relatively low flow rates of CO_2 , led to fibre formation instead of microspheres.

Coaxial devices have also been employed in which two capillary tubes continuously deliver the liquid solution and the supercritical antisolvent (York and Hanna, 1996). In this case, the high velocity of the supercritical fluid allows break-up of the solution into very small droplets. Thus, the formation of droplets depends on the turbulent mixing of the two flows. This method is known as Solution Enhanced Dispersion by Supercritical fluids (SEDS) (Hanna and York, 1994). In the United Kingdom, Bradford University developed this unique process in order to achieve smaller droplet size and intense mixing of supercritical fluid and solution for increased transfer rates. This process has recently been commercialised and pilot-plant scale-up is in progress (www.bpd.co.uk). A process schematic of SEDS is shown in Figure 1.13. The supercritical fluid is used both for its antisolvent properties and as a 'spray enhancer' by mechanical effect. A nozzle with two coaxial passages allows introducing the supercritical fluid and a solution of active substance(s) into the particle formation vessel where pressure and temperature are controlled. The high velocity of the supercritical fluid flow allows the break-up of the solution into very small droplets. Furthermore, the conditions are set up so that the supercritical fluid will effectively extract the solvent from the solution at the same time as it meets and disperses the solution. Researchers at University of Kansas have recently developed a unique nozzle design in which sonic waves were applied to the nozzle leading to 1 μm particles being produced (Subramaniam et al, 1997b). Robertson et al (1998) employed a premixed injector in which the liquid solution is mixed into the flowing CO_2 before the entrance to the reaction vessel. Other authors have used stirred autoclaves in a similar way (Schmitt et al, 1995; Wubbolts et al, 1997). The stirred autoclave device shows marked similarities in industrial crystallizers.

The SEDS process has been employed for several drug formulation applications. It has also been developed to process water-soluble materials, including sugars and proteins (Hanna and York, 1995). As shown in Figure 1.13, the process is based on a nozzle with three coaxial passages into a precipitator, to co-introduce the following;

- (i) A solution or suspension of active substance in solvent 1.
- (ii) A solvent 2 which is miscible with solvent 1 and soluble in the supercritical antisolvent.
- (iii) A supercritical antisolvent.

The dispersion of the active substance solution (in solvent 1) and solvent 2, and the extraction of these two solvents can occur simultaneously. Both solvents are then extracted by the supercritical antisolvent.

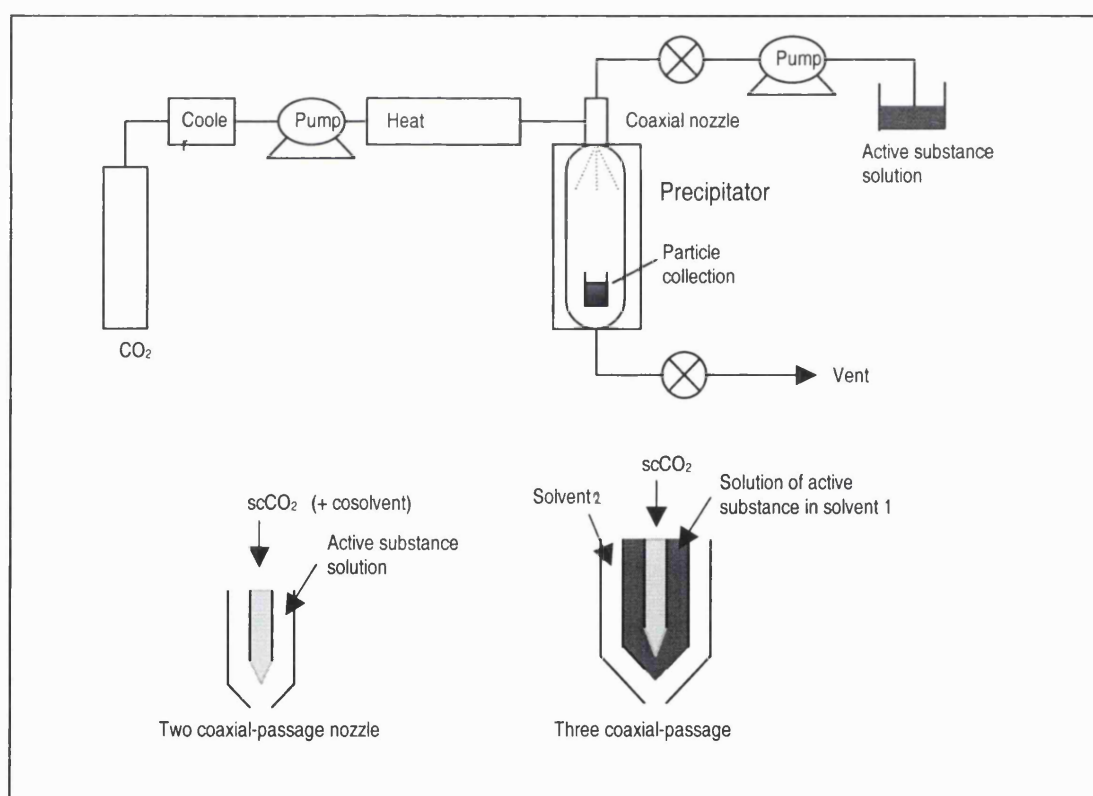


Figure 1.13 SEDS equipment concept along with a cross section of the two and three coaxial-passages nozzle.

Recently, Bradford Particle Design also patented the special antisolvent process which is suitable for particle formation of lipophilic materials and low polarity compounds (Hanna et al, 1999). In conventional GAS or SAS process, the sc-CO₂ expands an organic solution of active substance, decreasing its solvent power and causing the active substance precipitation. In this new method, the sc-CO₂ expands another supercritical solvent, in which the active substance is dissolved. Due to the second supercritical fluid action, precipitating particles of the active substance occurs. Ibuprofen particles were prepared by mixing a supercritical solution of ibuprofen in sc-CO₂ with supercritical nitrogen. Other lipophilic drugs, such as salicylic acid, ketoprofen, salmeterol xinafoate and nicotinic acid, have also been produced using this method.

Various fluid parameters can be used to control particle characteristics in semi-continuous precipitation processes. The type of injection device used can also strongly influence the precipitation process, the size of droplets and the mixing of the different fluids. In the ASES and PCA processes, the particle size and morphology are dependent on several factors such as the operating temperature, pressure, jet break-up, and the mass transfer rates between the supercritical fluid antisolvent phases and the sprayed droplet. Jet break up and the sizes of droplet depend on the relative magnitudes of the droplet deforming (inertial, external) and reforming (viscous, interfacial tension) forces. These forces are determined by the nozzle design, spray velocity, physical properties of the droplet and antisolvent phases. The mass transfer between the antisolvent phase and the sprayed droplet has two limiting paths. Firstly, the solvent evaporation with little carbon dioxide penetration into the droplet phase. Secondly, carbon dioxide swelling of the droplet phase with no solvent evaporation. In the case of polystyrene polymer, various particle morphologies have been obtained using this method (Dixon et al, 1993). The rate of particle formation is determined by the mass transfer of the antisolvent into the sprayed droplet, whereas particle agglomeration and aggregation are affected by the rate of solvent mass transfer into the supercritical fluid from the droplet. The mass transfer is influenced by atomisation efficiency and depends on dispersing and mixing phenomena between the solution droplet and supercritical fluid (Palakodaty and York, 1999). Therefore, an

understanding of mass-transfer rates is required to minimise particle agglomeration and to reduce drying time.

Antisolvent precipitation using sc-CO₂ yields a relatively more rapid precipitation in comparison with conventional solvent evaporation process. Surprisingly, many sc-processed products exhibit high levels of crystallinity. Micronized budesonide can be prepared using ASES (Steckel et al, 1997). Dichloromethane was used as the solvent and sc-CO₂ was used as the antisolvent. XRD analysis revealed that budesonide showed no change in crystallinity. Corrigan and Crean (2002) reported that Hydrocortisone-PVP coprecipitate prepared using gas antisolvent method (GAS) was more crystalline than corresponding system prepared by spray drying. Moneghini et al (2001) prepared carbamazepine-PEG4000 coprecipitate using gas antisolvent method (GAS). From XRD and DSC analysis, the crystalline carbamazepine was still detectable in all the coprecipitates.

Versatility of the antisolvent precipitation method has been demonstrated by producing a pure polymorphic form. Crystallization of Salmeterol xinafoate was prepared using SEDS of acetone and methanol solutions (Beach et al, 1999). Thermal analysis revealed that this compound can exist in two different polymorphic forms. Varying the temperature and pressure of preparation conditions can control the relative composition of the two polymorphs.

In some cases, amorphous products were obtained from the antisolvent precipitation method. Jaarmo et al (1997) produced Sodium chromoglycate using the SEDS technique employing methanol solution. Nanoparticles of catalyst precursor zinc acetate can be prepared using the Supercritical Antisolvent (SAS) method (Reverchon et al, 1999). Dimethyl sulfoxide was used as the solvent and sc-CO₂ was used as the antisolvent. XRD analysis revealed that the SAS-processed product at 150 bar, 40°C and 90 mg/ml was amorphous. Recently, Reverchon et al (2000) reported that amorphous amoxicillin can be obtained from continuous SAS process. The solution of drug in N-methylpyrrolidone was sprayed using sc-CO₂ as antisolvent. However, the effect of the storage time on the morphology and the crystalline structure has not been assessed.

As shown in Table 1.4, a significant number of recent publications demonstrates that the use of carbon dioxide as an antisolvent can clearly recrystallise many different polymers and pharmaceutical particles with a narrow size distribution using fewer organic solvents. In particular, Reverchon (1999) has published several reviews concerning supercritical antisolvent precipitation applications. Because the semi-continuous process (PCA, ASES and SEDS) permits faster depletion of the solvent relative to the GAS or SAS process, they have received increased attention in recent years. However, most of the reported studies deal with batch production of milligram quantities of product and of the proof-of-concept. As a result, continuous production of particles with desired product characteristics and consistency for the semi-continuous process requires investigation. Continuous harvesting of particles at high yield remains a challenge, especially with submicron size particles. Some useful attempts have been made to interpret the effects of process variables on particle size and morphology in terms of the dimensionless groups (Reynolds, Weber, and Ohnesorge numbers) that characterize the spray dynamics and jet breakup (Dixon et al, 1993; Saim et al, 1996; Eggers et al, 1996). At the same time a mathematical model of spray process, based on the underlying rate processes (spray dynamics, mass transfer, and nucleation process), is required for better understanding of mechanism. Such an understanding is essential for rational design and scale-up.

Table 1.4. Experimental results on the supercritical antisolvent precipitation of compounds.

Solute	Solution	SCF ^a	process	Solution, CO ₂ Flow Rate	T(°C)	P(bar)	Nozzle Diam (μm)/ Particle Diam(μm)	References
L-PLA ^b (MW 102 000)	1.5% (w/v) in CH ₂ Cl ₂	CO ₂	PCA	3 ml/min, 6.4 kg/h	40	90,200	400 /spheres 1-10	Bleich et al 1993
L-PLA (MW 100 000)	0.6% (w/w) in CH ₂ Cl ₂	CO ₂	PCA	1 ml/min, stagnant	31	76-97	75/spheres 0.6-1.4(0.5) ^g	Randolph et al 1993
	0.3% (w/w) in CH ₂ Cl ₂	CO ₂	PCA	1 ml/min, 5.34 SCFM	36	76-83	Ultrasonic/spheres 0.8-2.8 (0.3)	
L-PLA (MW 94100)	3% (w/v) in CH ₂ Cl ₂	CO ₂	PCA	-	0	81.6	100/<1	Bodmeier et al 1995
	3% (w/v) in CH ₂ Cl ₂	CO ₂	PCA	-	23, 32	81.6	100/spheres 1-5, fibers	
(+)-Chlorpheniramine maleate (10%/3.7%) ^c	4% (w/v) in CH ₂ Cl ₂	CO ₂	PCA	-	22	69	100/1-5	
(+)-Indomethacin (10%/0.7%) ^c	4% (w/v) in CH ₂ Cl ₂	CO ₂	PCA	-	22	69	100/1-5	
L-PLA (MW 102 000) (+)-Hyosine- butylbromide (20%/19.5, 19.8%) ^c	CH ₂ Cl ₂ /MeOH (85:15)	CO ₂	PCA	-	33-60	90-200	yield 81%(1.69) particle size < 20	Bleich et al 1994
L-PLA (MW 102 000) (+)-Hyosine- butylbromide (20%/19.5, 19.8%) ^c	2% (w/w) in CH ₂ Cl ₂	CO ₂	PCA	CO ₂ Density 0.5-0.8 g/ml 6 ml/min, stagnant	40	90/200	400/13.2 ^h (23.1) ⁱ , 14.9 ^h (26.4) ⁱ	Bleich and Muller 1996
(+)-Indomethacin (20%/0.5%) ^c	2% (w/w) in CH ₂ Cl ₂	CO ₂	PCA	6 ml/min, 6 kg/h	40	200	400/8.2 (15.3)	
(+)-Piroxicam (20%/6.8, 3.7%) ^c	2% (w/w) in CH ₂ Cl ₂	CO ₂	PCA	6 ml/min, 6 kg/h	40	90,200	400/3.5 (6.0), 2.8 (3.7)	
(+)-Thymopentine (5%/4.8, 4.9%) ^c	2% (w/w) in CH ₂ Cl ₂ /MeOH	CO ₂	PCA	6 ml/min, 6 kg/h	40	90,200	400/6.6 (12.1), 5.1(8.7)	
L-PLA (MW 115000 + MW 7000)	3% (w/w) in CH ₂ Cl ₂	CO ₂	PCA	-	30-45	85	300/7 ^h (9) ⁱ 26 ^h (36) ⁱ	Thies and Muller 1996
	3% (w/w) in CH ₂ Cl ₂	CO ₂	PCA	-	40	65-125	300/50 (55)-10 (20)	
HYAFF-7 ^d	200-500 ppm in DMSO	CO ₂	PCA	2.5 ml/min, 5 ml/min	40	104	100/50-500	Saim et al 1996
PLGA ^e	0.5 mg/ml in DMSO	CO ₂	PCA	2.5 ml/min, 5 ml/min	35	104	100/15	
Hydrocortisone	200-500 ppm in DMSO	CO ₂	PCA	2.5 ml/min, 5 ml/min	35	104	100/0.2-1	
Insulin	0.5-9.2 mg/ml in DMSO	CO ₂	PCA	0.9-1.7 ml/min, 9-26 L/min	28-46	91-142	30 or 50/ spheres1-5 ^h	Winters 1996
Lysozyme	2.2-6.8 mg/ml in DMSO	CO ₂	PCA	0.2-2.4 ml/min, 10-21 L/min	27-45	73-115	30 or 50/ spheres1-5 ^h	
Trypsin	0.1-4.0 mg/ml in DMSO	CO ₂	PCA	0.5-2.1 ml/min, 5-20 L/min	27-47	73-136	30 or 50/ spheres1-5 ^h	
Polystyrene (MW 200 000)	Toluene	CO ₂	PCA	CO ₂ Density 0.24-0.93 g/cm ³	0-40	39.6-224.7	100/ spheres, variety of size 0.1- 20 depending upon T and D	Dixon et al 1993
				D>0.7 g/cm ³	<30		100/0.1	

Table 1.4 (Continued)

Solute	Solution	SCF	process	Solution, CO ₂ Flow Rate	T(°C)	P(bar)	Nozzle Diam (micron)/ Particle Diam(micron)	References
Lactose	10% (W/V) Water	CO ₂ + EtOH or MeOH	SEDS	0.035 ml/min, 5 or 19 ml/min co-solvent flow rate 0.665 ml/min	50	150	p'cle morphology depends on the CO ₂ flow rate particle size 5-31	Palakodaty et al 1998
Steroids drug	1% (w/w) CH ₂ Cl ₂ and/or MeOH	CO ₂	ASES	63 ml/min, stagnant	40	8.5	300/5	Steckel et al 1997
Nicotinic acid	MeOH	CO ₂	SEDS	-	35	80	particle size 9.38 (0.47)	Rehman et al 1999
				-	120	80	particle size 3.93 (0.24)	
Carbamazepine	5% (w/v) CH ₂ Cl ₂ , 5% (w/v) MeOH	CO ₂	SEDS	0.5-1 ml/min, 500 L/hr	45-85	80-150	polymorphs can be formed depends on solvent choice, supersaturation rate and T	Edwards et al 2000
Terbutaline sulphate	MeOH/Water (92:8)	CO ₂	SEDS	-	35-80	90-250	variety of size 1.99-12.15 depending upon supersaturation rate and D	Rehman et al 2000
Superconductor precursors	5-65 mg/ml in DMSO	CO ₂ + DMSO	ASES	1 ml/min, 6500-12000 ml/min	40-60	70-160	22/0.1	Reverchon et al 1998
Lysozyme	0.5-1% (w/v) in DMSO	CO ₂	SEDS	0.2-0.6 ml/min, 18-30 ml/min	40-50	80-150	0.2, 0.3/ 1-5 at low P	Moshashae et al 2000
Cu-Indomethacin cpx ^f	90% (w/v) in DMF	CO ₂	GAS	-	25-40	59	P'cle morphology and Partice size 10-100 depends on expansion rate and conc of solution	Warwick et al 2000

^a super critical fluid. ^b poly(L-lactic acid). ^c (Expected drug loading/ actual drug loading): the amount of drug in the precipitate (actual) was less than amount of drug mixed with the polymer prior to precipitation (expected), due to partitioning of the drug into CO₂ during microparticle formation; eg. (20%/6.8,3.7%) means 6.8% drug loading at 90 bar, 3.7% drug loading at 200 bar. ^d Hyalurinic acid ethyl ester. ^e Poly(dl-lactide-glycolide). ^f Copper and Indomethacin complex. ^g Relative standard deviation. ^h After sonication. ⁱ Range: 10th – 90th percentile.

1.4 Techniques for characterizing amorphous solids

Various techniques have been proposed for the physical characterization of amorphous solids. These techniques include, Differential Scanning Calorimetry (DSC), X-ray Diffraction (XRD), Molecular spectroscopy, Isothermal Calorimetry, Modulated DSC, Solution Calorimetry, Density, Solubility and Water sorption. Buckton and Darcy (1999) reviewed both calorimetric (Isothermal microcalorimetry, solution calorimetry) and gravimetric methods, which can be used to characterise partially amorphous materials. Darcy and Buckton (1998) employed isothermal microcalorimetry to quantify the amorphous content of spray-dried lactose. Taylor and Zografi (1998b) used FT-Raman Spectroscopy to quantify the degree of crystallinity in milled indomethacin.

1.5 Dissolution studies

Many drugs exhibit poor solubility in water, thus presenting problems with regards to dissolution and hence bioavailability. The dissolution rate of drugs in the gastrointestinal fluids is often the rate-limiting step in the absorption of drugs rather than their diffusion rates across the gut wall.

The in vivo dissolution rate and the bioavailability of drugs for gastrointestinal absorption from solid dosage forms are relatively difficult to perform as the study involves human volunteers. In vitro dissolution experiments, which are comparatively simpler to perform, can be used to approximate the dissolution behaviour of the drugs in the body.

1.5.1. Factors affecting the dissolution rate of drugs

1.5.1.1 Solid phase characteristics

Many studies have shown that the crystalline form of a drug usually exhibits lower solubility and dissolution rate compared to that of the amorphous form. For example, novobiocin, phenobarbital, cortisone acetate, griseofulvin, and chloramphenicol (Banakar, 1992).

1.5.1.2 Polymorphism

The polymorphic forms of drugs and the states of hydration have been shown to affect the solubilising characteristics and dissolution rates of drugs. The anhydrous form usually has a higher aqueous solubility and faster dissolution rate than the hydrated form (Brittain and Grant, 1999). The influence of polymorphism on the dissolution rate has been reported for various pharmaceutical drug compounds, which included carbamazepine, tolbutamide, phenylbutazone, erythromycin, ampicillin and chloramphenicol (Banakar, 1992).

Al-Saieq et al (1982) studied the dissolution behaviour of chlorpropamide (CPM) polymorphs. The four metastable forms exhibited higher dissolution rates than that of the stable form. Ueda et al (1984) carried out further investigations on the dissolution profiles of CPM polymorphs in potassium chloride-hydrochloride acid buffer system. The polymorphic transformation of metastable form II to the stable form was observed during dissolution testing. Although the metastable polymorph exhibited a faster dissolution rate than the stable form, the use of the metastable form to improve the dissolution rates of poorly water soluble drugs is limited in application to commercial drug formulations. This limitation was due to the possibility of conversion from the highly soluble form to the less soluble crystalline form during manufacture and storage of the dosage forms (Horter and Dressman, 1997).

1.5.1.3 Particle size and surface area

The surface area of pharmaceutical solids plays an important role in controlling the dissolution. In general, the dissolution rate is directly proportional to the surface area of the drug. As a result, a higher dissolution rate can be obtained through a reduction in particle size. However, in the case of hydrophobic drugs with poor wettability, decreasing the particle size may not enhance the dissolution rate. Loth and Hemgesberg (1986) reported that dissolution rates of phenacetin powders micronised by jet milling and the Rapid Expansion of Supercritical Solution technique were nearly the same, even though they differed considerably in their surface areas. The insignificant difference in the dissolution rate was due to the agglomeration of the drug particles delaying dissolution medium penetration and subsequent wetting. The dissolution rate of micronised phenacetin was enhanced after mixing with hydrophilic

vehicles, such as mannitol and Aerosil R972. Once the wetting limitation was eliminated, the phenacetin micronised by RESS showed a higher dissolution rate than that produced via jet milling.

1.6 Thesis aims

The objectives of this work were to study the formation and stabilisation of drugs in the amorphous state, as a means of increasing dissolution and hence potentially bioavailability. A poorly water soluble drug, indomethacin, was selected as a model. Another objective was to construct and design a supercritical fluid based apparatus for preparing amorphous particles.

The aims of this study were to prepare amorphous particles using different methods. These included spray drying and precipitation using supercritical CO₂ as solvent and antisolvent. In addition the effect of different additives on the physical form of indomethacin would be investigated. A further aim was to understand how processing method and presence of additives affects dissolution and physical stability.

The hypothesis was that spray drying and supercritical fluid based techniques should make amorphous material, and that changes in production method would yield different morphologies and give different physical properties of products, especially with respect to dissolution rate.

Chapter 2

Materials and Methods

2.1 Materials

2.1.1 Drug

Indomethacin

The drug Indomethacin, having a poor solubility in water, was chosen as a model. Indomethacin is a non-steroidal anti-inflammatory drug (NSAID) having anti-inflammatory, analgesic and antipyretic activities (O'Brien et al, 1984; Laurence et al, 1997). NSAIDs are indicated for the treatment of moderate to severe rheumatoid arthritis, acute gouty arthritis and for the relief of mild to moderate pain (Mehta, 1993; Berkow et al, 1997).

Member drugs of the NSAID group act by inhibiting prostaglandin biosynthesis and share several adverse affects which include gastrointestinal bleeding and ulceration (Charles and Mogg, 1994). Previous thermodynamic and kinetic examinations of their behaviours in aqueous solutions reported a dominant hydrophobicity, weak acidity, low solubility and low dissolution rate in water but high partition coefficient in their acidic form (Fini et al, 1995). Many NSAIDs with expired patents are being developed as generic products with the possible risk of variable bioavailability due to differences between formulations. Indomethacin is one of them. There are more than one hundred NSAID drugs, which are presently available worldwide.

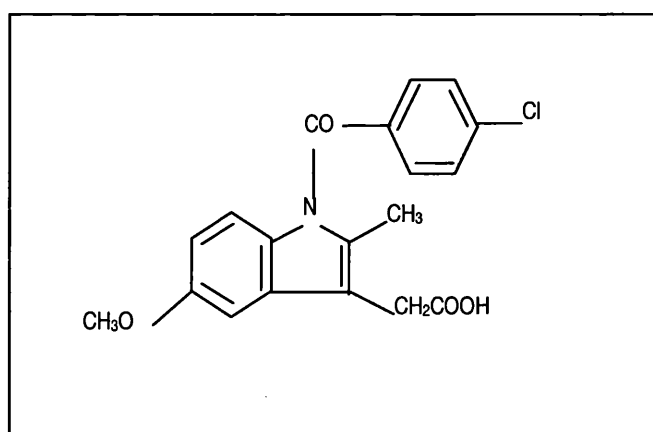


Figure 2.1. Structural formula of Indomethacin

Indomethacin ($C_{19}H_{16}ClNO_4$, 1-[p-chlorobenzoyl]-5-methoxy-2-methylindole-3-acetic acid} is a pale-yellow to yellow tan crystalline powder with a slightly bitter taste. It is odourless or almost odourless, practically insoluble in water (less than 1 g/l) and has a molecular weight of 357.79 g/mole. Table 2.1 shows the equilibrium solubilities of indomethacin in different solvents at 25 °C (O'Brien et al, 1984). Indomethacin is light sensitive but stable in air and heat under the normal temperature conditions.

Table 2.1. Indomethacin solubility in different solvents at 25 °C (adapted from O'Brien et al, 1984).

Solvent	Solubility (mg/100 ml)
Water	Practically Insoluble
Phosphate Buffer pH 5.6	3 (a)
Phosphate Buffer pH 5.6	5 (b)
Phosphate Buffer pH 7	54 (a)
Phosphate Buffer pH 7	80 (b)
Ethyl alcohol (95%)	200
Chloroform	330
Methanol	320
Benzene	40

(a) Form I, (b) Form II

Indomethacin is known to exist in two non-solvated crystalline modifications. There are consistent melting points, infra-red (IR) and powder X-ray diffraction data for these two polymorphic forms. Polymorphism is a phenomenon demonstrated by compounds that are able to crystallise in more than one crystal structure. Due to the different crystal packing arrangements, polymorphs display different chemical and

physical properties such as melting point, solubility, heat of fusion, density and refractive index (Rustichelli et al., 2000). Yamamoto (1968, through O'Brien et al, 1984) named the two forms of indomethacin as γ -type (melting point at about 162 °C) and α -type (melting point at about 155 °C). However, most of the researchers use Form I and Form II, respectively. Form I is the highest melting and lowest solubility polymorph. It is the thermodynamically stable crystalline form of indomethacin. Therefore, this form has been used in the pharmaceutical preparations. In addition to the polymorphic forms as described above, indomethacin can form solvates with benzene, t-butyl alcohol and other solvents (O'Brien et al, 1984).

Indomethacin (Lot No. 950012-254, Becpharm Ltd., England) of European Pharmacopeia quality was used as received.

2.1.2. Polymers

Polyvinylpyrrolidone (PVP)

Polyvinylpyrrolidone or Povidone {poly[1-(2-oxo-1-pyrrolidinyl) ethylene]} is a synthetic, water soluble polymer consisting of linear 1-vinylpyrrolidin-2-one group. The molecular weight of polyvinylpyrrolidone (PVP) depends on the degree of polymerization, which ranges between 2,500 and 3,000,000 g/mole. PVP is a fine, white to creamy coloured, odourless and hygroscopic powder. It is freely soluble in acids, chloroform, ethanol, ketones, methanol and water (Wade and Weller, 1994). It is stable to a short cycle of heat exposure at around 110-130 °C but it darkens if the temperature is higher than 150 °C.

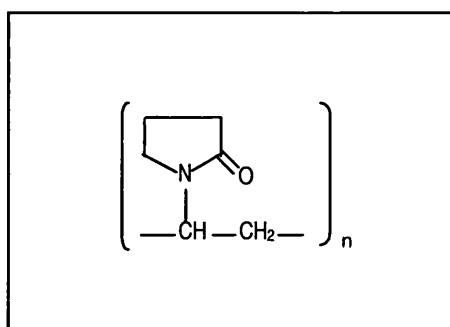


Figure 2.2. Structural formula of Polyvinylpyrrolidone

PVP has been employed in many preparations especially in solid-dosage forms. PVP can be used as binder, disintegrating agent, and dissolution enhancer (Wade and Weller, 1994). The main advantages of using PVP are non-toxicity and general applicability to most drugs. Many researchers investigated the effect of PVP as an excipient on the crystallisation of compounds. Sekikawa et al (1979) reported that PVP retarded or inhibited crystallisation of sulfoxazole, sulfamethizole, and sulfamerazine but has no effect in the crystallisation of nalidixic acid and caffeine. Corrigan et al (1985) showed that PVP inhibited the crystallization of indomethacin following co-spray drying. It has been shown that PVP can act as a stabilising agent for the amorphous state of certain materials. The mechanism of action of PVP as a stabiliser could be due to the formation of hydrogen bonds with the materials. In addition, PVP has an anti-plasticizing effect, and therefore increases the glass transition temperature of materials (Shamblin et al, 1998; Shamblin and Zografi, 1998; Taylor and Zografi, 1997; 1998a). PVP is known as a stabilising agent because of its ability to maintain a material in its amorphous state for a period of time.

PVP (MW 44,000Da, BDH Laboratory Supplies, England) was used as polymeric carriers for spray drying, precipitation using sc-CO₂ as solvent and as anti-solvent process.

Microcrystalline cellulose

Microcrystalline cellulose (MCC) in general has a wide range of uses in oral pharmaceutical solid dosage forms. It is basically used in tablet and capsule formulations, where it functions as a filler-binder, lubricant and also disintegrant (Wallace et al, 1983). The quantity of MCC used in a formulation may also alter depending on its functions. Table 2.2 presents the use of MCC and the corresponding concentrations (Wade and Weller, 1994). MCC is a white, odourless, and tasteless powder. There are several grades of MCC, which are commercially available in different particle sizes and moisture contents. It is slightly soluble in 5% w/v sodium hydroxide solution, practically insoluble in water, dilute acids, and most organic solvents (Wade and Weller, 1994).

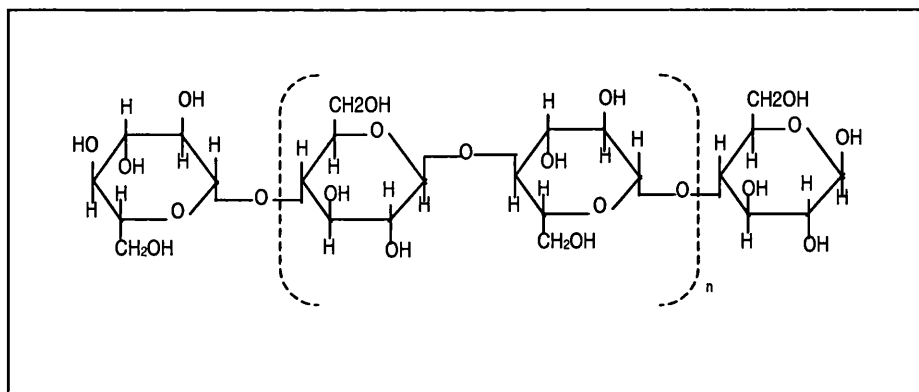


Figure 2.3. Structural formula of microcrystalline cellulose

Table 2.2 The functions and their corresponding concentrations of MCC.

Use	Concentration (%w/w)
Adsorbent	20-90
Anti-adherent	5-20
Capsule filler-binder	20-90
Tablet disintegrant	5-15
Tablet filler-binder	20-90

MCC is a non-toxic and non-irritant material. It is not absorbed readily into the body system following oral administration (Wade and Weller, 1994). It was found that MCC markedly affected the mechanical, microstructural and release characteristics of tablets (Landin et al, 1993). The study of cohesive properties of MCC indicated that these properties were related to hydrogen bonding. The hydrogen bond provides mechanical strength to the tablet by holding the particles together (Wan and Prasad, 1988) and the strength increases with increasing amount of cellulose (Pesonen et al, 1992). However, although MCC has excellent tablet binding characteristics, a rapid drug release from samples compressed with MCC is expected as this is due to the hydrophilic nature of the cellulose derivative (Shaikh, 1991). It has been documented

that the uptake of water into the tablet was increased by MCC. In consequence, the disintegration time was shortened (Wan and Prasad, 1988; Pesonen et al, 1992). This phenomenon occurred due to MCC accelerating the dissolution rate by the mechanism of enhancing water penetration into the tablet. As a result, the hydrogen bonds between MCC and drug were broken and the tablet structure loosened. It has also been shown that MCC absorbed water by capillary action. The molecular swelling is insignificant and the structure of MCC is retained even after water absorption (Wan and Prasad, 1988).

MCC (Emcocel 50M, mean particle size of 50 μm , Edward Mendell, Reigate, Surrey, England) was used as polymeric carriers for spray drying process. It was also used as a formulation excipient.

Silicified microcrystalline cellulose

Silicified microcrystalline cellulose (SMCC), achieved by silicification of the microcrystalline cellulose, resulting in an association between colloidal silica and microcrystalline cellulose. This particular grade has a median particle size in the region of 200 μm .

SMCC (Prosolv, LP200, Penwest, England) was used as polymeric carriers for spray drying process.

Polyethylene glycol

Polyethylene glycol (PEG) is an addition polymer of ethylene oxide and water. PEG grades 200-600 are liquids; grades 1000 and above are solids at ambient temperature. The liquid grades appear as clear, colourless, viscous liquids. They have a slight, but characteristic odour and a bitter, slightly burning taste. The solid grades are white and waxy flakes. They have a faint, sweet odour. PEG is widely used in a variety of pharmaceutical formulations. All grades of PEG are stable, soluble in water and miscible in all proportions with other PEG (after melting, if necessary). PEG 4000 has a melting range of 50-58 $^{\circ}\text{C}$.

PEG (MW 4,000 Da, BDH, England) was used as a polymeric carrier for precipitation using sc-CO₂ as a solvent.

2.1.3 Organic solvents

Organic solvents include acetone, chloroform, dichloromethane, and N,N-Dimethylformamide, ethanol, ethanol 96% and anhydrous methanol were used to dissolve indomethacin. The properties of the solvents described in the literature (British Pharmacopoeia 2002, Pharmaceutical codex, 1994) are summarized as follows:

Acetone

Acetone, propan-2-one, C₃H₆O, is a volatile and flammable liquid. Its boiling point is 56 °C.

Acetone (BDH, England) was used as a solvent to dissolve indomethacin.

Chloroform

Chloroform, trichloromethane, CHCl₃, contains 0.4 to 1.0% w/w of ethanol. It appears as a colourless, heavy, volatile liquid with a characteristic penetrating odour and a sweet burning taste. It is non-inflammable but the strongly heated vapour could be ignited and burn with production of noxious vapour. The boiling point is 60°C. It is soluble in 200 parts of water at 20 °C. It is miscible with dehydrated alcohol, ether, most other organic solvents, and fixed and volatile oils.

Chloroform (BDH, England) was used as a solvent to dissolve indomethacin.

Dichloromethane

Dichloromethane, Methylene chloride, CH₂Cl₂, appears as a volatile, sweet-smelling liquid. Its boiling point is 40°C.

Dichloromethane (BDH, England) was used as received. It was also mixed with ethanol (at ratio of 1 to 1, v/v). Both were used as solvents to dissolve indomethacin.

Dimethylformamide

Dimethylformamide C₃H₇NO, is a colourless liquid. The boiling point is 153°C.

Dimethylformamide (Sigma-Aldrich, England) was used as a solvent to dissolve indomethacin.

Ethanol

Ethanol (99.7-100% v/v) or absolute alcohol, $\text{CH}_3\text{CH}_2\text{OH}$, appears as a clear, colourless, mobile, volatile liquid with a characteristic spirituous odour and a burning taste. It is readily inflammable. The boiling point is 78°C . It is miscible with water, ether and chloroform. In addition, when mixed with water, contraction of volume and rise of temperature occur.

Ethanol (BDH, England) was used as received. It was also mixed with dichloromethane (at ratio of 1 to 1, v/v). Both mixtures were used as solvent to dissolve indomethacin.

Ethanol 96%

Ethanol 96% is a mixture of ethyl alcohol (ethanol), $\text{CH}_3\text{CH}_2\text{OH}$, and water. Ethanol 96% (BDH, England) was mixed with water (at ratio of 1 to 2, v/v). It was used as solvent to dissolve indomethacin in spray drying process.

Anhydrous methanol

Anhydrous methanol, CH_4O , contains water not more than 0.03% w/v. It appears as a colourless liquid. It is readily inflammable. The boiling point is 64 to 65°C .

Anhydrous methanol with less than 0.0050% water (Prolabo, England), was used as a solvent to dissolve indomethacin in solvent evaporation method.

2.1.4 Excipients

Sodium starch glycolate

Sodium starch glycolate is a sodium salt of a cross-linked partly o-carboxymethylated potato starch. It occurs as a white to off-white, odourless, tasteless, fine and free flowing powder. It is very hygroscopic, practically insoluble in methylene chloride. It gives a translucent suspension in water. It is commonly used in oral pharmaceuticals as a disintegrant in solid dosage form. It is widely used in tablets prepared using either direct-compression or wet-granulation process. Usually, the concentration employed

in a formulation is between 2-8%. Disintegration occurs by rapid uptake of water followed by immediate swelling.

Sodium starch glycolate (Explotab, Edward Mendell, England) was used as a disintegrant for direct-compression indomethacin tablet.

Magnesium stearate

Magnesium stearate is a mixture of magnesium salts of different fatty acids consisting chiefly of palmitic acid and stearic acid with minor proportions of other fatty acids. It appears as a white, very fine, precipitated or milled, light powder. The powder is greasy to the touch and readily adheres to the skin. It has a faint odour of stearic acid and a characteristic taste. It is practically insoluble in water and ethanol. Magnesium stearate is commonly used in cosmetics, food and pharmaceutical formulations. It is widely used as a lubricant in capsule and tablet formulations at concentrations between 0.25-5%.

Magnesium stearate (BDH, England) was used as a lubricant for direct-compression indomethacin tablet.

2.1.5 Distilled water

Freshly prepared distilled water (measured pH 5.2) was used as an antisolvent for Indomethacin precipitation, for preparing dissolution medium and saturated salt solution in RH stability studies.

2.1.6 Dissolution medium

A test solution described in the British Pharmacopoeia (BP 2002) was prepared to be the dissolution medium.

Phosphate buffer solution pH 7.2 (measured pH 7.2) was prepared by mixing 50 ml of 0.2 M potassium dihydrogen orthophosphate with 35 ml of 0.2 M sodium hydroxide and diluting to 200 ml with water. It was used as the dissolution medium for tablets and capsules containing indomethacin.

Potassium dihydrogen orthophosphate (Fisher, England) and Sodium hydroxide pellets (BDH, England) were used for preparing dissolution medium.

2.2 Methods

2.2.1 Scanning electron microscopy

The morphological properties of the indomethacin powder were characterised using a scanning electron microscope (Philips XL20, Eindhoven, Netherlands) at an accelerating voltage of between 10 and 15 kV. Prior to examination, samples were coated with a thin layer of gold by using a sputter coater (Emitech K550) to render them electrically conductive, after the powder had been mounted on double sided adhesive tape on aluminium stubs.

2.2.2 Differential scanning calorimetry (DSC)

Differential scanning calorimeter is a thermal analysis instrument. The substance under investigation is heated or cooled at a constant rate through a phase transition. The DSC provides solid-state transition data, such as melting points, glass transition and heat capacity. Determination of purity of materials and compatibility of excipient and drugs can be derived from DSC results (Ford and Timmins, 1998).

There are two basic types of DSC, the heat-flux DSC, and the power compensation DSC. For the heat flux DSC, the sample and reference are heated by the same furnace. The temperature difference, ΔT , between the materials is measured and recorded versus time (or temperature).

$$\Delta T = T_S - T_R$$

The area under the curve is related to the enthalpy of reaction, ΔH

$$\Delta H = k \times \text{area} = k \times \int \Delta T \times dt$$

where k is the calibration constant. The value of k can be determined by measuring the area of a known standard, A_S

$$k = \Delta H_S \times m_S / A_S$$

where ΔH_S is the enthalpy of fusion of the standard and m_S is the mass of the standard.

For the power compensation DSC, the sample and reference are heated by two separate furnaces. The power difference between the materials is plotted against time (or temperature) where the temperature difference ΔT is maintained at zero.

$$\Delta P = d\Delta q/dt = \beta \times (C_S - C_R)$$

where β is the heating rate, C_S is the heat capacity of the sample and C_R is the heat capacity of the reference. In this case, the area under the peak gives the enthalpy directly.

The heat capacity, the amount of energy required to raise one gram of sample by 1 °C, can also be determined from DSC data. The greater the heat capacity (ΔC_P), the greater the baseline deflection. Power is related to the heat capacity as in the following equation

$$\text{Power} = dq/dt = \Delta C_P \times dT/dt$$

To determine the heat capacity of a sample, it must be compared with a known standard, for example sapphire (Mc Naughton and Mortimer, 1975).

The International Confederation of Thermal Analysis (ICTA) suggested that the data obtained with a power-compensation type should show endotherms in an upward direction (Figure 2.4).

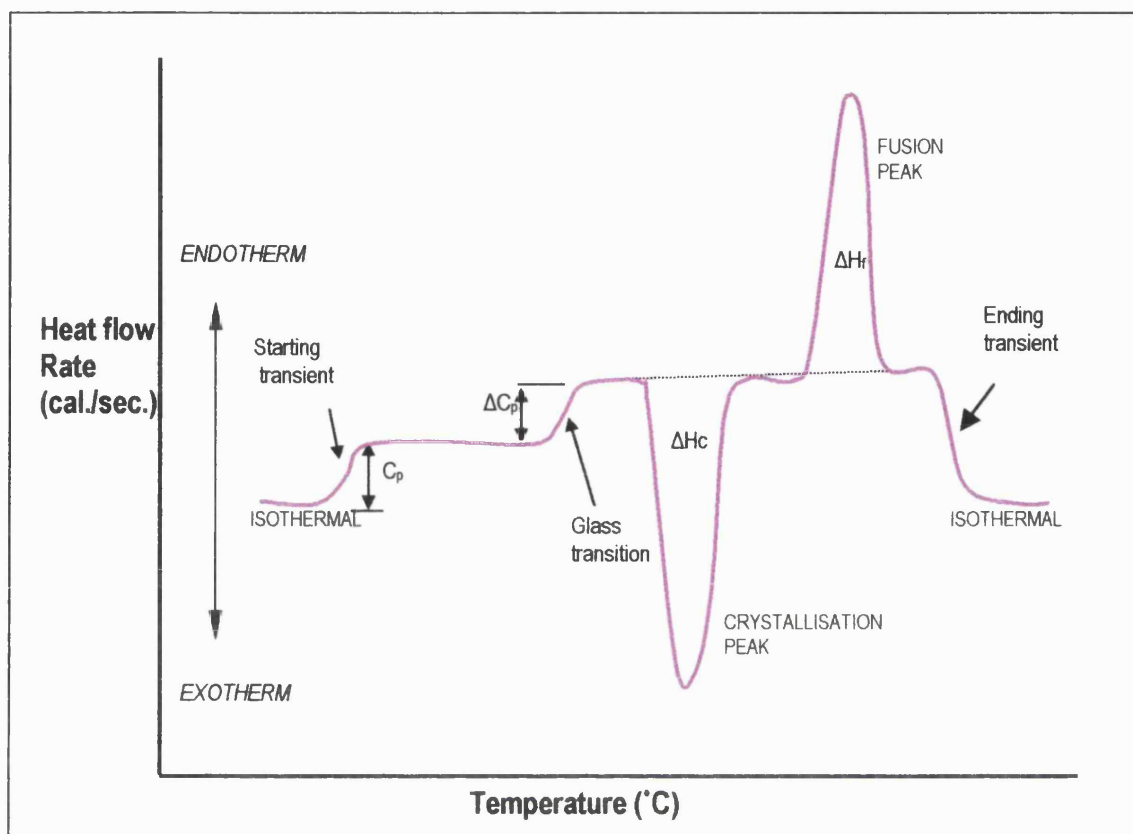


Figure 2.4 A typical thermogram generated from power compensation DSC (data adapted from Perkin-Elmer training paper).

A differential scanning calorimeter (Perkin Elmer DSC 7, USA) was employed. Samples of approximately 5 mg were carefully weighed and hermetically sealed in aluminium pans. A heating rate of 10 °C /min from 25 to 250 °C under nitrogen gas atmosphere was used.

2.2.3 Powder X- ray Diffraction Analysis

The crystalline nature of materials can be investigated using X- ray diffraction analysis, i.e. diffraction of x- rays from the planes of a crystal. The condition for diffraction of x-ray beams from a crystal is explained by the Bragg equation;

$$n\lambda = 2d \sin\theta$$

where λ is the wavelength of the X-ray beam, θ is the angle of diffraction, d is the distance between atomic planes in the crystal, and n is the order of the diffraction

The scattering power of atoms for X-rays depends on the amount of electrons they possess. Hence, the position of the diffraction beams from a crystal depends on the size and shape of the unit cell of a crystal and the X-ray beam wavelength. In contrast, the intensity of the diffracted beams depends on the type of atoms in the crystal and location of these atoms in the unit cell. No two substances would be expected to have exactly identical diffraction patterns. For this reason the X-ray pattern is a unique result for each crystalline compound.

X-ray diffraction is usually very useful for the initial identification of differences in morphology. However, variations in diffraction patterns may result from differences in orientation that are not related to differences in crystal structure (Szulzewsky et al, 1982). The Geometrical relationships among X-ray beam wavelength, diffraction angle and the distance of lattice space is shown in Figure 2.5.

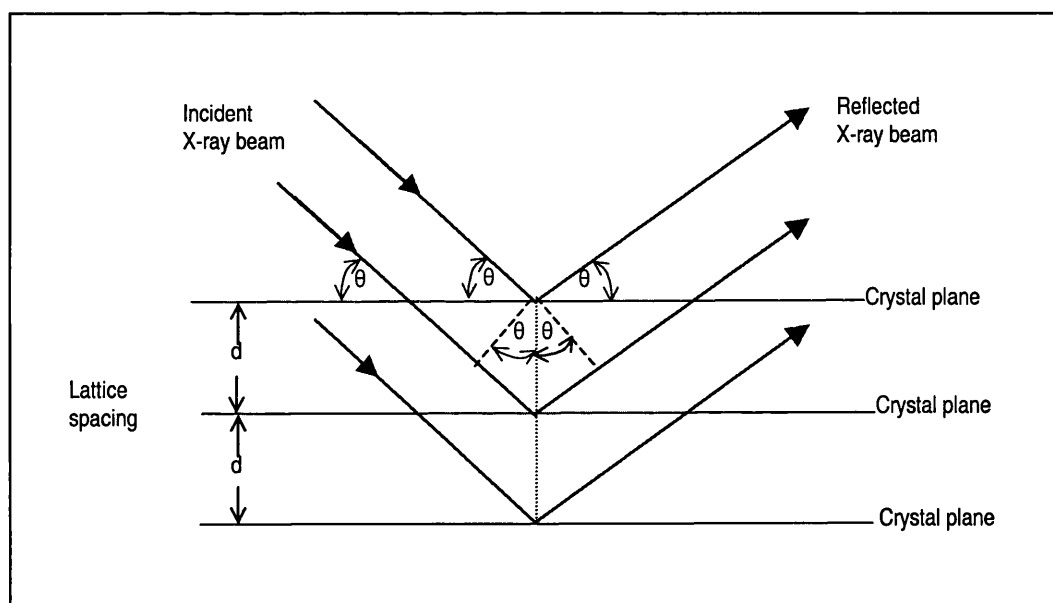


Figure 2.5 Geometrical relationships among X-ray beam wavelength, diffraction angle and the distance of lattice space.

If the baseline of spectra is flat between 5° and 50° 2θ and the peaks are sharp and well defined, the sample can be characterized as crystalline (Figure 2.6(a)). If the baseline increases in a form of a broad hump at about 20° 2θ before dropping again, and also has superimposed peaks, it can be explained that the sample may be a mixture of crystalline and amorphous material (Figure 2.6(b)). If a spectrum has a smooth hump without peaks it means the sample is a totally amorphous material (Figure 2.6(c)).

A Philips PW3710 scanning X-ray powder diffractometer (Philips, Netherlands) was used to quantify the presence of crystalline indomethacin in the various samples. The radiation used was generated by a copper $k\alpha$ filter, with a wavelength of 1.5418° \AA at 35 kV and 40 mA. Samples were scanned over a range of 2θ values from 5° to 50° at a scan rate of $2.5^\circ/\text{min}$.

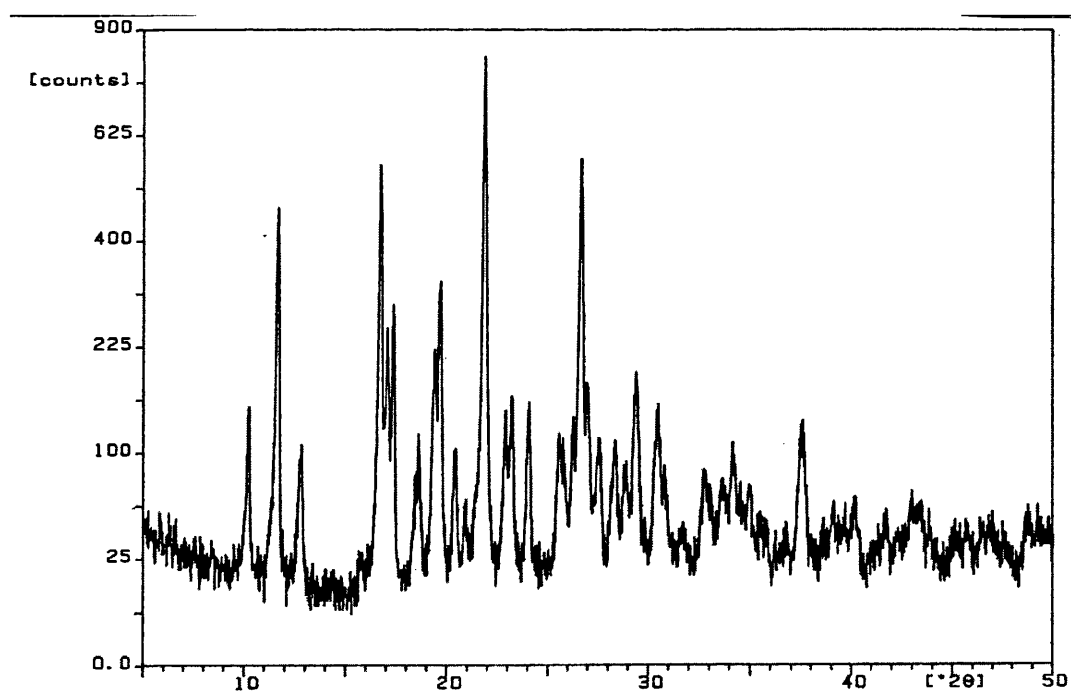


Figure 2.6(a) Typical spectra of crystalline material.

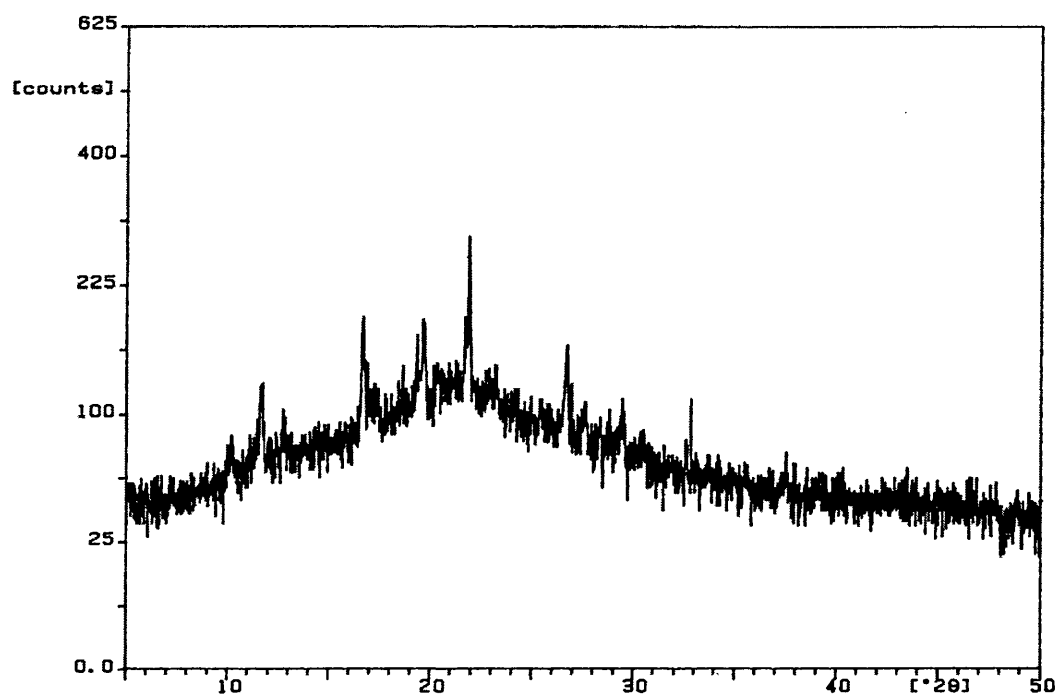


Figure 2.6(b) Typical spectra of partially amorphous material.

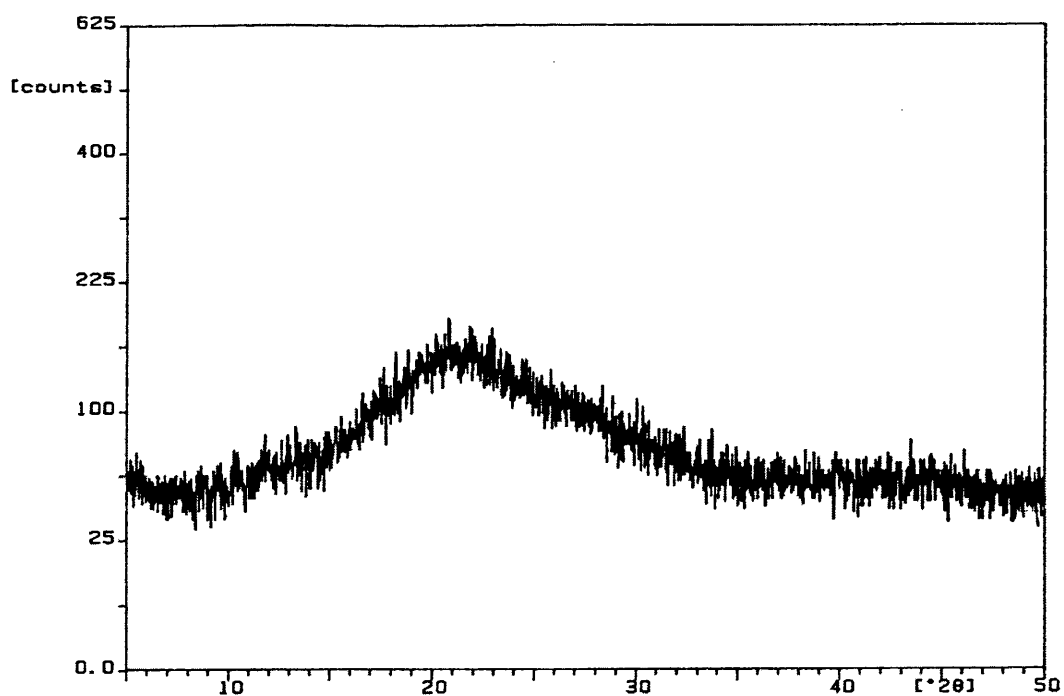


Figure 2.6(c) Typical spectra of amorphous material.

Chapter 3

Spray Drying

3.1. Introduction

It has been shown that the spray-drying process can change the physical state of drugs with a poor solubility in water and thus increase significantly their in vitro dissolution rates. For instance, spray dried indomethacin, phenobarbitone and hydroflumethiazide have shown enhanced drug dissolution due to the presence of amorphous content in the products (Corrigan et al, 1984; 1985). To change the physical state of poorly water soluble drugs and thus to enhance their dissolution and improve their bioavailability, polymers and other glass forming solids have been mixed with drugs prior to spray drying (Corrigan et al, 1985; Bootsma et al, 1989; Giunchedi and Conte, 1995; Corrigan and Crean, 2002).

The aim of this part of the study was to explore the potential of employing the spray-drying method in modifying the physical state of indomethacin. Indomethacin and polymer mixtures were studied using three different polymers, PVP, MCC and SMCC. The spray-dried powders were characterised using DSC and powder X-ray diffraction. In addition, the spray-dried samples were prepared in tablet dosage form and their dissolution behaviour was investigated.

3.2. Materials and Methods

3.2.1. Materials

Indomethacin, microcrystalline cellulose, polyvinylpyrrolidone, silicified microcrystalline cellulose, 96% ethanol, sodium starch glycolate, magnesium stearate, potassium dihydrogen orthophosphate, sodium hydroxide pellets, distilled water. The details of these materials are given in section 2.1.

3.2.2. Preparation of spray dried indomethacin

It was recommended that the Buchi B-190 Minispray dryer should be used only with aqueous systems but not used with organic solvents. However, combustible solvents could be used if their inflammable/explosion limit is not exceeded. Some examples of air/solvent ratio calculations are explained in Appendix. In the present study, a mixture of ethanol (96%) and water (2:1, v/v) was used as a solvent for the model drug indomethacin. Since increase in humidity content in the spray chamber could reduce

electrostatic charge build-up, water was added to the spray drying solution. The explosion limit of a solvent mixture could also be reduced in the presence of water and thus could minimize the potential risk.

Accurately weighed indomethacin of 100 mg was added slowly and dissolved in 360 ml of solvent mixture containing ethanol (96%) and water (2:1, v/v). The amount of drug dissolved before the supersaturation was recorded and taken as the maximum concentration of drug dissolved. Thus, indomethacin solubility in this solvent mixture was approximately 1.4% w/v.

Preliminary investigations were carried out to determine the effect of aspirator speed, inlet temperature and feed concentration on the physical characteristics and yield of the spray dried product. Solutions of indomethacin were prepared in ethanol (96%) and water (1:2, v/v) at concentrations of 0.7%w/v and 1.4% w/v. The solutions were spray dried using Buchi minispray dryer type 190 (Buchi Laboratory-Techniques Ltd., Switzerland), with a 0.7 mm pneumatic nozzle, under different conditions outlined in Table 3.1

Table 3.1 Spray drying parameters investigated for indomethacin

Settings Spray drying conditions	(a)	(b)	(c)	(d)	(e)	(f)
Feed concentration (%w/v)	1.4	1.4	1.4	1.4	0.7	0.7
Aspirator level	18	15	10	10	10	10
Pump flow rate (ml/min)	10	8.5	5.6	5.6	5.6	5.6
Compressed air flow rate (L/h)	600	600	600	600	600	600
Inlet temperature (°C)	150	150	150	100	150	100
Outlet temperature (°C)	85-90	80-85	75-80	75-80	75-80	75-80

Throughout the study, the material was obtained in the collecting vessel and the cyclone separator above the collecting vessel. The spray-dried product was desiccated immediately after drying at 0%RH over phosphorous pentoxide at 25 °C, to prevent uptake of moisture. The percentage yield was calculated using the weight of the materials collected from both sites. These preliminary experiments showed that the highest product yield was achieved with 1.4% w/v feed concentration, 5.6 ml/min feed input, level 10 (20 m³hr⁻¹) aspirator speed, 150 °C inlet temperature and 75-80 °C outlet temperature. Hence, these were the conditions chosen to produce spray dried materials for further investigation in this study.

3.2.3. Preparation of indomethacin and microcrystalline cellulose mixture

Mixtures of indomethacin and MCC at ratios of 8:2, 9:1 and 9.5:0.5, were ground for 30 min using a mortar and pestle. Another set of experiments comprising similar proportions of indomethacin and MCC was prepared but without grinding. The physical mixtures were dispersed in a solvent mixture consisting of ethanol (96%) and deionised water at ratio of 2:1 to produce 1.4 %w/v suspension. The suspension was stirred for 1 hr prior to spray drying using the settings as described above.

3.2.4. Preparation of indomethacin and polyvinylpyrrolidone mixture

Indomethacin and polyvinylpyrrolidone were dissolved in ethanol (96%) and deionised water solvent mixture at ratio of 2:1 to produce 1.4 %w/v solution. The proportions of indomethacin and PVP investigated were, 9.5:0.5, 9:1, 8:2, 7:3, 6:4, 5:5 and 4:6. The mixture was spray dried using the settings as described above.

3.2.5. Preparation of indomethacin and PVP mixtures with the inclusion of microcrystalline cellulose or silicified microcrystalline cellulose

Indomethacin and polyvinylpyrrolidone (8:2) was dissolved in ethanol/water solvent mixture at a concentration of 1.4% w/v. Microcrystalline cellulose or silicified microcrystalline cellulose was dispersed into the solution at 10%, 20% and 30% w/w of the indomethacin and PVP mixture.

Another set of experiment was prepared comprising fixed amount of indomethacin but different ratios of PVP and MCC or SMCC (Table 3.2). Indomethacin and polymer (8:2) were dissolved or dispersed in ethanol/water at a concentration of 1.4% w/v. The mixture was stirred and spray dried using the settings as described previously.

Table 3.2 The composition of indomethacin and different polymer for spray dried solutions.

Sample Compositions			
Indomethacin	PVP	MCC	SMCC
8	2	-	-
8	1	1	-
8	-	2	-
8	1	-	1
8	-	-	2

3.2.6. Thermal Analysis

Characterization method using DSC was described in section 2.2.2.

3.2.7. X-Ray Diffraction Analysis

Characterization method using XRD was described in section 2.2.3.

3.2.8. Preparation of tablets

The spray-dried powders of indomethacin and PVP (8:2), indomethacin, PVP and MCC (ratio of 8:2:1), indomethacin, PVP and SMCC (8:2:1) as well as crystalline indomethacin alone, were selected for the preparation of tablets. The spray-dried powders were mixed with microcrystalline cellulose (diluent), sodium starch glycolate (3%) and magnesium stearate (0.2%) for 30 minutes in a mortar and pestle. The powder mixture was weighed and fed manually into the die of a single punch tableting machine (F3

Manesty, England) fitted with a flat surface punch of 13 mm diameter. The powder mixture was compressed into tablets with weight of about 700 mg. Each tablet contained 50 mg of indomethacin.

3.2.9. Dissolution study

Selecting a suitable dissolution medium is an important step in dissolution studies, since the choice of medium can affect the dissolution rate of drugs. Indomethacin is a weak acid ($pK_a = 4.5$), thus its solubility and dissolution rate can be enhanced when a basic medium is used. In this study, phosphate buffer solutions at various pH (pH 6.4–8.0) were tested for appropriate dissolution media. At pH 8.0, the rapid dissolution of indomethacin was undesirable for the dissolution studies, as it was difficult to distinguish the difference between the dissolution profiles of the spray dried indomethacin and that of the original material. In order to prolong the dissolution time of indomethacin, dissolution media with lower pH were examined. This extended time span allowed more samples to be taken, giving more accurate and reliable dissolution profiles. However, if the pH was further reduced below 7.2, the dissolution time was unnecessarily long. The phosphate buffer solution, pH 7.2 was therefore used as the medium for the dissolution studies.

The dissolution study of tablets was performed using the paddle method (Pharmatest, Germany). The dissolution medium comprised 900 ml of phosphate buffer pH 7.2 (BP, 1998). The temperature of the dissolution medium was maintained at 37 ± 0.5 °C with a stirring speed of 50 rpm. The samples were collected by automated sampler at preset time intervals and analysed spectrophotometrically (Beckman DU-62 Spectrophotometer, USA) at the detection wavelength of 320 nm. The percentage drug released was calculated and the mean dissolution values versus time profiles were plotted.

3.3. Results and Discussion

Operating conditions for spray drying of indomethacin were preliminarily investigated. The aspirator setting alters the velocity of the atomising air which provides the energy for atomisation of the feed material, subsequently affecting a degree of separation in the cyclone. High aspirator speed results in a high degree of separation in the cyclone. In dealing with a combustible solvent, when high aspirator speed was employed, the feed

rate of solution must be high (calculated within explosion limit), otherwise an explosion can occur. In practice, at high aspirator speed (setting no18) and a liquid feed rate (10 ml/min), no product was collected, presumably because it was lost in the air stream exhaust. Decreasing the aspirator speed to level 15 (feed rate 8.5 ml/min) also produced the same problem. Eventually, when an aspirator speed of level 10 was employed (feed rate 5.6 ml/min), the powder was obtained in the collecting vessel and the cyclone separator. Consequently, an aspirator speed of level 10 was used for further studies in settings (d), (e) and (f).

Feed concentration and inlet temperature were investigated at a constant aspirator speed and outlet temperature. The yield of the spray drying process was calculated from the weight of the dried product collected from the collecting vessel and cyclone separator, as a percentage of the initial quantity used in the feed solution (Table 3.3)

Table 3.3 Results of % yield for indomethacin spray dried under different conditions

Drying conditions Feed concentration; Inlet temperature	% Yield (n=1)
0.7%; 100 °C	43.6
0.7%; 150 °C	24.0
1.4%; 100 °C	65.5
1.4%; 150 °C	70.9

The percentage yield obtained was greater for the more concentrated feed solution (1.4% w/v). The 0.7% w/v feed solution yielded less product as the inlet temperature was increased. As a result of this investigation, a feed concentration of 1.4% w/v and an inlet temperature of 150 °C, at a constant outlet temperature were chosen as optimum spray drying condition.

The DSC thermograms of spray-dried indomethacin, spray-dried indomethacin and MCC together with spray-dried indomethacin and MCC with grinding are given in Figures 3.1-3.3. The thermogram of spray-dried indomethacin exhibited two endothermic melting peaks, suggesting the presence of both the metastable and stable crystalline forms. It was reported previously that spray-dried indomethacin demonstrated a glassy amorphous form (Corrigan et al, 1985). However, no evidence of the amorphous form was seen in the present study, even though different operating conditions were employed. The inconsistency of the present findings might be attributed to the different drying parameters. Another contributing factor could be the use of different feed concentrations. Corrigan et al (1985) did not explain in detail the conditions used for spray drying.

The spray-dried indomethacin and MCC showed two endothermic melting peaks of metastable and stable crystalline forms (Figure 3.2). Similarly, the spray-dried indomethacin and MCC with grinding prior to spray drying depicted two endothermic peaks (Figure 3.3).

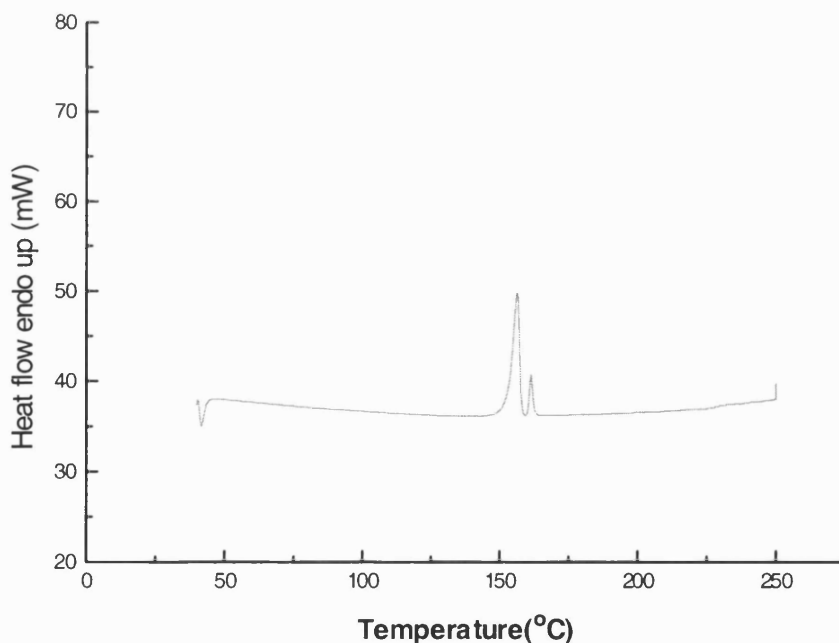


Figure 3.1 DSC scan of spray-dried Indomethacin in Ethanol/water

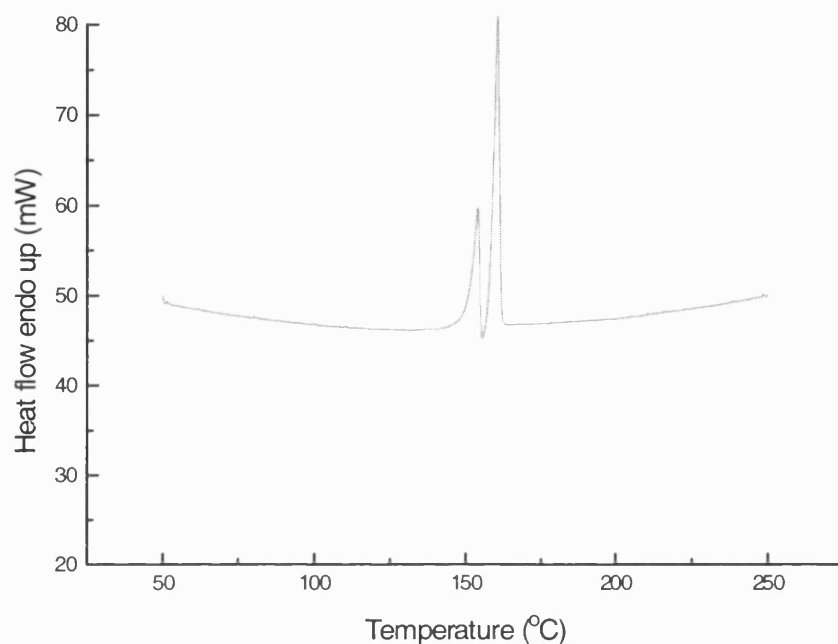


Figure 3.2 DSC scan of spray-dried dispersion of MCC in solution of Indomethacin in Ethanol/water

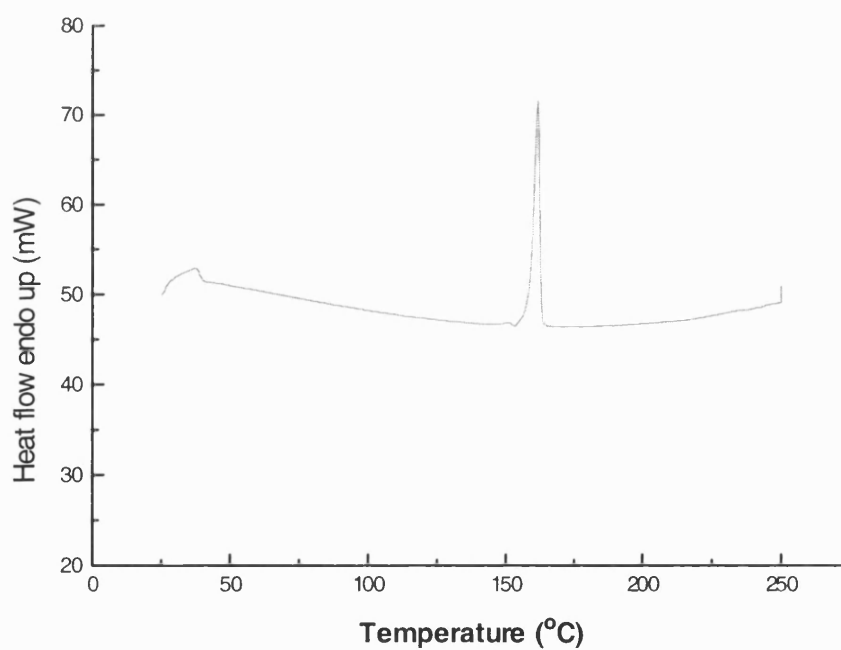


Figure 3.3 DSC scan of spray-dried ground mixtures of Indomethacin and MCC in Ethanol/water

In addition, the powder X-ray diffraction showed that the spray-dried samples were crystalline (Figures 3.4-3.6). The spray drying process did not alter the physical state of indomethacin or mixtures of indomethacin and MCC. Nakai et al. (1978a; 1978b) reported that MCC could convert crystalline volatile materials into the amorphous state by vibrational milling. However, grinding indomethacin with MCC could not produce the amorphous form in the present study. Moreover, grinding followed by spray-drying could not successfully change indomethacin into the amorphous form.

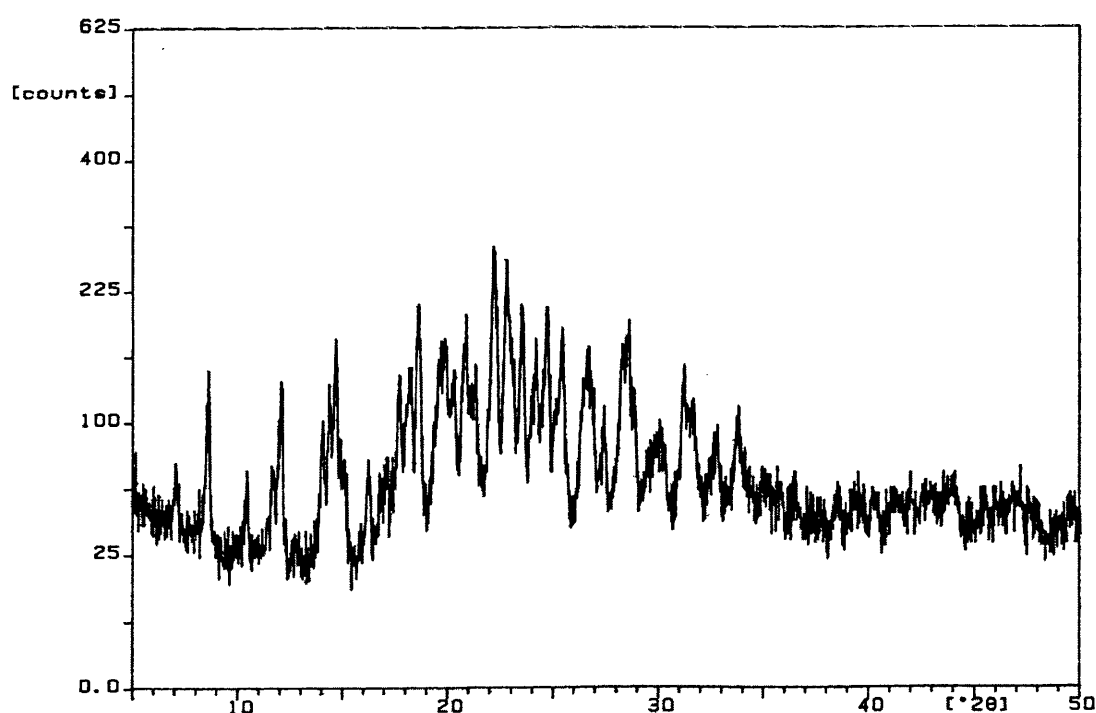


Figure 3.4 X-ray diffraction pattern of spray-dried Indomethacin in Ethanol/water

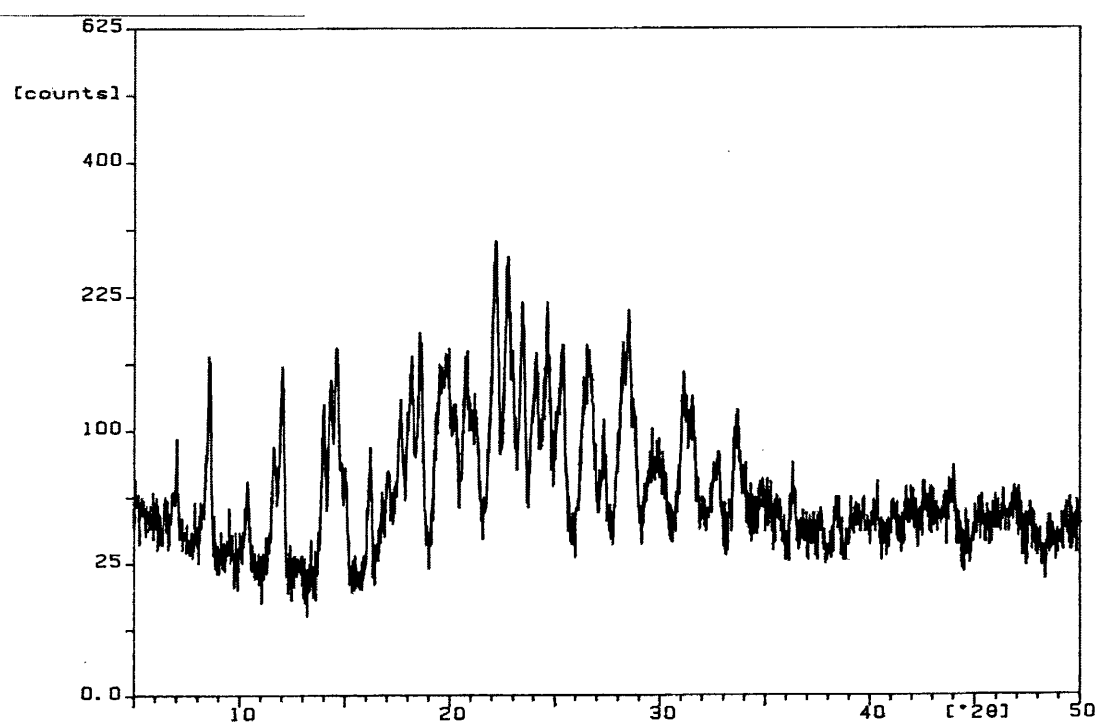


Figure 3.5 X-ray diffraction pattern of spray-dried dispersion on MCC in solution of Indomethacin in Ethanol/water.

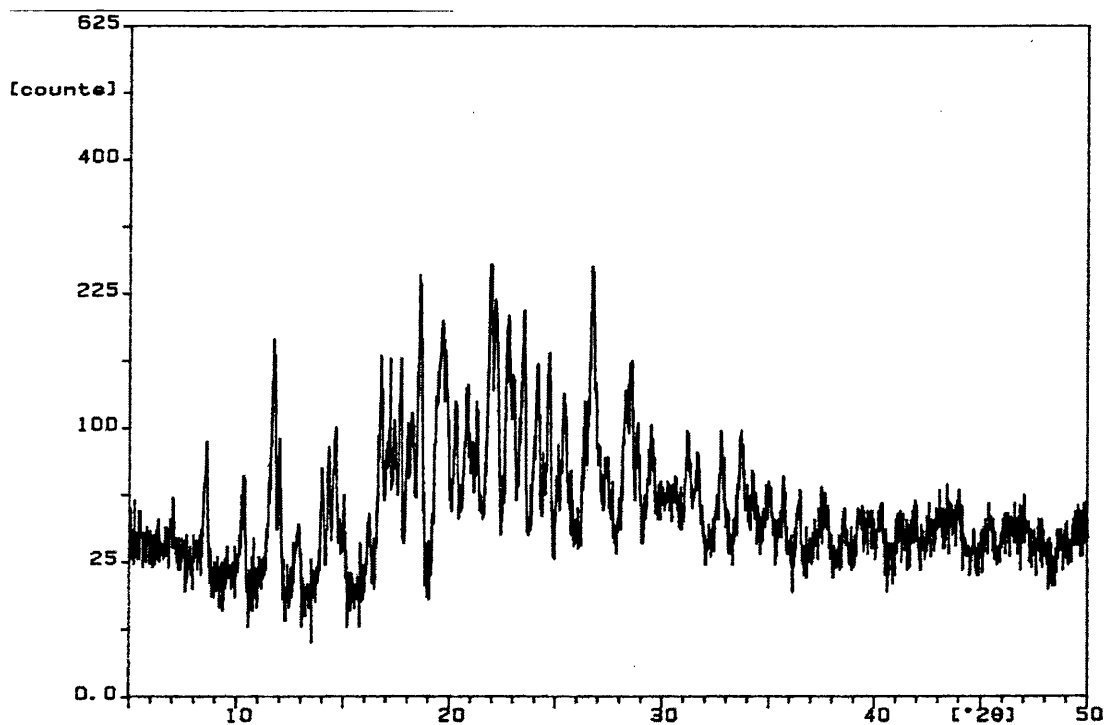


Figure 3.6 X-ray diffraction pattern of spray-dried ground mixtures of Indomethacin and MCC in Ethanol/water

A previous study of spray-dried indomethacin-PVP showed the existence of a higher energy amorphous drug phase in systems containing 20% PVP and above (Corrigan and Holohan, 1985). The DSC scans of spray-dried indomethacin and PVP systems generated in the current study are shown in Figures 3.7-3.10. The area under the single endothermic peak, which corresponded to melting of the drug at 155 °C, decreased with increasing PVP content. The peak disappeared at 20%PVP and above. The X-ray diffraction (Figures 3.11-3.14) results further suggested that for spray-dried indomethacin-PVP powders, at PVP ratio of 20% and above, indomethacin existed as an amorphous form.

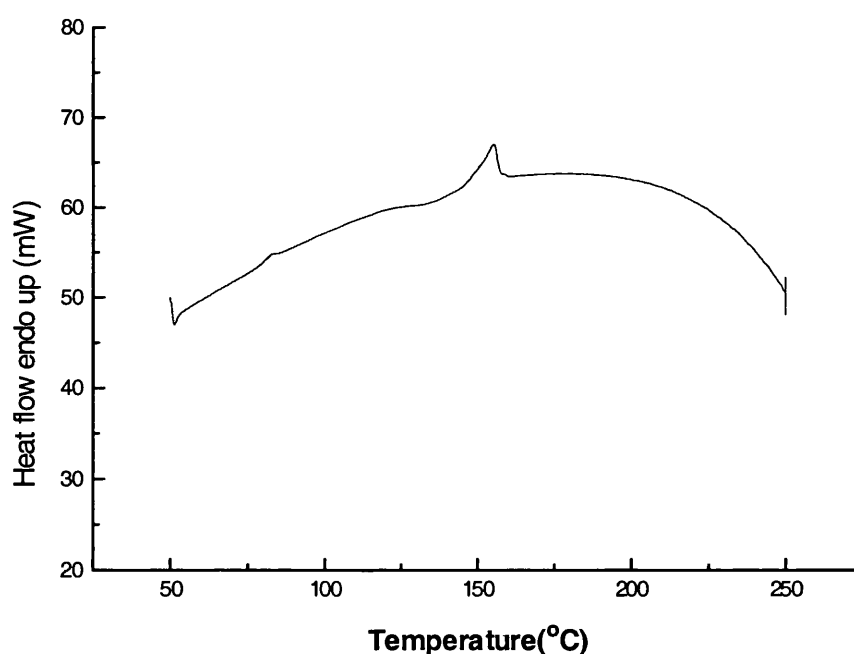


Figure 3.7 DSC scan of spray-dried Indomethacin with PVP 5%

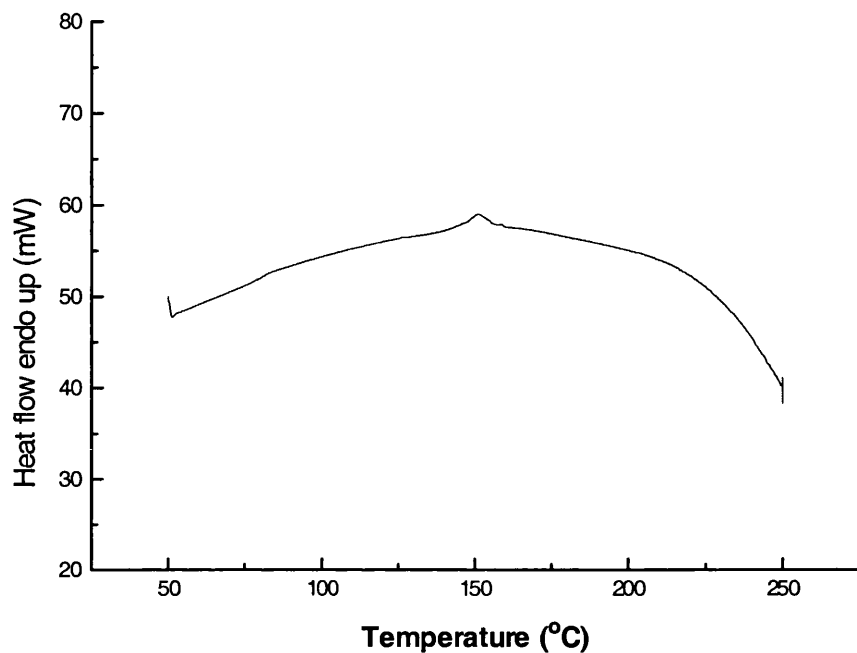


Figure 3.8 DSC scan of spray-dried Indomethacin with PVP 10%

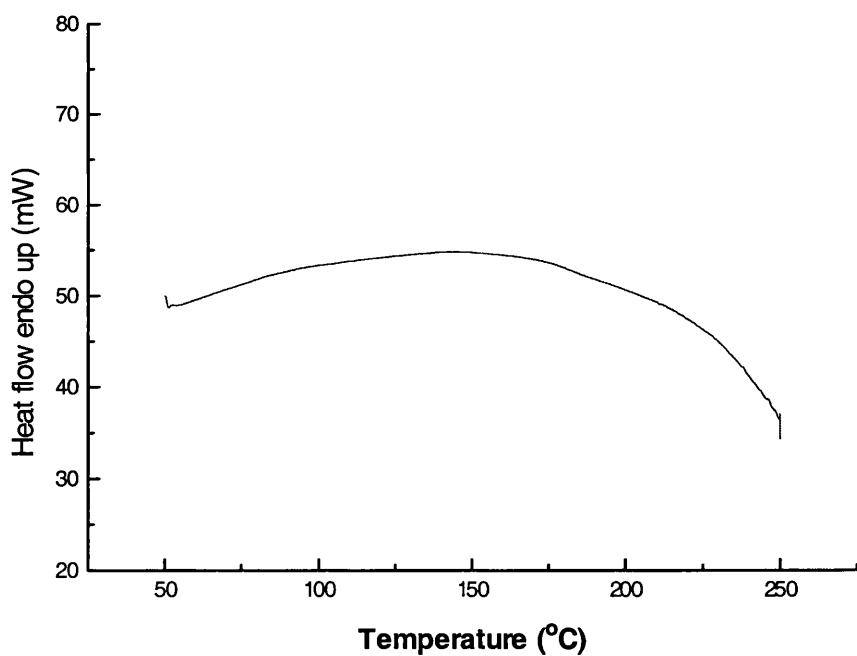


Figure 3.9 DSC scan of spray-dried Indomethacin with PVP 20%

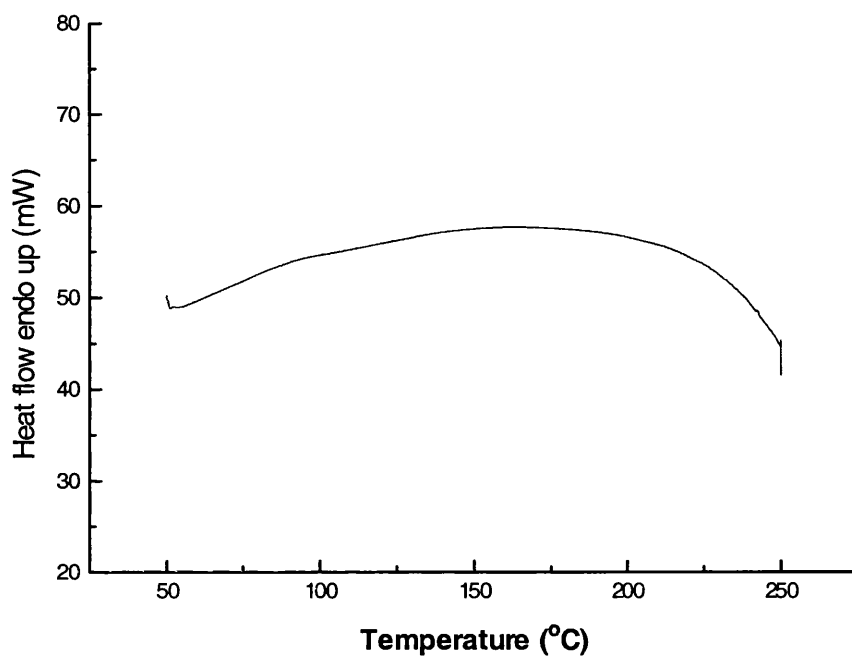


Figure 3.10 DSC scan of spray-dried Indomethacin with PVP 60%

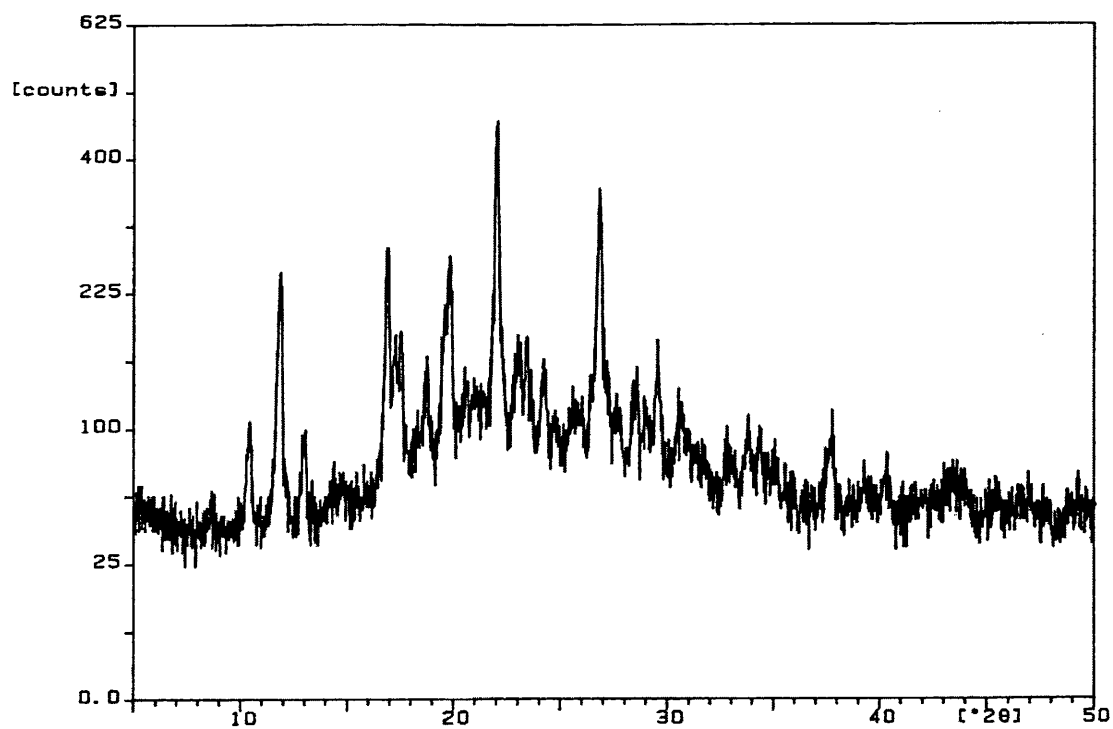


Figure 3.11 X-ray diffraction pattern of spray-dried Indomethacin with 5% PVP

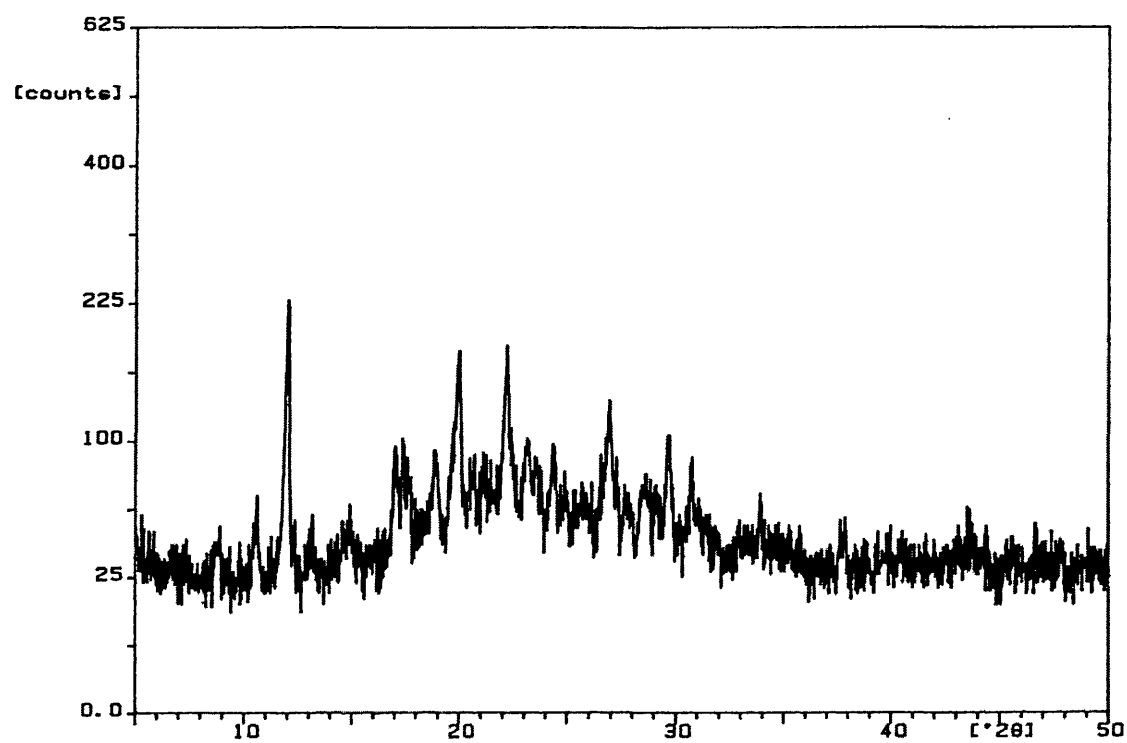


Figure 3.12 X-ray diffraction pattern of spray-dried Indomethacin with 10% PVP

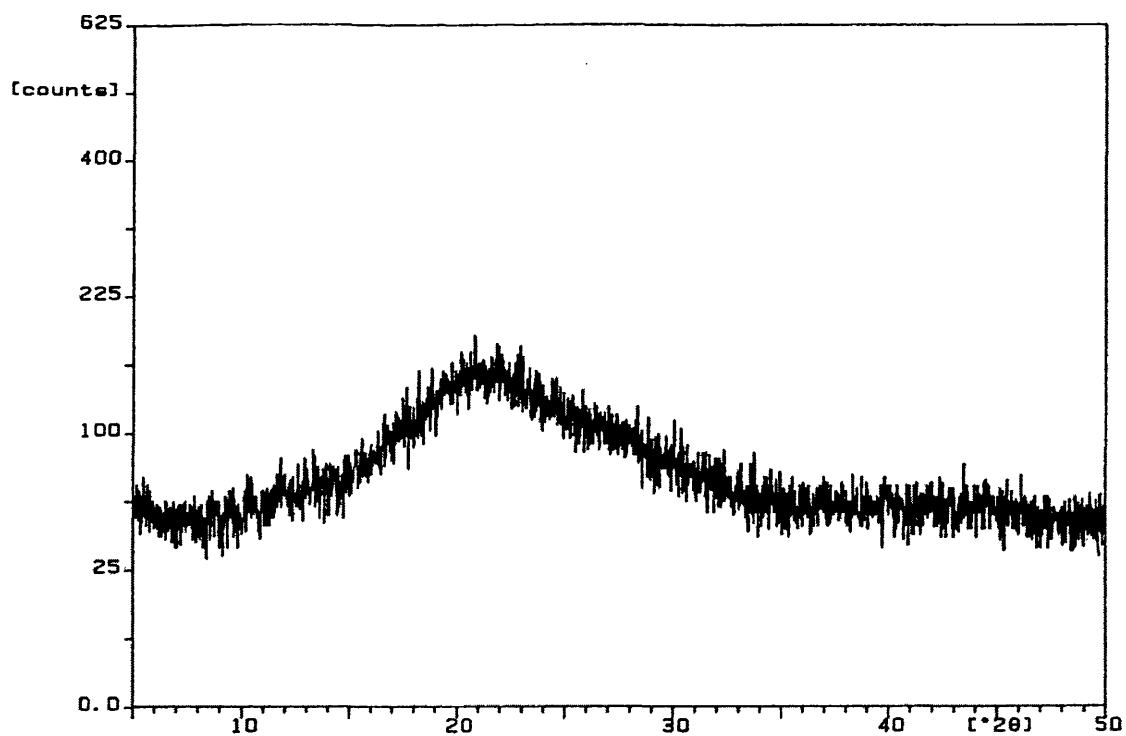


Figure 3.13 X-ray diffraction pattern of spray-dried Indomethacin with 20% PVP

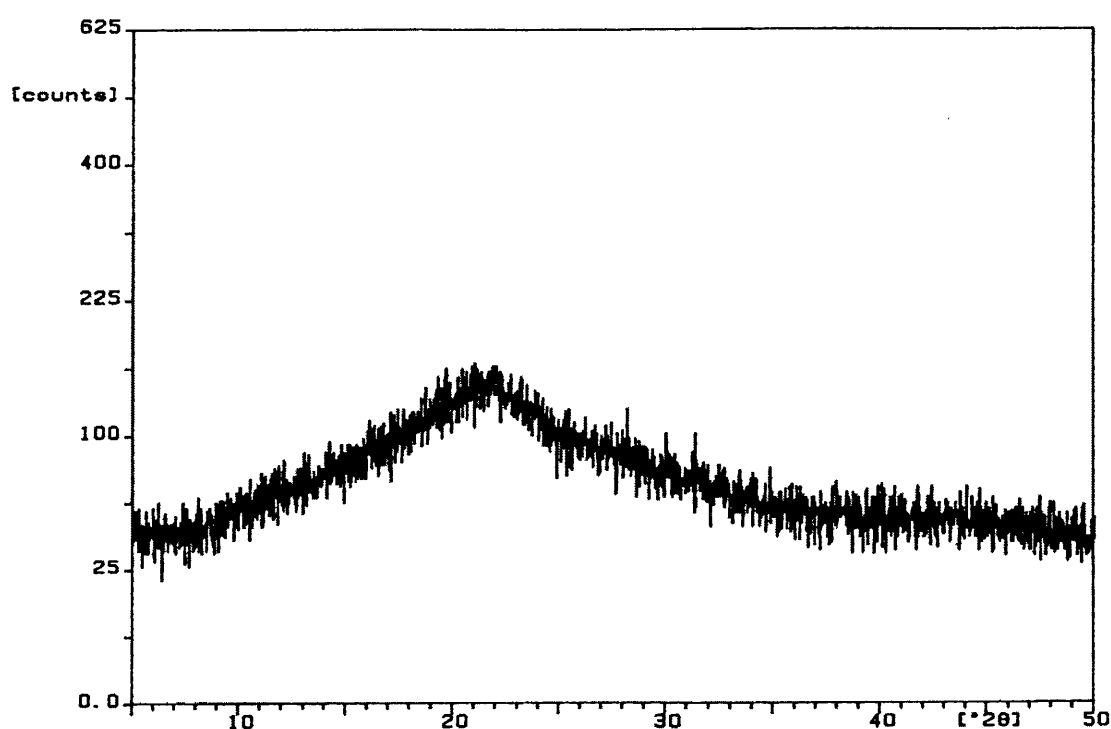


Figure 3.14 X-ray diffraction pattern of spray-dried Indomethacin with 60% PVP

Table 3.4. The powder X-ray diffraction results of indomethacin and PVP mixture at various compositions.

Sample Compositions		X-ray diffraction result
Indomethacin	PVP	
9.5	0.5	Crystalline
9	1	Crystalline
8	2	Amorphous
7	3	Amorphous
6	4	Amorphous
5	5	Amorphous
4	6	Amorphous

The x-ray diffraction results of spray-dried indomethacin with varied proportions of PVP and MCC are illustrated in Table 3.4.

Table 3.5. The powder X-ray diffraction results of indomethacin with various amount of PVP and MCC or SMCC.

Sample Compositions				X-ray diffraction result
Indomethacin	PVP	MCC	SMCC	
8	2	-	-	Amorphous
8	1	1	-	Crystalline
8	-	2	-	Crystalline
8	1	-	1	Crystalline
8	-	-	2	Crystalline

The X-ray diffraction results of indomethacin with various amount of PVP and MCC or SMCC are shown in Table 3.5. When the PVP content was reduced to less than 20%, crystalline indomethacin was obtained. Replacing part of PVP with MCC or SMCC could not produce amorphous indomethacin. The results further suggested that the presence of PVP and its concentration was crucial for preparing amorphous indomethacin.

The powder X-ray diffraction results of spray-dried indomethacin with 20% PVP with varied percentages of MCC and SMCC from 10% to 30% are given in Table 3.6. All these systems were amorphous. Furthermore, after 3-months storage at 25 °C with 0% relative humidity, all systems remained amorphous, indicating that the inclusion of MCC or SMCC was not essential as they did not affect the physical characteristics of spray-dried indomethacin with 20% PVP. In the presence of 20%PVP, amorphous indomethacin could be produced.

Table 3.6. The powder X-ray diffraction results of indomethacin and PVP with various percentages of MCC or SMCC.

Sample Compositions				X-ray diffraction result
Indomethacin	PVP	%MCC	%SMCC	
8	2	-	-	Amorphous
8	2	10	-	Amorphous
8	2	20	-	Amorphous
8	2	30	-	Amorphous
8	2	-	10	Amorphous
8	2	-	20	Amorphous
8	2	-	30	Amorphous

The mean dissolution profiles of tablets prepared from spray dried indomethacin, indomethacin and PVP (ratio of 8:2), indomethacin and MCC (ratio of 8:2), indomethacin and SMCC (8:2), indomethacin, PVP and MCC (ratio of 8:2:1), indomethacin, PVP and SMCC (8:2:1) as well as crystalline indomethacin are shown in Figure 3.15. It can be seen that the dissolution rates of all spray-dried powders were higher than that of the non-spray dried crystalline indomethacin. With regard to DSC results, the spray dried indomethacin produced a mixture of gamma and alpha crystalline forms (alpha metastable form was in the majority). The spray dried indomethacin with 20 % MCC and the spray dried indomethacin with 20% SMCC produced a mixture of gamma and alpha crystalline forms (gamma stable form was in the majority). Thus, it can be noted that both dissolution rate of the spray dried system containing indomethacin and 20% MCC and the spray dried system containing indomethacin and 20% SMCC were higher than that of the non-spray dried indomethacin but lower than that of the spray-dried indomethacin.

On the other hand, the mean dissolution profiles of indomethacin and 20%PVP, indomethacin with 20%PVP and 10%MCC or SMCC were superimposable. The incorporation of MCC did not seem to alter the drug release. The higher dissolution rate of the spray-dried powder was expected as indomethacin was in the amorphous form.

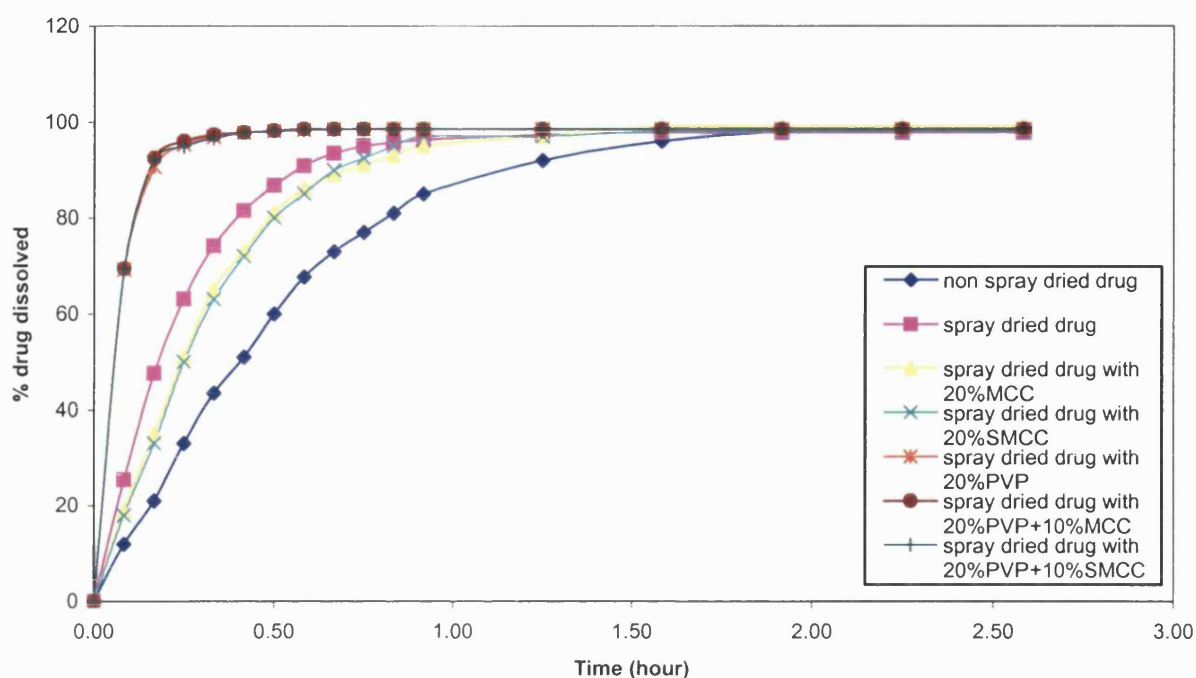


Figure 3.15 Dissolution profiles of spray-dried Indomethacin with polymer

3.4 Conclusions

Simple grinding of indomethacin with MCC did not yield indomethacin in an amorphous form. Spray dried indomethacin remained crystalline, as did co-spray dried indomethacin and MCC. The presence of PVP at 20% and above produced amorphous indomethacin. Adding the third component, either MCC or SMCC, did not affect the physical characteristics of the spray dried product.

The results of this element of the study showed that the physical characteristics of indomethacin solids spray-dried from non-aqueous solutions depended on the type and quantity of additives. The initial indomethacin dissolution rate of tablets prepared from co-spray dried indomethacin with 20%PVP was higher than that of non-spray dried tablets. In conclusion, to improve the dissolution rate of indomethacin, co-spray drying with 20% PVP was recommended.

Chapter 4

Precipitation using supercritical

CO₂ as an antisolvent

4.1 Introduction

In this part of the study, a new approach to enhance the dissolution of pharmaceuticals is presented, and the focus was particularly on indomethacin, a model compound with low water solubility. Precipitation using sc-CO₂ as an antisolvent may also be an alternative technique to prepare amorphous materials. Although supercritical fluids based methods often result in crystal formation, the fast precipitation should not allow the organization of the compound into a crystalline form. Consequently, in some cases the processed products show high levels of amorphous content. Amorphous sodium chromoglycate has been prepared using Solution Enhanced Dispersion by Supercritical Fluids technique (Jarrmo et al, 1997). Reverchon et al (1999, 2000) produced amorphous zinc acetate and amorphous amoxicillin using the Supercritical Antisolvent method.

The aim of this part of the study was to investigate the characteristics of indomethacin precipitated from different types of organic solvents using sc-CO₂ as an antisolvent. The method of preparation known as precipitation with compressed antisolvents (PCA) was employed. A small scale PCA apparatus was designed and constructed in the laboratory. The influence of process parameters, which included drug concentration and solution flow rate on the characteristics of the indomethacin powders were examined using SEM, DSC and powder X-ray diffraction.

4.2. Materials and Methods

4.2.1. Materials

Indomethacin, polyvinylpyrrolidone, ethanol, acetone, chloroform, dichloromethane, N,N-dimethylformamide, distilled water. The details of these materials are given in section 2.1. Industrial grade carbon dioxide (99.95% purity) was supplied by British Oxygen Company, England.

4.2.2. Precipitation of indomethacin using water as an antisolvent

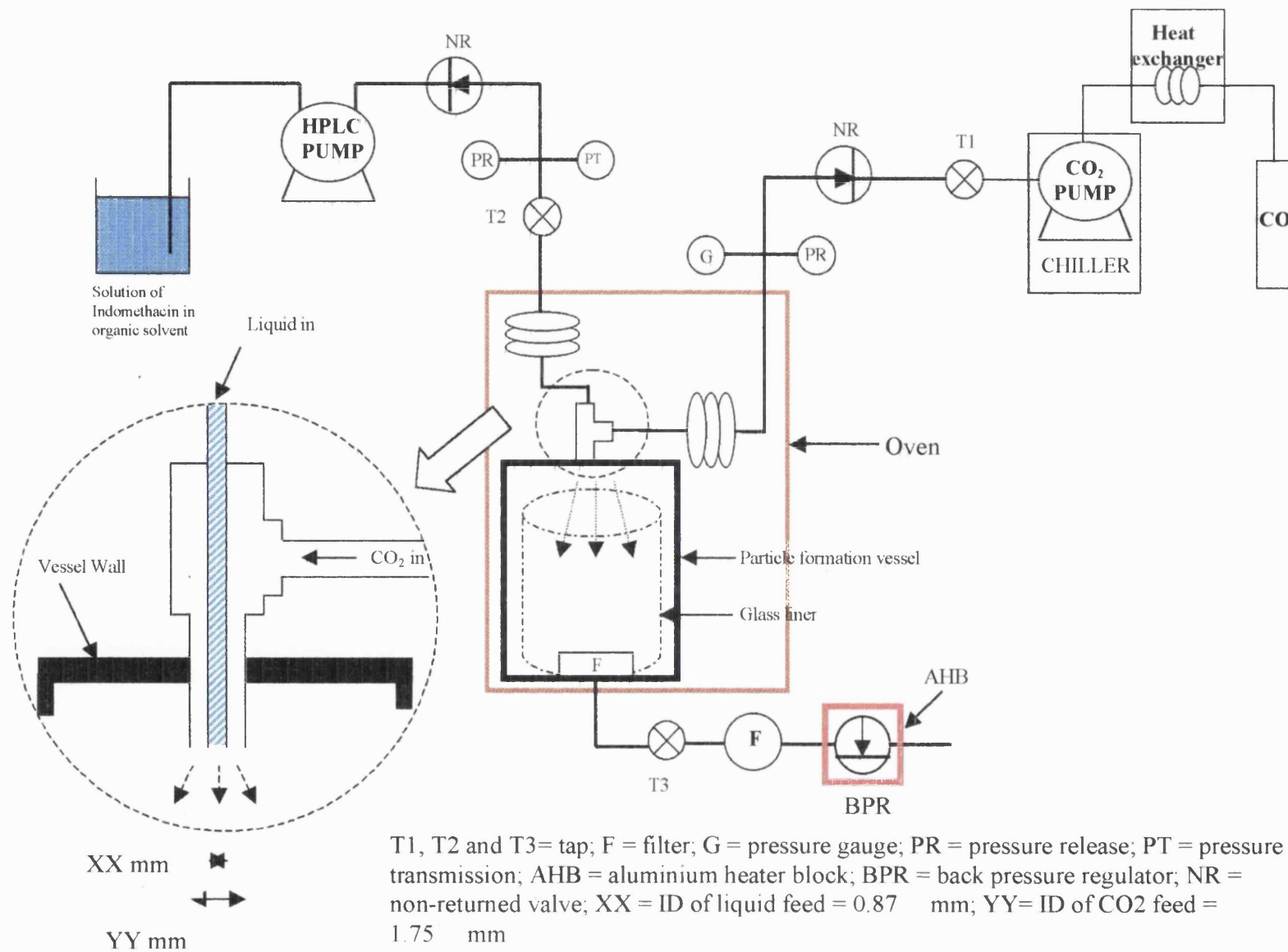
Indomethacin solutions of concentrations 5.0, 12.5, 20.0 and 33.3% w/v were prepared by dissolving in ethanol and heating at approximately 70 °C. Distilled water at room temperature was added to the indomethacin saturated ethanolic solution. The precipitated crystals were removed by filtration and dried under vacuum.

4.2.3. Construction and design of PCA apparatus

The schematic of the experimental apparatus is depicted in Figure 4.1. The liquid feed (internal diameter: 0.88 mm) and the CO₂ antisolvent feed (internal diameter: 1.75 mm) were brought together with the concentric nozzle (via a T-piece) into the reaction vessel (50 ml internal volume). Solution flow rate was controlled using an HPLC pump (model 302, Gilson, France). Liquid CO₂ was obtained from a 55 Bar liquid withdrawal CO₂ cylinder through a heat exchanger into the programmable HPLC pump (Model 305, Gilson, France). The pump head (10 ml) and pump inlet feed of CO₂ were chilled to approximately -10°C using a series of heat exchangers (Haake CH and F3, Fisons, Germany). CO₂ was warmed above its critical point via a coil inside the oven (TC 1900 temperature controller, ICI, Australia) before entering the high-pressure reaction vessel (40 ml internal volume). The vessel included a glass liner for ease of product recovery. Non-return valves were inserted in the liquid feed and CO₂ feed to avoid flow inversion in both feeds. The vessel was placed in an oven to maintain the temperature of the system. It was necessary to increase the supercritical-solution temperature to avoid liquid phase crossing during depressurization. A 7 µm stainless steel filter frit was situated at both the bottom of the reaction vessel and between the vessel and the back pressure regulator. It trapped any precipitated solid but allowed the CO₂-organic solvent solution to pass through in the washing step. The pressure in the whole system was regulated by a manually set back pressure regulator (BPR, Tescom, model 26-1762-24-194). Pressure in the CO₂ feed was measured using a pressure gauge. Pressure in the liquid feed was measured by a pressure transducer, housed in a custom made stainless steel body and connected to a digital read out (RDP electrics, model E705). The powders were collected in the vessel. At the end of the precipitation process, the vessel was washed with CO₂ to eliminate the organic solvent. The organic solvent was collected at the outlet pipe of the BPR. A temperature-controlled external heating block was located around the BPR to avoid intermittent freezing/blockage of the outlet pipe of the BPR.

The design of the PCA apparatus which included the reaction vessel, HPLC pump for liquid feed and adapted HPLC pump for CO₂ feed, was shown in Figures 4.2-4.4, respectively.

Figure 4.1 PCA Apparatus Schematic Diagram.



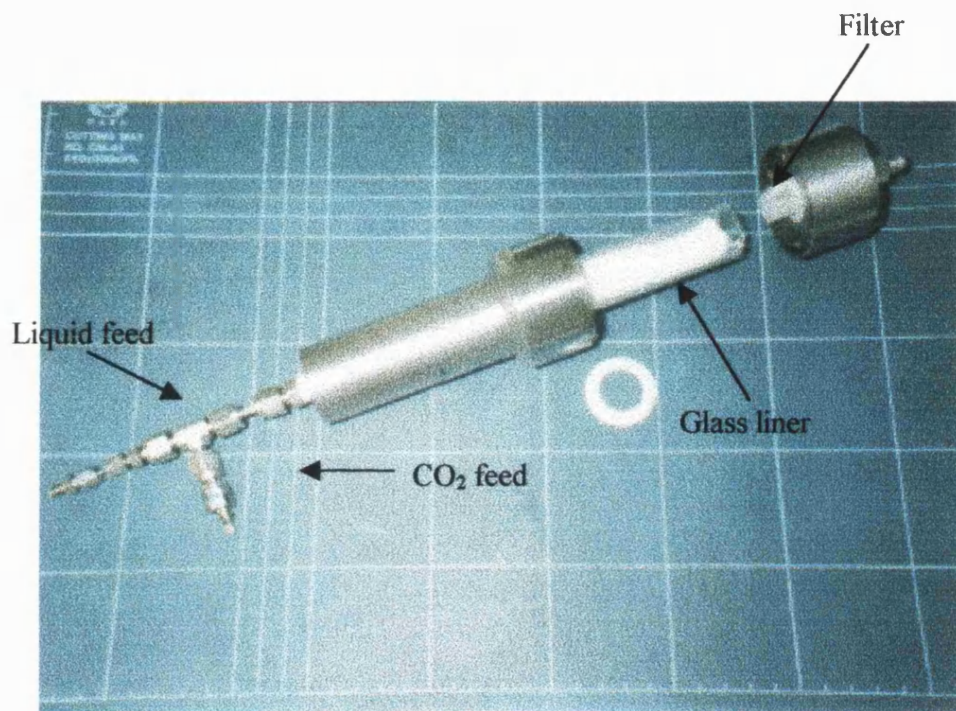


Figure 4.2 The reaction vessel required 6 screws at the bottom. The top of the vessel was connected with the concentric nozzle. The liquid and CO_2 feeds can clearly be seen. Notably this design has a glass liner within the vessel to enable the precipitated material to be removed without any disturbance.

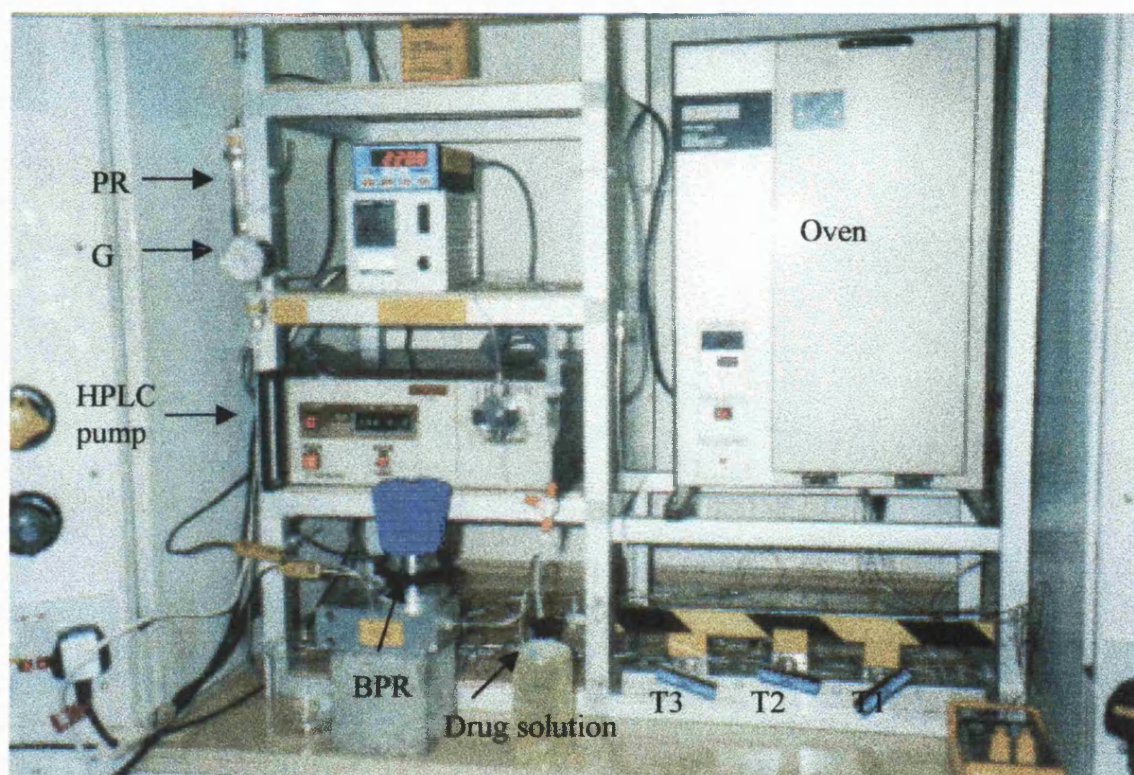


Figure 4.3 PCA apparatus. The HPLC pump was used to deliver the drug solution.

The vessel was placed in the oven.

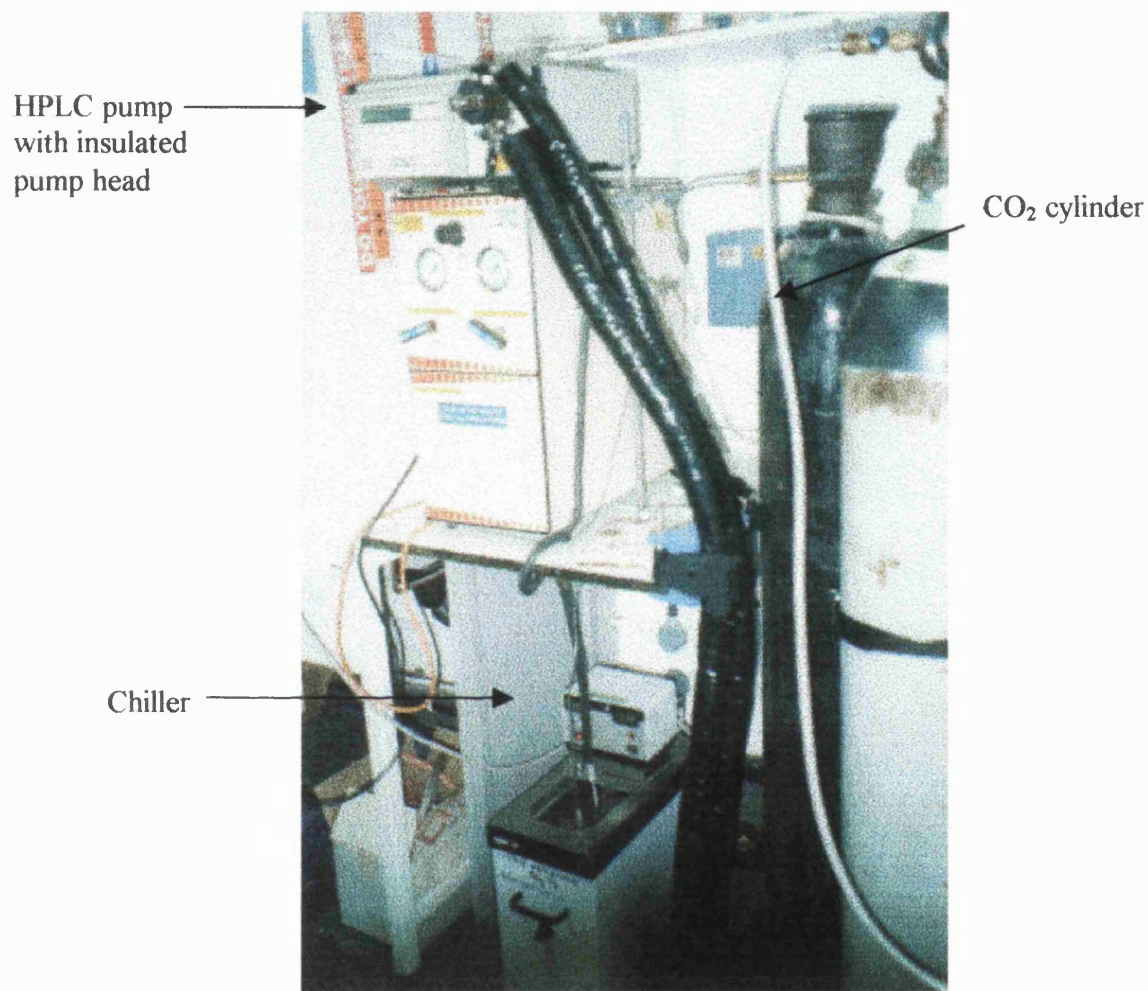


Figure 4.4 The adapted HPLC pump that has a chilled head for control of the CO_2 flow rate into the precipitation vessel.

4.2.4. Procedure

The oven was switched on and the required temperature of 22 °C or 40 °C was maintained. The chiller was switched on. Liquid CO₂ was directed from a cylinder into a pump at a constant flow rate of 10 ml/min, and delivered to the preheating coil which was inside the oven (Figure 4.1 taps T1 and T3 open). The reaction vessel was pressurised to the required pressure by adjusting BPR (Figure 4.1 tap T2 close). The drug solution pump was switched on. The antisolvent precipitations were started by opening the tap T2 to allow a flow of drug solution passing through a nozzle. At the end of the precipitation process, the drug solution pump was switched off and the tap T2 was closed. The sc-CO₂ continued to flow into the chamber. The product in the vessel was washed with 10 ml/min of supercritical CO₂ for 30 min to eliminate the organic solvent. After that, the CO₂ pump was switched off with tap T1 closed. The BPR was fully open to remove CO₂ from the system. The pressure was checked to be 0 bar before opening up the vessel. The product was collected in the vessel and stored in a silica gel desiccator at room temperature.

4.2.5. Precipitation of indomethacin from dichloromethane

Indomethacin solutions of concentrations 0.83, 1.67 and 3.33 %w/w were prepared by dissolving in dichloromethane. The sc-CO₂ was fed into the reaction vessel at a constant flow rate of 10 ml/min. The experiment started when the operating pressure reached 150 bar and the liquid solution was fed into the reactor chamber through the nozzle. The drug solution at flow rates between 0.5 and 1.0 ml/min and supercritical CO₂ at 10 ml/min were pumped into the reaction vessel. The precipitation process was allowed to continue for 30 min. Two different sets of parameters were used. One set was at ambient temperature (22 °C), pressure of 150 bar and CO₂ density of 0.5 g/ml and the other set at 40 °C, pressure of 150 bar and CO₂ density of 0.8 g/ml. At the end of the precipitation process, the product in the vessel was washed with supercritical CO₂ as described in section 4.2.4. The product was collected and stored in a silica gel desiccator at room temperature.

4.2.6. Precipitation of indomethacin from various organic solvents

Accurately weighed indomethacin (100 mg) was added slowly into various organic solvents, namely, dichloromethane, acetone, chloroform, dichloromethane:ethanol (1:1, v/v), ethanol and dimethyl-formamide. The amount of indomethacin dissolved before the drug supersaturate was recorded and taken as the maximum concentration of drug dissolved. The system was operated at a temperature of 40 °C, pressure of 150 bar and CO₂ density of 0.8 g/ml. The sc-CO₂ was initially fed into the reaction vessel at a constant flow rate. The experiment started when the operating pressure had been reached and the liquid solution was fed into the reactor chamber through the nozzle. The drug solution was pumped at flow rates between 0.125 and 1.0 ml/min and supercritical CO₂ at 10 ml/min into the reaction vessel and allowed to react for 30 min. At the end of the precipitation process, the product in the vessel was washed with sc-CO₂ as described in section 4.2.4. The product was collected and stored in a silica gel desiccator at room temperature.

4.2.7. Precipitation of indomethacin and PVP

Mixtures of indomethacin and polyvinylpyrrolidone in various proportions were dissolved in dichloromethane to produce a 3.33%w/v solution. The amount of PVP utilised in the experiments ranged from 5-60%w/w of the indomethacin content. Feeding rates of 0.5 ml/min and 10 ml/min were used to deliver the drug solution and sc-CO₂ into the reaction vessel. The experiment was run using similar parameters as described earlier.

4.2.8. Scanning electron microscopy

The details were explained in section 2.2.1.

4.2.9. Thermal analysis

The details were explained in section 2.2.2.

4.2.10. X-ray diffraction analysis

The details were explained in section 2.2.3.

4.3. Results and Discussion

Precipitation of indomethacin using water as an antisolvent

Prior to the construction of the PCA apparatus, a simple experiment was conducted to examine the feasibility of using supercritical CO₂ as an antisolvent in the precipitation of indomethacin from organic solvents. The experiment employed water as an antisolvent to precipitate indomethacin from ethanolic solution. The indomethacin precipitated from the organic solvents appeared to be white and fluffy. When the powder was viewed under SEM, all the particles were seem to be needle shaped irrespective of the concentrations employed. Figure 4.5(a) and (b) show the SEM of the original material and indomethacin precipitated from 33.3% indomethacin in ethanolic solution using water as an antisolvent, respectively. The DSC profiles indicated that indomethacin existed as mixtures of both α and γ crystalline forms when precipitates from solution at concentration between 5-20%w/v. The mixture contained a higher proportion of α crystalline form as shown from the larger area under the melting peak (Figures 4.6-4.7). As seen in Figure 4.8, precipitates from solution at a concentration of 33.3%w/v contained only the α crystalline form of indomethacin. Figures 4.9 and 4.10 show the PXRD profiles of indomethacin prepared from 20% and 33.3% w/v ethanolic solutions, respectively. It can be observed that they are both the same profiles. The particular peak at 8.5 °2 θ identified the α polymorphic form. (Figures 4.6-4.7) It is possible that the very small endothermic peak at 162 °C was material converted from α form to γ form during the DSC run.

The physical appearance, SEM, DSC and PXRD results of indomethacin precipitated using water as an antisolvent are summarised in Table 4.1.

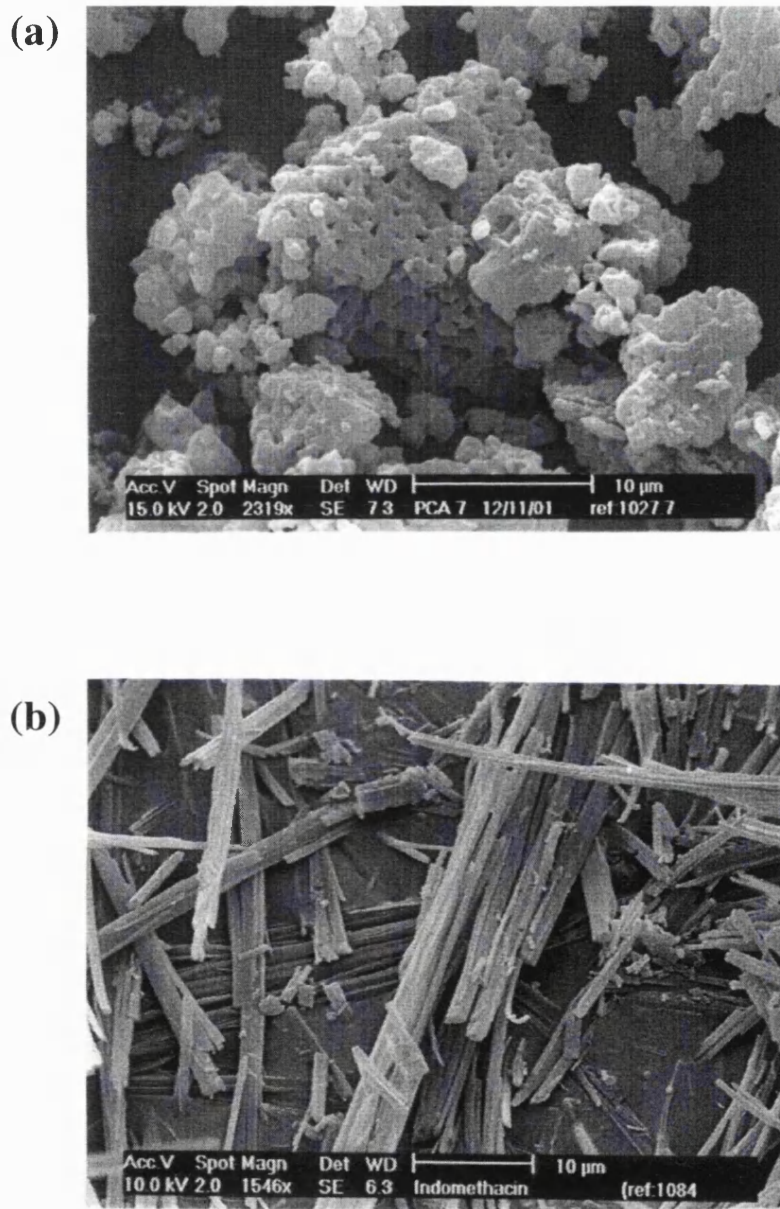


Figure 4.5 SEM photograph of indomethacin particles (a) unprocessed indomethacin (b) precipitated from 33.3% w/v ethanolic solution using water as an antisolvent.

Table 4.1 The physical appearance, SEM, DSC and PXRD results of indomethacin prepared at different concentrations precipitated using water as an anti-solvent.

Organic solvents	Maximum concentration (%w/v)	Observation	SEM	DSC & PXRD
Ethanol	33.3	Fluffy white powder	Needle shape	pure α
	20.0	Fluffy white powder	Needle shape	α and γ
	12.5	Fluffy white powder	Needle shape	α and γ
	5.0	Fluffy white powder	Needle shape	α and γ

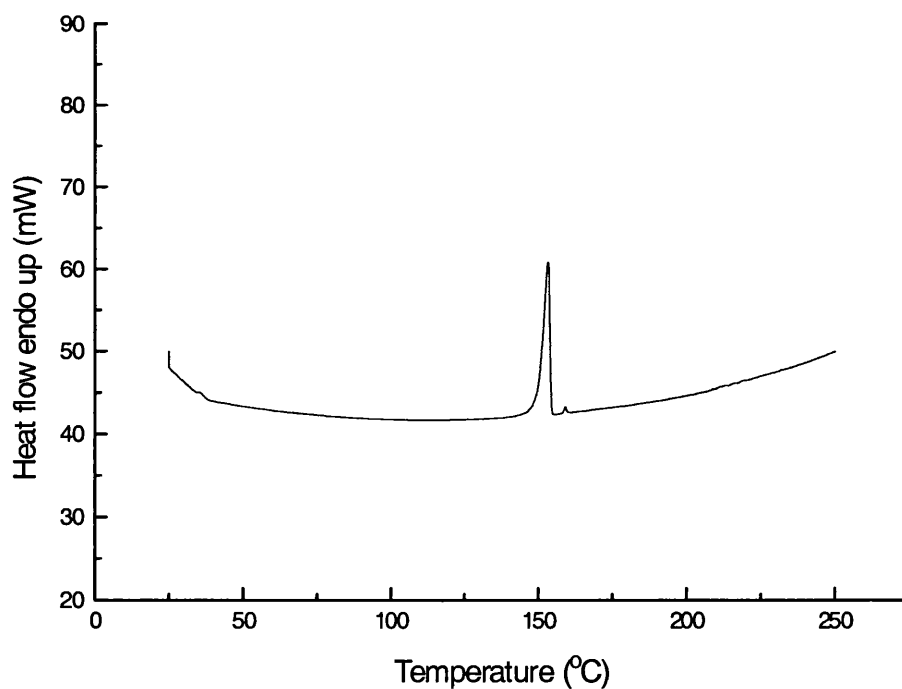


Figure 4.6 DSC scan of indomethacin recrystallized from 12.5% w/v of ethanolic solution using water as an antisolvent.

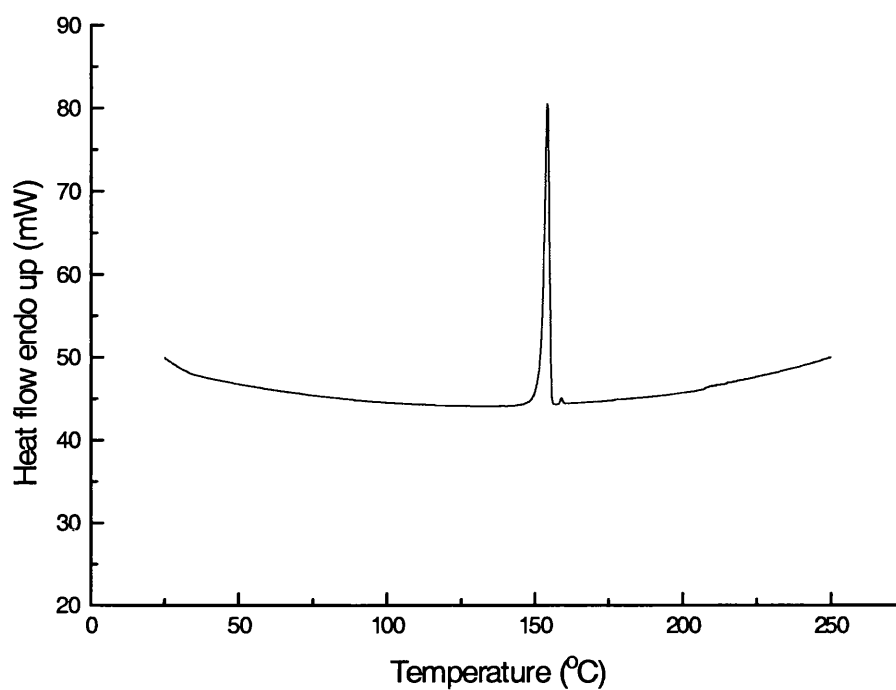


Figure 4.7 DSC scan of indomethacin recrystallized from 20% w/v of ethanolic solution using water as an antisolvent.

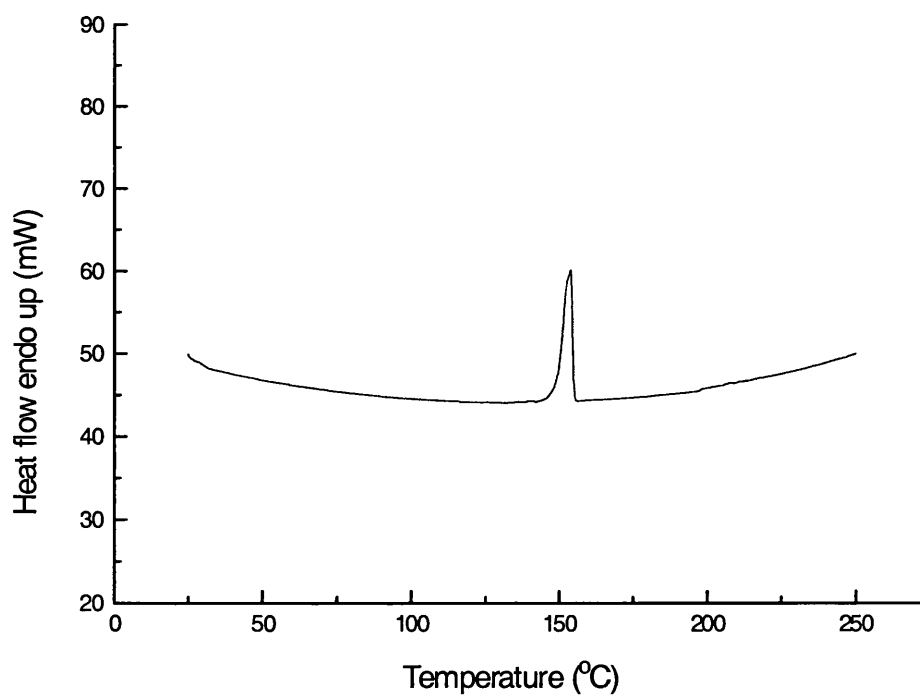


Figure 4.8 DSC scan of indomethacin recrystallized from 33.33% w/v of ethanolic solution using water as an antisolvent.

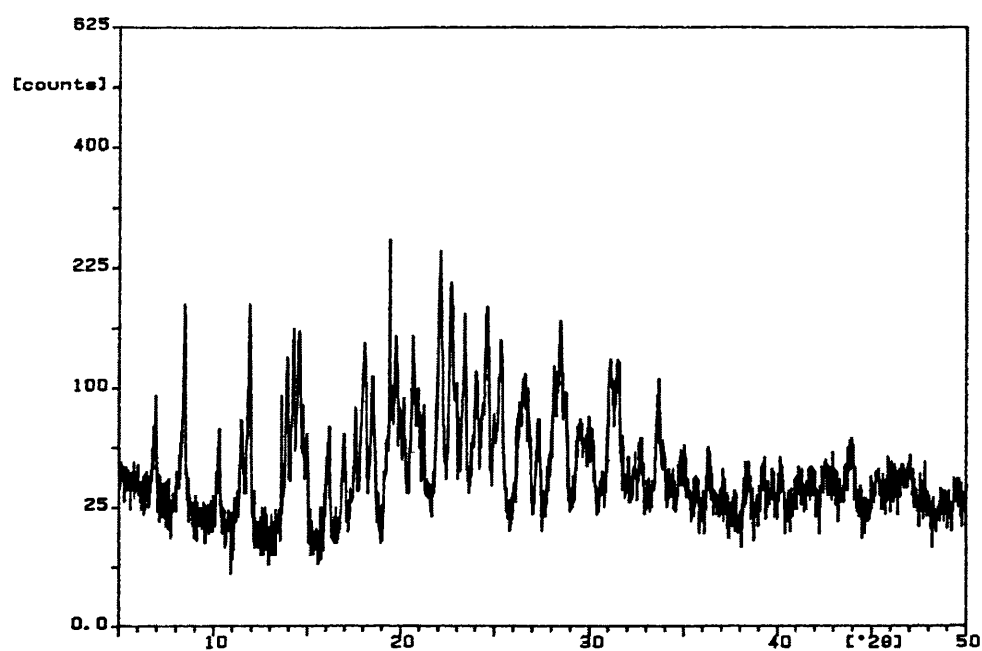


Figure 4.9 PXRD scan of indomethacin recrystallized from 20% w/v of ethanolic solution using water as an antisolvent.

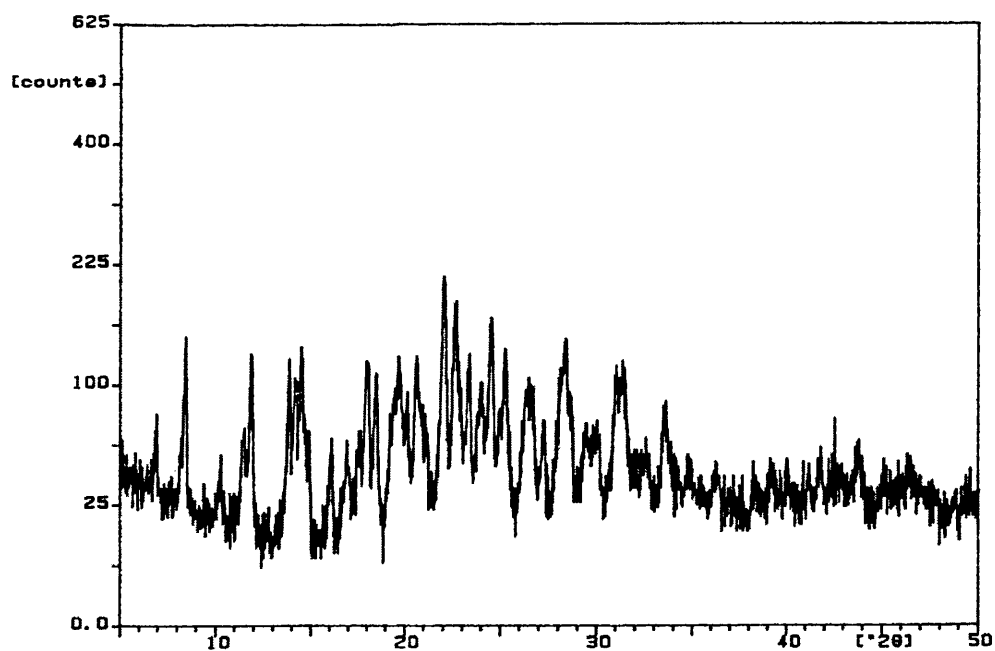


Figure 4.10 PXRD scan of indomethacin recrystallized from 33.33 % w/v of ethanolic solution using water as an antisolvent.

Precipitation of indomethacin using sc-CO₂ as antisolvent

Preliminary investigations were carried out to determine the effect of the processing temperature on the characteristics of precipitated particles. When the experiment was operated at ambient room temperature (22 °C), the temperature was below the critical point of CO₂ (31.1 °C) and sc-CO₂ could not be generated. As a result, the CO₂ used in the experiment consisted of two phases, namely, liquid and gas. Two types of powders having different colours, which stuck together, were obtained at all the different concentrations used. One was white and fluffy while the other one was yellow with rod-like shape. However, by increasing the temperature to 40 °C, the appearance of SCF products was homogeneous. Hence, this temperature was chosen to produce material for further investigations.

The SEM of the indomethacin particles prepared using dichloromethane as solvent and sc-CO₂ as antisolvent showed needle shapes (Figure 4.11). However, the DSC profiles of the indomethacin showed the presence of two crystalline peaks, α and γ crystalline forms (Figure 4.12). It can be noted that the composition of α form was higher than the γ form. PXRD further confirmed that indomethacin existed in α and γ crystalline forms (Figure 4.13). It seemed that the characteristics of indomethacin were not affected by varying the concentrations of indomethacin in dichloromethane solution and its feeding rate. The physical appearance, SEM, DSC and PXRD results of indomethacin precipitated from different concentrations and flow rates of drug solution using sc-CO₂ as antisolvent are given in Table 4.2.



Figure 4.11 Typical SEM photograph of indomethacin particles prepared using dichloromethane as solvent and sc- CO_2 as antisolvent.

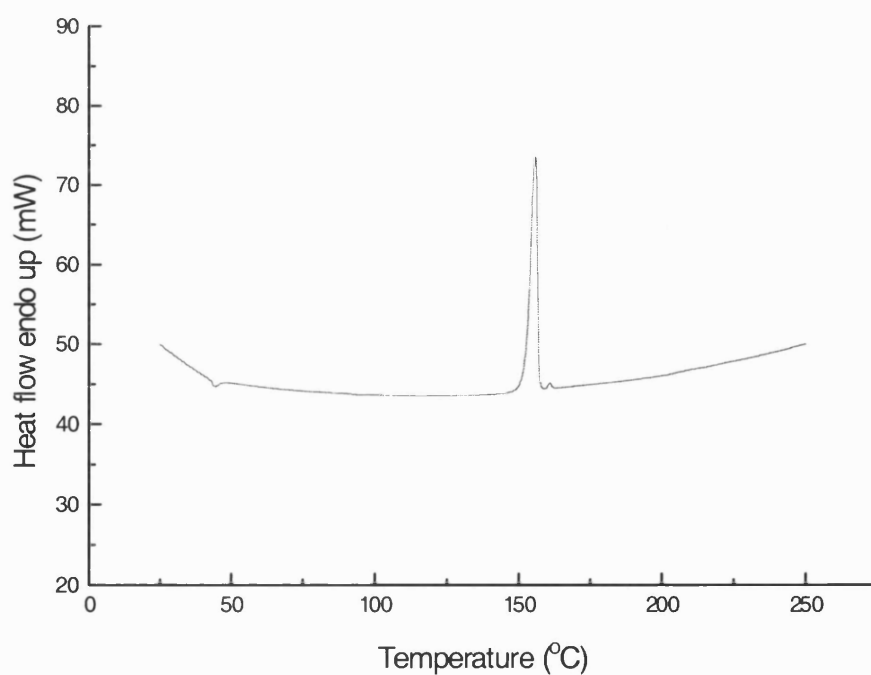


Figure 4.12 Typical DSC scan of indomethacin particles prepared using dichloromethane as solvent and sc- CO_2 as antisolvent.

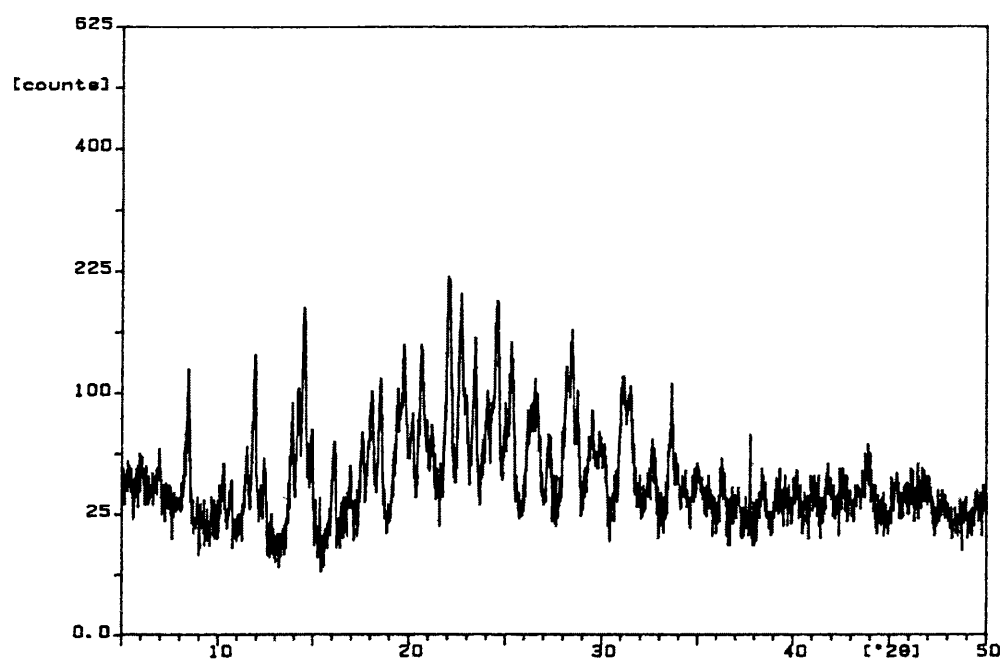


Figure 4.13 Typical PXRD profile of indomethacin particles prepared using dichloromethane as solvent and sc-CO₂ as antisolvent.

Table 4.2 The physical appearance, SEM, DSC and PXRD results of indomethacin precipitated from different concentrations and flow rates of drug solution.

Concentrations (%w/v)	Flow rate (ml/min)	Observation	SEM	DSC&PXRD
3.33	0.5	Fluffy powder white	Needle shape	α and γ
1.67	1.0	Fluffy powder white	Needle shape	α and γ
1.67	0.5	Fluffy powder white	Needle shape	α and γ
0.83	0.5	Fluffy powder white	Needle shape	α and γ
0.83	1.0	Fluffy powder white	Needle shape	α and γ

The maximum concentrations of indomethacin dissolved in the various organic solvents are shown in Table 4.3. Different solution flow rates were employed for indomethacin in different organic solvents because at values above those stated in Table 4.3, complete precipitation of indomethacin could not occur, which could be observed from the colour of the liquid removed through the vent of the back pressure regulator. When there was a complete precipitation, clear liquid could be seen through the vent. In contrast, if the precipitation process was not complete, yellow liquid could be seen, due to the presence of indomethacin in the liquid.

The SEM of indomethacin precipitated from dichloromethane and acetone showed needle shapes, indicating the presence of the α crystalline form. Figure 4.14(a) shows a needle shape of indomethacin prepared using acetone. In contrast, non-uniform rod-like particles were obtained when precipitated using ethanol, chloroform, dichloromethane:ethanol (1:1) and DMF. The SEM of indomethacin precipitated from chloroform is shown in Figure 4.14(b). The DSC results showed that indomethacin precipitated from various organic solvents composed of two crystalline peaks, α and γ crystalline forms (Figures 4.15-4.18). It can be noticed that in most samples the α form existed in a higher proportion than the γ form, especially when precipitated using acetone (Figure 4.17). Additionally, in Figure 4.17, the DSC curve of indomethacin precipitated from acetone had endo- and exothermic peaks at about 80-95 °C, which could be due to desolvation of acetone, and an endothermic peak at 155 °C which was due to fusion of the α form. Similarly, for Figure 4.18, DSC curve of indomethacin precipitated from chloroform had endo- and exothermic peaks at about 80-110 °C which was due to desolvation of chloroform and endothermic peaks at about 155 and 162 °C which could be due to fusion of α and γ form, respectively. The PXRD results confirmed that all the samples were composed of two polymorphs (Figures 4.19-4.21).

Table 4.3 The maximum concentration, physical appearance, SEM, DSC and PXRD results of indomethacin precipitated from various organic solvents using sc-CO₂ as antisolvent.

Organic solvents	Maximum concentration (%w/v)	Flow rate (ml/min)	Observation	SEM	DSC& PXRD
Dichloromethane	3.33	0.5	Fluffy white powder	Needle shape	α and γ
Acetone	3.75	0.25	Fluffy white powder	Needle shape	α and γ
Chloroform	3.75	0.25	Fluffy white powder	Non-uniform rod shape	α and γ
Dichloromethane :ethanol (1:1)	8	0.5	Fluffy white powder	Non-uniform rod shape	α and γ
Ethanol	1.25	0.5	Fluffy white powder	Non-uniform rod shape	α and γ^*
DMF	10	0.125	Fluffy yellowish powder with sticky liquid	-	NA

* DSC result only



Figure 4.14 (a) SEM of indomethacin particles prepared using Acetone as solvent and sc-CO_2 as antisolvent

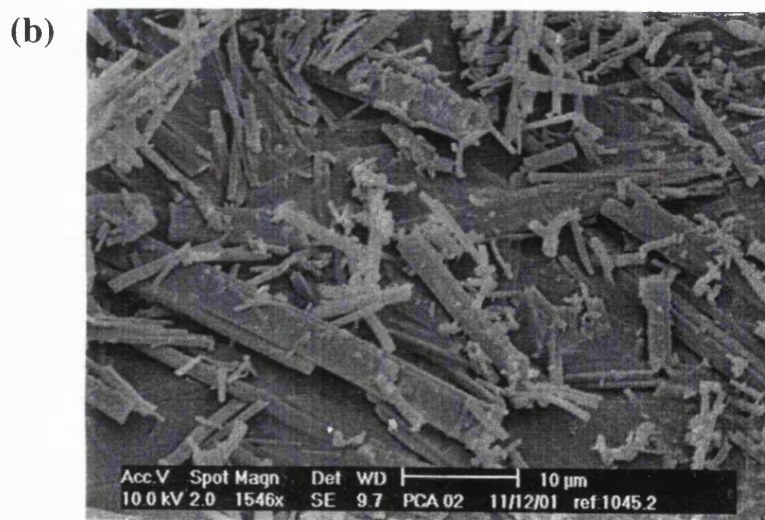


Figure 4.14 (b) SEM of indomethacin particles prepared using chloroform as solvent and sc-CO_2 as antisolvent

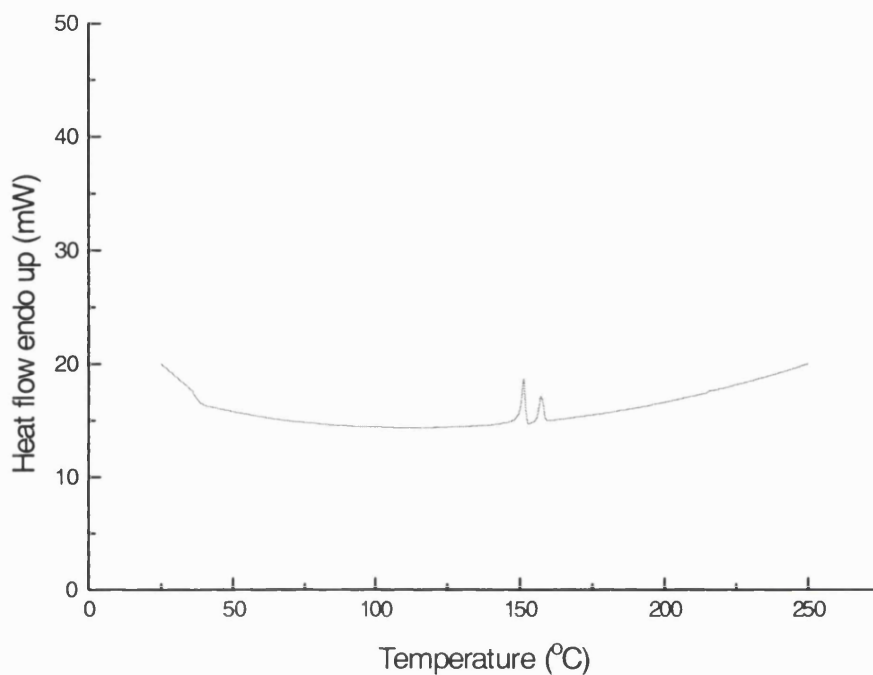


Figure 4.15 DSC of indomethacin particle prepared using ethanol as solvent and sc- CO_2 as antisolvent.

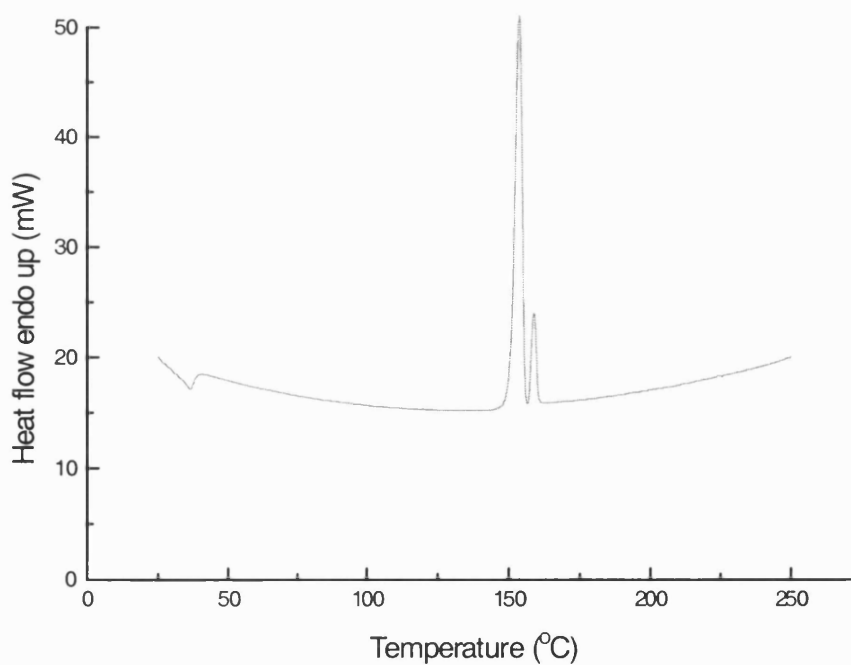


Figure 4.16 DSC of indomethacin particle prepared using dichloromethane: ethanol (1:1) as solvent and sc- CO_2 as antisolvent.

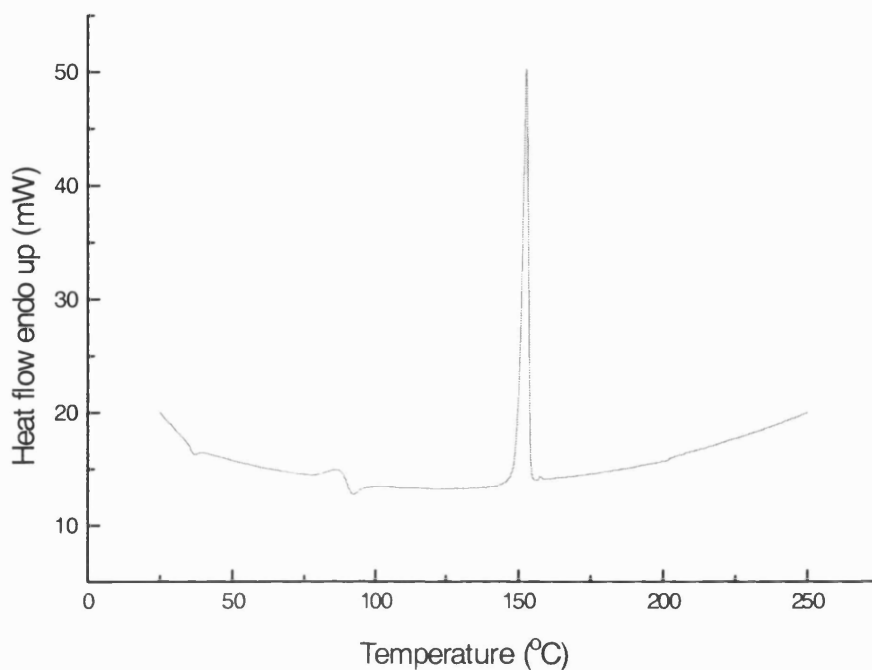


Figure 4.17 DSC of indomethacin particle prepared using acetone as solvent and sc- CO_2 as antisolvent.

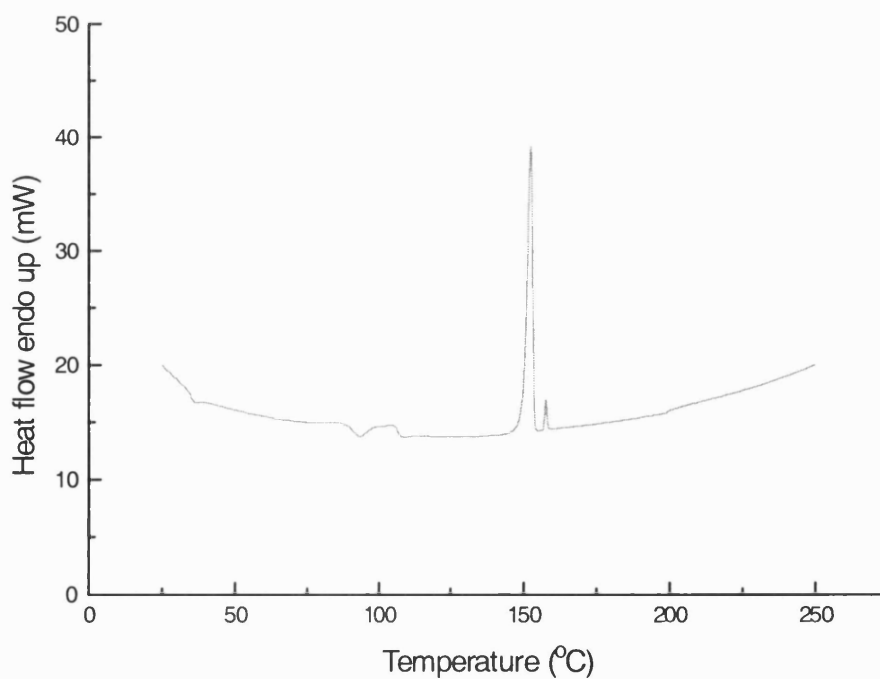


Figure 4.18 DSC of indomethacin particle prepared using chloroform as solvent and sc- CO_2 as antisolvent.

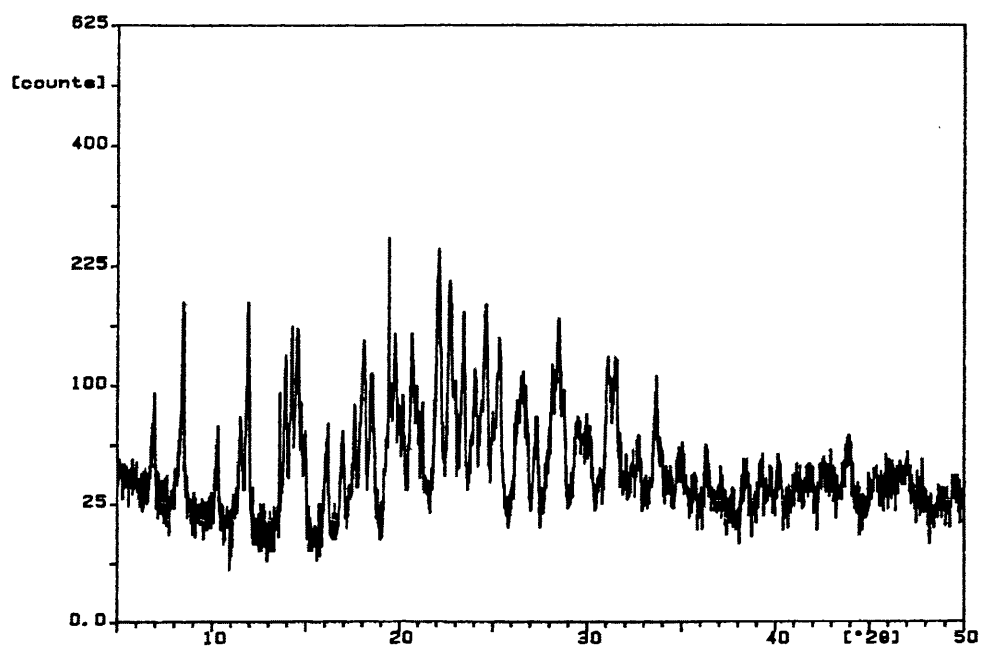


Figure 4.19 PXR D of indomethacin particle prepared using dichloromethane: ethanol (1:1) as solvent and sc- CO_2 as antisolvent.

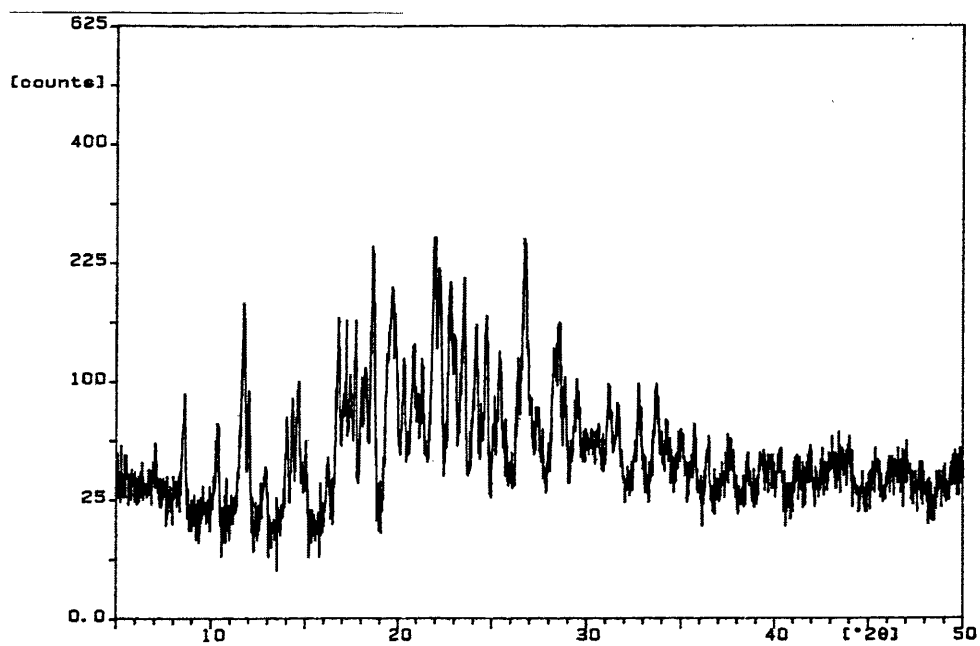


Figure 4.20 PXR D of indomethacin particle prepared using acetone as solvent and sc- CO_2 as antisolvent.

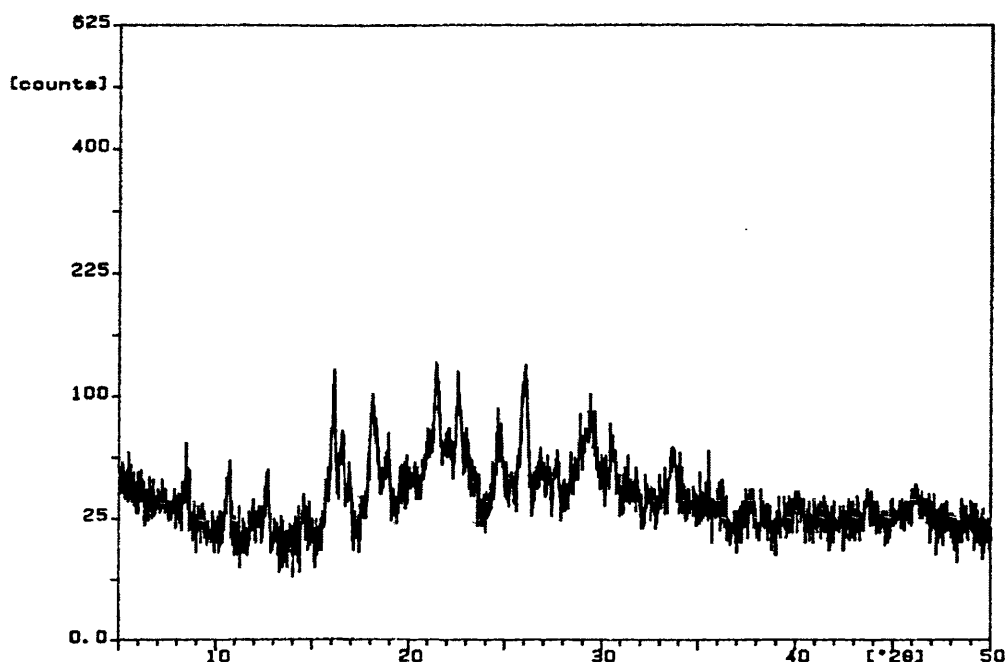


Figure 4.21 PXR D of indomethacin particle prepared using chloroform as solvent and sc-CO₂ as antisolvent.

A previous study of coprecipitating indomethacin and various proportions of PVP employing Solution Enhanced Dispersion by Supercritical fluids (SEDS) showed that all samples were non-crystalline, non-cohesive, fine web-like structures, easy-flowing powders with good handling properties (Wilkins et al, 1999). In this part of the study, unfortunately, coprecipitating indomethacin and PVP for the various ratios of PVP could not be obtained using our present PCA apparatus. It was noted that precipitation rendered sticky yellow liquid along the glass liner. As such, indomethacin and PVP coprecipitate could not be examined. Some of the means that might be able to overcome this setback are the use of PVP with higher molecular weight (for instance, above 50,000 Da), using a nozzle with a smaller internal diameter and a pump which could deliver CO₂ at a higher flow rate (for instance, above 10 ml/min).

4.4 Conclusions

The drug concentration and its feeding rate did not affect the characteristics of the product. The indomethacin precipitated from various organic solvents using sc-CO₂ (at 40°C and 150 bar) as anti-solvent was a mixture of α and γ crystalline forms. The scanning electron micrographs showed only needle or rod-like shape indicating the sole presence of α crystalline indomethacin. On the other hand, the DSC result showed two melting peaks inferring the presence of both α and γ crystalline forms. Obviously, the α crystalline form was present in a markedly higher proportion than γ crystalline form. Coprecipitation of indomethacin and PVP could not be produced due to the limitations of the current apparatus design.

Chapter 5
Precipitation using supercritical
CO₂ as solvent

5.1 Introduction

Supercritical carbon dioxide (sc-CO₂) has been extensively used as an environmentally acceptable alternative 'solvent' to some conventional hydrocarbon solvents. Rapid Expansion of Supercritical Solution (RESS) and Precipitation from Gas Saturated Solution or Suspension (PGSS) are both applying sc-CO₂ as a solvent. The RESS process involves solvating sample in the sc-CO₂ and immediately depressurising this solution through a nozzle, causing a rapid nucleation of the sample into a highly dispersed material. The advantages of this process are fine particles with a narrow size distribution can be produced via this technique without the need for additional solvents or surfactants. The use of low critical temperature solvents also makes this technique attractive for the precipitation of thermally labile materials. Unfortunately, its application is limited to products that have a considerable solubility in sc-CO₂ (nonpolar compounds). During the last decade, many publications are related to atomisation of pharmaceutical products, either to obtain microparticles, or microcapsules of an active into an excipient. On the other hand, the PGSS process basically dissolves a supercritical fluid into the melted or liquid-suspended substance(s). Then, it was rapidly depressurised through a nozzle causing the formation of solid particles. Particularly, this method allows forming of particles from substances that need not be soluble in sc-CO₂. Moreover, this method also can be used for suspensions of active substrate(s) in a polymer leading to the production of composite microspheres.

In Chapter 4, sc-CO₂ was used as an antisolvent for precipitation. α -metastable and γ -stable polymorphic forms of indomethacin were obtained. Coprecipitated indomethacin and PVP in the form of powder, for the various ratios of PVP, could not be obtained through the precipitation process. In this part of study, sc-CO₂ was used as solvent. A simple and unique apparatus was designed applying PGSS basic concepts. Instead of constructing a new apparatus, the PCA apparatus was duly modified to adapt to this change. The characteristics of processed pure indomethacin and coprecipitated indomethacin and PVP were investigated using SEM, DSC and powder x-ray diffraction. Moreover, the effect of different proportions of polymer on the crystallinity of the products was discussed.

5.2. Materials and Methods

5.2.1. Materials

Indomethacin, polyvinylpyrrolidone, polyethylene glycol. The details of these materials are given in section 2.1. Industrial grade carbon dioxide (99.95% purity) was supplied by British Oxygen Company, England. Tween 80 (Merck, England) was used as received. Lithium Fluoride (Prolabo, England) was used as received.

5.2.2. Design and construction of apparatus

The design of the apparatus had to be modified when supercritical CO₂ was used as a solvent. In the present design, which was modified from the PCA apparatus (Chapter 4), the HPLC pump for liquid feed was removed, as the present method did not require organic solvents. The special design of the CO₂ pump with a built-in chiller was made. Figure 5.1 shows the pump containing both input and output pressure meters. The desired output pressure was controlled by adjusting the air pressure. As shown in Figure 5.2, The design of the stirred batch reaction vessel was simplified by fastening the closure with only one screw to ease product recovery, compared to the reaction vessel of the PCA design, which required six screws. The glass liner was excluded as the product could be easily recovered directly from the reaction vessel. A paddle stirrer was included to improve mixing. The pressure in the vessel could be double checked from the pressure gauge which was installed on top of the vessel. Instead of employing the hot air oven (HPLC column thermostat) to maintain the temperature, a snug fitting aluminium heater block was used.



Figure 5.1 CO_2 pump with a built-in chiller.

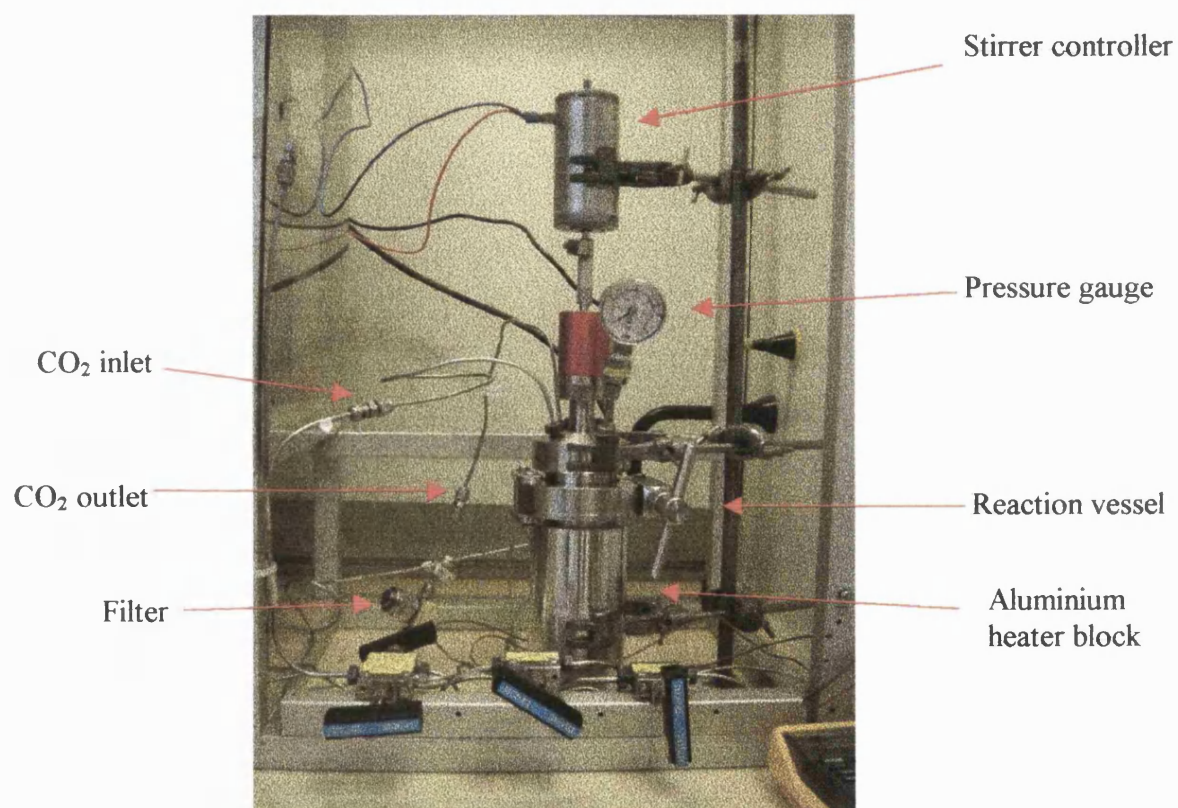
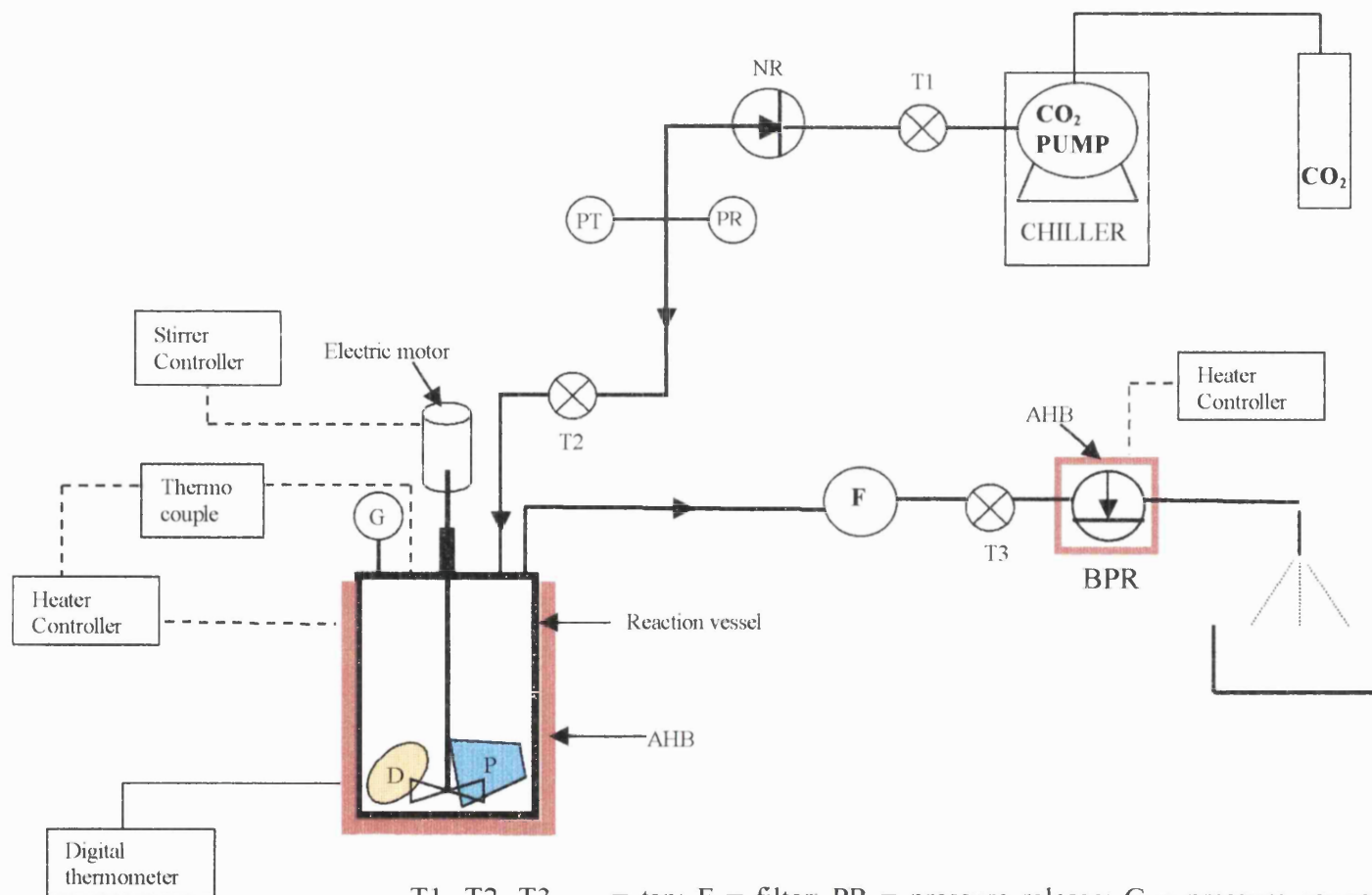


Figure 5.2 the stirred batch reaction vessel

Figure 5.3. Schematic diagram of an apparatus using CO₂ as solvent

T1, T2, T3 = tap; F = filter; PR = pressure release; G = pressure gauge; D = drug; P = polymer; AHB = aluminium heater block; PT = pressure transmission; BPR = back pressure regulator; NR = non-return valve.

The schematic of the experimental apparatus is depicted in Figure 5.3. The vessel was placed inside an aluminium heater block connected to the heater controller and thermocouple to maintain the temperature. The reaction vessel contained a stirrer connected to an electric motor. A non-returned valve was inserted between the CO₂ pump and the reaction vessel to avoid the flow inversion of CO₂. Cotton wool situated at the outlet of the vessel and a Nupro 7 µm stainless steel filter frit installed between the vessel and the back-pressure regulator was used to trap solids but allow the CO₂ to pass through during the depressurizing step. The pressure in the CO₂ feed was measured by a pressure transducer, housed in a custom made stainless steel body connected to a digital readout (RDP electronics, model E705). A temperature-controlled external heating block was located around the back-pressure regulator (BPR) to avoid intermittent freezing/blockage of the outlet pipe of the BPR.

5.2.3. Procedure

The basic procedures were the same in all cases for the mixtures; however, the reactions differed in the conditions of temperature and composition. The typical reaction was as follows; Indomethacin and PEG or PVP was accurately weighed and mixed in mortar and pestle for 15 min before being transferred into the reaction vessel. The vessel was sealed and placed into a snug fitting aluminium heater block. Liquid CO₂ was withdrawn from the CO₂ cylinder at 55 bar into the inlet of the pump. Then the liquid CO₂ was chilled by a built-in chiller for 30 minutes. The air pressure knob was opened prior to pressurized the CO₂ until the required output pressure of CO₂ was stable (Figure 5.1). The liquid CO₂ was delivered into the reaction vessel (Figure 5.3 Taps T1 and T2 open). The CO₂ was warmed above its critical point inside the reaction vessel. The stirrer controller was switched on. The heater controller was switched on and the temperature was raised. Upon reaching the desired temperature, the system was maintained for further 2 hr with taps T1, T2 and T3 closed. Lastly, the heater controller was switched off and the CO₂ was released steadily over a period of three minutes (T3 was fully opened while T1 and T2 were closed).

5.2.4. Investigation of the effect of sc-CO₂ on the characteristics of indomethacin

Preliminary investigations were carried out to determine if sc-CO₂ could produce amorphous indomethacin. The effect of different pressure of sc-CO₂ on the characteristics of indomethacin at 20°C was investigated. Indomethacin (200 mg) was exposed to sc-CO₂ in the reaction vessel for 2 hr at 20°C with pressures of 100 and 200 bar. The sample was collected after depressurizing of sc-CO₂.

5.2.5. Precipitation of indomethacin and PEG

Indomethacin and PEG 4000 (ratio of 1:4) was exposed to sc-CO₂ in the reaction vessel for 2 hr at 50 °C and 70 °C with pressures of 80, 100, 150 and 200 bar. The mixture was precipitated after depressurizing of sc-CO₂. The above settings was adapted from the study of Senca-Bozic (1997).

5.2.6. Precipitation of indomethacin and PVP

Preliminary investigations were carried out in order to determine the effect of sc-CO₂ temperature and pressure and different proportions of PVP on the characteristics of coprecipitates.

Mixtures of indomethacin and PVP at various ratios of 1.7:8.3, 4:6, 5:5, 7:3 and 8:2 were prepared. The mixtures were exposed to sc-CO₂ in the reaction vessel for 2 hr using the following parameters;

Pressure (Bar)	Temperature (°C)
80	40
150	40
150	75
150	90
200	75

Due to the limitation of the rig, the maximum pressure that could be reached was 260 bar. Therefore, all the pressure values employed were below 260 bar. As the temperature used was below 100 °C, it was lower than the melting point of indomethacin.

The mixtures were characterized using SEM (Section 2.2.1), DSC (Section 2.2.2) and PXRD (Section 2.2.3)

5.2.7. Scanning electron microscopy

Characterization method using SEM was described in section 2.2.1.

5.2.8 Particle size analysis

The mean size and span (90% undersize-10% undersize/ 50% undersize) of indomethacin (Becpharm, England) and indomethacin precipitated under different CO₂ pressure were measured using a laser diffractometer (Malvern Mastersizer S Ver. 2.18, UK), with a lens size of 14.3 mm. The instrument's software expresses particle size as the volume median diameter (VMD), i.e. the equivalent sphere diameter above and below which 50% of the volume of particles lies.

A saturated indomethacin stock solution was used as suspending medium for laser diffraction analysis. The stock solution was prepared by adding an excess of indomethacin to distilled water containing 0.01% of Tween 80 to facilitate the powder dispersion. It was agitated for 48 h at room temperature, thereafter left undisturbed for 12 h and then filtered through a 0.22 µm filter (Millipore, UK). To this solution, amounts of supercritical CO₂ processed indomethacin were added to make 35 mg/50 ml suspension. De-agglomeration of the particles was performed by ultrasonic treatment in a water bath for 1 minute before being loaded into a stirred sample cell.

5.2.9. Thermal analysis

A differential scanning calorimeter (Perkin Elmer DSC 7, USA) was employed. Samples of approximately 5 mg were carefully weighed in aluminium pans with a pinhole in the lid. The DSC was calibrated using pure samples of indium and Zinc.

In order to erase previous thermal history of the material and remove any residual moisture before the measurements of glass transition temperature (T_g), the samples were first heated to 145 °C and then cooled to -60 °C by an automated liquid nitrogen-cooling accessory at 20 °C/min. To check that this procedure did not result in degradation, each sample was subjected to a further three heating and cooling cycles and the T_g monitored. For all samples, there was no variation of the T_g suggesting that no degradation had occurred. Further experiment were conducted. After erasing thermal history, the samples were subsequently heated a second time from -60 °C to 220 °C at 20 °C /min, to check that the components were miscible. All T_g values were determined. Each sample was run in triplicate.

5.2.10. X-Ray diffraction analysis

Characterization method using PXRD was described in section 2.2.3.

5.2.11. Statistical analysis

The T_g values of indomethacin-PVP mixture prepared by sc-CO₂ based technique were analysed using a one-way analysis of variance. A post-hoc Tukey-HSD test was performed when there was a statistically significant difference, which was considered at $p < 0.05$.

5.2.12. Determination of the crystallinity of indomethacin

To estimate the % crystallinity of indomethacin, it was necessary to establish a powder X-ray diffraction calibration curve for known mixtures of amorphous and crystalline indomethacin. Since indomethacin can exist in both the α and γ crystalline forms, binary mixtures of each polymorph with amorphous material were prepared with 20% w/w of Lithium Fluoride (LiF) added as an internal standard. Figures 5.4 (a) and (b) show plots of the ratio of the peak areas at $2\theta = 8.5^\circ$ due to the α form and at $2\theta = 38.7^\circ$ due to LiF *versus* the content of the α form, and that of the peak areas at $2\theta = 11.6^\circ$ due to the γ form and at $2\theta = 38.7^\circ$ due to LiF *versus* the content of the γ form. Each plot was linear and the degree of crystallinity (X_c) of samples could be obtained using these calibration plots. Each value of X_c used in the calibration curve was the average of three independent measurements. This procedure allowed the % crystallinity due to either α or γ crystalline forms to be measured reproducibly down

to the level of $\pm 5\%$. Background diffraction due to PVP was negligible and did not interfere with the analysis.

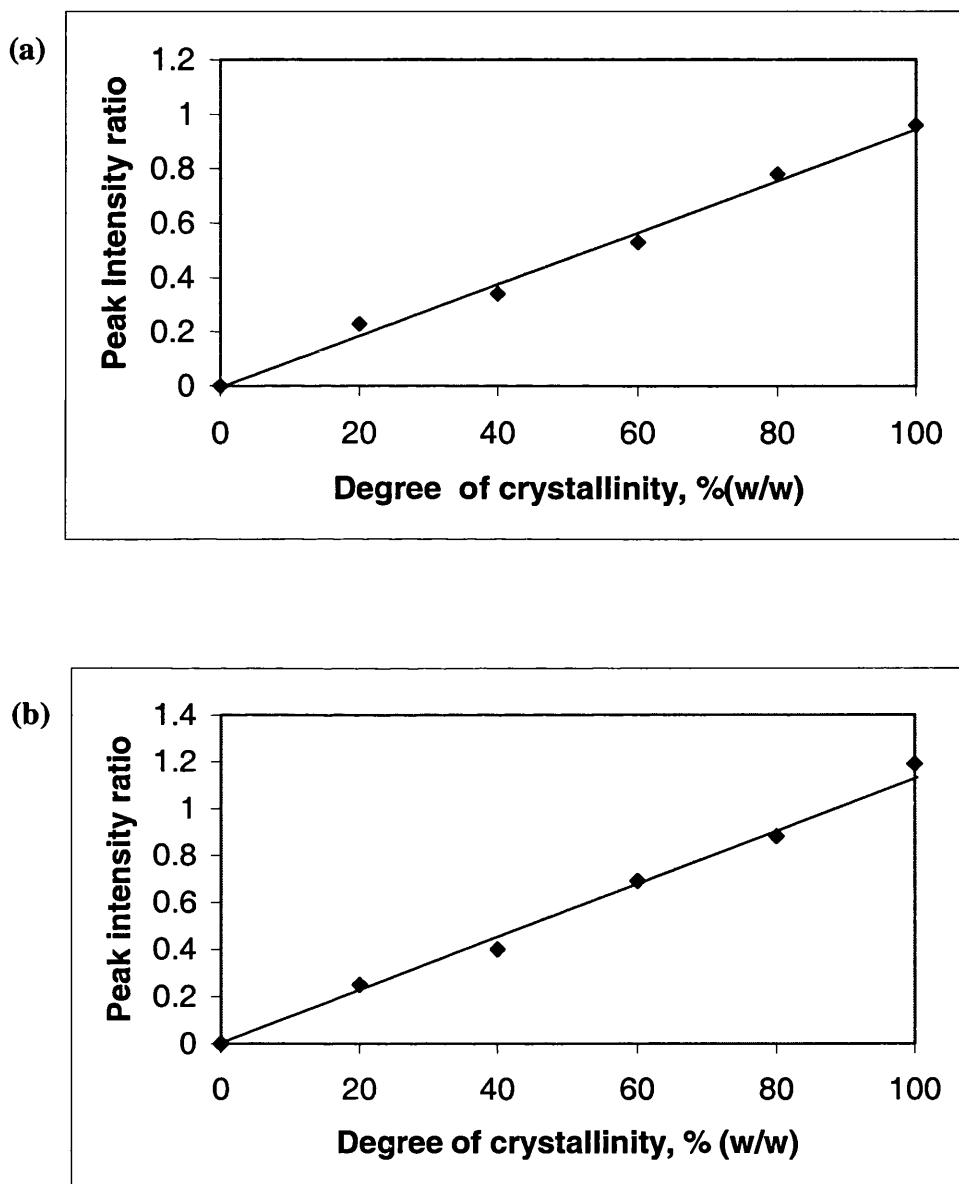


Figure 5.4 Peak intensity ratio versus degree of crystallinity of α and γ forms of indomethacin. (a) physical mixture of α form and noncrystalline solid (ratio of $2\theta=8.5^\circ$ versus 38.7°), (b) physical mixture of γ form and noncrystalline solid (ratio of $2\theta=11.6^\circ$ versus 38.7°).

5.3. Results and Discussion

The SEM image of the γ -crystalline indomethacin received from Becpharm (Becpharm, England) is shown in Figure 5.5(a). The unprocessed particles are crystalline in structure. Indomethacin particles precipitated by this method at various conditions have different size and morphology. CO₂ pressure is an important operation parameter of this process which can influence the properties of the precipitated product. This parameter was investigated at a constant temperature.

The particle size data from laser diffraction analysis of unprocessed and two independent samples are shown in Table 5.1. The yield of the products was calculated from the weight of the precipitated product collected from the vessel, as a percentage of the initial weight indomethacin (Table 5.1).

Table 5.1 Results of the particle size analysis for indomethacin precipitated under different conditions.

Operation parameter Temp.; Pressure	Volume median diameter (μm)	Span	% Yield (n=1)
Unprocessed indomethacin	28.17(± 0.07)	2.05(± 0.02)	-
20 °C; 100 bar	28.09(± 0.05)	2.17(± 0.02)	84.5
20 °C; 200 bar	3.54(± 0.02)	1.22(± 0.02)	77.9

n= 3 \pm sd

At 20 °C indomethacin precipitated under CO₂ pressure of 100 bar, the particle size was not changed in comparison with the unprocessed indomethacin. Although the values for the median particle size were slightly decreased, there was no significant difference ($p > 0.05$) in size when the operating CO₂ pressure was used at 100 bar. A CO₂ pressure increased from 100 bar to 200 bar in this precipitation process had an effect in reducing the size of particles. The median particle size decreased from 28.09 μm to 3.54 μm at a temperature of 20 °C. The low span value indicated that the

precipitated indomethacin at 200 bar have a narrow size distribution. The percentage yield obtained was lower for the higher CO₂ pressure condition. As the size of particle is smaller than the diameter of a filter, it could be lost during CO₂ depressurising step.

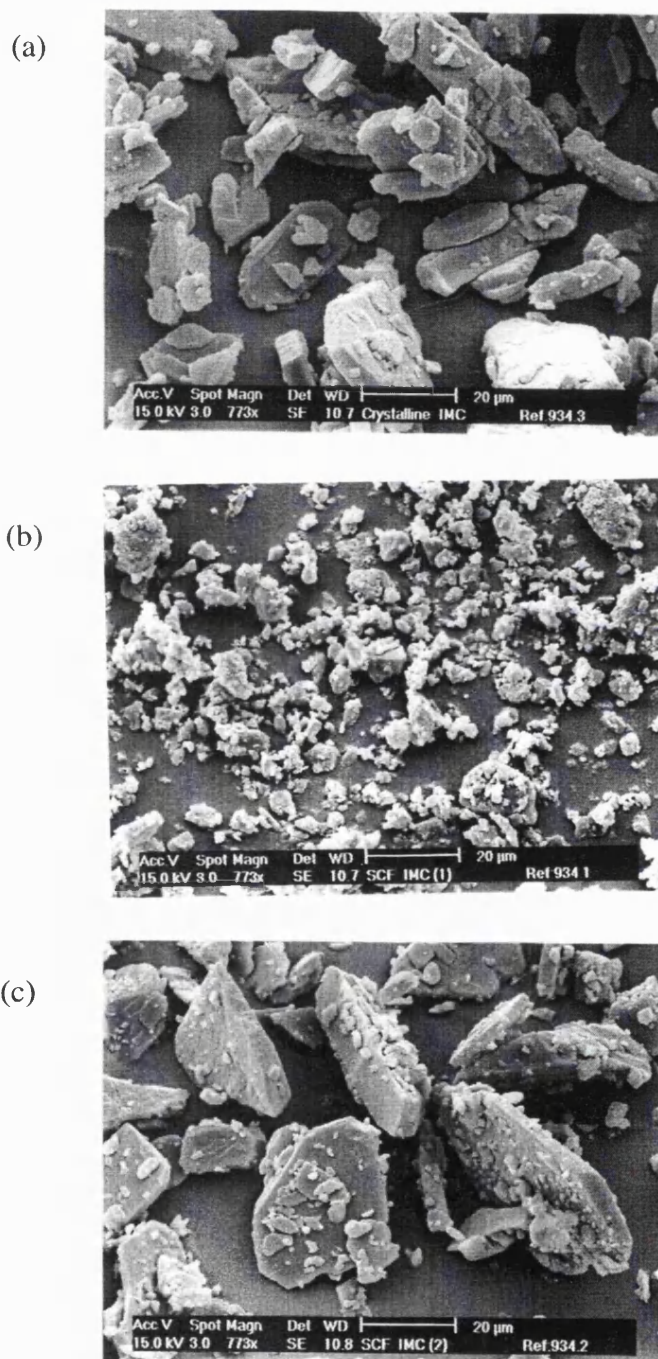


Figure 5.5 SEM images of indomethacin (a) original material and the precipitates obtained by SCF method at 20 °C (b) P=200 bar; (c) P=100 bar.

The SEM images of processed particles illustrated in Figures 5.5 (b) and (c) revealed that particles were irregular in shape and existed as aggregates. Thus, these results indicate that the micronisation of indomethacin using this apparatus is feasible. At 20 °C, the pressure influenced the particle size of products. The DSC profiles and PXRD scans indicated that indomethacin precipitated under CO₂ pressure of 100 and 200 bar were pure γ - stable crystalline form.

It has been reported that PEG 4000 could modify the characteristics of nifedipine, a poorly water soluble drug, using the Precipitation from Gas Saturated Solution (PGSS) technique (Sencar-Bozic et al., 1997). Sencar-Bozic et al (1997) found that addition of certain amounts of hydrophilic polymer, PEG 4000 to nifedipine resulted in a melting point decrease. They also reported the advantage of using PEG 4000 as it could lower the mixing temperature in PGSS process and hence avoid degradation of drug.

Since indomethacin is also a compound with low water solubility, it was thought that PEG 4000 could modify the physical state of indomethacin and potentially enhance the dissolution rate. Hence, similar drug to polymer ratio and process parameters were adopted in the present study as used by Sencar-Bozic et al (1997). However, the mixtures were obtained as yellow stone-like solid mass, consisting of indomethacin and PEG 4000, upon eventual loss of all CO₂ from the polymer matrix. This solid mass was stuck in the reaction vessel. The change in pressure between 200 and 80 bar at temperatures of 50 °C and 70 °C produced products of similar characteristics. The difficulty in product recovery and also different product characteristics from those reported by Sencar-Bozic et al (1997) could be due to the limitation of the present apparatus. In the study of Sencar-Bozic et al. (1997), the drug/polymer solution was sprayed via a heated nozzle into a separate chamber in which the final product was recovered.

The parameters of 150 bar and 40 °C which were used in the PCA method were selected for the precipitation of indomethacin and PVP initially. The γ crystalline form of indomethacin was obtained for all the ratios studied. Fine powdered mixtures were obtained. The SEM image of indomethacin and PVP mixture at ratio of 1.7:8.3

under sc-CO₂ 150 bar and 40 °C is shown in Figure 5.6. The round shapes of PVP and indomethacin crystals show that under this condition no reaction happened between indomethacin and PVP. Thus, under this condition sc-CO₂ could not plasticize PVP and could not assisted PVP and indomethacin mixing.

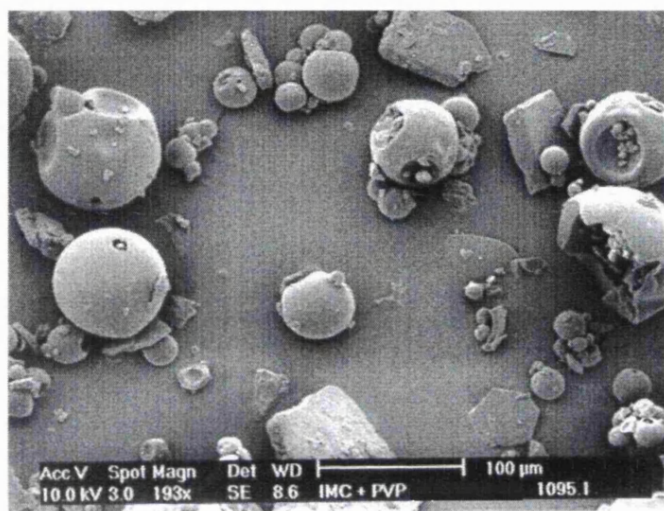
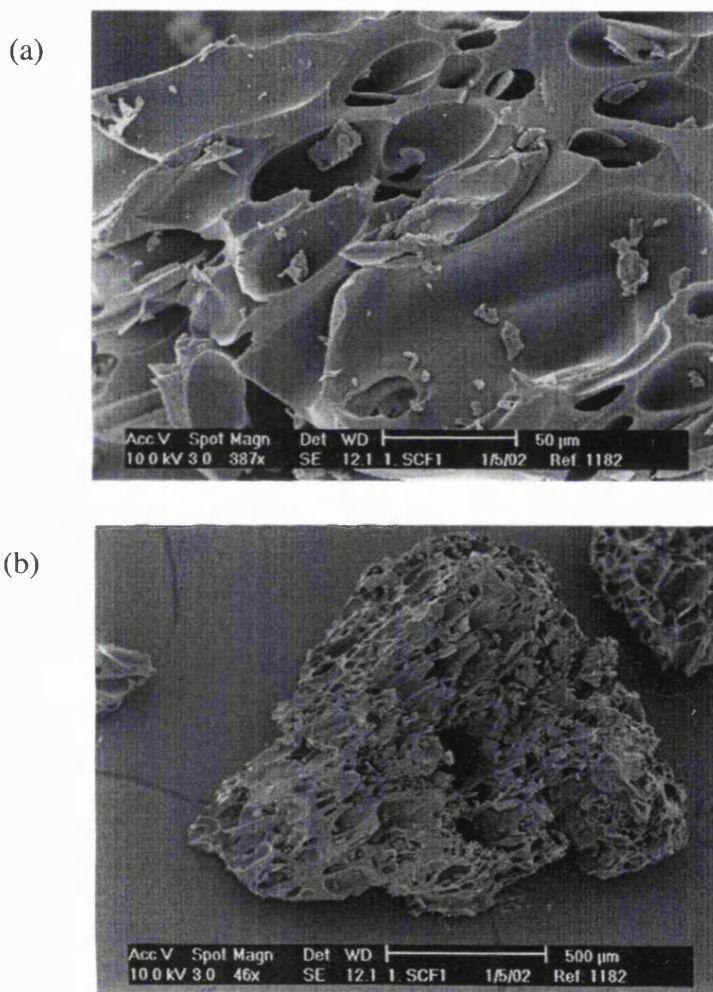


Figure 5.6 SEM images of indomethacin and PVP mixture at ratio 1.7: 8.3 prepared using sc-CO₂ as solvent (T=40 °C and P= 150 bar).

When the temperature was increased to 75 °C at the same pressure, the amorphous form of indomethacin was obtained at a PVP:indomethacin ratio of 8:2 and above. At lower proportions of PVP, only partially amorphous indomethacin was obtained. Under this condition, sc-CO₂ plasticized PVP and lowered its viscosity. Thus, sc-CO₂ could assist indomethacin and PVP blending.

The use of higher pressures (150 bar to 200 bar) yielded identical results with the same proportion of PVP being required to yield amorphous indomethacin. Similarly, temperatures higher than 75 °C produced similar results. Consequently, a pressure of 150 bar and a temperature of 75 °C were used for further studies.

The various proportions of indomethacin and PVP produced porous structures when viewed under the scanning electron microscope. This was presumably a consequence of foaming in the sc-CO_2 . A typical scanning electron micrograph of indomethacin and PVP mixture at a ratio of 1.7:8.3 under different magnification is shown in Figures 5.7 (a) and (b).



Figures 5.7 (a) and (b). SEM images of indomethacin and PVP coprecipitate at ratio 1.7:8.3, prepared using sc-CO_2 as solvent ($T=75^\circ\text{C}$ and $P=150\text{ bar}$), before grinding.

DSC scans were run for the various coprecipitates over the entire composition range. As seen in Figure 5.8 such a scan allowed an estimation of the glass transition temperature.

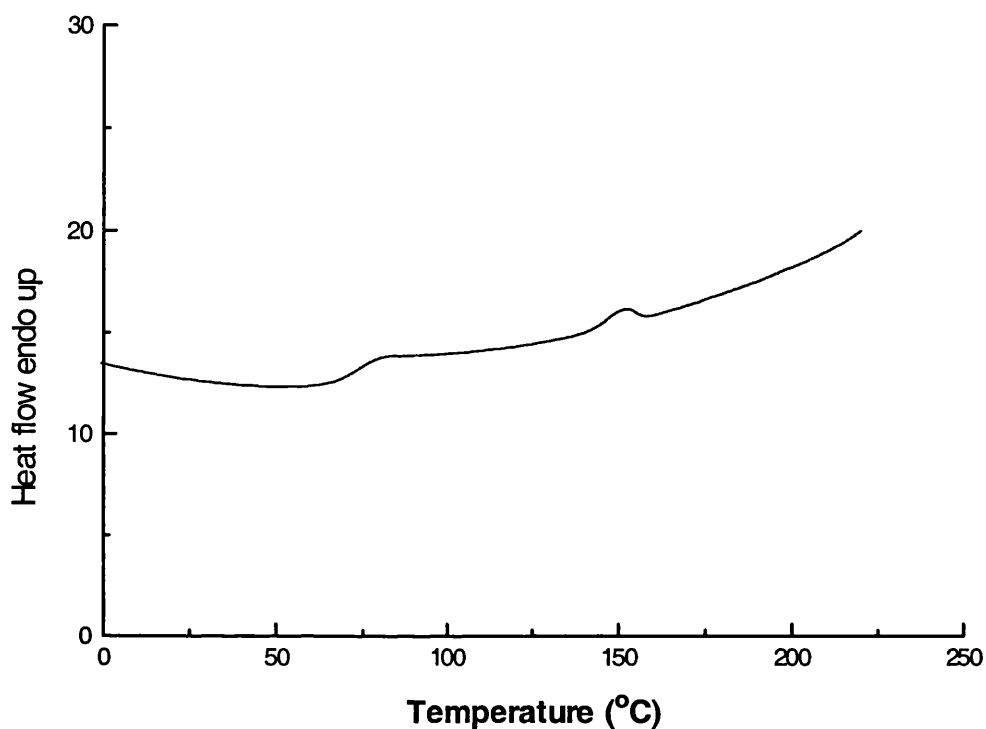


Figure 5.8 Typical trace obtained from differential scanning calorimetry of indomethacin-PVP coprecipitates using sc-CO₂ as solvent.

The PXRD profiles of coprecipitated indomethacin and PVP (0.2-0.83 PVP weight fraction) are shown in Figures 5.9-5.14. It can be noticed that there is only the peak at 11.6 °2 θ confirming that only the γ type was present in all coprecipitated indomethacin and PVP (0.2-0.6 PVP weight fraction).

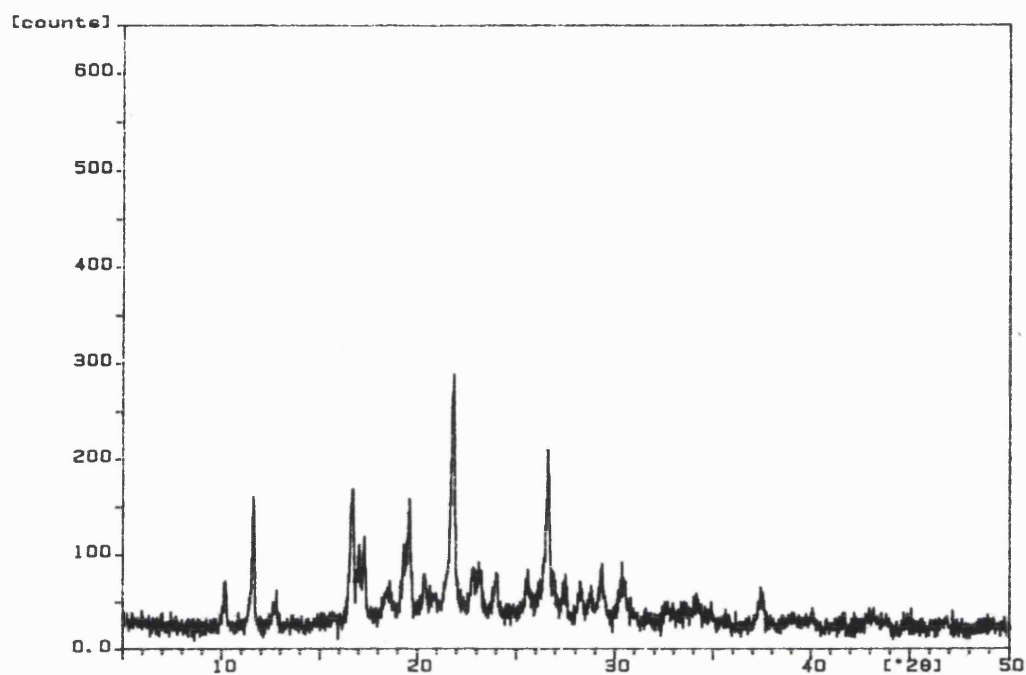


Figure 5.9 XRD pattern of the coprecipitation of indomethacin and 0.2 PVP weight fraction prepared using sc-CO_2 as a solvent.

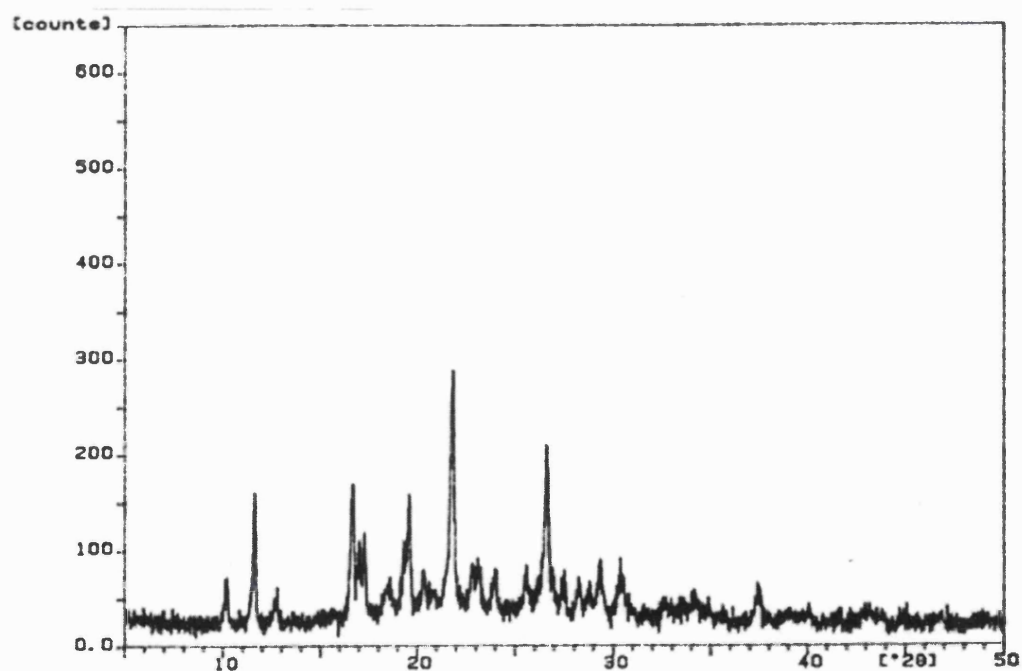


Figure 5.10 XRD pattern of the coprecipitation of indomethacin and 0.3 PVP weight fraction prepared using sc-CO_2 as a solvent.

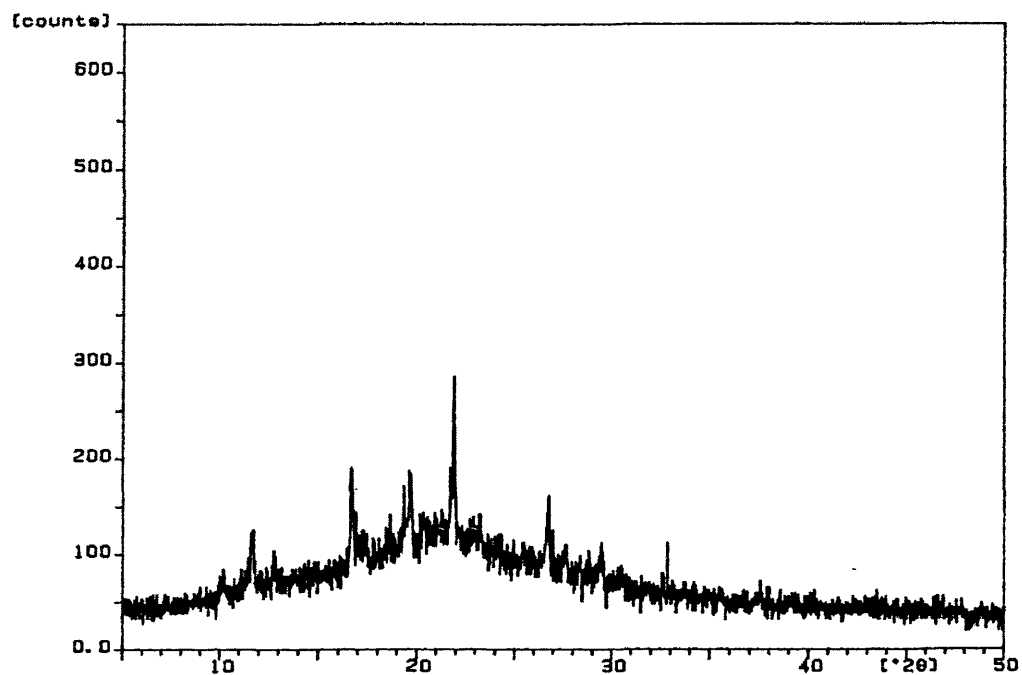


Figure 5.11 XRD pattern of the coprecipitation of indomethacin and 0.5 PVP weight fraction prepared using sc-CO₂ as a solvent.

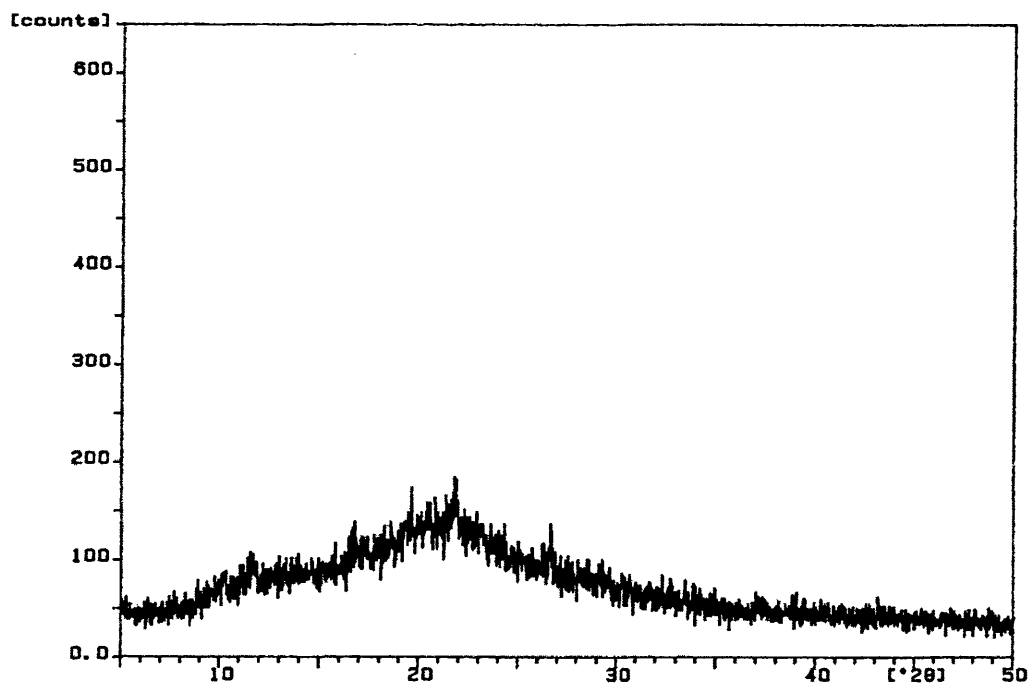


Figure 5.12 XRD pattern of the coprecipitation of indomethacin and 0.6 PVP weight fraction prepared using sc-CO₂ as a solvent.

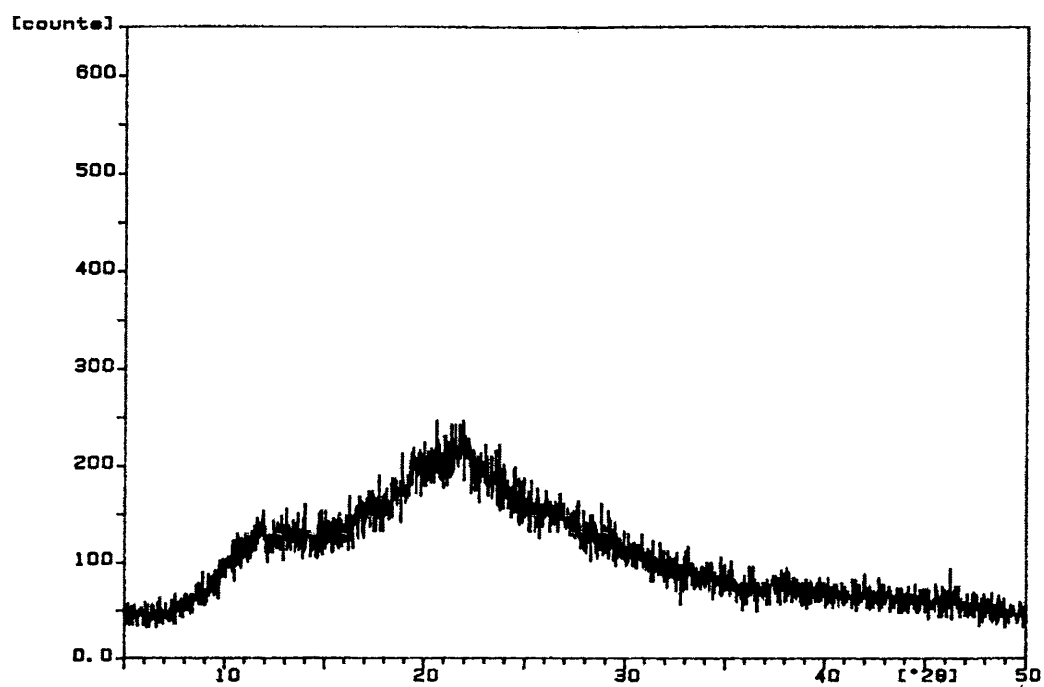


Figure 5.13 XRD pattern of the coprecipitation of indomethacin and 0.8 PVP weight fraction prepared using sc-CO₂ as a solvent.

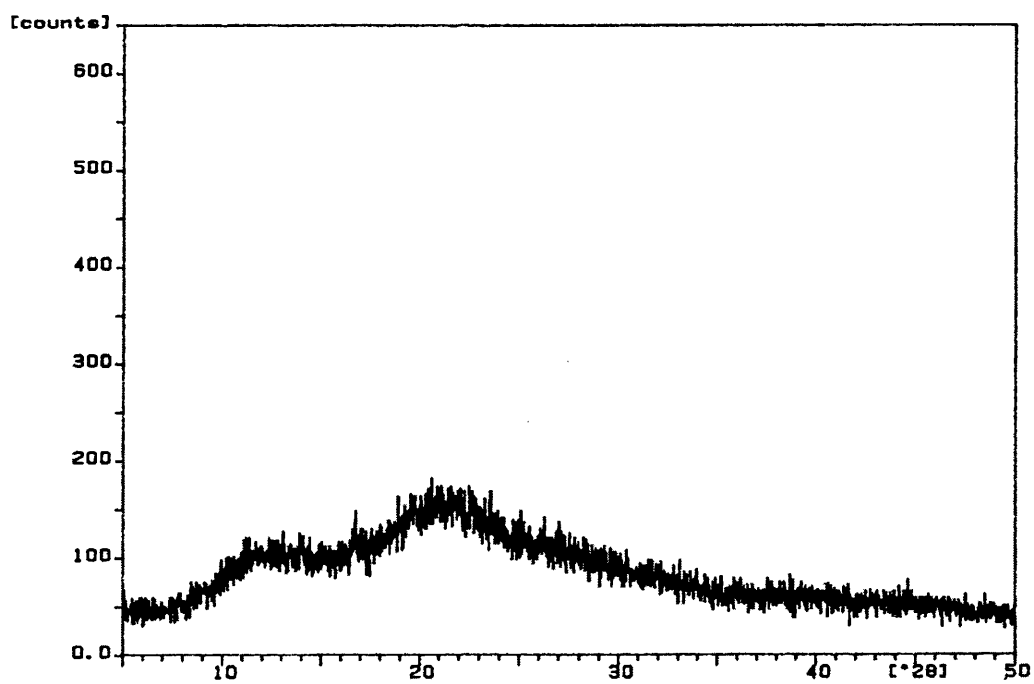


Figure 5.14 XRD pattern of the coprecipitation of indomethacin and 0.83 PVP weight fraction prepared using sc-CO₂ as a solvent.

Table 5.2 shows the effect of PVP on the T_g and the degree of crystallinity of the coprecipitates. The T_g value as a function of PVP weight fraction in the coprecipitates is presented in Figure 5.15. A single T_g value was observed over the entire range of PVP compositions, suggesting that indomethacin and PVP were miscible. The T_g values increased with an increase in the PVP content. When the T_g values were analysed statistically using one-way analysis of variance and post-hoc statistical analysis, they were significantly different (Tables 5.3 and 5.4).

Table 5.2 Glass transition temperature and degree of crystallinity for indomethacin coprecipitates with PVP obtained by Differential Scanning Calorimetry and PXRD, respectively.

PVP weight fraction	T_g (K)	Degree of crystallinity (% w/w)
0.2	333.98	55
0.3	344.89	41
0.5	366.78	18
0.6	370.84	15
0.83	397.45	0

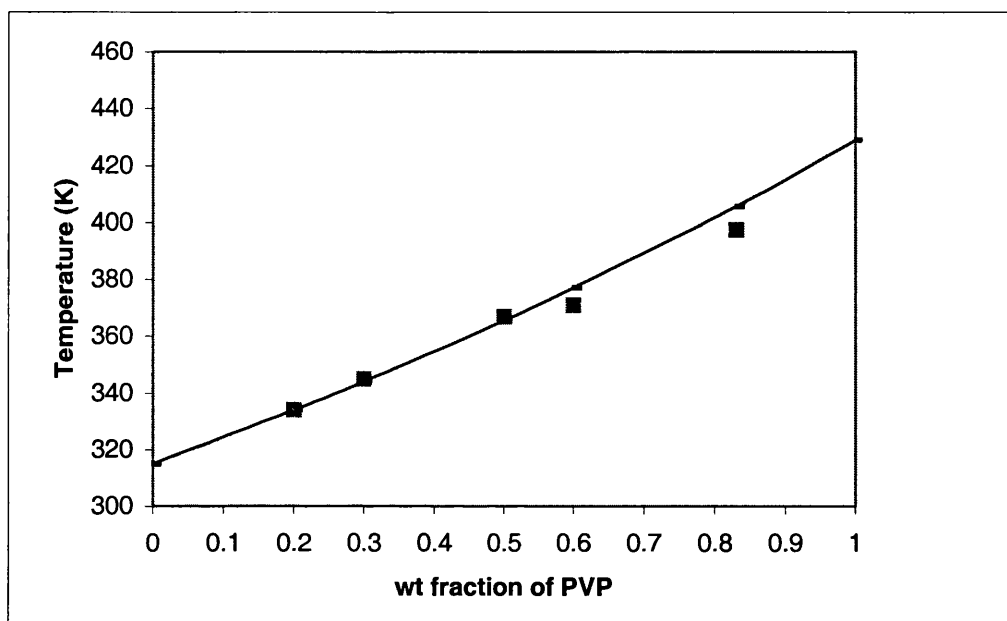


Figure 5.15. Plot of glass transition temperature *versus* weight percent of PVP for indomethacin-PVP coprecipitates using supercritical fluid based technique: the squares represent experimental data points and the solid line represents the fit to the Gordon-Taylor equation.

Table 5.3 One-way analysis of variance (ANOVA) results of T_g

	Sum of Squares	df	Mean Square	F	Sig.
Between Groups	7297.473	4	1824.368	1699.764	0.000
Within Groups	10.733	10	1.073		
Total	7308.206	14			

Table 5.4 Tukey HSD test results of $T_g(^{\circ}\text{C})$

	N	Subset for alpha = 0.05	do	do	do	do
PVP wt fraction		1	2	3	4	5
0.20	3	60.9767				
0.30	3		71.8867			
0.50	3			93.7800		
0.60	3				97.8367	
0.83	3					124.4467
Sig.		1.000	1.000	1.000	1.000	1.000

Means for groups in homogeneous subsets are displayed above.

The extent to which these mixtures might exhibit deviation from ideal mixing was evaluated by comparison of the experimental T_g with those predicted using the Gordon-Taylor equation (1952) as shown below;

$$T_{g\text{mix}} = (w_1 T_{g1} + K w_2 T_{g2}) / (w_1 + K w_2) \quad (1)$$

Where w_1 and w_2 are the weight fraction of each component. T_{g1} and T_{g2} are the corresponding glass transition values of each component. The constant K is related to the ratio of the free volumes of the two components and can be estimated from the density, ρ_1 and ρ_2 , of each component using the Simha-Boyer rule (1962).

$$K \approx (\rho_1 T_{g1}) / (\rho_2 T_{g2}) \quad (2)$$

The densities of the amorphous indomethacin and PVP samples used in this study were 1.31 (Yoshioka et al, 1994) and 1.20 g/cm³ (Matsumoto and Zografi, 1999), respectively. The T_g values of indomethacin and PVP were determined by DSC to be 315 and 429 K, respectively.

As can be seen in Figure 5.15, the solid line depicted the values of T_g predicted from Gordon-Taylor equation. The change in experimental T_g with PVP concentration follows the ideal mixing up to 50% PVP. However, experimental T_g values at 60 and 83% PVP were lower than those predicted indicating that mixing was not ideal at

these concentrations (Summers and Enever, 1977). These deviations could be attributed to the possibility of complex formation between indomethacin and PVP (Yoshioka et al, 1995; Taylor and Zografi, 1997). In addition, another reason could be due to a nonuniform distribution of the free volume between two components with very different T_g values (Shamblin et al, 1998). It was also proposed, but not shown, that these deviations could be resulted from molecular interactions formed between the two components which are fewer in number and/or strength relative to the interactions within each component (Hancock and Zografi, 1997).

5.4 Conclusions

Indomethacin could be “micronised” using sc-CO₂ as a solvent. Particles of processed indomethacin were found to be smaller than the unprocessed materials. At 20 °C, increasing the operating pressure from 100 to 200 bar reduced the particle size. The “micronised” indomethacin was found to be the γ -crystalline form.

An exploration of the potential of precipitation using sc-CO₂ as a solvent in modifying the physical state of indomethacin was continued after spray-drying and precipitation using sc-CO₂ as an antisolvent method were investigated. Instead of constructing a new rig, the PCA apparatus was modified applying PGSS concepts. Coprecipitation of indomethacin and PEG could not be produced due to the limitations of the present apparatus design.

Coprecipitated indomethacin and PVP at various weight fractions was successfully achieved at 75 °C and 150 bar. The totally amorphous products were obtained at relatively high PVP weight fraction of 0.80 and above. As the PVP weight fraction decreased, indomethacin displayed increasing degree of crystallinity.

Chapter 6

Dissolution and stability studies

6.1 Introduction

Poorly water-soluble crystalline drugs, often have low bioavailability when administered as oral solid dosage forms. Conversion of this material to the higher energy amorphous state can improve dissolution rates and hence bioavailability (Yamamoto et al, 1970; Chiou and Reigelman, 1970). However, the amorphous form, which is metastable relative to the crystalline form, can spontaneously crystallize under certain conditions of temperature and relative humidity during storage and use (Imaizumi et al, 1980; Otsuka and Kaneniwa, 1988; Andronis et al, 1997). Therefore, it is necessary to add excipients that could retard the instability over timescales. It has been suggested that co-solubilization or co-precipitation of drugs with excipients can form molecular dispersions which have higher glass transition temperatures (T_g) than the drug alone. An increase in T_g can be employed as a means of stabilizing amorphous material (Chiou and Reigelman, 1971; Simonelli et al, 1976). Principally, once the molecular dispersion has a T_g higher than that of the drug alone, the molecular mobility of the drug will be decreased and as a result, crystallization can be retarded. Polymers particularly with high T_g values, such as polyvinyl pyrrolidone (PVP), have been reported to enhance the physical stability of amorphous drugs (Imaizumi et al, 1983; Sekizaki et al, 1995; Matsumoto and Zografi, 1999).

In Chapter 5, a novel technique utilizing supercritical CO₂ for co-precipitation of indomethacin and PVP was described. In chapter 6, the study was conducted to investigate the dissolution rates of indomethacin and PVP mixtures of various proportions prepared using the method described in Chapter 5 in comparison with mixtures prepared using physical mixing and solid dispersion methods. Additionally, the dissolution rate of amorphous indomethacin, α -metastable indomethacin, γ indomethacin was also investigated. The stability of mixtures of indomethacin containing various PVP proportions, as solid dispersions (solvent evaporation technique), supercritical fluid based preparations and amorphous indomethacin itself were also investigated under different combinations of temperature and relative humidity.

6.2 Materials and Methods

6.2.1 Materials

Indomethacin, polyvinylpyrrolidone, ethanol, anhydrous methanol, potassium dihydrogen orthophosphate, sodium hydroxide pellets, distilled water. The details of these materials are given in section 2.1. Silica gel, magnesium chloride, sodium chloride and potassium sulphate which were supplied by BDH (England) and were used as received. Lithium Fluoride (Prolabo, England) was used as received.

6.2.2 Preparation of indomethacin and PVP physical mixtures

Indomethacin and PVP were mixed in a mortar and pestle for 15 min. The ratios of indomethacin and PVP mixtures were 8:2, 7:3, 5:5, 4:6 and 1.7:8.3. The samples were desiccated over silica gel at -20°C .

6.2.3 Preparation of indomethacin and PVP solid dispersions

Indomethacin and PVP solid dispersions were prepared using a solvent evaporation technique, wherein 5 g of the appropriate ratios of the two components, indomethacin:PVP at 8:2, 7:3, 5:5 and 1.7:8.3, were dissolved in 100 ml of anhydrous methanol at 50°C . The solvent was then removed using a rotary evaporator (Buchi Rotavapor R114, Switzerland) at 50°C . The organic solvent residue was dried in a vacuum oven at room temperature (25°C) for 24 hours. The co-precipitates were lightly ground in a mortar and desiccated over silica gel at -20°C . The solid dispersions were characterized using PXRD (Section 2.2.3). The T_g of solid dispersions was determined as method described in section 5.2.9. Determination of the % crystallinity of indomethacin in the solid dispersions was described in section 5.2.12.

6.2.4 Preparation of indomethacin and PVP mixture using supercritical CO_2

Mixtures of indomethacin and PVP at various ratios of 1.7:8.3, 4:6, 5:5, 7:3 and 8:2 were prepared. The mixtures were exposed to sc- CO_2 in the reaction vessel for 2 hr under sc- CO_2 pressure 150 bar and 75°C . The procedure for preparing indomethacin and PVP co-precipitates using supercritical CO_2 as solvent has been described in section 5.2.3. The co-precipitates were lightly ground in a mortar and desiccated over silica gel at -20°C .

6.2.5 Preparation of amorphous indomethacin

Amorphous indomethacin was prepared by the quenching method. 10 g of indomethacin was placed in a crucible and melted in an oven (Mettler, Germany) at 168-169 °C. Indomethacin was held at this temperature for 5 min and then cooled rapidly using liquid nitrogen. The amorphous indomethacin was warmed to room temperature under vacuum to prevent atmospheric moisture condensation on the sample. Then it was desiccated over silica gel at -20 °C. This temperature was previously shown to prevent crystallization of pure amorphous indomethacin for up to 6 months (Yoshioka et al, 1994). The resulting quenched indomethacin was found totally amorphous using PXRD (Section 2.2.3). Andronis et al (2000) reported that no change in the purity of the indomethacin glass was observed as a result of the melting and quenching. The amorphous sample was not ground before the experiments because mechanical activation of the sample during grinding was significant to the physical characteristic of the quenched indomethacin (Fukuoka et al, 1986).

6.2.6 Preparation of α -metastable indomethacin

The α -metastable indomethacin was prepared according to the method of Kaneniwa (1985), with modification. 10 g of indomethacin was dissolved in 50 ml of ethanol at 70 °C. 50 ml of distilled water at room temperature was then added to the indomethacin ethanolic solution. The precipitated crystals were removed by filtration and dried overnight under vacuum at -50 °C (Micromodulyo, England).

6.2.7 Drug content determination

The drug content of the indomethacin and PVP mixtures prepared using physical mixing, supercritical CO₂ and solid dispersion methods were determined. The indomethacin and PVP mixture at ratios of 8:2, 7:3, 5:5, 4:6 and 1.7:8.3 was examined. The quantity of powder mixture, equivalent to 25 mg of indomethacin, was dissolved in 500 ml of phosphate buffer pH 7.2 and the drug concentration was determined using a UV spectrophotometer (Beckman DU-62 Spectrophotometer, USA) at 320 nm. Each experiment was run 3 times.

6.2.8 Solubility determination

The solubility of the amorphous, α and γ indomethacin was determined. The indomethacin powder was added in excess into phosphate buffer pH 7.2. The preparations were stirred continuously for 7 days at ambient room temperature of approximately 22 °C. Samples were collected at preset time intervals and the drug concentrations measured using a UV spectrophotometer (Beckman DU-62 Spectrophotometer, USA) at 320 nm.

6.2.9 Dissolution study

The dissolution rates of amorphous indomethacin, α metastable indomethacin, γ indomethacin, mixtures of indomethacin and PVP at ratios of 8:2, 7:3, 5:5, 4:6 and 1.7:8.3, prepared from physical mixing, supercritical CO₂ and solid dispersion methods were investigated. The powders were sieved using a mechanical sieve shaker and powders with a particle size range between 93-150 μ m were selected for the dissolution study. The powders were filled manually into size 0 hard gelatin capsules. Each capsule contained a quantity of mixture to give the equivalent of 50 mg indomethacin. The dissolution study was undertaken according to the USPXXI dissolution test, apparatus II or paddle method (Pharmatest dissolution tester, Germany). The dissolution medium consisted of 900 ml of phosphate buffer pH 7.2, maintained at temperature of 37 ± 0.5 °C. A paddle rotation speed of 20 rpm was employed. The capsules were trapped at the bottom of a vessel with stainless steel mesh of 1/8".

The schematic illustration of this apparatus for dissolution study is shown in Figure 6.1. Samples of 5 ml each were collected automatically at predetermined time intervals of 5 min for the first hour and thereafter at intervals of 15 min for the subsequent 3 hours. The drug concentration in the sample was analysed using a UV spectrophotometer at a detection wavelength of 320 nm. The percentage of drug release versus time was calculated. The times for 50% ($T_{50\%}$) of drug released were estimated from the percentage of drug release versus time profiles.

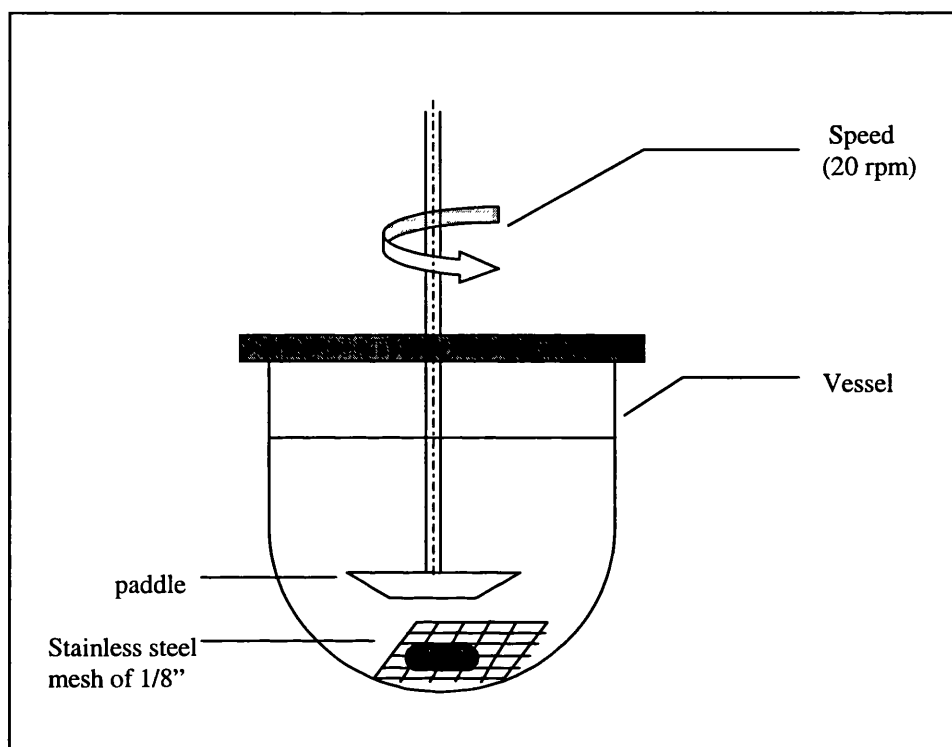


Figure 6.1. Paddle apparatus for dissolution testing.

6.2.10 Statistical analysis

The $T_{50\%}$ values of indomethacin-PVP mixture prepared by physical mix, solid dispersion and supercritical CO_2 methods were analysed using a one-way analysis of variance. A post-hoc Tukey-HSD test was performed when there was a statistically significant difference, which was considered at $p < 0.05$.

6.2.11 Stability study

The effect of temperature and relative humidity on the stability of amorphous indomethacin, indomethacin and PVP mixtures prepared using supercritical CO_2 and solid dispersion methods was also investigated. The indomethacin and PVP mixtures at ratios of 8:2, 5:5 and 1.7:8.3 were selected for the study.

For the study of temperature effect, the samples were kept in sealed glass bottles stored in desiccators containing silica gel at 30, 50 and 70 °C for a period of 3 months using a hot air oven (Pickstone, England and Memmert, Germany).

For the effect of relative humidity, the samples were kept at three different relative humidities in desiccators containing saturated salt solutions at 20 °C for a period of 3 months. Three saturated salt solutions, magnesium chloride, sodium chloride and potassium sulphate were used to create 35, 76 and 98%RH. (Nygqvist, 1983). The relative humidity of the desiccators was monitored by a hygrometer (Haenni, Switzerland).

Samples of 100 mg were withdrawn at preset time intervals over the 3 months of study period and mixed with 20% LiF (internal standard) before determination of crystallinity. The % crystallinity of the samples was determined by powder X-Ray diffraction analysis, using a Philips model PW 3710 X-Ray diffractometer as described in section 5.2.12. Calibration curves were prepared using known amounts of amorphous indomethacin mixed with either the α or γ crystal form to the level of 5%. Background diffraction due to PVP was negligible and did not interfere with the analysis. In this present study the period of observation was limited to 3 months because the higher temperatures chemical instability of indomethacin can arise on long term storage (Carstensen et al, 1993).

6.3 Results and Discussion

Solubility and dissolution studies of amorphous indomethacin, α -metastable indomethacin and γ indomethacin.

The solubility profiles of amorphous, α and γ indomethacin in phosphate buffer pH 7.2 at 22 °C are depicted in Figure 6.2. There was a steady increase in the amount of γ form dissolved and reached a plateau concentration at about 8 hr. On the other hand, the α metastable form showed a high solubility peak value after about 6 hr followed by a decline before reaching a plateau. The plateau level observed in this case was higher than that of the γ -crystal form. The α form could exist as a supersaturated solution and also it could convert to the γ stable form (Hancock and Parks, 1999). The quenched amorphous indomethacin showed a maximum in solubility after about 6 hr before values of solubility began to fall. The maximum in solubility suggested that the amorphous indomethacin existed as a supersaturated solution.

Imaizumi et al (1980) studied the solubility of amorphous indomethacin in 5 % aqueous methanol solution. It was reported that the solubility of the amorphous form became almost the same as that of α form after 2 hours. According to X-ray diffractometry, α metastable polymorph was formed from the amorphous at the initial stage of dissolution, and the resulting α form changed gradually to γ stable form. Hancock and Parks (2000) studied the solubility of amorphous indomethacin in water. It was shown that over the duration of the solubility experiments of amorphous indomethacin, the starting amorphous material partially converted to α and γ crystalline polymorphs.

The increase in solubility attained by both amorphous and α metastable form indomethacin may correspond to the solubility of an “activated state”. As activated state is a high energy metastable state by definition (Buckton and Beezer, 1992), it tends to resume more thermodynamically stable, lower energy states. The actual peak solubility value of amorphous and α metastable indomethacin might be higher than the measured peak during the experiments, since the change back to a more stable crystalline form of indomethacin, by crystallisation process, might compete with the dissolution of the amorphous or α indomethacin during the early dissolution phase (Rodrigues-Hornedo et al., 1992). This might explain the solubility profile of amorphous and α metastable indomethacin, where the initial phase of the profile is dissolution-dominated until the highest possible level of supersaturation is reached, i.e., the peak, while the second phase of the profile is dominated by a transition back to a more thermodynamically stable form of indomethacin, shown by a decline from the peak value. As can be seen in Figure 6.2, during the relatively short observation period of 7 days, slow reduction of solubility values of amorphous and α indomethacin were seen.

For comparison, the amorphous form exhibited the highest apparent solubility followed by the metastable (α) and lastly the stable form (γ). The apparent-saturated solubility values at steady state were 309.43, 143.97 and 73.67 mg/100 ml for the amorphous, α and γ indomethacin.

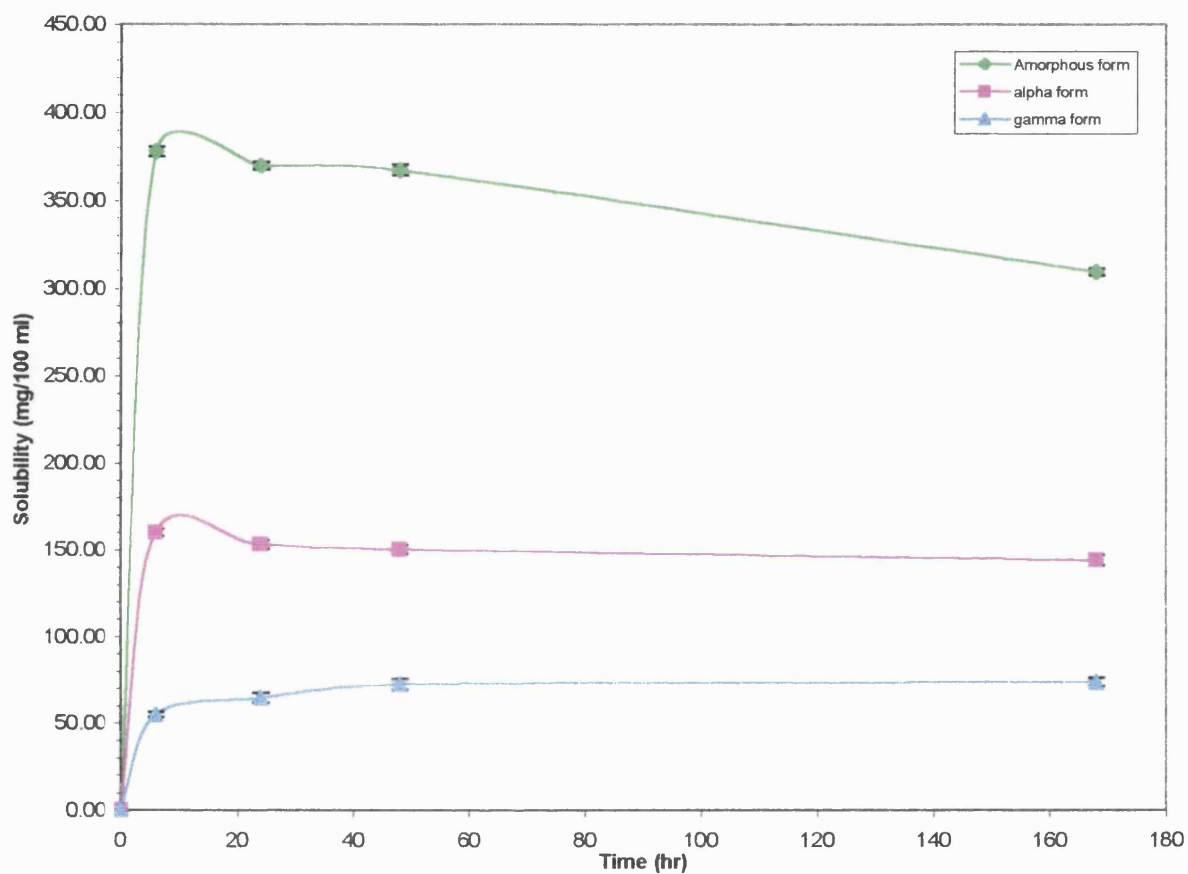


Figure 6.2 Solubility study of amorphous, α and γ form of indomethacin.

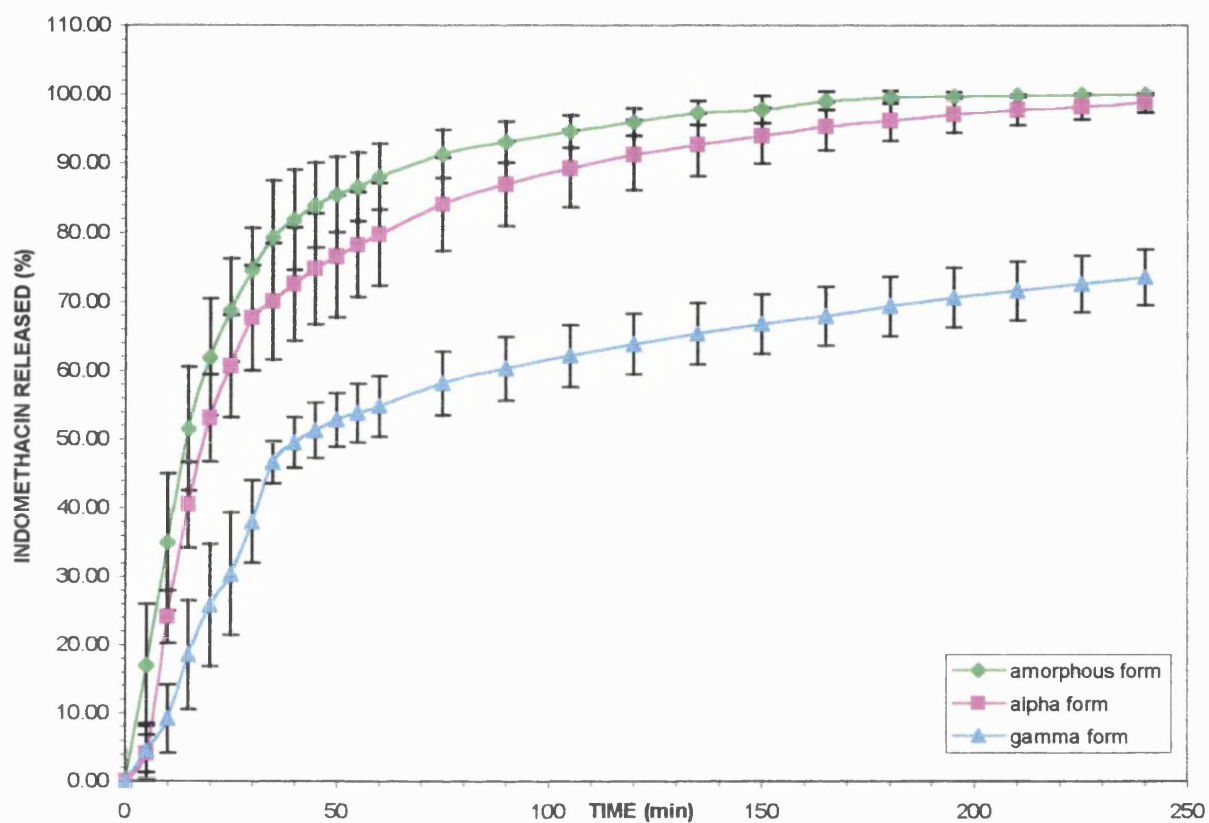


Figure 6.3 The dissolution profiles of amorphous, α and γ indomethacin

Table 6.1(a) ANOVA table of $T_{50\%}$ values of amorphous, α and γ forms of indomethacin

	Sum of Squares	df	Mean Square	F	Sig.
Between Groups	3142.390	2	1571.195	32.443	0.000
Within Groups	726.450	15	48.430		
Total	3868.840	17			

Table 6.1(b) Tukey HSD test results of $T_{50\%}$ values of amorphous, α and γ form indomethacin

Indomethacin	N	Subset for alpha = 0.05	do.
		1	2
Amorphous	6	14.5167	
α form	6	19.2667	
γ form	6		44.6167
Sig.		0.481	1.000

Means for groups in homogeneous subsets are displayed above.

Figure 6.3 shows the dissolution profiles of amorphous, α and γ indomethacin. The profiles indicated that the amorphous form had the highest dissolution rate, followed by the metastable (α) and finally the stable form (γ). It can be noted that the γ form was dissolved to the extent of about 70% at 240 min. The $T_{50\%}$ values were 15.4 minutes for amorphous, 19.3 minutes for α and 44.6 minutes for γ indomethacin. According to Noyes-Whitney equation, the dissolution rate is affected by the solubility of the compound in the medium. As such, the rank order of the dissolution rate was similar to that of the solubility.

When the $T_{50\%}$ values of amorphous, α and γ form indomethacin were analyzed statistically using one-way analysis of variance, they were significantly different. However, post-hoc statistical analysis showed that the $T_{50\%}$ values of the amorphous and the α forms of indomethacin were not significantly different. The reason amorphous and α form were not significantly different in post hoc analysis could be attributed to the particle size of α form used in the experiment, which was relatively small at around 20 μm , as compared to others at 93-150 μm as described in section 6.2.9. The fluffy nature of α indomethacin powder made sieving difficult. Additionally, the α form had needle shape and hence a high surface area.

The drug content of the indomethacin and PVP mixtures prepared using physical mixing, supercritical CO_2 and solid dispersion methods.

The drug content of indomethacin and PVP mixtures at various proportions produced using different methods is given in Table 6.2. The results showed that physical mixing and SCF samples gave nearly the same amount of drug content as expected. Whereas,

the solid dispersion did not give the drug content as predicted. It can be noted that mixing was affected by the method of preparation and composition.

Table 6.2 The indomethacin content in various mixtures of indomethacin and PVP.

Expected % indomethacin	Measured % indomethacin in SCF samples Mean \pm SD	Measured % indomethacin in Solid dispersion samples Mean \pm SD	Measured % indomethacin in Physical mixtures samples Mean \pm SD
80	79.7 (1.3)	78.9 (1.8)	81.4 (1.6)
70	71.1 (0.1)	69.8 (1.2)	69.2 (0.8)
50	49.6 (0.2)	53.6 (0.3)	50.6 (0.6)
40	39.5 (0.5)	42.3 (1.1)	39.9 (1.0)
17	17.2 (0.7)	20.1 (0.1)	17.9 (0.8)

Dissolution studies of indomethacin in mixtures of various proportions of PVP prepared using physical mixing , solid dispersion and supercritical CO₂ methods.

The dissolution profiles of physical mixtures of indomethacin and various proportion of PVP are presented in Figure 6.4. Increasing PVP content from 20% to 60% increased the dissolution rate of indomethacin. The dissolution profiles of both 50% and 60%PVP were similar and were almost superimposable. At 83%PVP, however, the dissolution rate was slower than at 50 and 60%PVP although higher than the 20 and 30%PVP. The indomethacin used in the physical mixtures is the stable gamma crystalline form (the form with poor dissolution). Incorporation of a hydrophilic polymer, such as PVP, enhanced the indomethacin dissolution when compared with the dissolution of indomethacin alone. Nevertheless, at high concentration the increase in viscosity in the diffusion layer as a result of gel formation of PVP could retard the drug release. Indomethacin in the physical mixtures dissolved rapidly in the first 15 minutes and then slowed down gradually. In the earlier stage, PVP from the physical mixture might lower the surface tension of the dissolution medium, resulted in wetting of the indomethacin crystal surface. Subsequently, PVP might increase the viscosity of the solution, resulting in slower diffusion and dissolution of the drug. The relationship between viscosity and drug diffusion has been discussed by Sarisuta and Parrott (1982, 1983) and Doherty and York (1987).

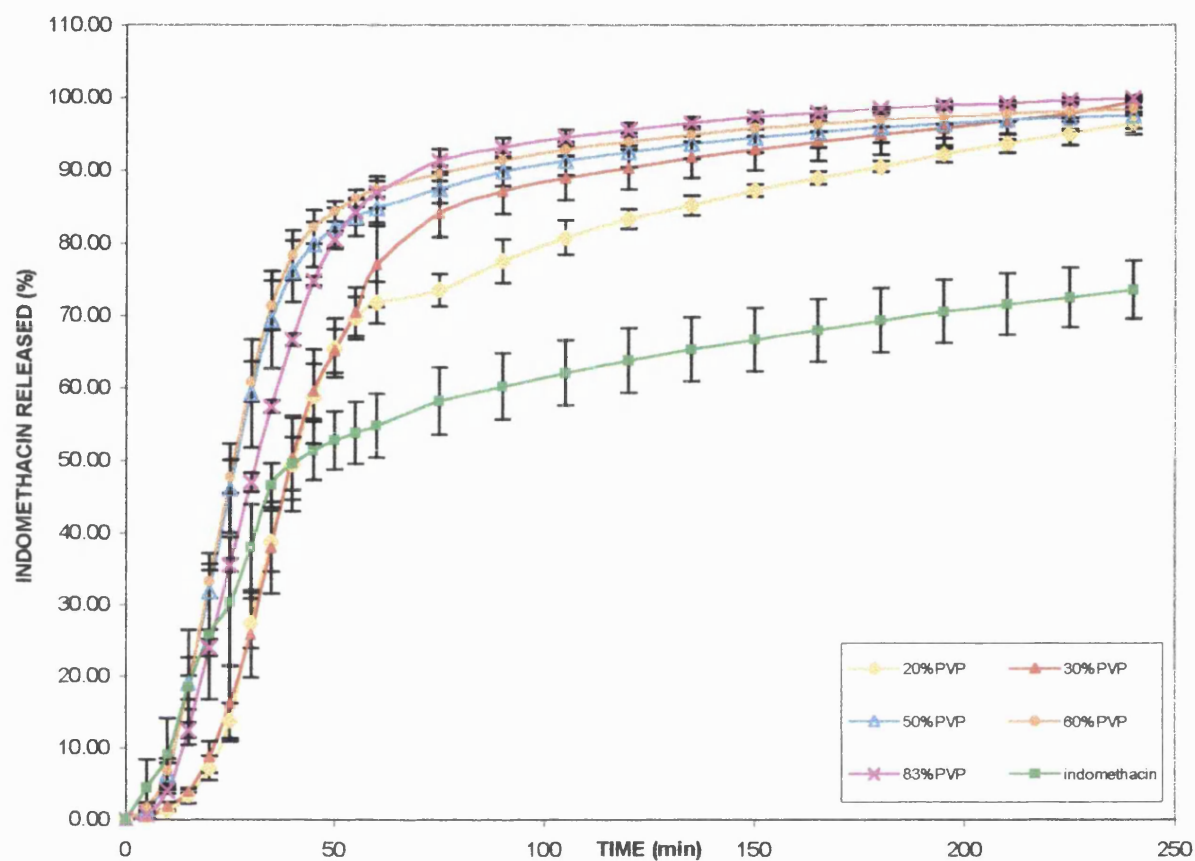


Figure 6.4 Dissolution profiles of pure indomethacin and physical mixture of indomethacin with 20-83% of PVP.

Table 6.3(a) ANOVA table of $T_{50\%}$ values of physical mixture of indomethacin with 20-83% of PVP.

	Sum of Squares	df	Mean Square	F	Sig.
Between Groups	857.398	4	214.350	17.367	0.000
Within Groups	308.565	25	12.343		
Total	1165.963	29			

Table 6.3(b) Tukey HSD test results of $T_{50\%}$ values of physical mixture of indomethacin with 20-83% of PVP.

%PVP	N	Subset for alpha = 0.05	do.	do.	do.
		1	2	3	4
60	6	24.9333			
50	6	26.8333	26.8333		
83	6		31.9500	31.9500	
20	6			35.0500	35.0500
30	6				39.5833
Sig.		0.880	0.117	0.555	0.200

Means for groups in homogeneous subsets are displayed above.

Indomethacin prepared using solid dispersion and supercritical CO₂ methods did not show similar trends to the trends noted for physical mixtures.

Table 6.4 shows the T_g and % crystallinity of solid dispersions of indomethacin and various proportions of PVP. Indomethacin existed in partially amorphous form at 20 and 30% PVP. An increase in the PVP content resulted in a decrease of % crystallinity. A totally amorphous sample could be obtained at 50% PVP and above. In contrast, Matsumoto and Zografi (1999) reported that solid dispersion of indomethacin and PVP at 5% and above prepared using solvent evaporation method was totally amorphous. According to PXRD data, there was a peak at 8.5° 2θ confirming that only the α type was detected in 20 and 30 % PVP solid dispersion samples. Figures 6.5-6.7 show PXRD profiles of solid dispersions of indomethacin with 20, 30 and 50% PVP, respectively.

Table 6.4 Glass transition temperature and degree of crystallinity for solid dispersions of indomethacin and PVP obtained by Differential Scanning Calorimetry and PXRD, respectively.

%PVP	T_g (K)	Degree of crystallinity (%)
20	341.67	20
30	347.89	13
50	356.78	0
60	372.12	0
83	397.45	0

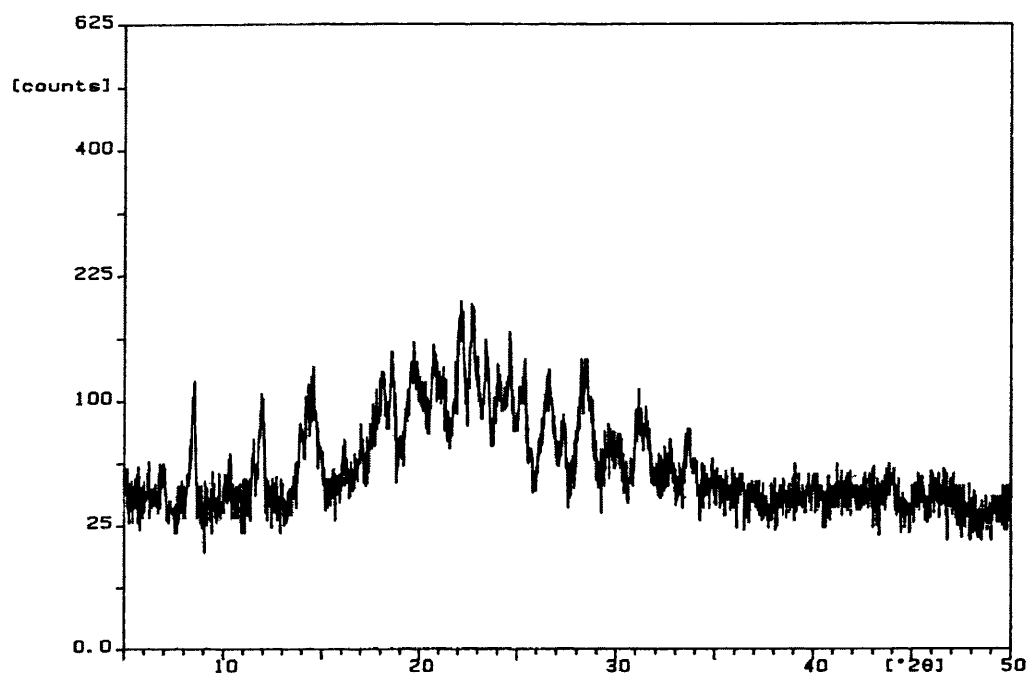


Figure 6.5 PXRD pattern of the solid dispersion of indomethacin and 0.2 PVP weight fraction prepared using solvent evaporation method.

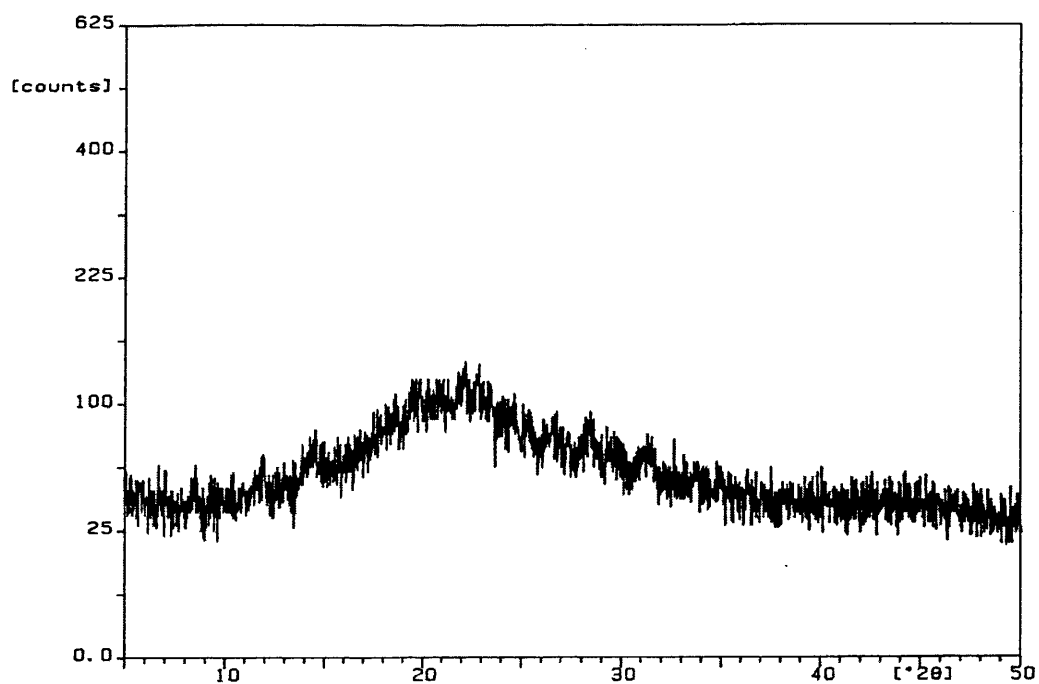


Figure 6.6 PXRD pattern of the solid dispersion of indomethacin and 0.3 PVP weight fraction prepared using solvent evaporation method.

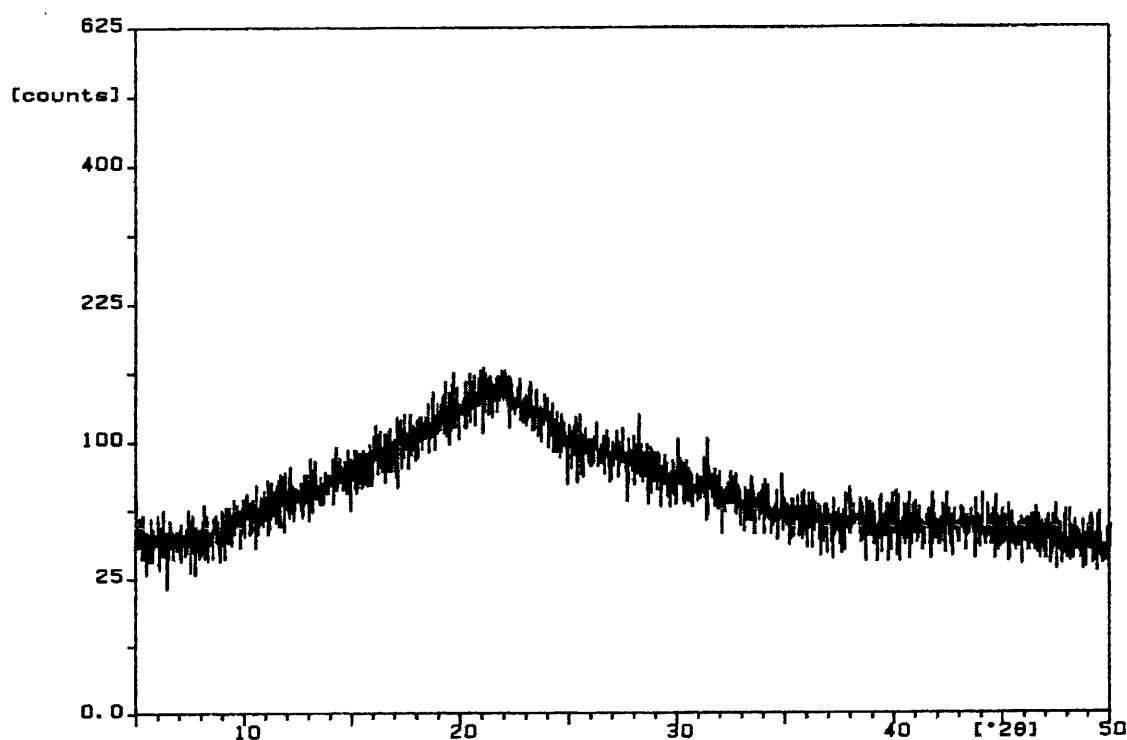


Figure 6.7 PXRD pattern of the solid dispersion of indomethacin and 0.5 PVP weight fraction prepared using solvent evaporation method.

The dissolution profiles of solid dispersions of indomethacin and various proportion of PVP are shown in Figure 6.8. The maximum dissolution rate was obtained by the dispersion having 20 % PVP and then followed by 30% PVP. Since both samples are partially amorphous and only the α -type exists, it may therefore be expected to have a fast initial dissolution rate due to the solution of amorphous content. This solution may become depleted with time and can be followed by a slow dissolution phase of the crystalline material. It should be noted that the release profiles of both 20 and 30%PVP samples were biphasic, these samples were both partially amorphous. The dissolution profiles of both 50% and 60%PVP were noted as being similar. The release profile of 83% deviated from those of others due to the high viscosity of PVP gel which could retard the drug release. However, at higher % PVP (50, 60 and 83%PVP), the dissolution rates were found to be lower than those of 20 and 30 %PVP. This trend could be related to the 2 factors involved, the viscosity/gel

formation and crystallinity. Should this be the case, the crystallinity effect might not be dominant compared to gel formation.

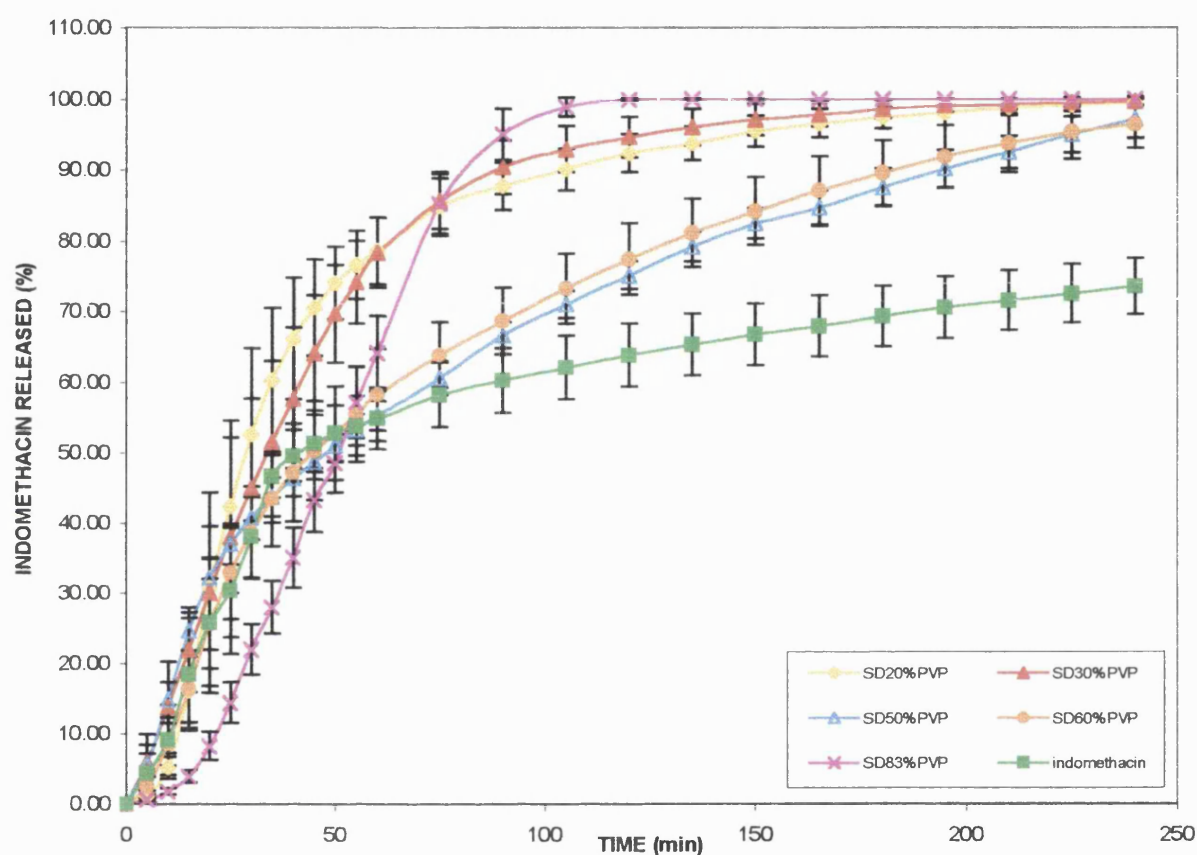


Figure 6.8 Dissolution profiles of pure indomethacin and solid dispersion (SD) of indomethacin with 20-83% of PVP prepared using solvent evaporation method.

Table 6.5(a) ANOVA table of $T_{50\%}$ values of solid dispersion indomethacin with 20-83% of PVP prepared using solvent evaporation method.

	Sum of Squares	df	Mean Square	F	Sig.
Between Groups	2308.071	4	577.018	10.412	0.000
Within Groups	1385.517	25	55.421		
Total	3693.588	29			

Table 6.5(b) Tukey HSD test results of $T_{50\%}$ values of solid dispersion indomethacin with 20-83% of PVP prepared using solvent evaporation method.

%PVP	N	Subset for alpha = 0.05	do.	do.
		1	2	3
20PVP	6	29.5000		
30PVP	6	35.1000	35.1000	
60PVP	6		43.0500	43.0500
83PVP	6			49.9667
50PVP	6			52.7833
Sig.		0.692	0.369	0.190

Means for groups in homogeneous subsets are displayed above.

With regard to Table 5.2 (Chapter 5), the coprecipitated indomethacin and 20-60% PVP samples prepared using the supercritical fluid method were partially amorphous. The PXRD profiles (Figure 5.9-5.14 in Chapter 5) showed that only γ -type was detected in all the co-precipitated indomethacin. For the dissolution of supercritical fluid samples shown in Figure 6.9, the 20%, 60% and 83% PVP samples displayed lower dissolution rates than those of 30 and 50% PVP. Referring to Tukey HSD test results of $T_{50\%}$ values of coprecipitates indomethacin shown in Table 6.6 (b), it can be noted that the 20%, 60% and 83% PVP samples were in one group and 30 and 50% PVP in another group. The 20%, 60% and 83% PVP samples displayed lower dissolution rate than those of 30 and 50% PVP. The 20% PVP had the highest % crystallinity whereas the 83% PVP was totally amorphous. In view of this, the gel forming effect of PVP was dominant in retarding drug release at higher content of PVP.

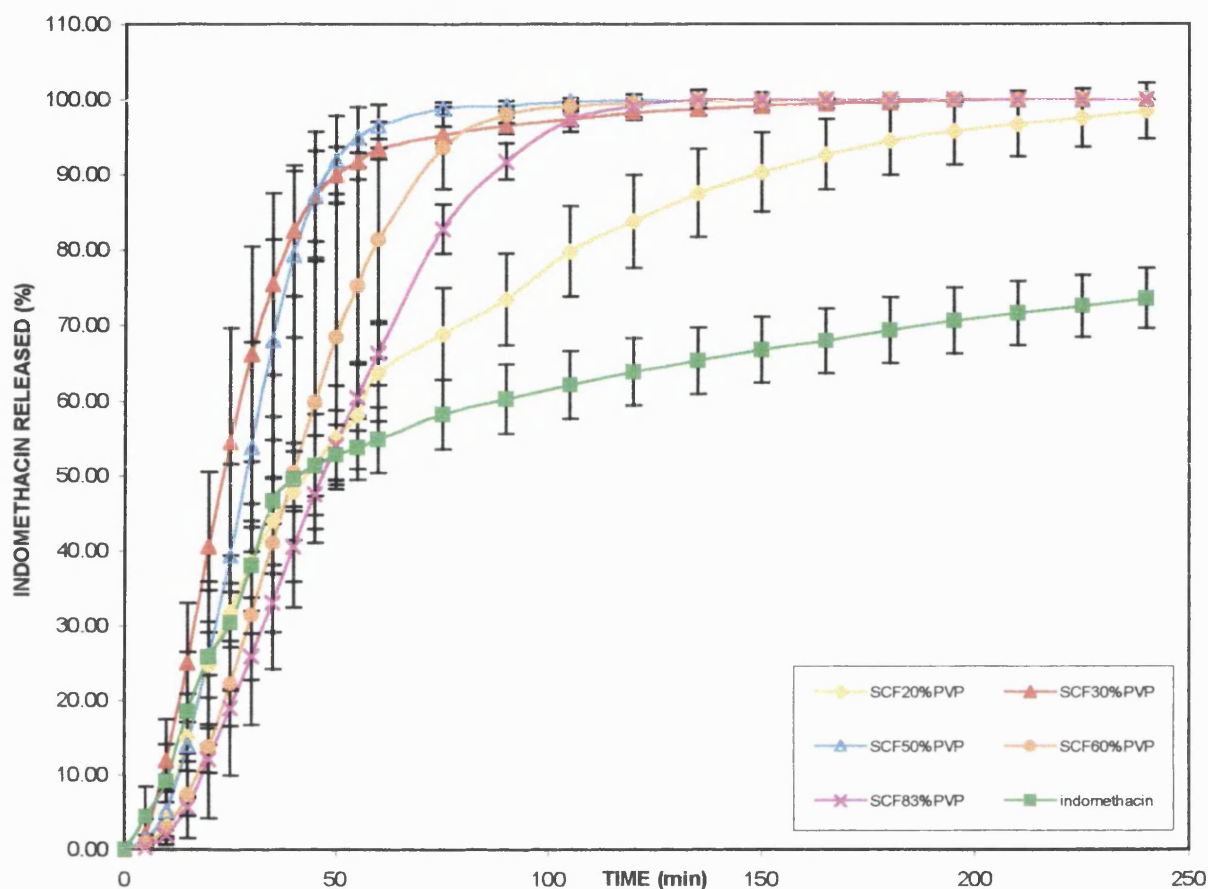


Figure 6.9 Dissolution profiles of pure indomethacin and coprecipitates of indomethacin with 20-83% of PVP prepared using supercritical CO₂ based technique.

Table 6.6(a) ANOVA table of T_{50%} values of coprecipitates indomethacin with 20-83% of PVP prepared using supercritical CO₂ based technique.

	Sum of Squares	df	Mean Square	F	Sig.
Between Groups	2607.255	4	651.814	9.598	0.000
Within Groups	1697.738	25	67.910		
Total	4304.994	29			

Table 6.6(b) Tukey HSD test results of $T_{50\%}$ values of coprecipitates indomethacin with 20-83% of PVP prepared using supercritical CO_2 based technique.

% PVP	N	Subset for alpha = 0.05	do.
		1	2
30PVP	6	23.5000	
50PVP	6	27.5833	
60PVP	6		42.3667
20PVP	6		42.9167
83PVP	6		47.0167
Sig.		0.909	0.863

Means for groups in homogeneous subsets are displayed.

Table 6.7 shows the comparison of values of $T_{50\%}$ using three different methods of preparation, and similar ratios of indomethacin and PVP. It should be noted that at 20% PVP, the $T_{50\%}$ of solid dispersion was lowest. However, at PVP contents of 30 and 50%, the supercritical fluid samples had the lowest value of $T_{50\%}$. At the higher concentration of PVP, at 60 and 83 % PVP, the physical mixtures had the lowest $T_{50\%}$. The $T_{50\%}$ values of indomethacin prepared using 3 different methods for similar ratio of indomethacin and PVP (20-83 %) which were analysed statistically using one-way analysis of variance and post-hoc statistical analysis are shown in Tables 6.8-6.12. It should be noted that except at 20% PVP, the mean $T_{50\%}$ values of other PVP concentrations prepared using physical mix, solvent evaporation and supercritical fluids based techniques were significantly different. In other words, the $T_{50\%}$ values were not affected by the methods used at 20% PVP. Nevertheless, the $T_{50\%}$ values of other PVP concentrations were highly dependent on the methods used.

Table 6.7 $T_{50\%}$ of mixtures of indomethacin and various proportion of PVP prepared using physical mixing, solid dispersion and supercritical fluids based technique. The numbers shown in the brackets are the respective standard deviations.

$T_{50\%}$ (min) %PVP	Physical mixing	Solid dispersion	Super critical fluids
20	35.05(5.90)	29.50(6.37)	42.92(13.57)
30	39.58(4.23)	35.10(4.70)	23.50(5.13)
50	26.83(1.66)	52.78(5.83)	27.58(7.08)
60	24.93(2.36)	43.05(13.10)	42.37(8.09)
83	31.95(0.85)	49.97(2.96)	47.02(3.68)

Table 6.8(a) ANOVA table of $T_{50\%}$ values of indomethacin from indomethacin and 20% PVP prepared by three different methods.

	Sum of Squares	df	Mean Square	F	Sig.
Between Groups	545.388	2	272.694	3.153	0.072
Within Groups	1297.243	15	86.483		
Total	1842.631	17			

Table 6.8(b) Tukey HSD test results of $T_{50\%}$ values of indomethacin from indomethacin and 20% PVP prepared by three different methods.

	N	Subset for alpha = 0.05
		1
Solid dispersion	6	29.5000
Physical mixture	6	35.0500
SCF	6	42.9167
Sig.		0.060

Means for groups in homogeneous subsets are displayed above.

Table 6.9 (a) ANOVA table of $T_{50\%}$ values of indomethacin from indomethacin and 30% PVP prepared by three different methods.

	Sum of Squares	df	Mean Square	F	Sig.
Between Groups	826.668	2	413.334	18.704	0.000
Within Groups	331.488	15	22.099		
Total	1158.156	17			

Table 6.9(b) Tukey HSD test results of $T_{50\%}$ values of indomethacin from indomethacin and 30% PVP prepared by three different methods.

	N	Subset for alpha = 0.05	do.
		1	2
SCF	6	23.5000	
Solid dispersion	6		35.1000
Physical mixture	6		39.5833
Sig.		1.000	0.256

Means for groups in homogeneous subsets are displayed above.

Table 6.10(a) ANOVA table of $T_{50\%}$ values of indomethacin from indomethacin and 50% PVP prepared by three different methods.

	Sum of Squares	df	Mean Square	F	Sig.
Between Groups	2618.010	2	1309.005	45.216	0.000
Within Groups	434.250	15	28.950		
Total	3052.260	17			

Table 6.10(b) Tukey HSD test results of $T_{50\%}$ values of indomethacin from indomethacin and 50% PVP prepared by three different methods.

	N	Subset for $\alpha = 0.05$	do.
		1	2
Physical mixture	6	26.8333	
SCF	6	27.5833	
Solid dispersion	6		52.7833
Sig.		.968	1.000

Means for groups in homogeneous subsets are displayed above.

Table 6.11(a) ANOVA table of $T_{50\%}$ values of indomethacin from indomethacin and 60% PVP prepared by three different methods.

	Sum of Squares	df	Mean Square	F	Sig.
Between Groups	1265.203	2	632.602	7.818	0.005
Within Groups	1213.742	15	80.916		
Total	2478.945	17			

Table 6.11(b) Tukey HSD test results of $T_{50\%}$ values of indomethacin from indomethacin and 60% PVP prepared by three different methods.

	N	Subset for $\alpha = 0.05$	do.
		1	2
Physical mixture	6	24.9333	
SCF	6		42.3667
Solid dispersion	6		43.0500
Sig.		1.000	0.991

Means for groups in homogeneous subsets are displayed above.

Table 6.12(a) ANOVA table of $T_{50\%}$ values of indomethacin from indomethacin and 83 % PVP prepared by three different methods.

	Sum of Squares	df	Mean Square	F	Sig.
Between Groups	1120.614	2	560.307	73.022	0.000
Within Groups	115.097	15	7.673		
Total	1235.711	17			

Table 6.12(b) Tukey HSD test results of $T_{50\%}$ values of indomethacin from indomethacin and 83% PVP prepared by three different methods.

	N	Subset for $\alpha = 0.05$	do.
		1	2
Physical mixture	6	31.9500	
SCF	6		47.0167
Solid dispersion	6		49.9667
Sig.		1.000	0.189

Means for groups in homogeneous subsets are displayed above.

Stability of amorphous indomethacin at different temperatures.

Figures 6.10-6.12 show the plots of percentage crystallinity against time for quenched amorphous indomethacin after storage over a 3-month period at 30, 50 and 70 °C, respectively. It can be noted that the amorphous indomethacin crystallized at 30 °C after an induction period of about 36 hours. This is in accordance with the periods of 28 hours reported by Otsuka and Kenikewa (1988) and 36 hours by Yoshioka et al (1994). It took approximately one month for crystallization to reach a steady state, and at this time the indomethacin had 90% crystallinity. At isothermal crystallization of 30 °C, the amorphous sample only changed to the γ crystal form. The plot in Figure 6.10(b) indicated that the transition of amorphous indomethacin to the crystalline form followed first order kinetic with a rate constant of 0.10 day^{-1} . This was also in accordance with the results of 0.12 day^{-1} reported by Otsuka and Kenikewa (1988) and 0.11 day^{-1} by Yoshioka et al (1994), respectively. Crystallization from the amorphous state of indomethacin could occur at 30 °C, a temperature which is below the T_g of 50 °C, since at this condition, indomethacin has sufficient rotational mobility to form a nucleus of critical size followed by crystal growth (Yoshioka et al, 1994).

Crystallization at 50 °C led to both α and γ forms as shown in Figure 6.11. It should be noted that the initial rate of appearance of the γ form was reduced in comparison with that at 30 °C and the α form appeared after a 4-day induction period. Both α and γ forms existed in almost equal proportions. It should be noted in Figure 6.12 that at 70 °C, both forms showed relatively higher initial crystallization rate than those of 50 °C. However, the curves were followed by abrupt plateau and the combination of % crystallinity for both forms was nearly 100%. It was found that at lower temperature, the condition favoured the crystallization of thermodynamically more stable γ form, whereas at higher temperature both polymorphs appeared but the α metastable form, which was thermodynamically less stable, showed a tendency to dominate. Yoshioka et al (1994) suggested that at a storage temperature above T_g , the particular polymorphic form existed under a particular set of conditions due to the thermodynamic factors, which included mechanisms and rates. From homogeneous nucleation theory (Turnbull and Fisher, 1949 through Yoshioka et al, 1994), the trends for either of the two polymorphs to crystallize from the amorphous state could be explained by a balance between the free energy at the nucleus/amorphous matrix

interface, and the free energy difference between the particular crystal form and amorphous matrix.

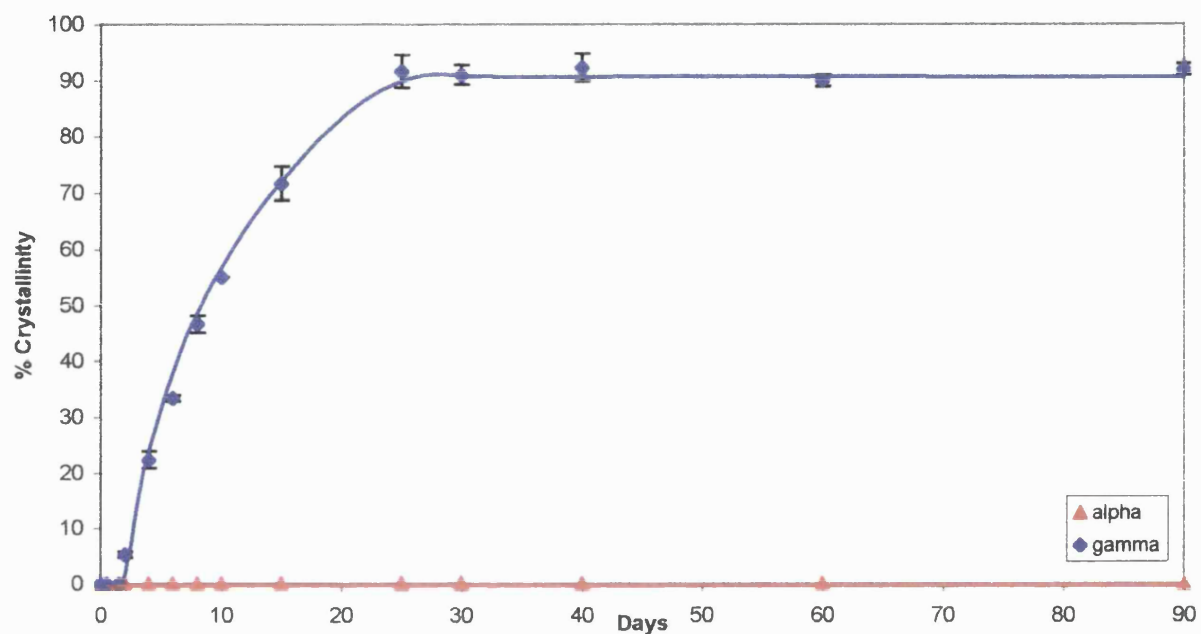


Figure 6.10 (a) percent crystalline phase *versus* time at 30 °C for the amorphous indomethacin

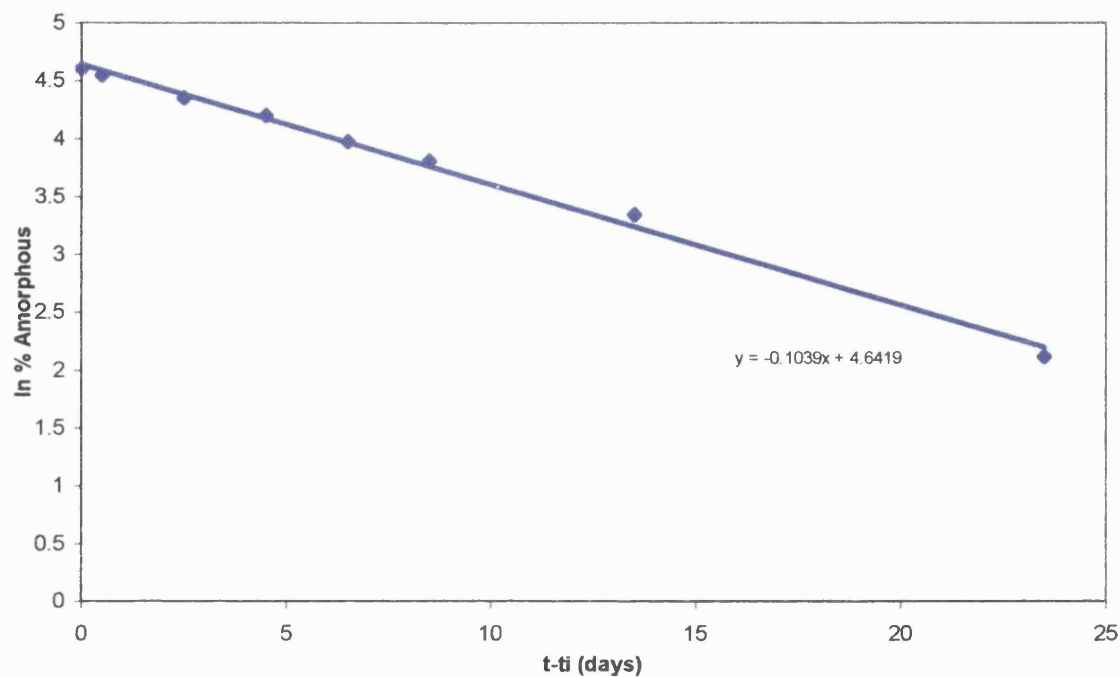


Figure 6.10 (b) plot of percent amorphous indomethacin remaining after storage at 30 °C for various time periods (t) after an induction time (t_i) for the amorphous indomethacin.

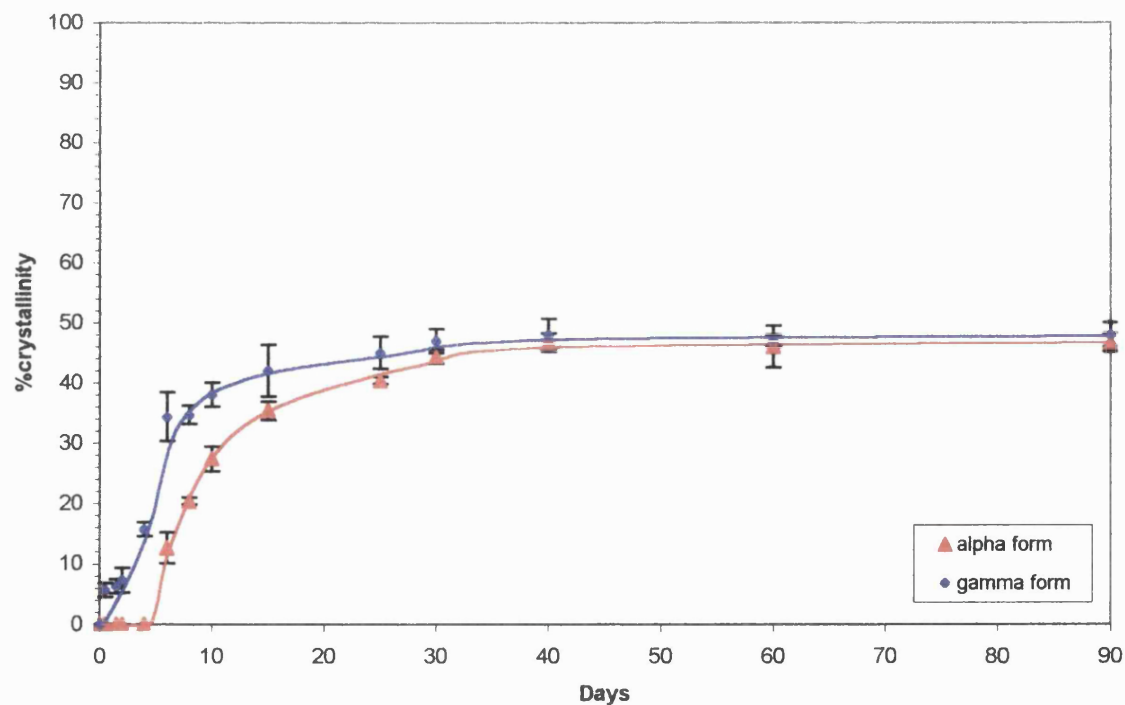


Figure 6.11 Percent crystalline phase *versus* time at 50 °C for the amorphous indomethacin

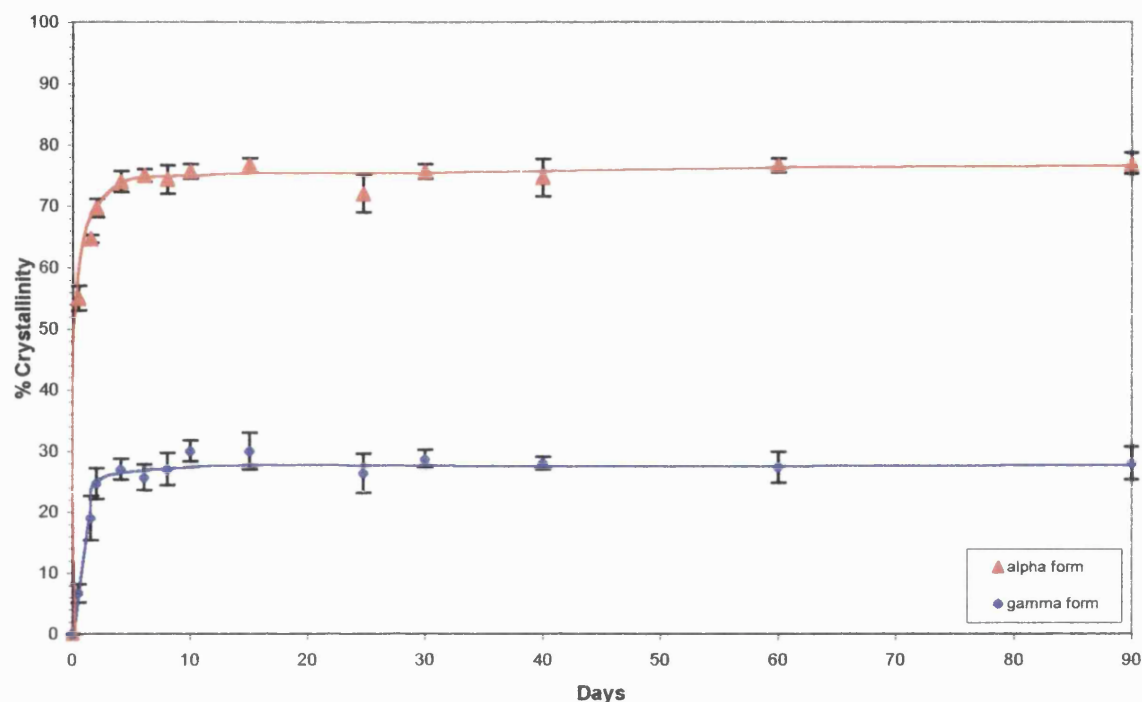


Figure 6.12 Percent crystalline phase *versus* time at 70 °C for the amorphous indomethacin.

Stability of coprecipitated indomethacin with PVP at different temperatures.

The stability of coprecipitated indomethacin and PVP at 20%, 50% and 83% prepared using solvent evaporation and sc-CO₂ methods was investigated. The degree of crystallinity results, determined by PXRD, of all freshly prepared solid dispersion (SD) and supercritical fluid (SCF) samples which were used to study the isothermal crystallisation at 30, 50 and 70 °C are given in Table 6.13. The appearance of crystalline indomethacin, either in the alpha or gamma crystalline form over a 3-month period at 3 different storage temperatures was monitored.

Table 6.13 Degree of crystallinity of indomethacin and PVP coprecipitated using solid dispersion and supercritical fluid technique.

Samples	% Crystallinity (t = 0 days)	Polymorph present
SD20PVP	20	α
SD50PVP	0	-
SD83PVP	0	-
SCF20PVP	55	γ
SCF50PVP	18	γ
SCF83PVP	0	-

Figures 6.13-6.15 show the %crystallinity versus time of SD 20%PVP, SCF 20%PVP and SCF 50%PVP, respectively. The α form presented in solid dispersion sample whereas the γ form presented in supercritical fluid samples. The higher the temperature, a more drastic change in % crystallinity was obtained. For SD 50%PVP, SD 83%PVP and SCF 83%PVP, there was no change in crystallinity over 3 months at 30, 50 and 70 °C. From these results, it can be concluded that indomethacin coprecipitated with PVP can have a significant inhibiting effect on crystallization rates at PVP levels of 50% and 83% for solid dispersion and 83% for supercritical fluid coprecipitate.

From Figure 6.13, it can be noted that the crystallinity of SD 20% PVP did not change up to 3 months at 30 °C. The percentage crystallinity changed from 20 % to 35% at 50 °C and to 38% at 70 °C, respectively. This phenomenon could be attributed to the seeding effect. As shown in Table 6.13, freshly prepared SD 20% PVP had 20 % crystallinity. The presence of α crystal in the coprecipitates could have enhanced crystallization.

From Figures 6.14 and 6.15, SCF 20% PVP was noted to exhibit a greater extent of % crystallinity change after a 3-month period. At 70 °C, the percentage crystallinity of SCF 20% PVP changed from 54% to 80%, whereas SCF 50%PVP changed from 19% to 40%. This phenomenon could be attributed to the seeding effect. As shown in Table 6.13, freshly prepared SCF 20% PVP had 54 % crystallinity, whereas SCF 50% PVP had 19% crystallinity. The presence of γ crystal in the coprecipitates could have enhanced crystallization. The more amount of γ crystal the higher the extent of crystallization.

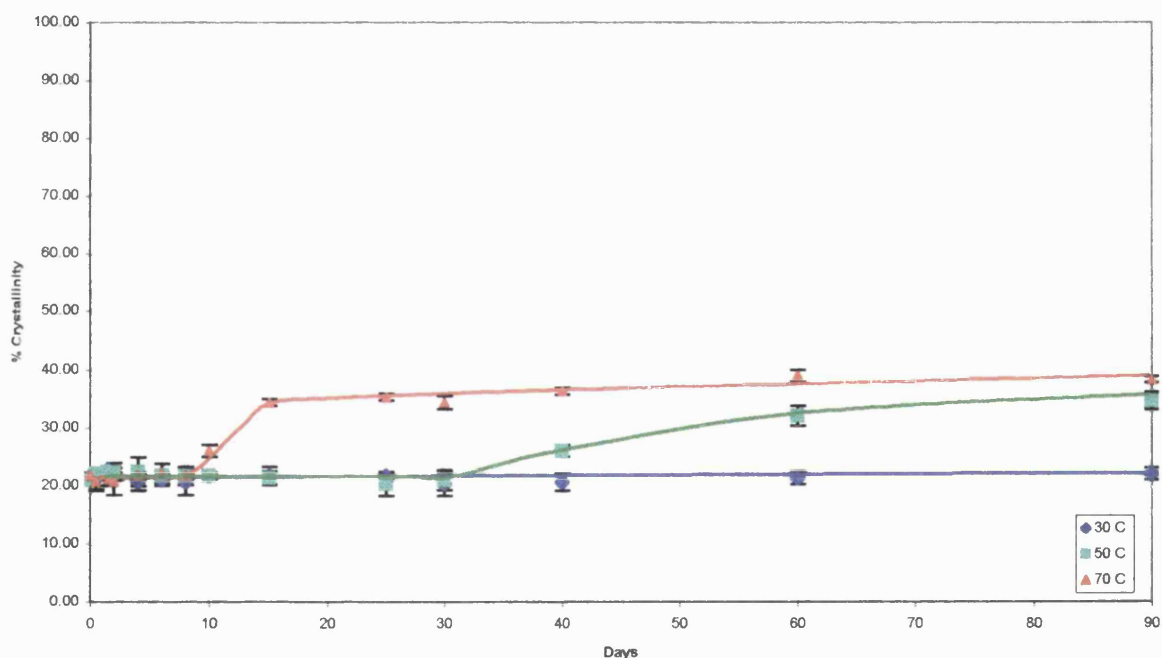


Figure 6.13 Percent crystalline phase *versus* time at 30, 50 and 70 °C for the solid dispersion of indomethacin and 20%PVP.

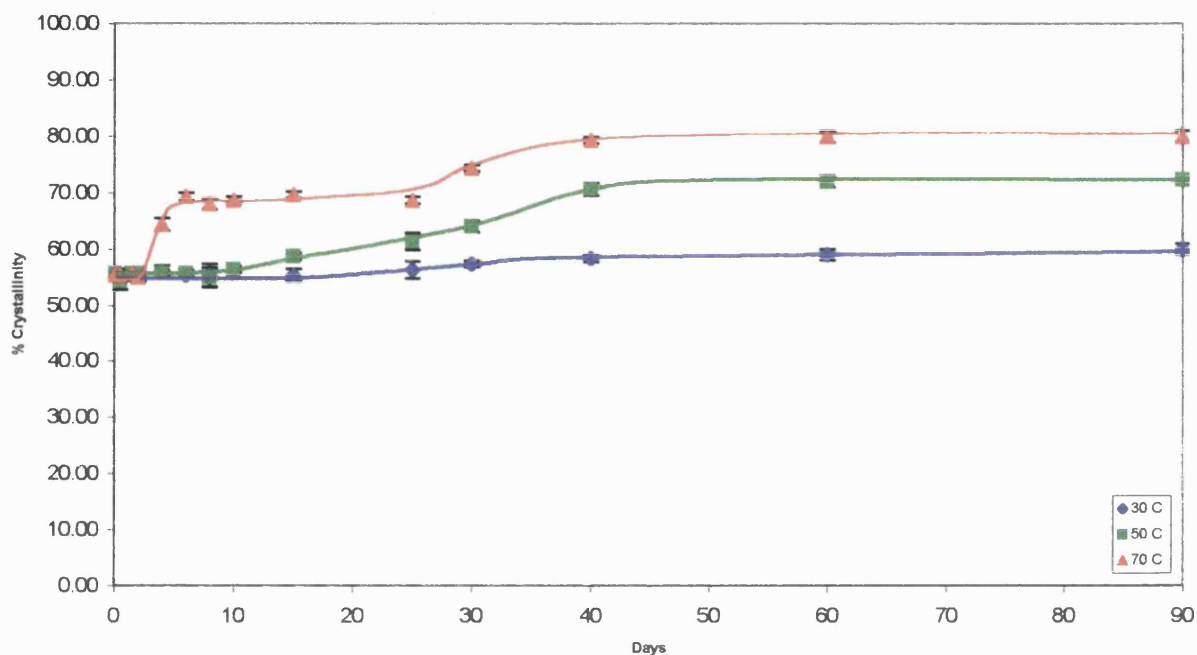


Figure 6.14 Percent crystalline phase *versus* time at 30, 50 and 70 °C for the coprecipitated indomethacin and 20%PVP prepared using the SCF based technique.

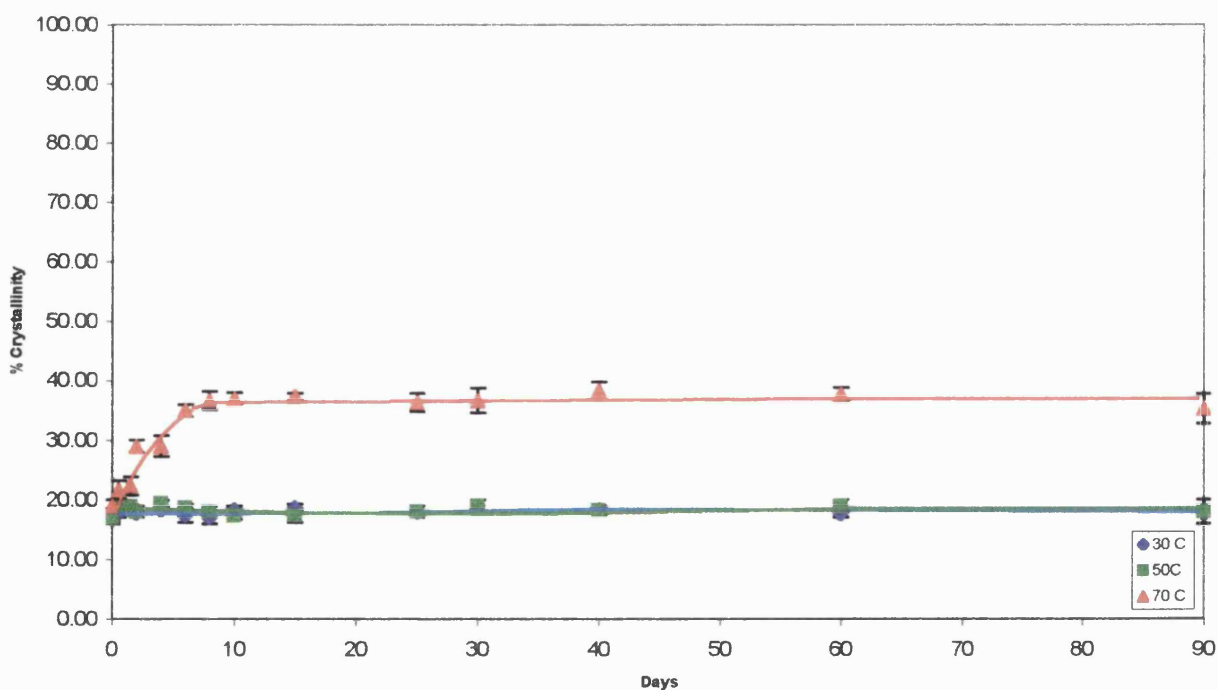


Figure 6.15 Percent crystalline phase *versus* time at 30, 50 and 70 °C for the coprecipitated indomethacin and 50%PVP prepared using the SCF based technique.

Previous studies of indomethacin-PVP coprecipitates showed that PVP acted as an inhibitor of crystallization (Imaizumi et al, 1983, Yoshioka et al, 1995). As reported by Imaizumi et al. (1983), coprecipitated samples at 75% PVP remained amorphous for at least 180, 60 and 30 days when stored at 40, 50 and 60 °C, while amorphous indomethacin exhibited 14% and 25% crystallinity after 2-day storage at 20 and 30 °C, respectively. In our present work, solid dispersion samples at 50% PVP, 83 % PVP and SCF samples at 83%PVP remained amorphous for at least 3 months, whereas amorphous indomethacin alone exhibited 22% crystallinity after storage for 4 days at 30 °C.

Stability of amorphous indomethacin at different relative humidity

Figure 6.16 shows the %crystallinity versus time profiles of amorphous indomethacin stored at 35%RH and 76%RH. Only the γ form was detected. On the other hand, as shown in Figure 6.17, α and γ forms appeared at 98%RH. It was well established that water, with a reported T_g of 135 K, acts as a plasticizer for amorphous and partially amorphous materials (Sugisaki et al 1968, through Hancock and Zografi, 1994). In this case, water might be absorbed into amorphous indomethacin and therefore, it can lower the glass transition temperature, T_g . Consequently, crystallization occurred. The more water absorbed at high % relative humidity, the lower the T_g and thus the increase in crystallization rate.

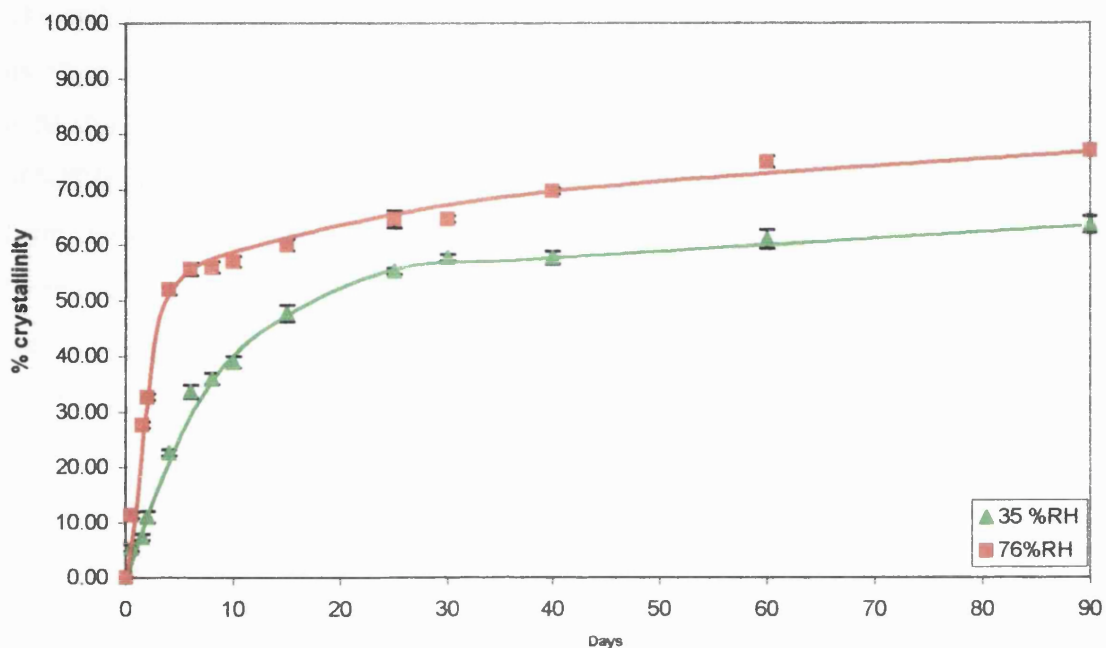


Figure 6.16 Plot of degree of crystallinity *versus* time of amorphous indomethacin stored at 35% and 76% RH and 25°C. Only γ form was found in the samples.

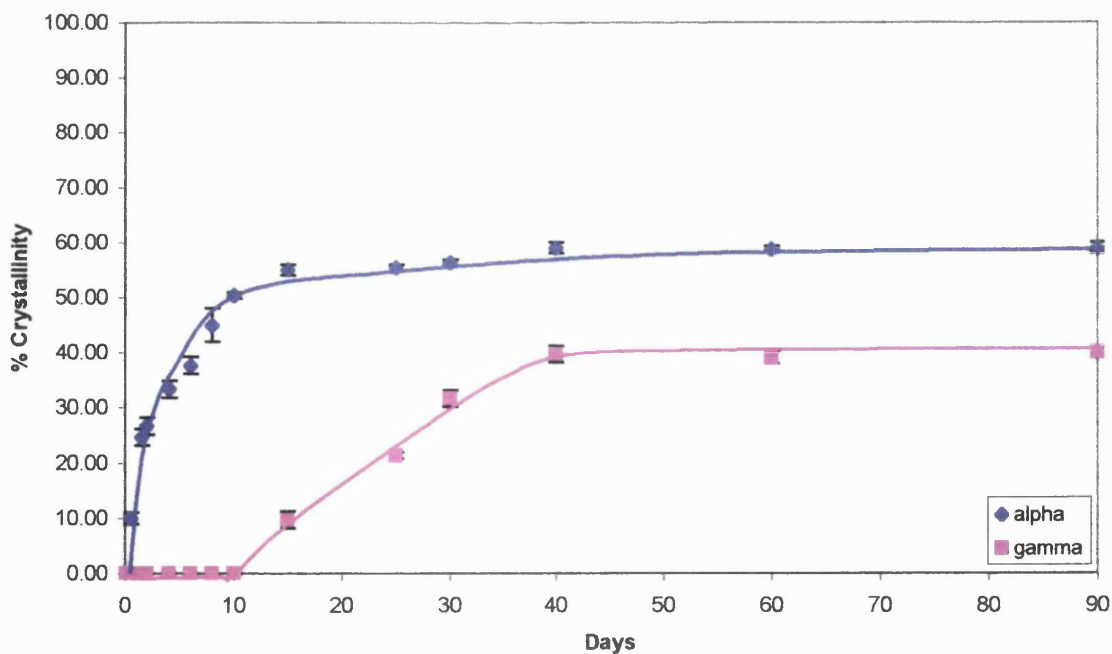


Figure 6.17 Plot of degree of crystallinity *versus* time of amorphous indomethacin stored at 98% RH and 25°C. Both α and γ form were found in the samples.

Stability of coprecipitated indomethacin with PVP at different relative humidity.

The stability of coprecipitated indomethacin and 20%, 50% and 83% PVP prepared using solvent evaporation method and sc-CO₂ method was investigated. Figures 6.18-6.20 show the %crystallinity versus time of SD 20%PVP, SCF 20%PVP and SCF 50%PVP, respectively. The α form presented in solid dispersion sample whereas the γ form presented in supercritical samples. The rate of change in % crystallinity increased with an increase in %RH. In Figure 6.20, the SCF 50% PVP sample was wet and sticky after kept at 76% RH for 30 days and 98% RH for 8 days. Consequently, the % crystallinity could not be determined by PXRD.

Monitoring the appearance of indomethacin coprecipitates, the SD 50%PVP, SD 83%PVP and SCF 83%PVP samples, revealed that there was no change in terms of appearance and also no crystallization occurred over a 3-month period at 35%RH. However, at higher %RH, the samples were wet and converted to a sticky mass within a month. The durations for the appearance of sticky indomethacin as observed at different %RH are given in Table 6.14. From this result, it can be concluded that indomethacin coprecipitated with PVP can have significant inhibiting effect on the crystallization rates at PVP levels of 50% and 83% for solid dispersion and at 83% for supercritical fluid coprecipitate. However, it was observed that the storage conditions could have an effect on the final results.

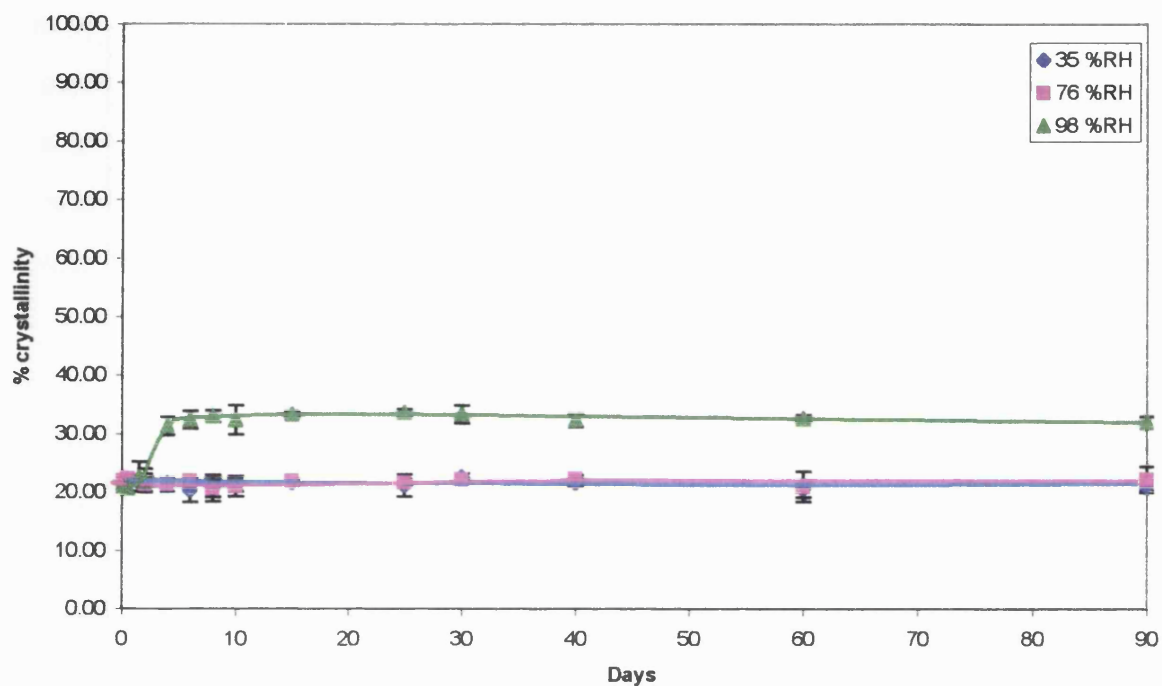


Figure 6.18 Percent crystallinity *versus* time at 35%, 76% and 98% RH for the solid dispersion of indomethacin and 20%PVP.

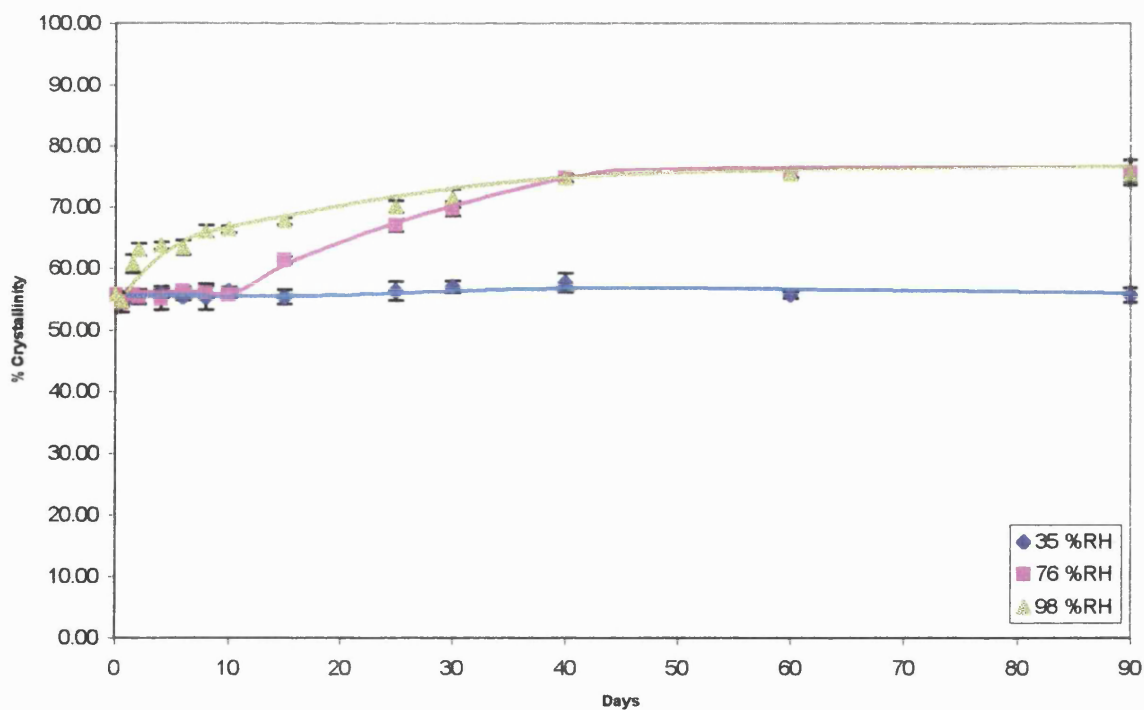


Figure 6.19 Percent crystallinity *versus* time at 35%, 76% and 98% RH for the coprecipitated indomethacin and 20%PVP prepared using SCF based technique. Only the γ form was found in the samples.

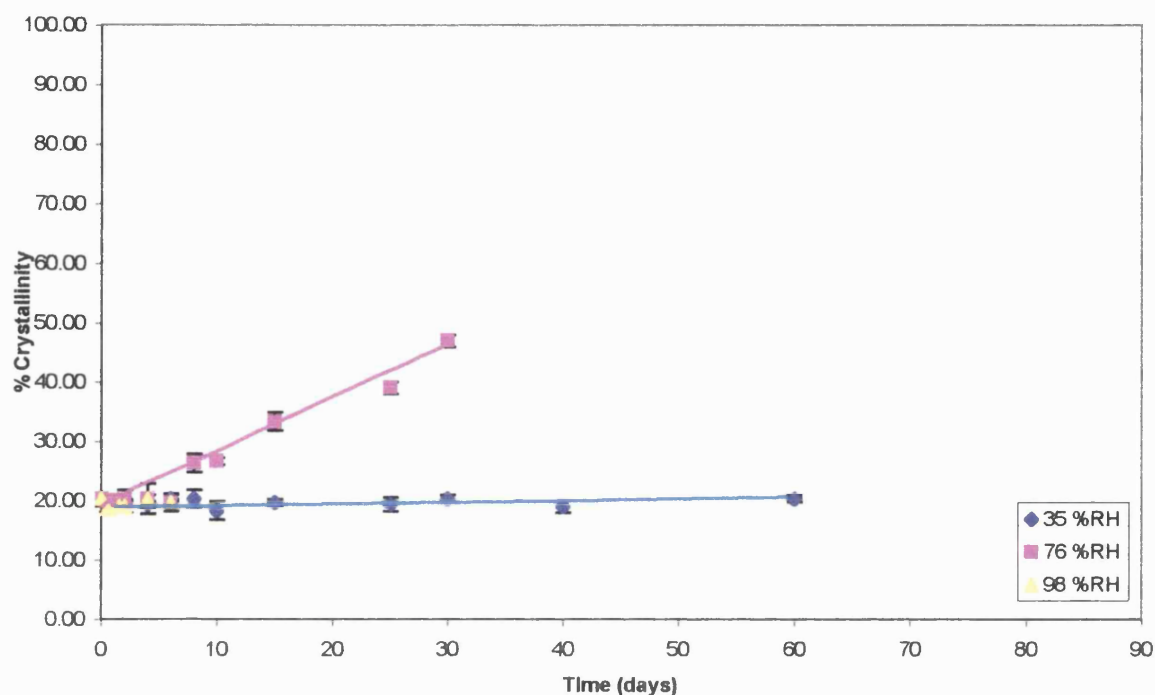


Figure 6.20 Percent crystallinity *versus* time at 35%, 76% and 98% RH for the coprecipitated indomethacin and 50%PVP prepared using SCF based technique. Only the γ form was found in the samples.

Table 6.14 The time measured for the changing of appearance from powder to sticky mass of indomethacin–PVP coprecipitates at various RH at 25 °C.

%RH	Time (days)		
	SD 50 PVP	SD 83 PVP	SCF 83 PVP
35	> 90	>90	>90
76	30	20	20
98	8	5	5

6.4 Conclusions

The dissolution rate and solubility studies of amorphous indomethacin, α and γ indomethacin polymorphs showed that the amorphous form had the highest solubility and dissolution rate, followed by the metastable form (α) and lastly the stable form (γ).

The dissolution studies of various proportions of indomethacin and PVP mixture prepared using sc-CO₂ as solvent, physical mixing and solid dispersion methods showed that PVP could enhance the dissolution of indomethacin at low concentration but an increase in PVP content could retard the dissolution rate. The results were dependent on the amount of PVP in the mixture and additionally the method of preparation. It should be noted that the T_{50%} results obtained using environmental friendly method of employing sc-CO₂ as solvent showed dissolution rate which was comparable and in some cases even better than those results of physical mixing and solid dispersion.

The stability studies for 3 months were carried out on the coprecipitates and amorphous indomethacin. The quenched amorphous indomethacin reached approximately 90% crystallinity within a month at a temperature of 30 °C and only the γ crystalline form was observed. At higher temperatures (50 and 70 °C), crystallization rate increased and both α and γ crystalline forms were obtained. Coprecipitation of indomethacin with PVP retarded the crystallization process. The coprecipitates where indomethacin existed in complete amorphous form did not crystallize after storage at 30, 50 and 70 °C for 3 months. Nevertheless, for coprecipitates with indomethacin existed in partially amorphous form, crystallization occurred at a rate which was dependent on temperature. When the amorphous indomethacin was stored at 35%RH and 76%RH, only the γ form was detected, but both α and γ forms appeared at 98%RH. Similarly, coprecipitation of indomethacin with PVP also retarded the crystallization process at lower %RH. At higher %RH, the powder turned sticky.

Chapter 7

Conclusions and Recommendations

7.1 Introduction

The main objective of this work was to study the preparation and stabilisation of poorly water-soluble drugs in the amorphous state, as a means of producing solid oral dosage forms with rapid dissolution. Indomethacin, a nonsteroidal anti-inflammatory drug (NSAID), was chosen as a model compound because its dissolution rate is limited by its poor solubility in water. The coprecipitation with a water-soluble polymer, polyvinylpyrrolidone (PVP), was used as the means to alter the physical state of indomethacin, i.e. conversion to amorphous content and hence increase in the dissolution rate of indomethacin. The spray-drying of non-aqueous solutions of indomethacin in the presence of various additives were investigated. Additionally, an environmental friendly method using supercritical CO₂ as an antisolvent and solvent were also employed.

Prior to the coprecipitation using supercritical fluid based technique, the rigs were specially designed, fabricated and modified under safety precautions. The feasibility of using supercritical CO₂ to prepare indomethacin and PVP coprecipitates was then investigated. The products were characterized using DSC, SEM and PXRD. Finally, the dissolution and stability of coprecipitates of indomethacin and PVP prepared using supercritical CO₂ was examined.

7.2 General conclusions

Spray drying is a process whereby a solution or suspension is atomised into a fine spray, mixed with warm air and allowed to evaporate to a dry particulate powder. Spray drying has the advantage of being a one-stage process. However, it is limited by low yield and the presence of solvent residue could affect the stability of the final products. Spray drying often produces amorphous material, but spray dried indomethacin from non- aqueous solution remained crystalline, as did co-spray dried indomethacin and microcrystalline cellulose (MCC). Co-spray drying with 20-60% PVP could produce amorphous indomethacin. Combining the third component, either the MCC or SMCC did not affect the physical characteristics of the product. It has been shown that the type and quantity of additives can be instrumental in altering the physical state of indomethacin. The dissolution rate of a direct compression tablet of co spray-dried indomethacin with 20%PVP was higher than that of non-spray dried

indomethacin. To improve the dissolution rate of indomethacin, co-spray drying with 20% PVP is recommended.

An alternative method, using supercritical CO₂ as an antisolvent was performed. Indomethacin precipitated from various organic solvents using supercritical CO₂ (at 40 °C and 150 bar) as antisolvent comprised a mixture of α and γ polymorphs. Based on DSC, PXRD and SEM analyses, it was observed that the α form was present in a higher proportion than the γ form. No significant effect on the drug characteristic was observed when the drug concentration and its feeding rate were varied within the range of operating conditions studied. Due to the limitation of the current experimental set-up, coprecipitation of indomethacin and PVP could not be produced.

The feasibility of precipitation of indomethacin using supercritical CO₂ as a solvent was then assessed after the modification of the previous rig. Application of this process to the precipitation of indomethacin resulted in the γ crystalline form and obviously smaller particle size than that of the original material. At 22 °C, an increase in the operation pressure from 100 to 200 bar resulted in a decrease in particle size.

The dissolution rates of poorly water-soluble drugs can also be enhanced by coprecipitation with water-soluble polymers such as PVP. Numerous studies have demonstrated the feasibility of forming coprecipitates of indomethacin and PVP. Coprecipitation not only can enhance the dissolution rate of indomethacin, but also minimise the side effects such as gastric irritation, ulcers and stomach bleeding upon oral administration. The main objective of this study was to prepare indomethacin-PVP coprecipitates using supercritical CO₂. A successful coprecipitate was obtained upon mixing indomethacin and PVP under supercritical CO₂. Coprecipitation experiments involved studying the effect of pressure and temperature on the characteristic of the drug in the mixture. It was found that coprecipitated indomethacin at various weight fractions was successfully achieved at 75 °C and 150 bar. The amorphous products were obtained at PVP weight fraction of 0.80 and above. As the PVP weight fraction decreased, indomethacin displayed increasing degree of crystallinity. The SEM photographs of the coprecipitates showed a foamy and porous structure.

The dissolution studies of coprecipitates of various proportions of indomethacin and PVP mixture prepared using supercritical CO₂ as solvent and unprocessed crystalline indomethacin in a phosphate buffered solution were determined. The dissolution rate of coprecipitates exhibited comparatively higher dissolution rates than that of crystalline indomethacin alone. The enhanced dissolution rate of the coprecipitate was attributed to the reduction in the degree of crystallinity of the product after processing.

The stability studies for 3 months were carried out on the coprecipitates and amorphous indomethacin itself. The powders were stored under different temperature and relative humidity. Increasing the temperature or relative humidity enhanced the rate of conversion of amorphous indomethacin into crystalline indomethacin. On the other hand, coprecipitation of indomethacin with PVP could retard the crystallization rate.

In summary, this project has demonstrated clearly that the dissolution rate of poorly water-soluble indomethacin was enhanced successfully by the coprecipitation with PVP using “the clean technology”, supercritical CO₂ based process.

7.3 Recommendations for Future Work

Development and evaluation of rapid dissolution dosage forms

The SCF indomethacin-PVP could be used to formulate into tablet or capsule dosage form with rapid dissolution. Equipped with a better dissolution, the dose of indomethacin could be reduced leading to a decrease in side effects. The final dosage form should be evaluated using methods stated in standard monograph such as BP.

Application of SCF onto other poorly soluble drugs and polymers

In the present study, PVP has been used to modify the physical state of indomethacin and increase its stability. Amorphous form of indomethacin was produced with higher dissolution rate. The incorporation of PVP has further improved the stability of the compound. Other hydrophilic polymers such as HPMC, HPC should be investigated. In addition, other poorly water soluble drugs should also be explored.

Further improvement of apparatus

In the present study, some of the components used in the experiments were designed manually. There is still room for improvement in terms of the design of the apparatus. For example, a bigger reaction vessel might be constructed to accommodate a larger quantity of samples per batch. Recycling of CO₂ might be controlled to reduce production cost.

Chemical stability

The chemical stability of indomethacin-PVP mixture should be evaluated to establish the shelf life of the compound. As indomethacin exists in the amorphous form in the mixture, it will be interesting to know if the presence of PVP could reduce its chemical stability without compromising on its physical state.

Exploring more sophisticated and sensitive techniques in measuring amorphous compounds

In the present study, DSC and X-ray diffraction are the tools used in establishing the amorphous or crystalline form of indomethacin. Other alternative techniques such as Isothermal microcalorimetry, Solution calorimetry, Water Absorption and FT-Raman Spectroscopy, should be explored.

References

- Alessi, P.; Cortesi, A.; Kikic, I.; Foster, N.R.; McNaughton, S. J.; Colombo, I. Particle Production of Steroid Drugs Using Supercritical Fluid Processing. *Ind. Eng. Chem. Res.*, 1996, 35, 4718-4726.
- Al-Saieq, S.S.; Riley, G.S. Polymorphism in Sulfonylurea Hypoglycemic Agents, II, Chlopropamide. *Pharm. Acta. Helv.*, 1982, 57(1), 8-11.
- Andronis, V.; Yoshioka, M.; Zografi, G. Effects of sorbed water on the crystallization of indomethacin from the amorphous state. *J. Pharm. Sci.*, 1997, 86(3), 346-351.
- Molecular mobility of supercooled amorphous indomethacin as a function of temperature and relative humidity. *Pharm. Res.*, 1998, 15(6), 835-842.
- Andronis, V.; Zografi, G. Crystal nucleation and growth of indomethacin polymorphs from the amorphous state. *J. Non-cry. Solids.*, 2000, 236-248.
- Angell, C. A. Formation of glasses from liquids and biopolymers. *Science.*, 1995, 267, 1924-1935.
- Banakar, U.V. Pharmaceutical Dissolution Testing; in: Drug and the Pharmaceutical Science Vol. 49; New York, USA, 1992.
- Barth, J.; Mollmann, H.W.; Armbruster, B.; Florke, W.; Hovhhaus, G.; Mollmann, C.R.; Derendorf, H. Analysis of shape, particle size distribution and aggregation of the crystals of sodium cromoglycate and nedocromil sodium. *Eur.J.Hosp.Pharm.*, 1993, 3, 20-28.
- Beach, S.; Latham, D.; Sidgwick, C.; Hanna, M.; York, P. Control of the physical form of salmeterol xinafoate. *Organic Process Research & Development*, 1999, 3, 370-376.
- Berkow, R.; Beers, M.H.; Fletcher, A.J., The Merck manual of medical information, home edition, Merck research laboratories, NJ, 1997.

Bleich, J.; Kleinebudde, P.; Muller, B.W. Influence of gas density and pressure on microparticles produced with the ASES process. *Inter. J. Pharm.*, 1994, 106, 77-84.

Bleich, J.; Muller, B.W. Production of drug loaded microparticles by the use of supercritical gases with the Aerosol Solvent Extraction System (ASES) process. *J. Microencapsulation.*, 1996, 13(2), 131-139.

Bleich, J.; Muller, B.W.; Waßmus, W. Aerosol solvent extraction system- a new microparticle production technique. *Int. J. Pharm.*, 1993, 97, 111-117.

Bodmeier, R.; Wang, H.; Dixon, D.J.; Mawson, S; Johnston, K.P. Polymeric microspheres prepared by spraying into compressed carbon dioxide. *Pharm. Res.*, 1995, 12(8), 1211-1217.

Bootsma, H.P.R.; Frijlink H.W.; Eissens A.; Proost JH.; Van Doorne, H.; Lerk, CF. β -cyclodextrin as an excipient in solid oral dosage forms : in vitro and in vivo evaluation of spray-dried diazepam- β -cyclodextrin products. *Inter. J. Pharm.*, 1989, 51, 213-223.

British Pharmaceutical Codex 1994 Pharmaceutical society of Great Britain, Pharmaceutical Press, 1994.

British Pharmacopoeia 2002, The stationary office, London, 2002.

Brittain, H.G.; Bogdanowich, S.J.; Bugay, D.E.; De Vincentis, J.; Lewen, G.; Newman, A.W. Physical chracterization of pharmaceutical solids. *Pharm.Res*, 1991, 8, 963-973.

Brittain, H.G.; Grant, D.J.W. Effects of Polymorphism and Solid-State Solvation on Solubility and Dissolution Rate. *Drug. Pharm. Sci.*, 1999, 95, 279-330.

Broadhead, J.; Edmond Rouan, S.K.; Rhodes, C.T. The spray drying of pharmaceuticals. *Drug Dev. Ind. Pharm.*, 1992, 18(11-12), 1169-1206.

Buckton, G.; Beezer, A.E. The relationship between particle size and solubility. *Int. J. Pharm.*, 1992, 82, R7-R10.

Buckton, G.; Darcy, P. Assessment of disorder in crystalline powders- a review of analytical techniques and their application. *Inter. J. Pharm.*, 1999, 179, 141-158.

Carstensen, J.T.; Morris, T. Chemical stability of indomethacin in the solid amorphous and molten states. *J. Pharm. Sci.*, 1993, 82(6), 657-659.

Charles, B.G.; Mogg, G.A.G. *Biopharm. Drug. Disp.*, 1994, 15, 121-128.

Charoenchaitrakool, M.; Dehghani, F.; Foster, N.R.; Chan, H.K. Micronisation by RESS to enhance the dissolution rates of poorly water-soluble pharmaceuticals. *Ind. Eng. Chem. Res.*, 2000, 39(12), 4794-4802.

Chiou, W.L.; Riegelman, S. Oral absorption of griseofulvin in dogs. Increased absorption via solid dispersion in polyethylene glycol 6000. *J. Pharm. Sci.*, 1970, 59, 937-942.

Chiou, W.L.; Riegelman, S. Pharmaceutical applications of solid dispersion systems. *J. Pharm. Sci.*, 1971, 60, 1281-1302.

Corrigan, O.I.; Timoney, R.F. Influence of Polyvinylpyrrolidone on the dissolution Properties of Hydroflumethiazide. *J. Pharm. Pharmacol.*, 1975, 27(10), 759-764.

Corrigan, O.I.; Holohan, E.M. Amorphous spray-dried hydroflumethiazide –polyvinyl pyrrolidone systems: Physicochemical properties. *J. Pharm. Pharmacol.*, 1984, 36(4), 217-221.

Corrigan, O.I.; Holohan, E.M.; Sabra, K. Amorphous forms of thiazide diuretics prepared by spray-drying. *Int. J. Pharm.*, 1984, 18(1-2), 195-200.

Corrigan, O.I.; Holohan, E.M.; Reilly, M.R. Physicochemical properties of indomethacin and related compounds co-spray dried with polyvinylpyrrolidone. *Drug Dev. Ind. Pharm.*, 1985, 11(2-3), 677-695.

Corrigan, O.I.; Crean, A.M. Comparative physicochemical properties of hydrocortisone-PVP composites prepared using supercritical carbon dioxide by the GAS anti-solvent recrystallization process, by coprecipitation and by spray drying. *Int. J. Pharm.*, 2002, 245, 75-82.

Crosby, E.J.; Marshall W.R.Jr. Effects of drying conditions on the properties of spray-dried particles. *Chem. Eng. Prog.*, 1958, 54(7), 56-63.

Darcy, P.; Buckton, G. Quantitative assessments of powder crystallinity: Estimates of heat and mass transfer to interpret isothermal microcalorimetry data. *Thermochim. Acta.*, 1998, 316, 29-36.

Debenedetti, P.G. Precipitation of poly (L-lactic acid) and a composite poly (L-lactic acid) -pyrene particles by rapid expansion of supercritical solutions. *J. Supercrit. Fluids.*, 1994, 7, 9.

Debenedetti, P.G.; Lim GB.; Prud'homme, RK., Formation of Protein Microparticles by antisolvent precipitation, European Patent, 0542314 A1, 1992.

Dixon, D.J.; Johnston, K.P.; Bodmeier, R.A. Polymeric materials formed by precipitation with a compressed fluid antisolvent. *AIChE. J.*, 1993, 39, 127-139.

Doherty, C.; York, P. Mechanisms of Dissolution of Frusemide/PVP Solid Dispersions. *Int. J. Pharm.*, 1987, 34, 197-205.

Ediger, M.D.; Angell, C.A.; Nagel, S.R. Supercooled liquids and glasses. *J.Phys.Chem.*, 1996, 100, 13200-13212.

Edwards, A.D.; Shekunov, B.U, Forbes, R.T.; York, P. Crystallisation of pure anhydrous carbamazepine polymorphs using SEDS process. *J. Pharm. Pharmacol.*, 2000, 52 (Supplement), 301.

Egawa, H.; Maeda, S.; Yonemochi, E.; Oguchi, T.; Yamamoto, K.; Nakai, Y., "Solubility parameter and dissolution behaviour of cefalexin powders with different crystallinity" *Chem Pharm Bull.*, 1992, Vol. 40, 819-820.

Eggers, R.; Wagner, H.; Jaeger, P., "Extraction of spray-particles with supercritical fluids", In High pressure Chemical Engineering, Process Technology Proceedins, Vol 12, Von Rohr, PhR.; Trepp, ChEds., Elsevier, Amsterdam, 1996,49-54.

Fini, A.; Fazio, G.; Feroci, G., "Solubility and solubilization properties of non-steroidal anti-inflammatory", *Inter. J. Pharm.*, 1995, 126, 95-102.

Florence, A.T.; Attwood, D. Physicochemical principles of pharmacy, 3rd Ed, Macmillan press Ltd, London, U.K., 1998.

Ford, J.L.; Timmins, P. Pharmaceutical thermal analysis techniques and applications, Ellis Horwood Limited, Chichester,U.K., 1998.

Fukuoka, E.; Makita, M.; Yamamura, S. Some physicochemical properties of glassy indomethacin. *Chem. Pharm. Bull.*, 1986, 34(10), 4314-4321.

Gallagher-Wetmore, P.; Coffey, M.P.; Krukonis, V. Application of supercritical fluids in recrystallization: Nucleation and Gas Antisolvent (GAS) Techniques. *Respiratory Drug Delivery*, IV, 1994, 287.

Gil, H-J.; Kim, H.; Chi, S. Release of flurbiprofen from poloxamer 407 gel. *Arch. Pharm. Res.*, 1994, 17(4), 240-243.

Gordon, M.; Taylor, J.S. Ideal co-polymers and the second order transition of synthetic rubbers 1. non-crystalline co-polymers. *J. Appl. Chem.* 1952, 2, 493-500.

Giunchedi, P.; Conte, U. Spray-drying as a preparation method of microparticulate drug delivery systems: An over view. *STP. Pharma Science.*, 1995, 5(4), 276-290.

Hancock, B.C.; Parks, M. What is the true solubility advantage for amorphous pharmaceutical?. *Pharm. Res.*, 2000, 17(4), 397-404.

Hancock, B.C.; Zografi, G. Characteristics and significance of the amorphous state in pharmaceutical systems. *J. Pharm. Sci.*, 1997, 86(1), 1-12.

Hancock, B.C.; Zografi, G. The relationship between the glass transition temperture and the water content of amorphous pharmaceutical solids. *Pharm. Res.*, 1994, 11(4), 471-477.

Hanna, M.; York, P., Patent WO 95/01221, 1994.

Hanna, M.; York, P., Patent WO 96/00610, 1995.

Hanna, M.; York, P., Hanna, MH., Patent WO 99/59710, 1999.

Hill, V. An investigation into the use of MTDSC as a technique for the characterization of pharmaceutical materials. PhD thesis, University of London, 1999.

Horter, D.; Dressman, J.B., "Influence of Physicochemical Properties on Dissolution of Drugs in the Gastrointestinal Tract." *Adv. Drug Delivery Rev.*, 1997, 25(1), 3-14.

Imaizumi, H.; Nambu, N.; Nagai, T. Stability and several physical properties of amorphous and crystalline forms. *Chem. Pharm. Bull.*, 1980, 28, 2565-2569.

Imaizumi, H.; Nambu, N.; Nagai, T. Stabilization of amorphous state of indomethacin by solid dispersion in polyvinylpyrrolidone. *Chem. Pharm. Bull.*, 1983, 31, 2510-2512.

Jaarmo, M.; Rantakyla, M.; Aaltonen, O. Particle tailoring with supercritical fluids: production of amorphous pharmaceutical particles. In: K. Arai (Ed.), *Proceedings of the Fourth International Symposium on Supercritical Fluids*, Sendai, Japan, 1997, 263-267.

Jung, J.; Perrut, M. Particle design using supercritical fluids: literature and patent survey. *J. Supercrit Fluids.*, 2001, 20, 179-219.

Kerc, J.; Srcic, S.; Knez, Z.; Sencar-Bozic, P. Micronization of drugs using supercritical carbon dioxide. *Int. J. Pharm.*, 1999, 182, 33-39.

Kim, J.H.; Paxton, T.E.; Tomasko, D.L. Microencapsulation of Naproxen Using Rapid Expansion of Supercritical Solutions. *Biotechnol. Prog.*, 1996, 12(5), 650-661.

Landin, M.; Gonzalez, M.P.; Souto, C.; Concheiro, A.; Gomez-Amoza, J.L.; Martinez-Pacheco, R. Comparison of two varieties of microcrystalline cellulose as filler-binders II. Hydrochlorothiazide tablets. *Drug. Dev. Ind. Pharm.*, 1993, 19(10), 1211-120.

Larson, K.A.; King, M.L. Evaluation of super critical fluid extraction in pharmaceutical industry. *Biotechno. Prog.*, 1986, 2, 73-82.

Laurence, D.R.; Bennett, P.N.; Brown, M.J. *Clinical Pharmacology*, 8th Ed, Churchill Livingston, U.K, 1997.

Lele, A.K.; Shine, A.D. Effect of RESS dynamics on polymer morphology. *Ind. Eng. Chem. Res.*, 1994, 33, 1476-1485.

Loth, H.; Hemgesberg, E. Properties and Dissolution of Drugs Micronized by Crystallization from Supercritical Gases. *Int. J. Pharm.*, 1986, 32, 265-367.

Martin, H.J.; Schmidt, P.C.; Wahl, M.A.; Hils, P.; Helfgen, B.; Turk, M.; Schaber, K. Nanoscale particles for pharmaceutical purpose by rapid expansion of supercritical solutions (RESS): Part II: Characterization of the product and use. *Proceed. 7th Meeting on Supercritical fluids*, Tome 1; M. Perrut, E. Reverchon (Eds), ISBN 2-905-267-33-10, December 6-8, Antibes, 2000, 53-57.

Masters, K., spray drying handbook, 5th Ed., Longman (U.K.)& J. Wiley & Sons (U.S.), 1990.

Matson, D.W.; Fulton, J.L.; Peterson, R.C.; Smith, R.D. Rapid expansion from supercritical fluid solution solutions: solute formation of powder, thinfilms and fibres. *Ind. Eng. Chem. Res.*, 1987, 26, 2299-2306.

Matsumoto, T.; Zografi, G. Physical properties of solid molecular dispersion of indomethacin with poly(vinylpyrrolidone) and poly(vinylpyrrolidone-co-vinylacetate) in relation to indomethacin crystallization. *Pharm. Res.*, 1999, 16(11), 1722-1728.

McCabe, W.L.; Smith, J.C.; Harriott, P. Unit operations of chemical engineering, 5th Ed, McGraw-Hill international edition, 1993.

McHugh, M.A.; Krukonis, V.J., Supercritical Fluid Extraction: Principles and Practice. Butterworths, Boston, 1986.

McNaughton, J.L.; Mortimer, C.T. Differential Scanning Calorimetry, In *IRS, Physical chemistry Series 2*, Vol. 10, Butterworths, 1975.

Mehta, M., Physicians' Desk Reference guide to drug interactions, side effects, indications, 47th Ed, Medical Economics Data Production, N.J., 1993.

Moneghini, M.; Kikic, I.; Voinovich, D.; Perissutti, B.; Filipovic-Grcic, J. Processing of carbamazepine-PEG 4000 solid dispersions with supercritical carbon dioxide: preparation, characterisation, and in vitro dissolution. *Int. J. Pharm.*, 2001, 222, 129-138.

Moshashae, S.; Bisrat, M.; Forbes, R.T.; Nyqvist, H.; York, P. Supercritical fluid processing of proteins I: Lysozyme precipitation from organic solution. *Euro. J. Pharm. Sci.*, 2000, 11, 239-245.

Mullin, J.W., Crystallization, 3rd Ed, Butterworth-Heinmann, Oxford, U.K., 1997.

Nakai, Y.; Fukuoka, E.; Nakajima, S-I.; Iida, Y. Effects of Grinding on Physical and Chemical Properties of Crystalline medicinals with Microcrystalline Cellulose II. Retention of volatile medicinals in ground mixtures. *Chem.Pharm. Bull.*, 1978a, 2983-2989.

Nakai, Y.; Nakajima, S.; Yamamoto, K.; Terada, K.; Konno, T. Effects of Grinding on Physical and Chemical Properties of Crystalline medicinals with Microcrystalline Cellulose III. IR spectra of medicinal in ground mixtures. *Chem. Pharm. Bull.*, 1978b, 3419-3425.

Nernst, W. Theorie der Reaktionsgeschwindigkeit in heterogenen Systemen. *Z. Phys. Chem.*, 1904, Vol. 47,52-55.

Noyes, A.; Whitney, W. The rate of solution of solid substances in their own solutions. *J. Am. Chem. Soc.*, 1897, 19, 930-934

Nyquist, H. Saturated salt solutions for maintaining specified relative humidities. *Int. J.Pharm.Tech.Prod.Mfr.*, 1983, 4, 47-48.

Oakley, D.E. Produce uniform particles by spray drying. *Chem. en. prog.*, Oct 1997, 48-54.

O'Brien, M.; Mc Cauley, J.; Cohen, , Analytical profiles of drug substances, 1984, Vol 13. 211-238

Ochoa Machiste, E.; Giunchedi, P.; Setti, M.; Conte, U. Characterization of Carbamazepine in Systems Containing a Dissolution Rate Enhancer. *Int. J. Pharm.*, 1995, 126, 65-72.

Ohgaki, K.; Kobayashi, H.; Katayama, T. Whisker formation from jet of supercritical fluid solution. *J. Supercrit. Fluids.*, 1990, 3, 103-107.

Otsuka, M.; Kaneniwa. A kinetic study of the crystallization process of noncrystalline indomethacin under isothermal conditions. *Chem. Pharm. Bull.*, 1988, 36, 4026-4032.

Palakodaty, S.; York, P. Phase behavioural effects on particle formation processes using supercritical fluids. *Pharm. Res.*, 1999, 16, 976-985.

Palakodaty, S.; York, P.; Pritchard, J. Supercritical fluid processing of materials from aqueous solutions: The application of SEDS to lactose as a model substance. *Pharm. Res.*, 1998, 15(12), 1835-1843.

Pesonen, T.; Paronen, P.; Ilkka, J. Dissolution properties of direct compression tablets containing an agglomerated cellulose powder. *Drug Dev. Ind. Pharm.*, 1992, 18(2), 159-173.

Phillips, E.M.; Stella, V.J. Rapid expansion from supercritical solutions: application to pharmaceutical processes. *Inter. J. Pharm.*, 1993, 94, 1-10.

Randolph, T.W.; Randolph, A.D.; Mebes, M.; Yeung, S. Sub micrometer-sized biodegradable particles of poly(l-lactic acid) via the Gas Antisolvent Spray precipitation process. *Biotechnol. Prog.*, 1993, 9, 429-435.

Raynie, DE., Chapter 5 Meeting the Natural Products Challenge with Supercritical Fluids, In: Abraham, MA.; Sunol, AK.(Eds.), Supercritical Fluids: Extraction and Pollution Prevention. ACS Symposium Series 670, American Chemical Society, Washington DC, 1997, 68-75.

Rehman, M.U.; Shekunov, B.Y.; York, P.; Colthorpe, P. Supersaturation profile and particle formation of nicotinic acid using the SEDS process. *J. Pharm. Pharmacol.*, 1999, 51 (Supplement), 275.

Rehman, M.U.; Shekunov, B.Y.; York, P.; Colthorpe, P. Crystallisation of inhalation compound in supercritical fluids: optimisation of particulate and solid properties. *J. Pharm. Pharmacol.*, 2000, 52 (Supplement), 27.

Reverchon, E. Supercritical antisolvent precipitation of micro- and nano-paarticles. *J. Supercritical fluids*, 1999, 15, 1-21.

Reverchon, E.; Donsi, G.; Gorgoglione, D. Salicylic acid solubilization in supercritical CO₂ and its micronization by RESS. *J. Supercritical fluids*, 1993, 6(4), 241-248.

Reverchon, E.; Porta, G.D.; Taddep, R.; Pallado, P.; Stassi, A. Solubility and micronization of griseofulvin in supercritical CHF₃. *Ind. Eng. Chem. Res.*, 1995,34, 4087-4091.

Reverchon, E.; Pallado, P. Hydrodynamic modelling of RESS Process. *J. Supercrit. fluids*, 1996, 9, 216-221.

Reverchon, E.; Perrut, M. Particle design using supercritical fluids: Review and Examples. Proceedings of the 7th meeting on supercritical fluids, Antibes/ Juan-Les-Pins, France., 2000, 1, 3-20.

Reverchon, E.; Porta, G.D.; Falivene, M.G. Process parameters and morphology in amoxicillin micro and submicro particles generation by supercritical antisolvent precipitation. *J Supercrit. fluids.*, 2000, 17, 239-248.

Reverchon, E.; Porta, G.D.; Trolino, A.D.; Pace, S. Supercritical antisolvent precipitation of nanoparticles of superconductor precursors. *Ind. Eng. Chem. Res.*, 1998, 37, 952-958.

Robertson, J.; King, M.B.; Seville, J.P.K. Particle production using near-critical solvents." In: M. Perrut, P. Subra (Eds.), Proceedings of the 5th meeting on Supercritical Fluids, INPL, Vandœuvre (Fr), 1998, Vol. 1, 339.

Rodrigues-Hornedo N.; Lechuga-Ballesteros D.; Wu, H.J. Phase transition and heterogenous/epitaxial nucleation of hydrated and anhydrous theophylline crystals. *Int. J. Pharm.*, 1992, 85, 149-162.

Rustichelli, C.; Gamberini, G.; Ferioli, V.; Gamberini, M.C.; Ficarra, R.; Tommasini, S. Solid-State Study of Polymorphic Drugs: Carbamazepine. *J. Pharm. Biomed. Anal.*, 2000, 23(1), 41-54.

Saim, S.; Subramaniam, B.; Rajewski, R.A.; Stella, V. Particle micronization with compressed gas antisolvent. *Pharm. Res.*, 1996, 13, S-273.

Sarisuta, N.; Parrott, E.L. Comparison of several diffusion equations in the calculation of viscosity and its relation to dissolution rate. *Drug. Dev. Ind. Pharm.*, 1982, 8, 605-616.

Sarisuta, N.; Parrott, E.L. Diffusivity and dissolution rates in polymeric solutions. *Drug. Dev. Ind. Pharm.*, 1983, 9, 861-875.

Simonelli, A.P.; Mehta, S.C.; Higuchi, W.I. Dissolution rates of higher energy sulfathiazole-povidone coprecipitates 2: Characterization of form of drug controlling its dissolution rate via solubility studies. *J. Pharm. Sci.*, 1976, 65, 355-361.

Schmitt, W.J.; Salada, M.C.; Shook, G.G. Finely-divided powders by carrier solution injection into a near or supercritical fluids. *AIChE J.*, 1995, 41, 2476.

Sekikawa, H.; Nakano, M.; Arita, T. Dissolution mechanisms of drug-polyvinylpyrrolidone coprecipitates in aqueous solution. *Chem. Pharm. Bull.*, 1979, 27(5), 1223-1230.

Sekizaki, H.; Danjo, K.; Eguchi, H.; Yonezawa, Y.; Sunada, H.; Otsuka, A. Solid-state interaction of ibuprofen with polyvinylpyrrolidone. *Chem. Pharm. Bull.*, 1995, 43, 988-993

Sencar-Bozic, P.; Srcic, S.; Knez, Z.; Kerc, J. Improvement of nifedipine dissolution characteristics using supercritical CO₂. *Int. J. Pharm.*, 1997, 148, 123-130.

Shaikh, N.H.; De Yanes, S.E.; Block, L.H.; Collins, C.C.; Pria, J.C. Effect of different binders on release characteristics of theophylline from compressed microspheres. *Drug Dev. Ind. Pharm.*, 1991, 17(6), 793-804.

Shamblin, S.L.; Taylor, L.S.; Zografi, G. Mixing behavior of colyophilized binary systems. *J. Pharm. Sci.*, 1998, 87(6), 694-701.

Shamblin, S.L.; Zografi, G. Enthalpy relaxation in binary amorphous mixtures containing sucrose. *Pharm. Res.*, 1998, 15(12), 1828-1834.

Shaube, G.R.; Brennecke, J.F.; McCready, M.J. Radial model for particle formation from the rapid expansion of supercritical solutions. *J Supercrit Fluids.*, 1995, 8, 318-328.

Shine, A.; Gelb, J., Patent WO 98/ 15384, October, 1997.

Simha, R.; Boyer, R.F. On a general relation involving the glass temperature and coefficients of expansion of polymers. *J.Chem.Phys.*, 1962, 37, 1003-1007.

Steckel, H.; Thies, J.; Muller, B.W. Micronizing of steroids for pulmonary delivery by supercritical carbon dioxide. *Inter. J. Pharm.*, 1997, 152, 99-110.

Subra, P.; Debenedetti, P. Application of RESS to several low molecular weight compounds. In *High pressure Chemical Engineering, Process Technology Proceedings*, Vol 12, Von Rohr, PhR.; Trepp, ChEds., Elsevier, Amsterdam, 1996, 49-54.

Subramaniam, B.; Rajewski, R.A.; Snavely, K. Pharmaceutical processing with supercritical carbon dioxide. *J. Pharm. Sci.*, 1997a, 86, 885-890.

Subramaniam, B.; Saim, S.; Rajewski, R.A.; Stella, V. Patent WO 97/31691, 1997b.

Summers, M.P.; Enever, R.P. Effect of primidone concentration on glass transition temperature and dissolution of solid dispersion systems containing primidone and citric acid. *J. Pharm. Sci.*, 1977, 66(6), 825-828.

Szulzewsky, K.; Kulpe, S.; Schulz, B.; Fichtner Schmittler, H. Crystallographic results on the polymorphism of chloramphenicol palmitate. *Acta Pharm Suec.*, 1982, 19(6), 457-470.

Taylor, L.S.; Zografi, G. Spectroscopic characterization of interactions between PVP and indomethacin in amorphous molecular dispersions. *Pharm. Res.*, 1997, 14(12), 1691-1698.

Taylor, L.S.; Zografi, G. Sugar-polymer hydrogen bond interactions in lyophilized amorphous mixtures. *J. Pharm. Sci.*, 1998a, 87(12), 1615-1621.

Taylor, L.S.; Zografi, G. The Quantitative Analysis of Crystallinity Using FT-Raman Spectroscopy. *Pharm. Res.*, 1998b, 15(5), 755-761.

Thies, J.; Muller, B.W. Production of large sized microparticles with supercritical GASES. *Pharm. Res.*, 1996, S-161.

Tom, J.W.; Debenedetti, P.G. Formation of bioerodible polymeric microspheres and microparticles by Rapid expansion of supercritical solutions. *Biotechnol. Prog.*, 1991, 7, 403-411.

Tom, J.W.; Debenedetti, P.G. Precipitation of poly(hydroxy acids) and coprecipitation of polymer/drug particles by Rapid Expansion of Supercritical Solutions. *Polym. Prepr. (Am. Chem. Soc. Div. Polym. Chem.)*, 1992, 33(2), 104-105.

Tom, J.W.; Debenedetti, P.G.; Jerome, R. Precipitation of poly(L-lactic acid) and composite poly (L-lactic acid)- pyrene particles by Rapid Expansion of Supercritical Solutions. *J. Supercrit. Fluids.*, 1994, 7, 9-29.

Tom, J.W.; Lim, G.B.; Debenedetti, P.G.; Prud'homme, R.K. Applications of supercritical fluids in the controlled release of drugs. *ACS Symp. Ser.*, 1993, 514, 238-257.

Trelfall, T.L. Analysis of organic polymorphs: a review. *Analyst.*, 1995, 120, 2435-2460.

Ueda, H.; Nambu, N.; Nagai, T. Dissolution behaviour of chlorpropamide polymorphs. *Chem. Pharm. Bull.*, 1984, 32(1), 244-250.

Wade, A.; Weller, P.J., Handbook of pharmaceutical excipients 2ndEd., The pharmaceutical press, London, 1994.

Wallace, J.W.; Capozzi, J.T.; Shangraw, R.F. Performance of pharmaceutical filler/binders as related to methods of powder characterization. *Pharmaceut Technol.*, 1983, 7(9), 94-104.

Wan, L.S.C.; Prasad, K.P.P. Effect of Microcrystalline cellulose and cross-linked Sodium carboxy methylcellulose on the properties of tablets with methylcellulose binder. *Int. J. Pharm.*, 1988, 41(1-2), 159-167.

Warwick, B.; Dehghani, F.; Foster, N.R.; Biffin, J.R.; Regtop, H.L. Synthesis, Purification, and micronization of pharmaceuticals using the Gas Antisolvent Technique. *Ind. Eng. Chem. Res.*, 2000, 39, 4571-4579.

Weidner, E.; Knez, Z.; Novak, Z. Proceed. Of the 3rd International Symposium on Supercritical Fluids, Tome 3; G. Brunner, M. Perrut (Eds), ISBN 2-905-267-23-8, October 17-19, Strasbourg, 1994, 229.

Weidner, E.; Steiner, R.; Knez, Z. Powder generation from polyethylene glycols with compressible fluids. In High pressure Chemical Engineering, Process Technology Proceedings, Vol 12, Von Rohr, PhR.; Trepp, Ch(Eds.), Elsevier, Amsterdam, 1996, 223-228.

West, A.R. Basic solid state chemistry, John Wiley & sons, Inc, U.K., 1997.

Wilkins, S.A.; York, P.; Roberts, R.J.; Rowe, R.C.; McConvey, I.F. The formation of indomethacin: polymer co-precipitates by the solution enhanced dispersion by supercritical fluids (SEDS) process. *J. Pharm. Pharmacol.*, 1999, 51 (Supplement): 291.

Winters, M.A.; Knutson, B.L.; Debenedetti, P.G.; Sparks, H.G.; Przybycien, T.M.; Stevenson, C.L.; Prestrelski, S.J. Precipitation of Proteins in Supercritical Carbon Dioxide. *J. Pharm. Sci.*, 1996, 85, 586-594.

Wubbolts, F.E.; Bruinsma, O.S.L.; de Graauw, J.G.; van Tosmalen, G.M. Continuous gas anti-solvent crystallisation of hydroquinone from acetone using carbon dioxide. Proceeding of 4th International Symposium on Supercritical Fluids, Tohoku Univ. Press, Sendai (Jap), 1997, 63.

Yeo, S.D.; Lim, G.B.; Debenedetti, P.G.; Bernstein, H. Formation of microparticulate protein powders using a supercritical fluid antisolvent. *Biotech. Bioeng.*, 1993, 41, 341.

Yonemochi, E.; Ueno, Y.; Ohmae, T.; Oguchi, T.; Nakajima, S-I.; Yamamoto, K. Evaluation of amorphous ursodeoxycholic acid by thermal methods. *Pharm. Res.*, 1997, 14(6), 798-803.

York, P.; Hanna, M. In *Respiratory Drug Delivery V: Program and Proceedings*; Dalby, R.N., Ed.; Interpharm Press: Buffalo Grove, IL., 1996, 231-239.

York, P. Strategies for particle design using supercritical fluid technologies. *Pharm. Sci. Tech. Today.*, 1999, 2(11), 430-440.

Yoshioka, M.; Hancock, B.C.; Zografi, G. Crystallization of Indomethacin from the Amorphous state below and above its glass transition temperature. *J. Pharm. Sci.*, 1994, 83, 1700-1705.

Yoshioka, M.; Hancock, B.C.; Zografi, G. Inhibition of indomethacin crystallization in poly(vinylpyrrolidone) coprecipitates. *J. Pharm. Sci.*, 1995, 84(8), 983-986.

Yamamoto, K.; Nakano, M.; Arita, T.; Takayama, Y.; Nakai, Y. Dissolution behavior and bioavailability of phenytoin from a ground mixture with microcrystalline cellulose. *J. Pharm. Sci.*, 1970, 65, 1484-1488

Yamaguchi, T.; Nishimura, M.; Okamoto, R.; Takeuchi, T.; Yamamoto, K. Glass formation of 4"-O-(4-methoxyphenyl)acetyltylosin and physical stability of the amorphous solid. *Int. J. Pharm.*, 1992, 85, 87-96.

Yu, L.; Reutzel, S.M.; Stephenson, G.A. Physical characterization of polymorphic drugs: an integrated characterization strategy. *Pharm. Sci. Tech. Today.*, 1998, 1, 118-127.

Appendix

Spray Drying with combustible solvents

With regard to the presence of spray drying with combustible solvents, special precautions were necessary. Working out the correct proportion of the combustible solvent in the air is the best approach to prevent any incidents occurring during spray drying with combustible solvents. Additionally, this proportion of air/solvent mix must be within the upper and lower explosion limits.

Calculation of air/solvent ratio (% v/v)

The maximum aspirator flow rate is $40 \text{ m}^3 \text{ hr}^{-1}$ (setting 20). Setting the aspirator rate at 10, the aspirator flow rate is therefore calculated value of $20 \text{ m}^3 \text{ hr}^{-1}$; setting the aspirator rate at 5, the rate is therefore evaluated at $10 \text{ m}^3 \text{ hr}^{-1}$ and so on.

Example 1

Calculate the maximum feed rate of a 50% ethanol content by using inlet temperature 100°C (The lower explosion limit of ethanol is 3.28 % v/v. Molecular weight of ethanol 46 g/mole and

ρ 0.79 g/ml)

a) Aspirator at 10

b) Aspirator at 5

Solution

From reference lists, the values of the lower explosion limit for higher safety is 1/5 of the lower limit (3.28% v/v), which means 0.656% v/v. Thus, for this calculation 0.656% v/v is the ratio of vapour solvent / total vapour of ethanol.

(a) For setting aspirator at 10:

The maximum capacity of vapour solvent authorised can be calculated as follow:

$$20000 \text{ l/hr} \times 0.656\% = 131.2 \text{ l/hr}$$

The equivalent of solvent can be calculated from The Law of Perfect Gas

$$PV = nRT \quad \dots\dots\dots (1)$$

where P is the atmospheric pressure, V is the volume of solvent liquid, n is the number of solvent mole, R is the molar constant gas and T is the inlet temperature in degree Kelvin.

Equation (1) may be rearranged to facilitate the direct determination of the mole/hr as follow:

$$n = PV/(RT)$$

where $P = 1 \text{ atm}$, $R = 0.0823 \text{ atm l mol}^{-1} \text{ K}^{-1}$.

In the operational condition, the inlet temperature is $100^\circ\text{C} + 273 = 373 \text{ K}$.

Therefore $n = 1 \times 131.2 / (0.0823 \times 373) = 4.274 \text{ mole/hr}$.

Since Molecular weight of ethanol = 46 g/mole and $\rho = 0.79 \text{ g/ml}$

The maximum feed rate of ethanol in ml/hr is

$$\frac{4.274 \text{ mole/hr} \times 46 \text{ g/mole}}{0.79 \text{ g/ml}} = 248.87 \text{ ml/hr}$$

Thus, feed rate of ethanol 248.87 ml/hr can be spray-dried with the aspirator at 10 in the safety conditions.

For a solution of 50% ethanol content, this mean that a maximum feed rate is

$$248.87 \times \frac{100}{50} = 497.74 \text{ ml/hr}$$

note: the feed pump was set at 8

(b) For setting aspirator at 5, the maximum feed rate of a 50% ethanol content solution would be half of the former which is 248.87 ml/hr (the feed pump was set at 4)

Another mode of calculation can be checked to ascertain that the conditions desired are safe.

Example 2

Could a 64% ethanol content solution be spray-dried at the inlet temperature 100°C and feed rate 400 ml/hr with the maximal capacity of the aspirator.

Solution

Ethanol feed rate $400 \times 64/100 = 256 \text{ ml/hr}$

From the density and molecular weight of ethanol, the rate of ethanol in mole/hr is

$$\frac{256 \text{ ml/hr} \times 0.79 \text{ g/ml}}{46 \text{ g/mole}} = 4.4 \text{ mole/hr}$$

From equation (1) can be rearranged and calculate the rate of vapour in l/hr as follow.

$$V = nRT/P$$

Therefore

$$V = \frac{4.4 \text{ mole/hr} \times 0.0823 \text{ atm l mole}^{-1} \text{ K}^{-1} \times 373 \text{ K}}{1 \text{ atm}}$$
$$= 135.07 \text{ l/hr}$$

air/solvent ratio can be obtained from the rate of vapour and aspirator flow rate

$$\text{air/solvent ratio} = \frac{135.07 \times 100}{(135.07 + 40,000)} = 0.34\% \text{ v/v}$$

$$0.34\% < 0.656\%$$

Since this value is lower than the lower explosion limit of ethanol, it can be concluded that the process is safe.